

Diversity, evolution and function of *Ralstonia solanacearum* TALE-likes

Dissertation

der Mathematisch-Naturwissenschaftlichen Fakultät
der Eberhard Karls Universität Tübingen
zur Erlangung des Grades eines
Doktors der Naturwissenschaften
(Dr. rer. nat.)

vorgelegt von
Niklas Schandry
aus München

Tübingen
2016

Gedruckt mit Genehmigung der Mathematisch-Naturwissenschaftlichen Fakultät der
Eberhard Karls Universität Tübingen.

Tag der mündlichen Qualifikation:	11.05.2016
Dekan:	Prof. Dr. Wolfgang Rosenstiel
1. Berichterstatter:	Prof. Dr. Thomas Lahaye
2. Berichterstatter:	Prof. Dr. Thorsten Nürnberger
3. <i>Berichterstatter, falls zutreffend</i>	-

Zusammenfassung	5
Abstract	6
Preface and contributions	7
1 Introduction	7
<i>1.1 Organismic interactions</i>	7
1.1.1 Evolutionary interplay between host and pathogen	8
1.1.2 Molecular interplay between host and pathogen in plants	9
1.1.2.1 Pattern triggered immunity	9
1.1.2.2 The role of effectors in disease development	10
1.1.2.3 Transcription activator like effectors (TALEs)	11
1.1.2.3.1 Structural features of the TALE CRD	13
1.1.2.3.2 TALE function in planta	15
1.1.2.3.3 TALEs as virulence factors	16
1.1.2.3.4 TALE mediated resistance	16
1.1.2.3.5 Drivers and mechanisms of TALE diversification in Xanthomonads	18
<i>1.2 The plant pathogenic Ralstonia solanacearum species complex</i>	19
1.2.1 What is <i>R. solanacearum</i> ?	19
1.2.2 <i>Ralstonia solanacearum</i> life cycle	20
1.2.3 Effectors of the Rssc	21
<i>1.3 Goals of this work</i>	22
2 Results	24
<i>2.1 TALE-likes of R. solanacearum</i>	24
2.1.1 Goals of this project	24
2.1.2 Strains were selected to cover much of the Rssc diversity	24
2.1.3 RipTALs can be found across the Rssc	27
2.1.4 RipTAL classification based on sequence characteristics	28
2.1.4.1 RipTAL classification and nomenclature	28
2.1.4.2 RipTAL CRD diversity is limited	30
2.1.5 Functional characterization of RipTALs	32
2.1.5.1 RipTALs localize to the nucleus	32
2.1.5.2 RipTALs are sequence specific transcriptional activators	34
2.1.5.2.1 RipTALs encode a Guanine requirement in the NTR extending the similarity between EBEs	34
2.1.5.2.2 RipTAL cross activation profiles and strain host range correlate	35
2.1.5.2.3 Repeat 8 of RipTAL classes I and III shows relaxed base specificity in its native context	37

2.1.5.2.4	RipTALs might be involved in host range adaptation	38
2.1.6	Characterizing evolutionary forces acting on TALE-like effectors	39
2.1.6.1	Harnessing polymorphisms found in RipTAL repeats to study evolution of TALE-like DNA binding domains	40
2.1.6.2	Mechanistic principles of RipTAL CRD evolution	47
2.2	<i>RipTALs in disease</i>	51
2.2.1	Natural recognition in <i>A. thaliana</i>	51
2.2.1.1	<i>P. fluorescens</i> as a heterologous delivery system for RipTALs	51
2.2.1.2	Analysis of candidate accessions using Rssc strains	57
2.2.1.3	A R based statistical analysis tool for Rssc infections	58
2.2.1.3.1	Input data formatting	58
2.2.1.3.2	Loading of require packages	59
2.2.1.3.3	Data import	59
2.2.1.3.4	Converting disease indeces to survival data	60
2.2.1.3.5	Plotting Kaplan-Meier survival curves and statistical analysis of plant lines treated with a single strain	62
2.2.1.3.6	Visual assessment of predictors in the dataset	64
2.2.1.3.7	Excluding batches from subsequent analysis	66
2.2.1.3.8	Statistical analysis of differential survival using variants of the log-rank test	66
2.2.1.3.9	Statistical analysis of differential survival based on Cox-proportional hazards	71
2.2.1.3.10	Statistical analysis assuming non-proportional hazards	72
2.2.1.4	Validation of the initial Pf-0 phenotypes with <i>R. solanacearum</i>	76
2.3	<i>Engineering resistance based on synthetic RipTAL receptors</i>	78
2.3.1	Project definition	78
2.3.2	Strategy	79
2.3.3	Composition of the synthetic RipTAL-activated R gene.	79
2.3.3.1	Promoter	79
2.3.3.2	Coding sequence	80
2.3.3.3	Selection markers, terminator sequences and cloning of the construct	82
2.3.4	Functional validation of hypersensitive response elicitation	86
2.3.5	Plant lines generated and project continuation	94
3	Discussion	100
3.1	<i>RipTALs are part of the accessory effectome in Rssc</i>	100
3.1.1	Abundance, distribution and phylogeny of RipTALs in the Rssc indicates monophyletic origin	100
3.1.2	RipTALs in comparison to other Rips	101

3.1.3	Functional overlap between RipTALs indicates role in host adaptation	101
3.2	<i>Evolutionary constraints of TALE-like effectors</i>	103
3.2.1	Analysis of repetitive sequences in an evolutionary context	103
3.2.2	RipTALs provide an angle to trace evolutionary mechanisms acting on TALEs	104
3.2.3	Evolvability of host-exposed pathogen proteins	108
3.2.4	Mechanistic, structural and ecological comparison of antigenic variation and <i>Xanthomonas</i> TALEs	109
3.2.5	Relationship between evolvability of pathogen features and host range	112
3.3	<i>RipTAL recognition in plants</i>	114
3.3.1	Natural recognition in <i>A. thaliana</i>	114
3.3.2	Considerations on the survival analysis of Rssc infected plants	115
3.3.3	Engineered RipTAL recognition	119
3.3.4	Broad range synthetic resistance	120
4	Material and Methods	121
4.1	<i>Methods for the isolation and modification of Deoxyribonucleic acids (DNA)</i>	121
4.1.1	Transformation of bacteria	121
4.1.2	DNA Isolation	121
4.1.3	Polymerase chain reaction and related methods	122
4.1.3.1	General Procedure	122
4.1.3.2	PCR amplification and cloning of <i>ripTALs</i>	128
4.1.3.3	Cloning of GUS reporter constructs	130
4.1.3.4	Gel electrophoresis of DNA	130
4.2	<i>Protein methods</i>	130
4.2.1	Protein extraction, PAGE, and Western blot on <i>P. fluorescens</i>	130
4.2.2	GUS-Assays using <i>A. thaliana</i> protoplasts	131
4.2.3	Confocal laser scanning microscopy of <i>ripTAL</i> expressing protoplasts	132
4.2.4	Analysis of RipTAL-YFP fusion protein levels in protoplasts by flow cytometry	133
4.3	<i>Plant and microbe Methods</i>	133
4.3.1	Leaf infiltration of <i>A. thaliana</i> plants and cell death assays	133
4.3.2	Transient transformation of leaf cells via <i>A. tumefaciens</i> infiltration of <i>N. benthamiana</i>	133
4.3.3	Transformation of <i>A. thaliana</i> by floral dip	134
4.3.4	Cotyledon transformation of <i>S. lycopersicum</i>	134
4.3.5	Infection of <i>A. thaliana</i> with Rssc strains by soil soaking	134

4.4	<i>Computational methods and additional R scripts</i>	134
4.4.1	Alignments and calculations of alignment sequence identities or similarities	134
4.4.2	Extraction of individual <i>repeat</i> sequences from <i>repeat</i> arrays (<i>CRD</i> sequences)	135
4.4.3	Visualization of sequence similarities	137
	References	139
	Acknowledgements	151
	Curriculum Vitae	152
	Data Supplement	153

Zusammenfassung

Der bakterielle *Ralstonia solanacearum* Spezienkomplex verfügt über eine große Anzahl an Effektoren und zeichnet sich unter den bakteriellen Krankheitserregern durch ein sehr breites Wirtsspektrum von über 200 Pflanzenarten, sowie den für die Pflanze tödlichen Ausgang der Krankheit aus. Dies führt vor allem in tropischen Regionen zu starken Einschränkungen in der Kultivierbarkeit bestimmter Pflanzen bzw. zu Ernteaussfällen. Viele der Wirte sind Nachtschattengewächse (z.B. Kartoffel, Tomate, Paprika), jedoch sind auch Erreger von Krankheiten einkeimblättriger Pflanzen, die ökonomisch relevante Vertreter der Bananengewächse infizieren und töten, teil des Spezienkomplexes.

Unter den Effektoren finden sich Homologe der "Transcription activator like effectors" (TALEs), die RipTALs, die in der Lage sind spezifische DNS Sequenzen zu erkennen und die Transkription benachbarter Gene zu aktivieren. Die vorliegende Arbeit bietet den ersten umfassenden Überblick über die Verteilung von RipTAL Genen im Spezienkomplex, sowie deren kodierende Sequenzen. Darüber hinaus konnte experimentell gezeigt werden, dass alle RipTALs sequenzspezifische Transkriptionsfaktoren sind. Im Gegensatz zu TALEs sind RipTALs wenig divers in ihren Zielsequenzen, jedoch bilden sie, in Abhängigkeit der präferierten Wirtspflanzen, nicht überlappende Spezifitätsgruppen. Auf Basis eines Vergleichs von RipTAL und TALE Genen wird ein erklärendes Konzept zum Verhalten dieser Gene in natürlichen Bakterienpopulationen vorgestellt.

Zusätzlich war die Nutzbarkeit von RipTALs im Kontext von pflanzlicher Resistenz eine zentrale Fragestellung. Hierzu wurde die natürliche Diversität der Modellpflanze *Arabidopsis thaliana* hinsichtlich RipTAL abhängiger Resistenz untersucht. Es konnten vier Ökotypen identifiziert werden, die einen RipTAL-abhängigen Krankheitsphänotyp zeigen.

Darüber hinaus wurde ein synthetisch-translatinaler Ansatz zur Etablierung RipTAL-induzierter Resistenz gegen *R. solanacearum* im Nutzpflanzenmodell *Solanum lycopersicum*, sowie in *A. thaliana*, verfolgt. Experimentell konnte eine RipTAL abhängige Resistenzreaktion in, mit dem synthetischem Konstrukt transformiertem, pflanzlichem Gewebe gezeigt werden.

Abstract

The bacterial *Ralstonia solanacearum* species complex (Rssc) possesses a large effector repertoire and is set apart from many other bacterial plant pathogens by its broad host range of over 200 plant species and the lethality of the disease. Diseases caused by the Rssc impact the yield and possibility to cultivate certain plant species in tropical areas, where these bacteria are endemic. Most host plants are solanaceous, such as tomato, pepper or potato, but certain lineages within the Rssc specialized on economically important crops of the Musa family, such as banana or plantain.

Among the large effector repertoire are homologs of the Transcription Activator Like Effectors (TALEs), termed RipTALs. RipTALs are able to recognize specific DNA sequences and activate transcription of neighbouring genes.

This work provides a comprehensive overview of the abundance of RipTAL genes within the Rssc, as well as their coding sequences. It is demonstrated that all identified RipTALs act as sequence specific transcription factors in plants. In contrast to TALEs, the diversity of RipTAL target sequences is limited. Yet, RipTALs form distinct functional groups of overlapping sequence specificity, which can be correlated to strain host ranges. Based on the comparison of RipTALs and TALEs a model explaining the behavior of these genes in natural bacterial populations is presented.

The utilization of RipTALs in the context of disease resistance in plants constitutes a second central theme of this work. Two distinct approaches were followed. Firstly, the natural diversity of the model plant *Arabidopsis thaliana* was assessed regarding naturally occurring RipTAL mediated defense reactions. This unveiled four candidate ecotypes that exhibit a RipTAL dependent disease phenotype.

Secondly, a translational, synthetic approach to establish RipTAL-dependent disease resistance in the model plant *A. thaliana*, as well as in the crop model *Solanum lycopersicum* was employed. Experimental results showed a RipTAL-dependent resistance response, in plant tissues transformed with the synthetic construct.

Preface and contributions

Parts of this work, in particular the results described in section 2.1, are part of a manuscript (N. Schandry, O. de Lange, P. Pior, T. Lahaye; “TALE-likes are an Ancestral Feature of the *Ralstonia solanacearum* Species Complex and Converge in DNA Targeting Specificity”) currently under consideration for publication in “Frontiers in Plant Science”. The experiments shown in figures 8, 9, 10, 11 / 12 and 13 were partially performed by Orlando de Lange. His contributions were: protoplast transfections for microscopy and flow cytometry and protoplast transfections for, and subsequent measurements of, GUS reporter activity. I performed microscopy, GUS reporter assays not carried out by Orlando de Lange and was responsible for data handling, statistical analysis and interpretation and figure preparation.

Although performed as part of my doctoral studies, my contributions to de Lange et al. 2013, are not explicitly discussed in this work. The same applies to my contributions to a manuscript on the applicability of TAL-like repeats in a biotechnological and synthetic biology context (joint first authorship with Orlando de Lange), currently in preparation.

1 Introduction

1.1 Organismic interactions

The interplay between different organisms is a fundamental aspect of all life. No organism is able to exist in isolation and large eukaryotic organisms serve as an ecological niche to many smaller organisms (Walter and Ley 2011; Berendsen et al. 2012; Turner et al. 2013). These interactions are an important topic of ongoing research. Accumulating evidence, uncovered largely by genome sequencing of all genomes found on, around and within a eukaryotic organism has highlighted how complex inter-organismic relationships shape the development and general abilities of an organism (Berendsen et al. 2012; Cho and Blaser 2012; Turner et al. 2013). The nutrient uptake of eukaryotic organisms appears to rely heavily on the action of small organisms, such as bacteria (Hacquard et al. 2015). Research into

the rhizome (collection of organisms in rhizosphere (close proximity of a plant root)) has shown that large diversity can be found there (Berendsen et al. 2012). A well studied example of nutrient uptake facilitated by small organisms in plants is root symbiosis, with either fungal or bacterial symbionts (Kistner and Parniske 2002). Plants closely interact with root symbionts and exchange various organic and in-organic substances for mutual benefit. While interactions for mutual benefit exists, many cases of interactions are only beneficial to one of the partners involved (Berendsen et al. 2012). Microbial pathogens cause disease, meaning that the host organism can no longer function normally (D'Arcy 2001). Diseases can be manifold, ranging from localized lesions, to full infection (colonization) of tissues or organs, vascular systems and other structures. For the sake of simplicity this work will largely focus on situations, where the host is a multi-cellular eukaryote of the Plantae kingdom, and the pathogen is a bacterial organism.

1.1.1 Evolutionary interplay between host and pathogen

Disease is rarely beneficial to the host organism; thereby being diseased often results in a direct fitness penalty. Natural selection will select for host traits that reduce, or prevent disease. This has lead to the immune systems we see in many organisms. Eukaryotic immune systems are often conceptualized into different layers. These range from basal recognition of certain pathogen features, such as structure or composition of conserved pathogen features on a molecular level (pathogen associated molecular patterns, PAMPs), to the sophisticated adaptive immune system found in vertebrates (Nürnbergger et al. 2004; Chisholm et al. 2006; Cooper and Alder 2006; Jones and Dangl 2006).

Conversely, successful host-colonization is beneficial for the pathogen, and traits that lead to higher colonization success will be favored by natural selection. The consequence of this are antagonistic selection pressures on the host and pathogen, which lead to co-evolution of both partners (Chisholm et al. 2006; Jones and Dangl 2006). This is sometimes referred to as an evolutionary arms race between host and pathogen (Jones and Dangl 2006).

1.1.2 Molecular interplay between host and pathogen in plants

1.1.2.1 Pattern triggered immunity

The evolutionary arms race translates into a molecular arms race between host and pathogen. The molecular consequence of the evolutionary and ecological relationship is an intimate molecular co-evolution of pathogenicity and immunity determinants of the pathogen and its host, respectively (Jones and Dangl 2006). Basal immunity, in both plants and animals, is upheld by non-self recognition of molecular patterns outside of a host cell (Nürnberger et al. 2004). This recognition is conferred by pattern recognition receptors (PRRs), acting as receptor like kinases (RLKs), usually composed of an extracellular sensor domain and an intracellular kinase domain (Jones and Dangl 2006). In plants, the extracellular sensor domain often belongs to the class of leucine rich repeats (LRR) or bear a resemblance to prokaryotic LysM receptors (Gómez-Gómez and Boller 2002; Miya et al. 2007). The recognized PAMPs include for example bacterial flagellin, EF-Tu or fungal chitin, recognized by *A. thaliana* membrane localized receptors FLS2, EFR and LYK5/CERK1, respectively (Gómez-Gómez and Boller 2000; Zipfel et al. 2006; Miya et al. 2007; Cao et al. 2014). Upon ligand perception, PAMP triggered immunity (PTI) is elicited by these receptors through complex MAP (mitogen activated protein) kinase (MAPK) signaling networks (Nürnberger et al. 2004; Zipfel 2008). Activation of these kinase signaling networks often involves bridging, membrane localized proteins such as BAK1 and SOBIR, which are able to form complexes with different RLKs upon ligand perception, and enable kinase signaling leading to the activation of various genes involved in plant defense and thereby eliciting PTI (Zipfel 2008; Liebrand et al. 2014; Albert et al. 2015).

As PTI relies on the recognition of basal, conserved pathogen features, outside of the plant cell, subversion of PTI constitutes a primary step in successful infection.

1.1.2.2 The role of effectors in disease development

One strategy pathogens employ to subvert PTI is the injection of proteins into host cells via type III secretion. These injected proteins are commonly known as effectors, and are directly injected into host cells using highly specialized molecular needles, able to penetrate the physical boundaries of a host cell (Grant et al. 2006), the type III secretion system. Effectors can be considered the second layer of pathogen attack, after initial contact to the host. Commonly, the evolution of effectors is considered to be the consequence of the first layer of plant defense, PTI (Jones and Dangl 2006).

Effector functions are diverse, and range from subversion of host defense such as interference of PAMP recognition, to manipulation of host metabolism to the benefit of the pathogen (Grant et al. 2006). For example, a regulator of PAMP signaling in *A. thaliana*, RIN4, is the target of multiple effectors, e.g. *Pseudomonas syringae* effectors AvrRpt2 and AvrRpm1, function by inhibiting RIN4 mediated signaling (Kim et al. 2005; Abramovitch et al. 2006). Plants in turn make use of resistance (*R*) proteins to recognize effectors. Multiple models of effector recognition have been proposed. These include the guard model, where an *R* protein is thought to “guard” the biochemical target of an effector (the guardee) (van der Hoorn and Kamoun 2008). In this model the *R* protein is triggered by a specific, effector-mediated modification of the guardee and upon recognition of such a modification the guard *R* protein elicits a resistance response (van der Hoorn and Kamoun 2008). However, it has been indicated that some effector targets appear to solely exist in the plant cell to be targeted by an effector, likely serving as a decoy from the original effector substrate. For example, tomato *R* protein Prf recognizes inhibition of the intracellular kinase Pto, which is inhibited by *P. syringae* effector AvrPto. AvrPto has been shown to also inhibit the kinase function of FLS2, which is likely the biological target of AvrPto, thereby interfering with PAMP signaling (van der Hoorn and Kamoun 2008). It thus appears likely that Pto is serving as decoy for AvrPto, competing with FLS2 (van der Hoorn and Kamoun 2008). This model is known as the decoy model, and it entails that the decoy protein partially mimics the true effector target, structurally or otherwise, thereby serving as an effector substrate. Upon effector-mediated modification of the decoy, *R* proteins elicit an immune response, similar to the

guard model (van der Hoorn and Kamoun 2008). The main difference between the guard and decoy model relates to the biological function of the protein monitored by a given *R* protein. In the guard model, the guardee is presumed to be the direct target of an effector and important for host function, whereas in the decoy model the guardee is thought to solely function as a decoy, with no additional function (van der Hoorn and Kamoun 2008).

R protein mediated resistance responses are collectively referred to as effector triggered immunity (ETI). ETI usually leads to a strong defense response, entailing a hypersensitive response (HR). The HR is the strongest immune response known in plants, and leads to localized cell death in the infected tissue (Jones and Dangl 2006). A unique class of *R* genes mediates the recognition of transcription activator like effectors (TALEs) (van der Hoorn and Kamoun 2008; Zhang et al. 2015).

1.1.2.3 Transcription activator like effectors (TALEs)

TALEs are a unique class of effectors initially discovered in plant pathogenic *Xanthomonas* species (Boch and Bonas 2010). TALEs can be divided into three domains: an N-terminal region (NTR), the central repeat domain (CRD) and the C-terminal region (CTR) (Gao et al. 2012; de Lange, Wolf, et al. 2014) (Figure 1).

TALE-like effectors were described in *Ralstonia solanacearum* (Salanoubat et al. 2002; Heuer et al. 2007; de Lange et al. 2013; Li et al. 2013), and TALE-like without proven effector function from *Burkholderia rhizoxinica* (BATs) and in marine metagenomes (MOrTLs) have been shown to contain a functional CRD with similar properties to that of TALEs (Juillerat et al. 2014; de Lange, Wolf, et al. 2014; de Lange et al. 2015).

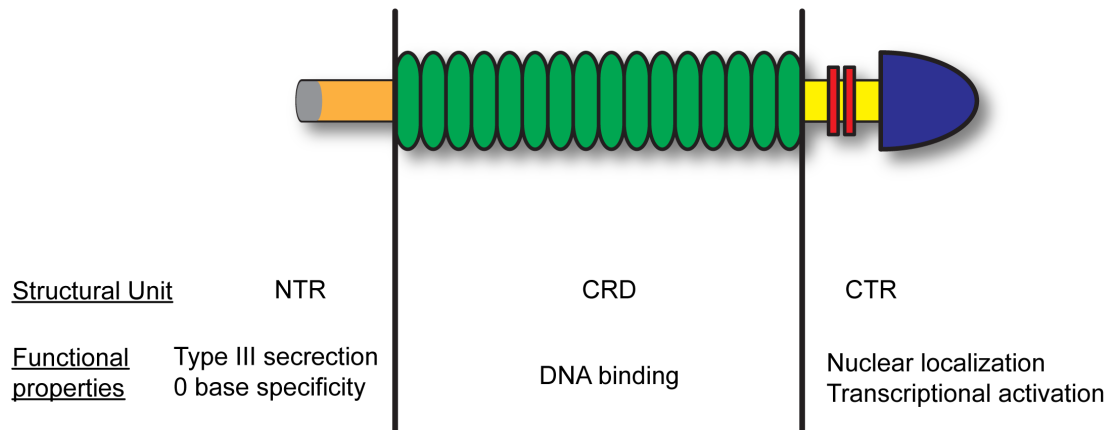


Figure 1. General structural features of a TAL-like effector. The putative type III secretion signal is colored in grey, NTR in orange, CRD in green with repeats shown as ovals, CTR in yellow, with the exception of nuclear localization signals (red) and activation domain (blue).

The NTR of TALEs contains a, far N-terminal, type III secretion signal necessary for translocation by the type III secretion system. Adjacent to the CRD the NTR harbors sequence degenerate repeats, which in concert confer recognition of one DNA base, and are assumed to structurally stabilize the CRD (Boch and Bonas 2010; Gao et al. 2012). The CTR of TALEs contains nuclear localization signals and a transcriptional activation domain, both are required for proper function in a plant cell (Figure 1) (Van den Ackerveken et al. 1996; Boch and Bonas 2010). Early experiments have shown that the transcriptional activation domain can be functionally replaced with a VP16 activation domain (Zhu 1999).

The most striking feature of TALEs is the CRD, which is made up of 1 to 33 near perfect repeats of 33-35 amino acids in length (Boch and Bonas 2010). Most TALEs display between 15 and 19 repeats in their CRD (Boch and Bonas 2010). These repeats are highly conserved in DNA and protein sequence, and most polymorphisms between repeats are found at amino acids position 12 and 13. These residues have therefore been termed repeat variable diresidue (RVD) (Moscou and Bogdanove 2009). Early experiments have indicated that the CRD takes an important role in *in planta* TALE function (Yang et al. 2005). Rigorous studies on genes activated upon TALE translocation or expression have uncovered that TALEs act as sequence specific transcription factors *in planta* (Römer et al. 2007). DNA-sequence specificity of TALEs is conferred by the CRD and the sequence of RVDs in the CRD has successfully been linked to the bound DNA sequence, thereby

allowing for the prediction of bound sequences solely based on the sequence of RVDs found in a TALE (Boch et al. 2009; Moscou and Bogdanove 2009). Vice versa, it is possible to design TALEs (designer TALEs, dTALEs) for virtually any desired sequence (Morbiter et al. 2011).

1.1.2.3.1 Structural features of the TALE CRD

Crystallization of TALE PthXo1 bound to DNA and subsequent structure elucidation uncovered that tandem arranged TALE repeats form a right-handed helix, which forms a super-helix around the DNA double helix along the major groove (Figure 3a,b). Each repeat in the TALE CRD consists of two alpha helices, one made up of 8 amino acids (short helix) and a second helix formed by 16 amino acids (long helix) (Figure 2) (Bochtler 2012; Gao et al. 2012; Mak et al. 2012). The long and short helices are separated by two loops. The loop, which is N-terminally flanked by the short helix, contains the RVD (RVD loop) (Figure 2), while the other loop connects short and long helices of adjacent repeats.

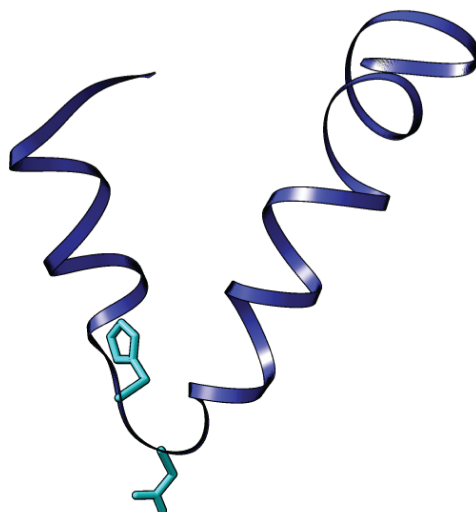


Figure 2. Structure of an individual TALE repeat. The short helix leading to the RVD loop is on the left, the RVD side chains (Histidine (12), Aspartic acid (13)) are shown in cyan, and the long helix is shown to the right. The image was rendered based on the PthXo1 structure (Mak et al. 2013) (pdb accession 3UGM) using UCSF Chimera (Pettersen et al. 2004).

The RVD loop is in close physical proximity to the DNA bases, coordinated by the rigid short and long helix (Figure 3b,c). Often, position 13 is able to form

either van-der-Waals contacts, or hydrogen bonds, with certain DNA bases, thus mediating base specificity (Bochtler 2012; Deng et al. 2014).

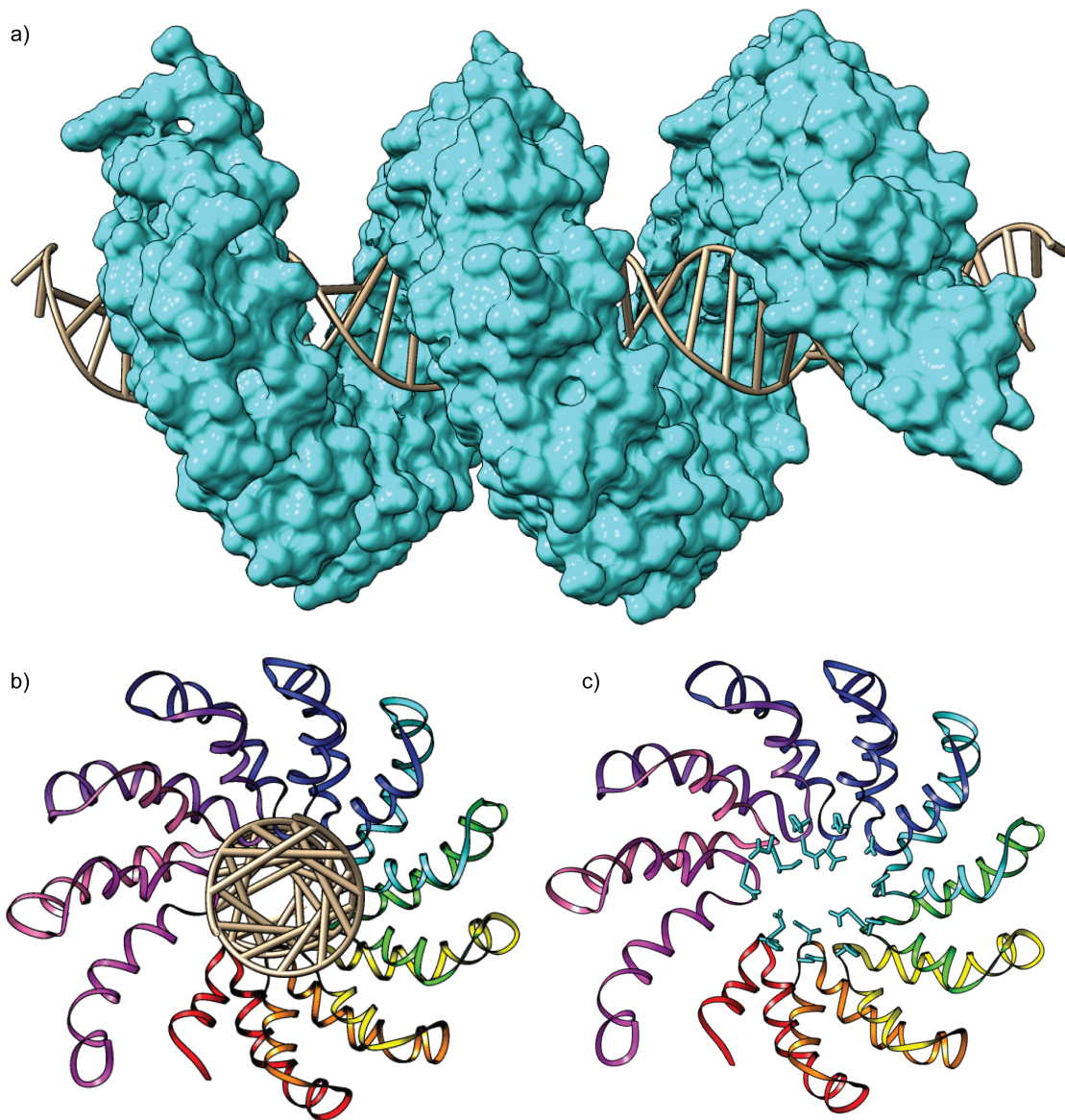


Figure 3. Crystal structure of a TALE. a) Surface structure of a TALE CRD (cyan, N-terminus to the left) bound to a matching DNA double strand (brown). b) View downwards the DNA double helix (3' facing "out"), with 10 TALE repeats, shown as ribbons, bound. Each repeat is colored individually, with the most N-terminal repeat being red. c) Display of the same repeats as in b, but with the DNA structure hidden and the side chains of the RVD residues shown (cyan). All structures were rendered based on the PthXo1 structure (Mak et al. 2013) (pdb accession 3UGM) using UCSF Chimera (Pettersen et al. 2004).

However, it is known that certain residues at position 13 are unable to form any contact with DNA bases, and instead do not sterically fit to certain DNA bases, thereby abolishing DNA binding of a given sequence by negative

discrimination (Wicky et al. 2013). It has been shown that CRDs made up of less than 11 repeats confer poor DNA binding (Streubel et al. 2012), and it appears that CRDs made up of 15-19 repeats archive an optimal balance between affinity to DNA and base sequence specificity, explaining why CRDs of this length are most abundant in nature (Boch and Bonas 2010). Together all repeats found in one CRD confer binding of an effector binding element (EBE). The sequence of the bound EBE is determined by the sequence of RVDs in a CRD together with the base specificity of the NTR (Hummel et al. 2012; Doyle et al. 2013; Lamb et al. 2013).

1.1.2.3.2 *TALE function in planta*

While the basic molecular function of a TALE, the activation of transcription of a gene, is clear the biological consequences of this molecular action are diverse. The biological consequence is directly dependent on the activated gene. The activated gene depends on the RVD sequence in the CRD and the plant genotype. The function of the resulting gene-product determines the biological outcome. So far TALEs have been shown to activate a variety of protein coding genes in plants (Kay et al. 2007; Römer et al. 2007; Bogdanove et al. 2010; Strauss et al. 2012; Verdier et al. 2012; Pereira et al. 2014; Tian et al. 2014; Hutin et al. 2015). Depending on the TALE and plant genotype studied, different outcomes have been described. Since TALEs are effectors of pathogens, these outcomes can be grouped into two distinct biological groups (Figure 4). On one hand, TALEs can act as virulence factors, meaning that their action is beneficial to pathogen growth, or otherwise promotes disease (Figure 4a). On the other hand, instances of TALE mediated resistances in specific plant genotypes have been reported (Figure 4b).

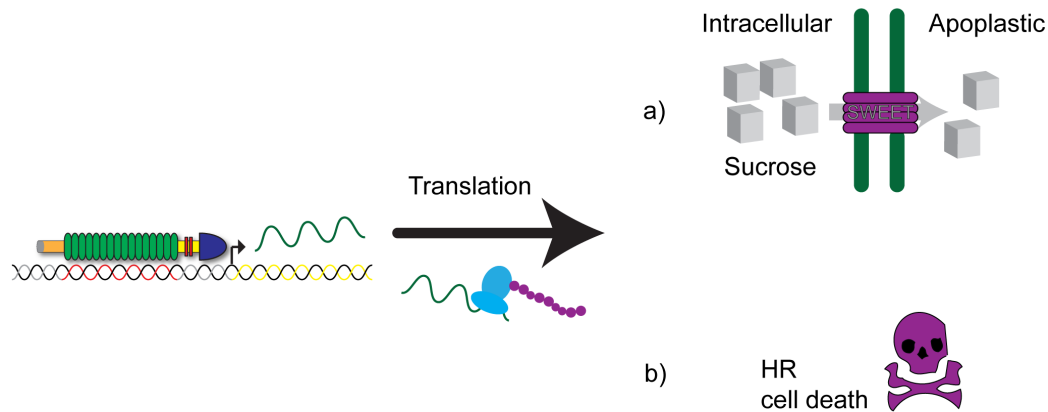


Figure 4. Possible outcomes of transcriptional activation of a coding sequence by a TAL-like effector. To the left binding and transcription are illustrated, with mRNA shown in green. Upon translation by the ribosome (light blue) into peptide chains (purple), the resulting proteins can take different disease relevant functions. a) Example of the assumed function of TALE-mediated SWEET expression, with an increase in apoplastic sugar content being beneficial for the pathogen. b) Translation into an executor R protein (skull and bones) leads to the induction of a hypersensitive response (HR), restricting pathogen growth.

1.1.2.3.3 *TALEs as virulence factors*

To date a number of TALE activated genes have been characterized that lead to a increased bacterial proliferation in the diseased tissue. These include among others, sugar transporters of the SWEET/Mtn3 family and transcription factors (Kay et al. 2007; Verdier et al. 2012; Pereira et al. 2014). Sugar transporters of the SWEET family mediate sugar efflux from the cell (Chen 2014). TALE mediated up regulation of SWEETs is thought to increase sugar content in the apoplast (Figure 4a). As Xanthomonads primarily colonize the apoplastic space of plant tissues, this is thought to provide nutrients, thereby providing a fitness advantage (Chen 2014).

1.1.2.3.4 *TALE mediated resistance*

A single *R* protein, mediating structural recognition of TALEs has been characterized in tomato (*Lycopersicon esculentum*), Bs4 (Schornack et al. 2004). Bs4 is a classical toll/interleukin-1-receptor (TIR) nucleotide binding (NB), leucine rich repeat (LRR) *R* protein, and appears to structurally

recognize a combination of NTR and repeat units of AvrBs4 (Schornack et al. 2004).

However, the more prominent mechanism of TALE based resistance elicitation appears to be based on the transcriptional activation of otherwise silent plant genes (Zhang et al. 2015), whose promoters may be considered as decoys in the larger effector / *R* protein framework. These genes have been termed executor *R* genes, as they directly execute a resistance response upon expression. Executor *R* genes have been identified in rice, conferring resistance to *Xanthomonas oryzae* pv. *oryzae* (Xoo) and *X. oryzae* pv. *oryzicola* (Xoc), and in *Capsicum annuum* and *C. pubescens*, where they confer resistance to *X. euvesicatoria* in a TALE-CRD dependent manner (Zhang et al. 2015). The uniting feature of all executor *R* genes is the absence of transcription in a non-infected plant, and the occurrence of TALE bound EBEs in their promoter. Upon expression most executor *R* genes lead to a hypersensitive resistance response. Zhang and White have grouped executor *R* genes into two groups based on biochemical properties of the produced proteins (Zhang et al. 2015). The larger of the two groups contains Xa10, Xa21 and Xa23 from Rice, as well as Bs4C from pepper (Strauss et al. 2012; Tian et al. 2014; Zhang et al. 2015). This group is characterized by containing (predicted) trans-membrane domains, and they are assumed to form pores in membranes, thereby leading to a disruption of cell homeostasis (Tian et al. 2014; Zhang et al. 2015). The smaller group contains only a single protein, Bs3 from pepper. Bs3 bears close homology to flavin-dependent monooxygenases, as well as proteins of the YUCCA family, involved in auxin biosynthesis (Römer et al. 2009; Zhang et al. 2015). The biochemical properties of Bs3 have so far not been characterized.

Generally, the mode of action of all executor *R* proteins remains largely unknown. This may be related to the generally poor molecular understanding of plant hypersensitive responses, which are mainly characterized phenotypically by the accompanying cell death reaction (Zhang et al. 2015).

Besides elicitors of HR, another example of resistance conferring, TALE dependent, genes is *xa27* from rice. *Xa27* expression is up-regulated by TALE AvrXa27 and GFP fusions of Xa27 localize to the apoplast (Wu et al. 2008). Additionally, expression of Xa27 leads to secondary thickening of the

cell wall in vascular elements (Gu et al. 2005). Xa27 inhibits growth of both, Xoo and Xoc (Hummel et al. 2012).

1.1.2.3.5 *Drivers and mechanisms of TALE diversification in Xanthomonads*

TALEs can be the subject of both, positive and negative selection, depending on their function as virulence factors or elicitors of plant defense, respectively. The CRD of TALEs is highly diverse between different *Xanthomonas* strains, and even within a single *Xanthomonas* genome, multiple TALE encoding genes can be found, which may exhibit completely different RVD sequences (Pérez-Quintero et al. 2015). As the RVD sequence found in the CRD dictates the bound DNA sequence in the host genome, natural selection will act on the CRD during a pathogen host interaction (Yang and Gabriel 1995; Yang et al. 2005).

TALE CRDs may exhibit convergent DNA binding preferences, meaning that TALEs from distinct *Xanthomonas* strains adapted to the same host plant, target the same promoter, despite targeting different sequences in that promoter. This has, for example, been shown for Xoo TALEs converging on the promoter of *OsSWEET14* (Pérez-Quintero et al. 2015; Hutin et al. 2015). However, this selection for convergent host gene activation requires an initial variation, which has to be created by certain processes. So far, different mechanisms have been implicated in creating TALE CRD diversity. In particular both intra- and intergenomic recombinatorial mechanisms have been implicated in creating CRD diversity (Yang and Gabriel 1995; Yang et al. 2005). More recently, Ferreira et al. proposed alterations during the transposition of TALE genes, in particular caused by slipped strand mis-pairing during replication, as a mechanism which creates new CRD variants (Ferreira et al. 2015). Booher and colleagues showed that TALE genes undergo intra-genic recombination, which may lead to the loss of intervening genomic regions. They further showed that TALE repertoires of *Xanthomonads* are dynamic, even if these bacteria are cultured and propagated in laboratory conditions and thought to be the same strain (Booher et al. 2015). This indicates that the TALE repertoire of a strain is dynamic even within a limited time of observation.

1.2 The plant pathogenic *Ralstonia solanacearum* species complex

1.2.1 What is *R. solanacearum*?

The *Ralstonia solanacearum* species complex (Rssc) consists of many related plant pathogenic, gram-negative, β -proteobacteria, which may actually constitute different species, and are therefore referred to as a species complex (Fegan and Prior 2005). Collectively the species complex is able to infect over 200 plant species across 50 botanical families (Genin and Denny 2012). Parts of the species complex are listed as quarantine organisms in the European Union and as bioterrorism agents in the United States (N'guessan et al. 2012), highlighting the devastating impacts of these pathogens on agriculture. The global economic damages caused by brown rot strains on potato (excluding all other hosts) are estimated at \$950 million per year (Milling et al. 2009).

Members of the Rssc have been found on all modern continents, except Antarctica, and are largely limited to tropical regions (Genin and Denny 2012). Historically, the species complex has been divided into biovars, based on the ability to metabolize certain carbohydrates, and races, based on host ranges. As the race-biovar typing scheme is not based on genetic evidence, this typing scheme has been replaced by the one proposed by Fegan and Prior, which divides the species complex into four major phylogenetic divisions, based on sequence similarity of the internally transcribed spacer (ITS) (Fegan and Prior 2005). These divisions are referred to as phylotypes, and the phylotypes reflect the geographic distribution of these strains (Genin and Denny 2012; Wicker et al. 2012). Phylotypes are further divided into sequevars, based on the sequence of the *egl* gene (Wicker et al. 2012). The last common ancestor of the Rssc is presumed to date back to Gondwana, which would explain the geographic distribution and phylogeny of the individual phylotypes as seen today (Wicker et al. 2012).

As accumulating evidence has indicated that two closely related species, blood disease bacterium and *R. syzygii*, form a single genomic species with phylotype IV of the Rssc (Remenant et al. 2011), and given the fact that

phylotypes I and III qualify as one genomic species, the Rssc has recently been taxonomically divided into separated species (Safni et al. 2014; Prior et al. 2016).

Rssc phylotype	Taxonomic species according to Safni et al.
I	<i>R. pseudosolanacearum</i>
II	<i>R. solanacearum</i>
III	<i>R. pseudosolanacearum</i>
IV (pathogenic on solanacea)	<i>R. syzygii</i> subsp. <i>indonesiensis</i>
IV (blood disease bacterium)	<i>R. syzygii</i> subsp. <i>celebensis</i>
IV (<i>R. syzygii</i> , pathogenic on clove)	<i>R. syzygii</i> subsp. <i>syzygii</i>

Table 1. Species classification of Rssc phylotypes

The molecular characterization performed in this work is in-line with the phylotype scheme of the Rssc, and therefore the phylotype scheme will be used throughout this work.

Members of the Rssc generally exhibit a bi-partite genome structure, with two circular chromosomes, the smaller of which is often referred to as the megaplasmid (Genin and Denny 2012). This genome structure is conserved across all members of the Rssc. However, genes are not necessarily in synteny between different strains and Rssc genomes are dynamic (Remenant et al. 2011). Generally, it appears that most house-keeping genes are located on the larger chromosome, while strain specific genes, including effectors and pathogenicity determinants, tend to be more abundant on the megaplasmid (Genin and Denny 2012).

1.2.2 *Ralstonia solanacearum* life cycle

Most members of the Rssc are soil-borne, but some, such as blood disease bacterium strains and *R. syzygii* are insect transmitted (Remenant et al. 2011). The soil-borne character of this disease makes it hard to control infection, as infectious bacteria are retained in soil and water for a long time (Genin and Denny 2012). This renders commonly used control measures,

such as crop rotation, ineffective (Jyothi and Santhosha 2012). Soil-borne infection starts by invasion of the root vasculature, and subsequent spread of bacteria to the plant hypocotyl (Genin and Denny 2012). Upon successful colonization of the hypocotyl, bacteria spread throughout the plant xylem vessels, leading to inhibition of nutrient transport (sometimes referred to as xylem clogging) (Guidot et al. 2014). Insect vectored infection skips many of the early steps of soil-borne infection, as the bacteria are transmitted directly into the xylem. Xylem colonization leads to wilting of the whole plant, hence the name bacterial wilt for diseases caused by the Rssc on solanaceous plants. Diseases caused by members of the Rssc have received different names, depending on the affected host plant and country (Genin and Denny 2012).

1.2.3 Effectors of the Rssc

Collectively, at least 94 groups of orthologous effectors can be found across the Rssc (Peeters, Carrère, et al. 2013). Historically, different identifiers have been used for Rssc effectors, including hrpB regulated gene (brg), hrpB dependent expression (hpx), avirulence (avr), pseudomonas outer protein (pop) and Ralstonia injected protein (Rip) (Peeters, Carrère, et al. 2013). Recently, Peeters and colleagues have proposed to unify the nomenclature of Rssc effectors, by prefixing the name of every gene which produces an effector with Rip, followed by a alphabetic gene identifier (XY) and a numeric paralogue identifier (#) and appended with the name of the strain which contains this particular gene in subscript, resulting in RipXY#_{Strain} (Peeters, Carrère, et al. 2013).

Several Rips have been characterized; with RipP2 (popP2) being the best characterized one so far. RipP2 is an acetyltransferase, and is specifically recognized by the RRS1-R allele in *A. thaliana*, but not by the allelic RRS1-S (Deslandes et al. 1998; Peeters, Carrère, et al. 2013; Saucet et al. 2015). Recognition of RipP2 by RRS1-R leads to the elicitation of ETI, presumably mediated by the WRKY domain of RRS1-R, rendering the plant more resistant to infection by RipP2 delivering Rssc strains (Deslandes et al. 1998; Van der Linden et al. 2013). RRS1-R forms a complex with the RPS4 R-protein, and

depending on the allelic variants of both this complex is also able to confer resistance to the *P. syringae* pv. *tomato* effector AvrRps4 (Saucet et al. 2015). The GALA effectors (ripG family) of Rssc strains are also well characterized, and belong to the class of coiled-coil (CC) LRR proteins, bearing structural resemblance to the aforementioned plant LRRs. GALA effectors have been proposed to be the consequence of horizontal gene transfer from plants (Kajava et al. 2008). GALA proteins further contain an F-box domain, which enables them to interact with the eukaryotic SCF-type E3 ubiquitin-ligase complex, by interacting with SKP1 (Angot et al. 2006; Kajava et al. 2008). The overall family of GALA Rips is conserved across the Rssc, but diversity has been reported. GALAs thereby are part of the core effectome of the Rssc, and have also been indicated to be involved in determining host range (Remigi et al. 2011).

On average, a Rssc strain carries around 70 effectors (Genin and Denny 2012), of which around 50 are conserved among all phylotypes. Within one phylotype, the number of conserved effectors increases, to about 60 when comparing phylotype II strains to each other. However, the number and type of effectors per strain has not been successfully linked to host range (Genin and Denny 2012). This may indicate that either subtle changes in effector sequence impact on host specificity in a so far unrecognized manner, or that other secreted factors take an important role in the host range determination.

1.3 Goals of this work

Among the large number of effectors found within the Rssc, are homologues of TALEs from *Xanthomonas*, which are the topic of this work. An initial molecular characterization of RipTALs (Rip; Transcription Activator Like) has been carried out on RipTALs found in phylotype I of the Rssc, revealing that their DNA binding behavior can be predicted with a code similar to that of TALEs with the exception of an NTR encoded G0 requirement, different from the NTR encoded T0 requirement known from TALEs (de Lange et al. 2013). Additionally it has been shown that RipTALs localize to the nucleus when expressed *in planta*, and that this localization depends on nuclear localization sequences found in the CTR (de Lange et al. 2013; Li et al. 2013).

This work set out to expand the knowledge on RipTALs in multiple directions. A description of RipTALs found across all phlotypes was carried out. These RipTALs were then analyzed regarding their ability to activate reporter constructs in a sequence specific manner, and the overlap in activated sequences was quantified. These studies indicated functional convergence, depending on strain host range. A detailed analysis of the relationships of repeats found in a RipTAL CRD uncovered their adaptive potential, a consequence of their heightened evolvability, and these results are discussed in the light of TALEs and disease contribution of TALE-likes.

Further, natural RipTAL recognition in *A. thaliana* across 80 ecotypes was analyzed using heterologous expression systems and validated using Rssc strains. To validate results, an R based statistical analysis script for Rssc infections has been developed, tailored towards the unique characteristics of Rssc infections.

Finally, synthetic, RipTAL receptive, HR eliciting gene constructs were designed based on the knowledge gained from the analysis of RipTALs across all phlotypes and used to generate transgenic lines in *A. thaliana* and *Solanum lycopersicum*.

2 Results

Throughout this and the following sections, DNA sequences encoding protein units, such as NTR, CRD, CTR or repeats, are italicized.

2.1 TALE-likes of *R. solanacearum*

2.1.1 Goals of this project

The analysis of abundance and diversity of RipTALs within the Rssc constitutes a first step in understanding their biological role in this bacterial species complex. Information on abundance can be used to understand more about the history of RipTALs within the species complex and clear up ongoing discussion on the phylogenetic origin of these effectors (Salanoubat et al. 2002; Fall et al. 2007; Heuer et al. 2007; Peeters, Carrère, et al. 2013).

Knowledge on the diversity of RipTALs will facilitate the generation of plants that contain RipTAL responsive *R* genes. Additionally, a detailed description of RipTAL DNA binding domains, and the diversity found between and within phylotypes, combined with intimate knowledge on the strains analyzed, will facilitate future studies into their role in disease.

Following up the description of RipTALs, these were functionally characterized on the molecular level, to understand their function in plant cells. This will enable future research endeavors relating to their role in specific host plants, and could constitute a first step in the generation of Rssc resistant plants.

Additionally, this project set out to understand the evolutionary forces shaping RipTALs and TALEs, with a particular interest in understanding more about the highly diverse repeat arrays of TALEs. This line of research may provide means for researches working on TALEs or RipTALs in an agricultural context (e.g. generation of disease resistant crops) to anticipate durability of such efforts.

2.1.2 Strains were selected to cover much of the Rssc diversity

Strains from across the species complex were analyzed regarding their *RipTAL* repertoire. The set of strains analyzed is given in Table 2. These

strains were largely acquired from Dr. P. Prior, who handles one of the largest Rssc strain collections. Due to the large plasticity found in the Rssc (Guidot et al. 2007; Peeters, Guidot, et al. 2013; Peeters, Carrère, et al. 2013), different rationales influenced the strain selection. For strains belonging to phylotype I, a limited, but representative collection of 10 strains found on Mayotte, a small island in the Indian Ocean, was included. T. Chesneau and P. Prior have previously characterized the diversity of strains found on Mayotte (manuscript in preparation) and despite the low number of strains, these cover the full genetic diversity of strains found in this small Island population. One reason for focusing on this unusual, isolated population was that RipTALs from phylotype I strains from Asia, and in particular China, had previously been studied and described (Heuer et al. 2007; de Lange et al. 2013). Besides the Mayotte strains, three strains, which were originally typed as phylotype IV turned out to be phylotype I strains and were therefore included in the phylotype I set.

Phylotype II of the Rssc has received most attention previously, and the genomes of a number of strains were sequenced at the time of strain selection. From the available genomes it appeared like RipTALs were restricted to MolK2 (Li et al. 2013; Peeters, Guidot, et al. 2013), a strain causing Moko disease of banana, belonging to phylotype IIB (Ailloud et al. 2015). The strains belonging to phylotype II analyzed contained the sequenced *R. solanacearum* type-strain K60, the sequenced strain MolK2 and three previously uncharacterized strains (Table 2).

Rssc phylotype III, which is geographically restricted to Africa, is the least studied phylotype of the Rssc. Prior to this work, no RipTAL had been discovered within this phylotype. To explore the diversity of RipTALs across the species complex, a total of 23 strains spanning much of the diversity of phylotype III were acquired (Table 2).

Finally, for strains belonging to phylotype IV, the strain selection was influenced by an interest in host specialization. Phylotype IV of the Rssc contains a species of bacteria, which cause blood disease of banana (Remenant et al. 2011). This subspecies is unusual in comparison to other members of the Rssc, because it has undergone large genomic rearrangements and simultaneous genome reduction (Remenant et al. 2011)

and is unable to infect solanaceous plants (Ailloud et al. 2015). Interestingly, the published genome sequence of blood disease bacterium strain R229 indicates presence of a RipTAL CDS (Peeters, Carrère, et al. 2013). Of the 14 analyzed phylotype IV strains, four belong to the *R. syzygii* species and are exclusively able to infect clove trees, seven are classified as blood disease bacterium, and three strains belong to phylotype IV of the Rssc not further sub-classified. Among the not further classified phylotype IV strains is Ps107, for which the genome sequence is available and thus is known to contain a RipTAL (Li et al. 2013; Peeters, Carrère, et al. 2013).

In total the strain collection analyzed contained 53 strains, given in Table 2.

Phylotype	Sequevar	Strain-ID	Geographic Origin	Isolated From
I	31	RUN2108	Mayotte	Tomato
I	31	RUN2120	Mayotte	Tomato
I	46	RUN2127	Mayotte	C. annuum
I	15	RUN2140	Mayotte	Aubergine
I	15	RUN2143	Mayotte	C. annuum
I	46	RUN2146	Mayotte	Tomato
I	31	RUN2165	Mayotte	S. nigrum
I	31	RUN2170	Mayotte	Aubergine
I	18	RUN2083	Mayotte	C. frutescens
I	18	RUN2150	Mayotte	Tomato
I	ND	RUN1359	Indonesia	Clove
I	ND	RUN064	Indonesia	Clove
IIA	7	K60	Wake Co, N.C.	Tomato
IIB	4	UW160	Isla Padre, Peru	Plantain
IIB	3	Molk2	Philippines	Musa sp.
IIB	4	UW163	Nauta, Peru	Musa sp.
IIB	1	UW551	WI (originally Kenya)	geranium
III	43	RUN369	Guinea	Potato
III	22	RUN075	Zimbabwe	Potato
III	29	RUN133	Cameroon	Tomato
III	ND	RUN362	Guinea	Potato
III	23	RUN39	Burkina Fasi	Eggplant
III	29	RUN53	Cameroon	Morella
III	19	RUN60	Reunion	Pelargonium
III	20	RUN76	Zimbabwe	Nicotiana tabaccum
III	29	RUN145	Cameroon	Huckleberry

III	20	RUN146	Cameroon	Tomato
III	49	RUN166	Cameroon	Huckleberry
III	29	RUN174	Cameroon	Pepper
III	19	RUN331	Madagascar	Potato
III	43	RUN362	Guinea	Potato
III	42	RUN368	Guinea	Potato
III	22	RUN478	Zimbabwe	Solanum panduraforme
III	21	RUN479	Angola	Potato
III	20	RUN480	Zimbabwe	Symphytum sp
III	ND	RUN2340	Madagascar	Potato
III	ND	RUN2532	Madagascar	Potato
III	ND	RUN2594	Madagascar	Potato
III	ND	RUN2717	Madagascar	Potato
III	43	RUN376	Guinea	Potato
IV	10	RUN62	Indonesia	Banana
IV	11	RUN1327	Indonesia	Clove
IV	9	RUN88	Indonesia	Clove
IV	9	RUN89	Indonesia	Clove
IV	9	RUN1357	Indonesia	Clove
IV	9	RUN089	Indonesia	Clove
IV	10	RUN1314	Indonesia	Musa sp.
IV	10	RUN1347	Indonesia	Musa sp.
IV	10	RUN1348	Indonesia	Musa sp.
IV	10	RUN1350	Indonesia	Musa sp.
IV	10	RUN1351	Indonesia	Musa sp.
IV	10	RUN1349	Indonesia	Musa sp.
IV	11	RUN14	Australia	Tomato
IV	10	RUN083	Indonesia	Tomato

Table 2. Overview of the strains investigated regarding RipTALs. ND = not determined

2.1.3 RipTALs can be found across the Rssc

To gain a first insight into the abundance of RipTALs in the strain collection, a PCR on genomic DNA of these strains was performed. The PCR was carried out using a set of primers (#48 & #49, Table 13), which bind a sequence stretch in the *NTR* and *CTR*, close to the *CRD*. The priming region was picked based on aligned DNA sequences of *ripTALs* found in public genomes and a conserved stretch of 30 bp on up- and downstream of the *CRD* was identified. Using these primers, *ripTAL* presence in 10 of 13 phylotype I strains was demonstrated. Within the five phylotype II strains, only Molk2 contained a *ripTAL*, which is in-line with published genome sequences. Out of the 23 phylotype III strains, only a single strain, RUN369, contained a *ripTAL*. Among

the phylotype IV strains, all 8 BDB strains contained a *ripTAL*, but none of the *R. syzygii* strains did. Out of the three remaining Rssc phylotype IV strains, two contained a *ripTAL*. An overview of *ripTAL* abundance in different phlotypes is shown in Figure 5.

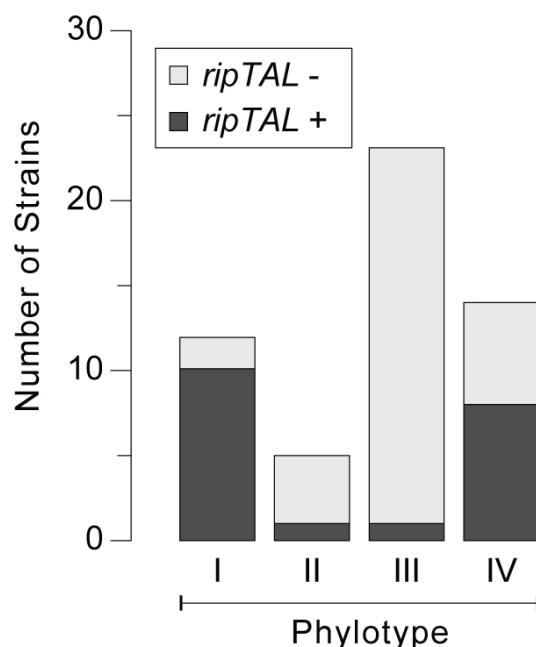


Figure 5. *ripTAL* abundance across strains from different phlotypes.

2.1.4 RipTAL classification based on sequence characteristics

2.1.4.1 RipTAL classification and nomenclature

After having gained an overview of strains, which do or do not contain a *ripTAL*, the PCR products were sequenced. As the PCR products of the initial analysis correspond to the *CRD*, these sequences can already be used to predict possible target sequences, based on the established RipTAL code, which is very similar to the TALE code (de Lange et al. 2013; Miller et al. 2015). In the case of uncharacterized RipTAL RVDs, the base preferences were assumed to be analogous to that of TALE RVDs (Miller et al. 2015). The *CRD* sequences already hinted at redundancy in the RipTALs found in the collection, i.e. multiple strains from the same phylotype contained identical DNA binding domains (Figure 7). The full coding sequences (CDS) of RipTALs, from at least one strain per binding domain was cloned. To clone

these, primers deduced from published genomes containing *ripTALs*, of strains belonging to phylotype I, II and IV were used. Since no published genome of a phylotype III strain contains a *ripTAL*, the sequences up- and downstream of the *CRD* were elucidated by genome walking (Leoni et al. 2011). This then allowed for the design of primers to amplify the full *ripTAL* from RUN369.

Since RipTALs, like TALEs, are modular proteins, the sequences of the NTR, CRD and CTR were analyzed separately. Sequences of all NTRs were compared against all, and the same was done for the CTRs (Figure 6). The similarities of RipTALs from the same class were initially compared. The NTR and CTR of RipTALI-1 and RipTALI-8 as well as the similarities between RipTALIV-1 and RipTALIV-2 are given in Figure 6a, showing that RipTALs of the same class show more than 98% similarity in both regions.

More generally, the sequence similarities observed for the NTR and CTR correspond well to the overall strain phylogeny. In line with these observations, all RipTALs are more similar to any other RipTAL than to TALE representative AvrBs3 (Figure 6b). Based on these observations, RipTALs were classified in two ways. First a roman numeral denotes the phylotype these RipTALs are derived from. For example RipTALs from phylotype I strains are classified as RipTALI. Following the phylotype designation (also referred to as RipTAL class) and separated by a dash, a binding domain identifier is appended, which is used to unambiguously identify the RVD composition (order and number of RVDs found in the CRD). The binding domain identifier is an Arabic numeral, and numbering is only reflecting the chronological order of the identification of these CRDs, but carries no further information. If necessary, this can be followed by a strain identifier in subscript, to precisely refer to a *ripTAL* from a specific strain, which may differ in, for example, silent SNPs. For example the first known *RipTAL* from phylotype I strain GMI1000, which has the genomic identifier Rsc1815 and the gene name *brg11*, is called RipTALI-1_{GMI1000}.

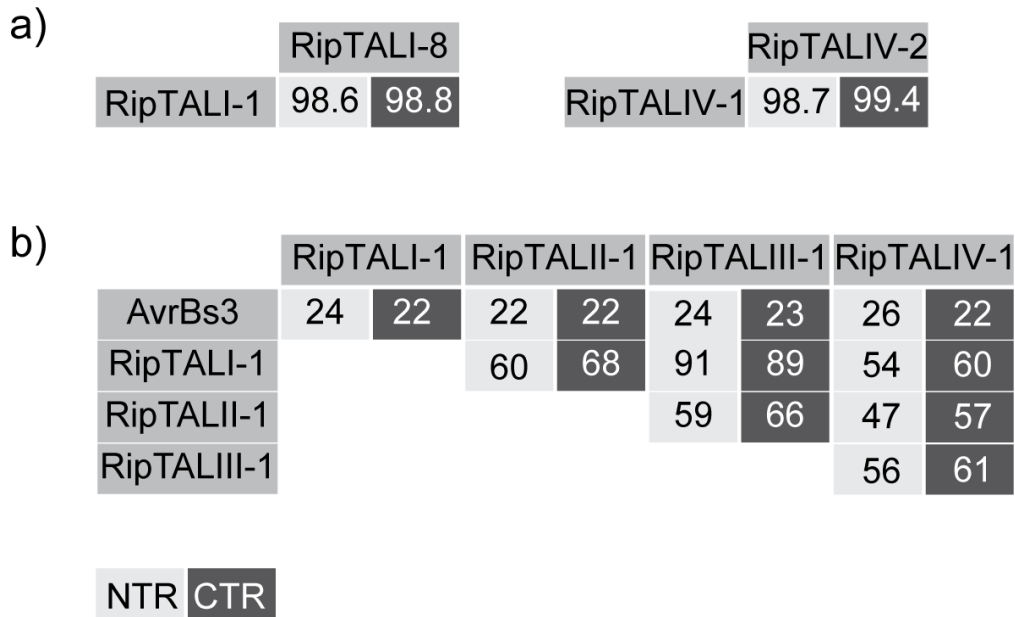


Figure 6. Overview of NTR and CTR similarities. a) Comparison of the NTR (black text) and CTR (light grey text) within class I and class IV RipTALs. b) NTR and CTR comparisons across different RipTAL classes, and to TALE AvrBs3. Color code is given at the bottom.

2.1.4.2 RipTAL CRD diversity is limited

The picture that emerged from the sequencing of RipTAL CRDs was different from the one that is observed for *Xanthomonas* TALEs. *Xanthomonas* TALEs are highly variable in the sequence of the CRD, and generally the predicted EBEs differ quite drastically even between TALEs from closely related strains (Pérez-Quintero et al. 2015). RipTALs display very limited diversity in the CRD, defined by the RVD composition (Figure 7). Many Rssc strains contain identical binding domains, and even between different CRD variants differences in RVD composition are mostly subtle, often differing mainly by the number of copies of a given repeat in the array. As can be seen in Figure 7, RipTALI-1 and RipTALI-8 differ by only one RVD polymorphism. RipTALI-1 and RipTALI-9 differ by an insertion/deletion polymorphism of a single HD repeat as displayed in Figure 7. RipTALI-8 and RipTALIII-1, although originating from different phylotypes, have an identical predicted EBE (Figure 10b). RipTALIV-1 and RipTALIV-2 differ in the number of NN repeats, but look overall similar (Figure 7). The only RipTAL that appeared to be unique in its RVD composition was RipTALII-1 (Figure 7).

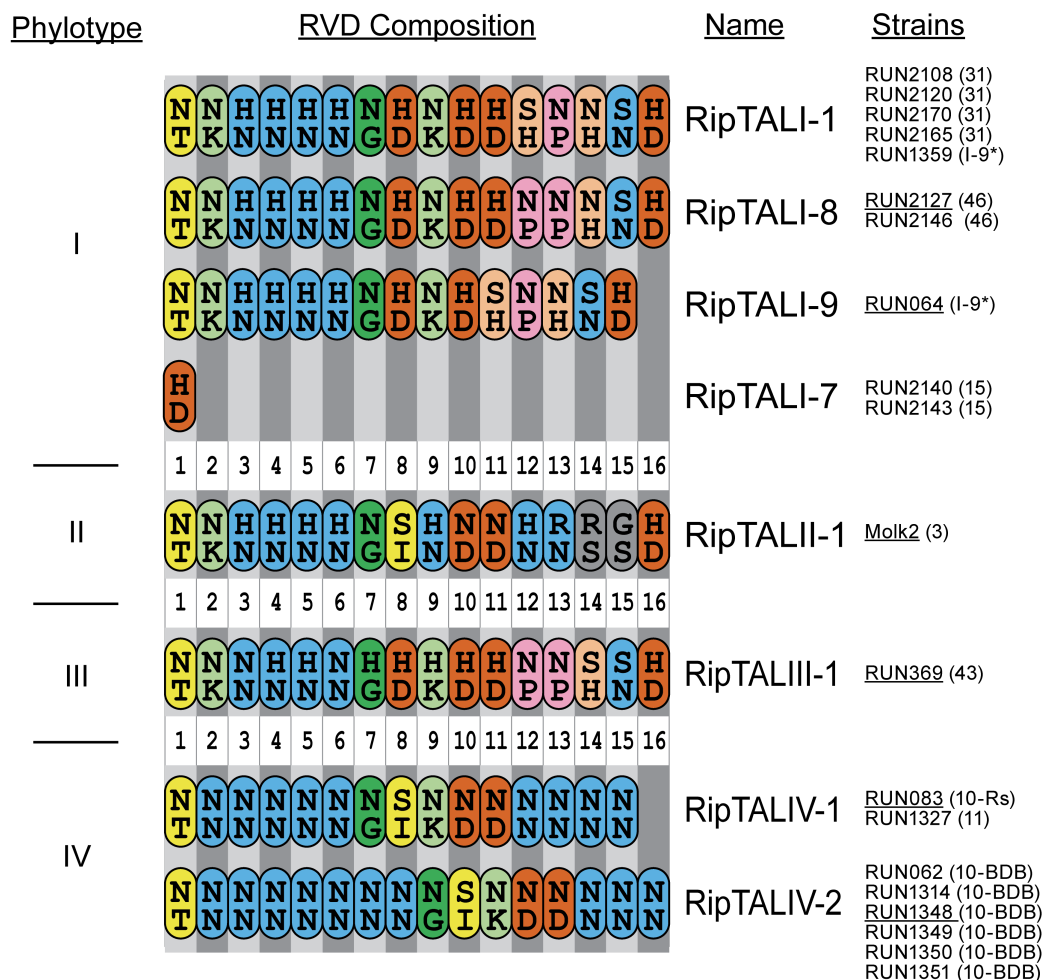


Figure 7. CRD diversity of newly identified RipTALs, grouped by class. Underlined strains indicate RipTALs cloned for functional assays. Numbers in brackets indicate the strain sequevar.

However, the conclusions that can be made on sequence analysis alone are limited, and therefore a molecular characterization was carried out *in planta*.

2.1.5 Functional characterization of RipTALs

Since RipTALI-7 was previously analyzed and was shown to retain localization, but not transcriptional activation, it was not included in the functional characterization (de Lange et al. 2013).

2.1.5.1 RipTALs localize to the nucleus

To get a first idea of the *in planta* function of RipTALs from all classes, their subcellular localization in Arabidopsis protoplasts was analyzed. Using YFP tagged RipTALs (in gateway binary vector pGWB641 (Nakamura et al. 2010)) and a constitutively expressed, nuclear localized mCherry fluorophore (in vector *pCF205*), both transfected into protoplasts under constitutive promoters, microscopy was performed to assess if RipTALs localize to the nucleus, as required for a transcription factor. Indeed, microscopy showed that all RipTALs can be expressed *in planta* and localize to the nucleus (Figure 8). However it appeared that RipTALII-1 was expressed poorly in comparison to the other RipTALs (Figure 8).

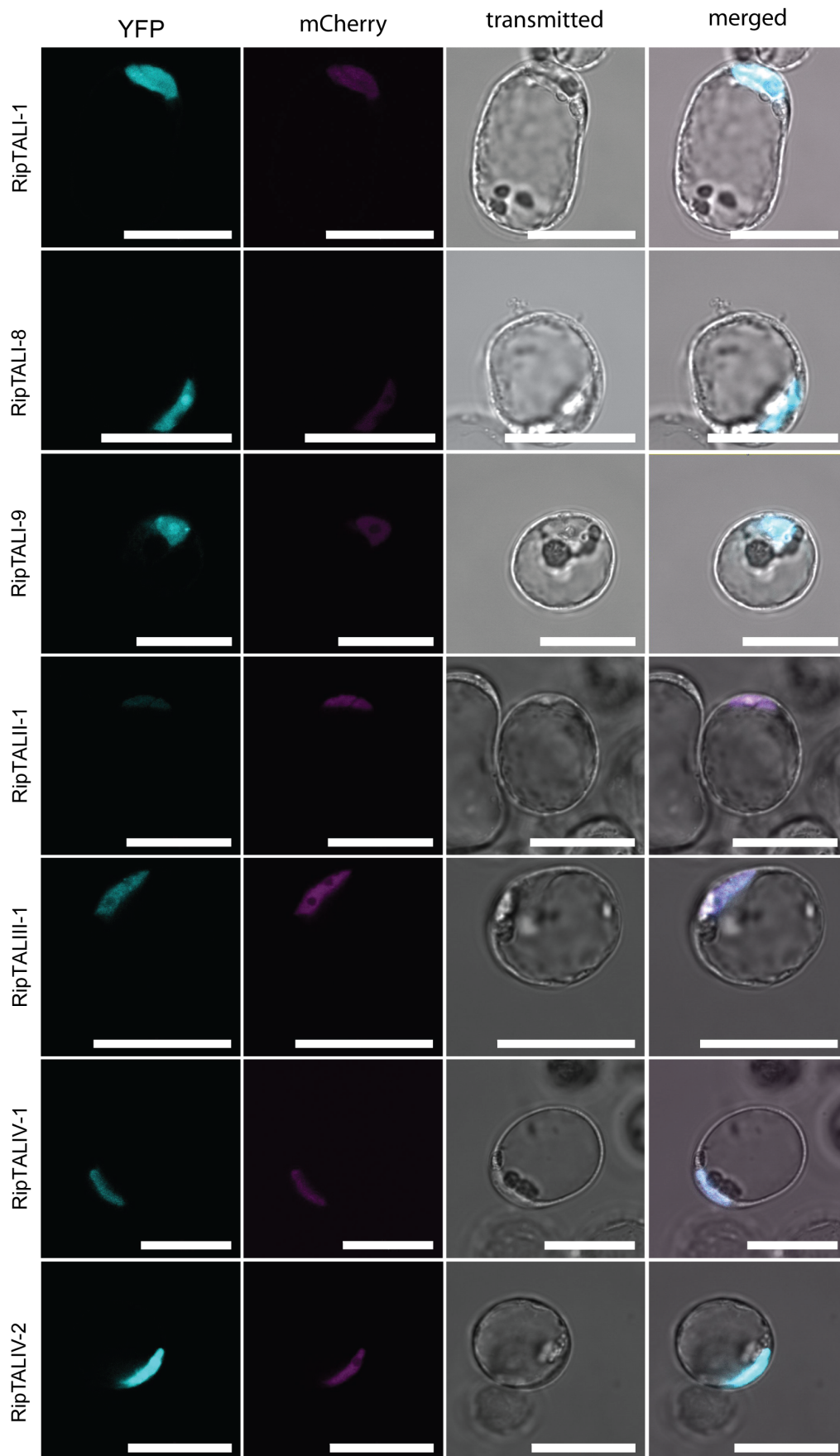


Figure 8. Microscopy of YFP tagged RipTALs, with mCherry-NLS as a nuclear marker in *A. thaliana* protoplasts. Scalebars represent 50 μ m.

The comparatively poor expression of RipTALII-1 was validated by flow cytometry (Figure 9).

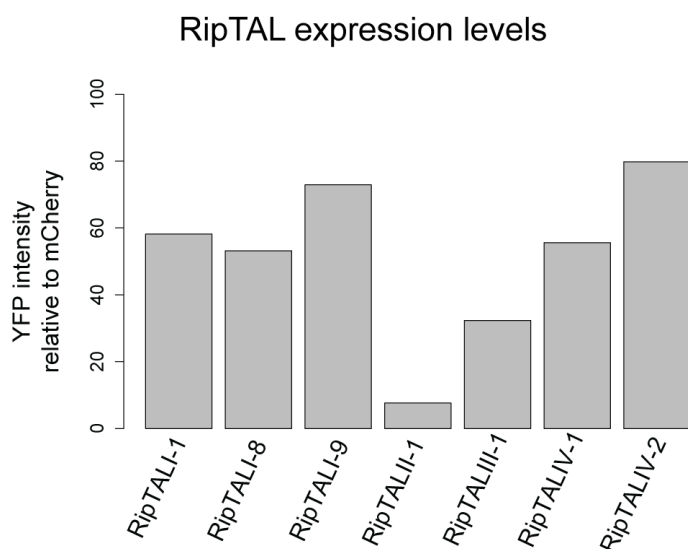


Figure 9. Expression levels of YFP tagged RipTALs in *A. thaliana* protoplasts. Quantification was performed by flow cytometry and is shown as a relative value to co-transfected mCherry-NLS.

2.1.5.2 RipTALs are sequence specific transcriptional activators

2.1.5.2.1 *RipTALs encode a Guanine requirement in the NTR extending the similarity between EBEs*

One of the key characteristics of class I RipTALs, shown in earlier work (de Lange et al. 2013), is the requirement for a guanine base preceding the RVD-defined EBE. This base is known as the 0-base (Doyle et al. 2013; Lamb et al. 2013) in the context of TALE-likes. Since the NTR, which confers this requirement, is diverse between RipTAL classes (Figure 6), all RipTALs were tested against their own predicted EBE, with all four possible 0-bases. Experiments were performed using *A. thaliana* root culture protoplasts, transfected with a RipTAL expression construct in vector pGWB641 (35S promoter driven, C-terminal YFP-tag (Nakamura et al. 2010)), a Bs3 promoter derivative containing a RipTAL EBE instead of the AvrBs3 EBE (EBE_AvrBs3) upstream of an *uidA* reporter gene (encodes a β -Glucuronidase, GUS) in pENTR, and a plasmid containing a *luciferase* gene

under the control of the constitutive ubiquitin promoter. GUS and luciferase activity were quantified using a plate reader. Subsequently, GUS activity was normalized to luciferase (to control for transfection efficacy, raw data given in Table S1) and then compared to the appropriate luciferase normalized background control (identical reporter co-transfected with pGWB641:AvrBs3, negative control, data given in Table S2). It was found that RipTALs of all classes activated their EBE with a Guanine 0-base most strongly (Figure 10a). This extends the number of conserved DNA bases found between all EBEs with the exception of EBE_IV-2 to position 0, to a stretch of 8 bases in total (Figure 10b).

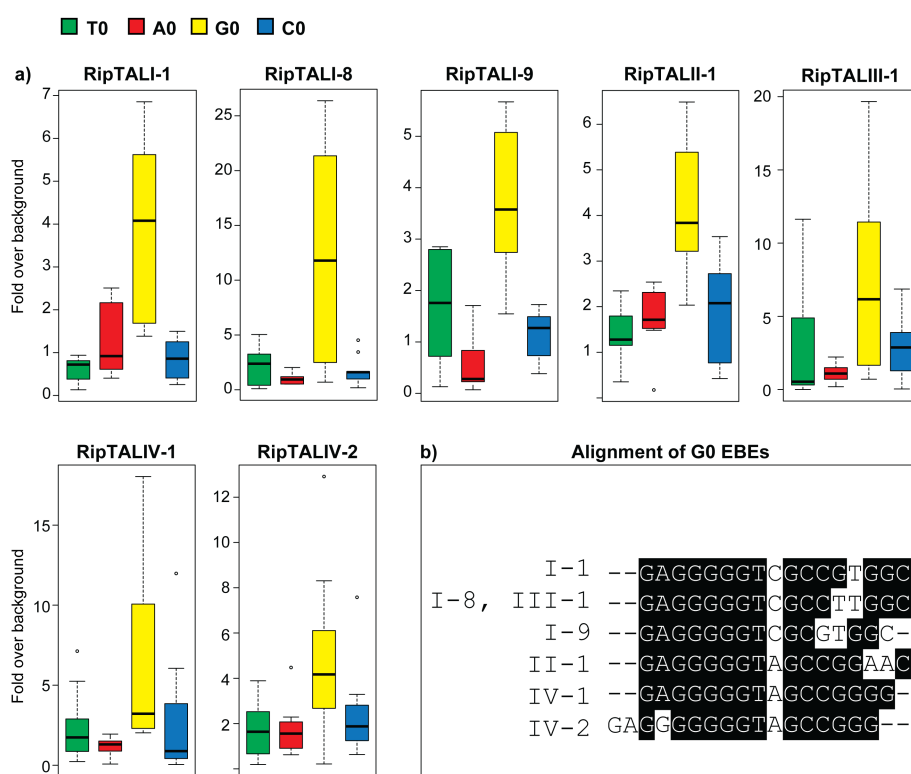


Figure 10. All RipTALs encode a G0-preference in the NTR. a) All RipTALs were tested against their predicted EBE, with either T, A, G or C at the 0 position. b) Alignment of G0-EBEs of all RipTALs, colored with boxshade.

2.1.5.2.2 *RipTAL cross activation profiles and strain host range correlate*

As described earlier, the diversity of binding domains found among RipTALs is limited (Figure 7). To understand if these similarities lead to a functional

overlap in bound and activated promoter sequences, reporter assays using all G0-EBE reporters in combination with all RipTALs were performed. All G0-EBE reporters were co-transfected with all individual RipTALs into *A. thaliana* protoplasts, and reporter activation was quantified (Figure 11).

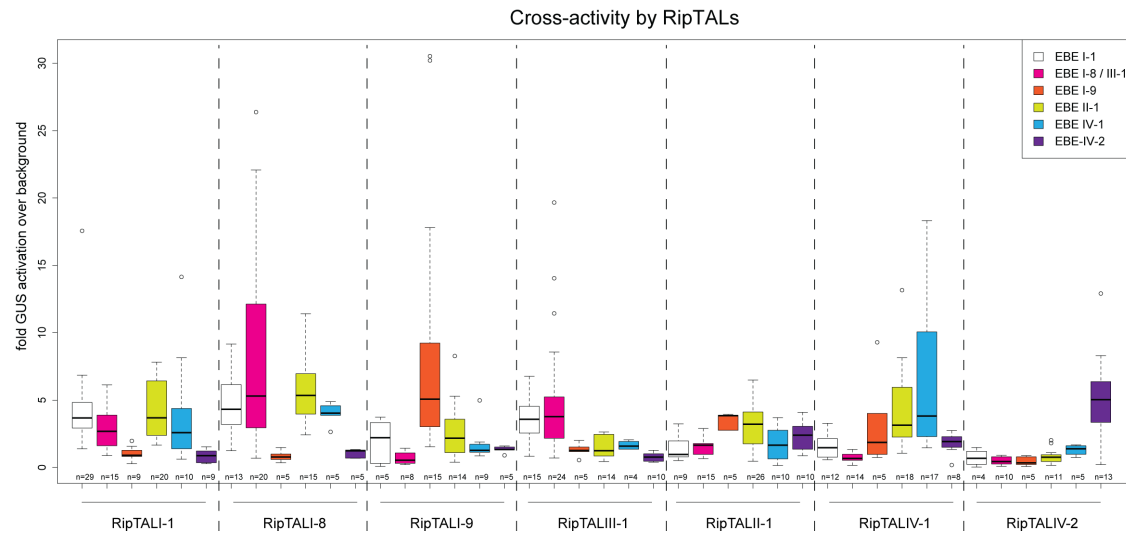


Figure 11. Boxplot of RipTAL cross-activity on predicted EBEs of other RipTALs. All RipTALs were tested against all RipTAL EBEs. Boxplots ordered by RipTAL, and the legend in the top-right indicates the EBE tested.

From Figure 11 it becomes evident that RipTALs display overlap in the activation of reporter constructs containing the EBE of other RipTALs. For example, RipTALI-1 and RipTALI-8 are able to activate the EBE of many other RipTALs, while RipTALIV-2 appears to be highly specific for its own EBE.

As detailed strain host range information was available for each RipTAL bearing strain (Table 2), the observed overlaps in promoter activation were analyzed in the context of strain host ranges. Two groups of RipTALs could be defined, based on overlap in reporter activation and strain host-range. One group constitutes of RipTALI-1, RipTALI-8 and RipTALIII-1, all isolated from strains that are able to infect a broad range of solanaceous hosts (Figure 12). The second group consists of RipTALII-1 and RipTALIV-1 (Figure 12), which were isolated from strains pathogenic on banana plants (Table 2).

Effector \ EBE	I-1	I-8 III-1	I-9	II-1	IV-1	IV-2	Lifestyle Group (number of ripTAL bearing strains in this group)
RipTALI-1	<u>3.7</u>	2.7	0.9	3.7	2.6	0.9	Broad host range on solanaceous plants (7 strains)
RipTALI-8	4.3	<u>5.3</u>	0.8	5.4	4	1.2	
RipTALIII-1	3.6	<u>3.8</u>	1.3	1.2	1.6	0.8	
RipTALII-1	1	1.7	3.8	<u>3.2</u>	1.7	2.4	Restricted to banana (7 strains)
RipTALIV-2	0.7	0.4	0.3	0.8	1.4	<u>5</u>	
RipTALI-9	2.2	0.5	<u>5.1</u>	2.2	1.3	1.3	Undefined (3 strains)
RipTALIV-1	1.5	0.7	1.9	3.1	<u>3.8</u>	1.9	

Figure 12. Overlapping EBE activation by RipTALs, correlated to strain lifestyle. Numbers in cells give median fold GUS readout over background, for the given RipTAL / EBE combination. Blue background indicates p-value < 0.01 (Wilcoxon test, null hypothesis: median =< 1 (no change)) for the given RipTAL / EBE combination. Underlined values indicate perfectly matching (predicted) RipTAL-EBE combinations.

2.1.5.2.3 Repeat 8 of RipTAL classes I and III shows relaxed base specificity in its native context

The overlap in EBE activation indicates that RipTALs are flexible in their bound and activated DNA sequences. One major polymorphism between class I/III and class II/IV EBEs is a prominent Cytosine / Adenine exchange in the center of the predicted EBE (Figure 10b). Yet, RipTALI-1 and RipTALI-8 are able to activate the EBE of RipTALII-1 (EBE_II-1) and to a lesser extent EBE_IV-1 (Figure 12). The repeat in RipTALI-1 and RipTALI-8, which interacts with the Adenine at position 8 in EBE_II-1 contains HD at the RVD position. To investigate, if those CRDs are able to tolerate an Adenine at position 8, an EBE was created that is identical to EBE_I-1, with the exception of position 8, which was exchanged to Adenine (EBE_I-18A). RipTALI-1, RipTALI-8 and RipTALIII-1 were tested against EBE_I-1A8 and EBE_I-1 (Figure 13).

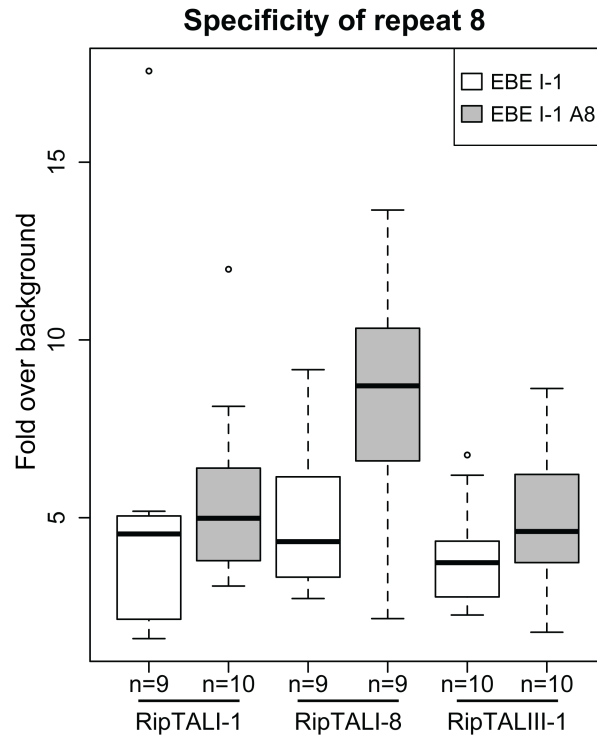


Figure 13. Investigation of the specificity of HD repeat 8 in RipTALI-1, I-8 and III-1. All RipTALs were tested against the predicted EBE_I-1 and against the mutated EBE_I-1A8. Data are shown as fold reporter activation over background levels.

Assessment of the specificity of class I and III RipTAL repeat 8, showed that both, the original reporter and the reporter where base 8 of the EBE was changed to Adenine, are activated to similar levels, with slightly stronger induction of EBE_I-1 A8 by RipTALI-8, compared to the induction of the original reporter construct (Figure 13). This is in clear contrast to previous work (de Lange et al. 2013), where this repeat was tested in a trimer against all possible base homo-trimers. In the trimeric context repeat 8 of RipTALI-1 was highly specific for C (de Lange et al. 2013).

2.1.5.2.4 *RipTALs might be involved in host range adaptation*

The functional characterizations of RipTALs (Figure 8, Figure 9, Figure 10, Figure 12, Figure 13) performed point towards a role of RipTALs in host-range adaptation. In particular, the overlap in activated sequences found for RipTALII-1 and RipTALIV-2 (Figure 12), could be an indication on how these

strains were able to acquire banana as a new host. It seems probable that these RipTALs converged towards targeting the same banana S gene. It is worth noting that strains carrying RipTALIV-1 are able to infect tomato, whereas those carrying RipTALIV-2 exclusively infect banana plants (Ailloud et al. 2015). Yet, on a genomic level these strains form one single species (Remenant et al. 2011). Strains from phylotype II, containing RipTALII-1 are able to infect both, banana and tomato plants (Ailloud et al. 2015).

As the results presented in this section provide hints on how RipTALs could be involved in host-adaptation, a special interest was placed on understanding their evolutionary potential and providing a glimpse at the mechanisms driving RipTAL evolution.

2.1.6 Characterizing evolutionary forces acting on TALE-like effectors

One key question that remains after the molecular characterization of RipTALs, is how TALE-like effectors behave in evolutionary terms. Of particular interest in this context is the DNA binding domain. One can easily envision how injected transcription factors contribute to host specificity, as they are able to functionally discriminate different host genotypes on the nucleotide level. Additionally, due to the plethora of knowledge available on the molecular action and resulting pathogenicity function of TALE-like CRDs, in particular of TALEs, such studies can be related directly to protein function (via sequence specific DNA binding), and thereby indirectly to disease (via the activation of disease related genes in a host-genotype dependent manner). Yet, the highly repetitive character of the TALE *CRD* makes bioinformatic phylogenetic approaches highly challenging (Booher et al. 2015; Pérez-Quintero et al. 2015), as the sequence information content of TALE *repeats*, which is required to reconstruct *repeat* phylogenies, is very low. The low information content is due the restriction of polymorphic residues to mainly two of the 34 codons (Boch and Bonas 2010) within one *CRD*. This is different in RipTAL *repeat* arrays that generally exhibit it a higher number of polymorphic residues. Additionally, the newly identified RipTALs presented in the previous section, come from bacterial strains with known phylogenies. Thereby bioinformatic, sequence-based studies of the *CRD* of RipTALs and

the individual *repeat* units that make the *CRD* combined with known strain phylogeny, could provide a complementary approach to the available knowledge on TALE evolution.

2.1.6.1 Harnessing polymorphisms found in RipTAL repeats to study evolution of TALE-like DNA binding domains

The following experiments were conducted using nucleotide sequences of *repeats*. Each *repeat* found within a *CRD* was extracted, aligned to all other *repeats* from the same *CRD*, and the alignment was ordered by the position of the *repeat* in the *CRD*. From these alignments pairwise identities were calculated, and the resulting matrix of pairwise identities was colored based on the value found in each cell of the table. An initial comparison was performed for TALEs AvrBs3, AvrBs4 and AvrXa27 (not shown). It was found that *repeat* identities are generally very high (92-100%, Figure 14). Additionally it was observed that TALE *repeats*, which contain the same amino acids at the RVD position, are more similar to each other. This again highlights the limited information that can be gained from TALE repeat comparisons. No patterns in *repeat* sequence similarities were observed within a *CRD*.

A different picture emerged from the comparison of *repeats* found within one RipTAL *CRD*. Generally RipTAL *repeats* are less similar to each other than TALE *repeats* are to each other (e.g. within RipTALI-1 they range from 65% to 97%, Figure 14). Yet, some *repeats* are more similar to each other. Within RipTALI-1 these are *repeats* two to six, which are 85% to 94% identical (Figure 14). *Repeats* eight, ten and eleven are also highly similar to each other with *repeat* identities ranging from 95% to 97% (Figure 14).

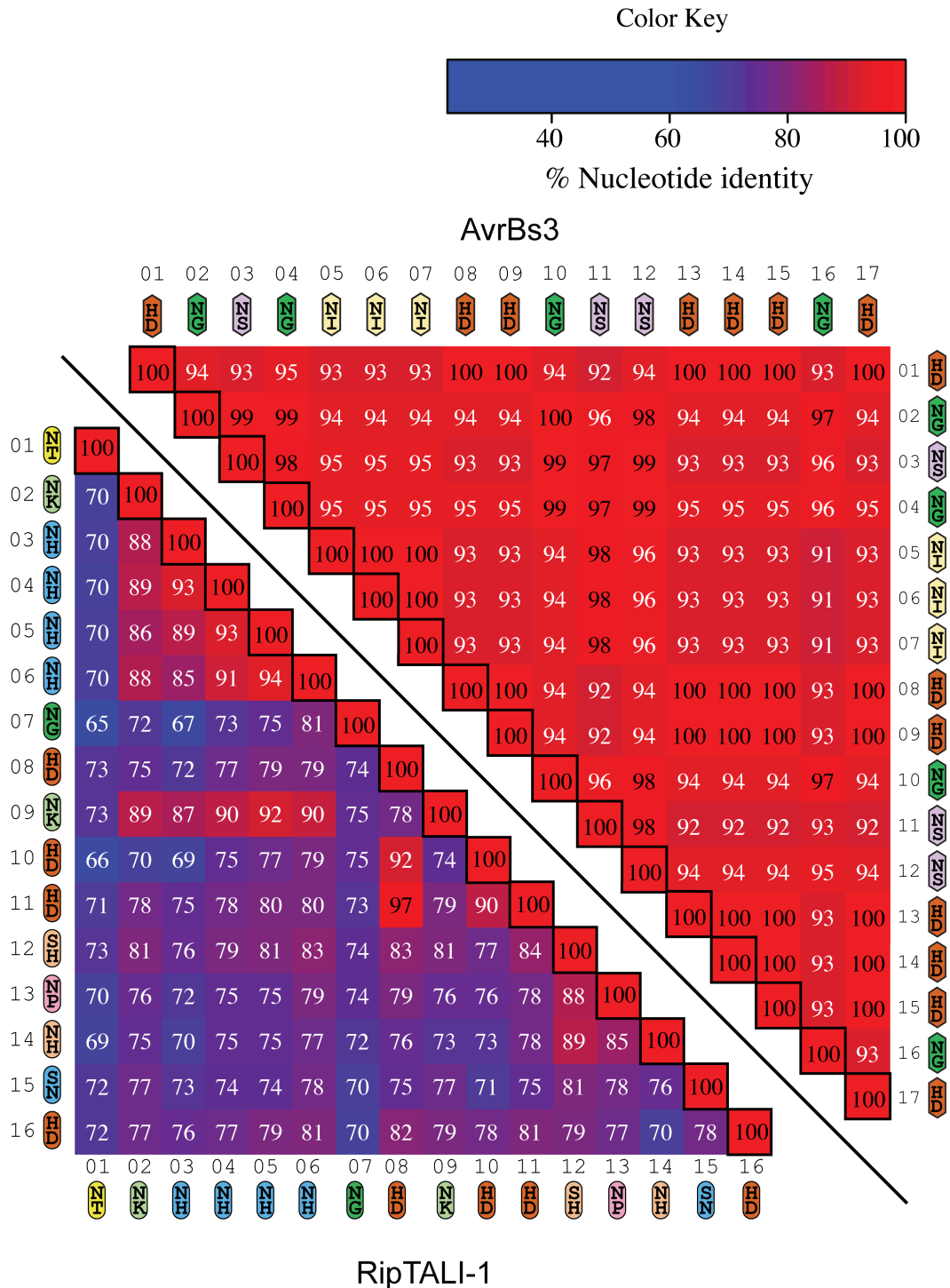


Figure 14. Pairwise identities of TALE and RipTAL repeats from the same CRD. Top-left: all repeats from the CRD of AvrBs3 compared against all. Bottom-right: All repeats from the CRD of RipTALI-8 compared against all others. Cells are colored by value according to the color code at the top. Values ≥ 97 are colored in black, all others in white. Black frames around cells indicate self-comparisons. Repeats are numbered according to their position in the CRD, and ovals are used to represent RipTAL repeat amino acid translations with the RVD of that repeat given in black text. TALE repeats are annotated in the same way, but with pointed ovals.

Understanding the differences found between different *ripTAL* CRDs could facilitate insights into CRD evolution. Therefore, CRDs of *ripTAL*s from the same class, found in one phylotype, were compared using the approach described above. These CRDs represent naturally evolved effectors and therefore can be used to track changes over time, by investigating the status quo. Again, as a reference CRDs of very closely related TALEs, *AvrBs3* and *AvrBs4*, were compared. Sequence similarities of TALE repeats stemming from different, but closely related, CRDs are similar to those found within the same TALE, ranging from 91% to 100% (Figure 14, Figure 16).

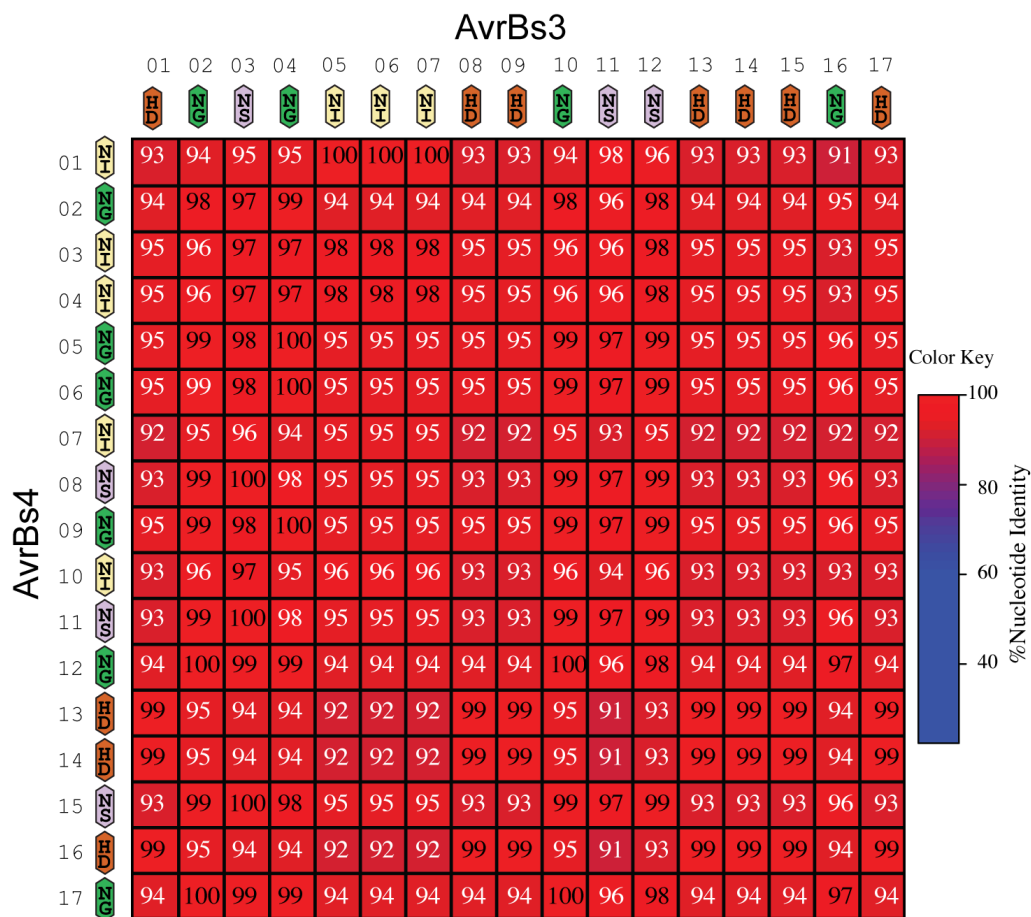


Figure 16. Per-repeat comparison of TALEs AvrBs3 (columns) and AvrBs4 (rows). Cells are colored by value according to the color code to the right. Values ≥ 97 are colored in black, all others in white. Repeats are numbered according to their position in the CRD, and pointed ovals are used to represent TALE repeat amino acid translations with the RVD of that repeat given in black text.

However, a different picture emerges when *repeats* from *CRDs* from closely related *ripTALs* are compared. Most strikingly, it appears that *repeats* that are at the same position in different arrays are very similar. This is clearly observable from a red diagonal of high sequence similarity in Figure 17a, for a comparison of *ripTALI-1* to *ripTALI-8*. A similar pattern, of *repeats* at similar position in the *CRDs* being conserved, is observed for *RipTALIV-1* in comparison to *RipTALIV-2* (Figure 17b), from closely related phylotype IV strains. However, in Figure 17b one can see a red block, of different length in both dimensions. This stems from a different number of similar *repeats* in the first half of the compared *CRDs*. More generally, the pattern of sequence similarities of *repeats* found in different, closely related *CRDs*, indicates that *ripTAL repeats* retain a rather fixed position in the *repeat* array, and do not freely shuffle positions.

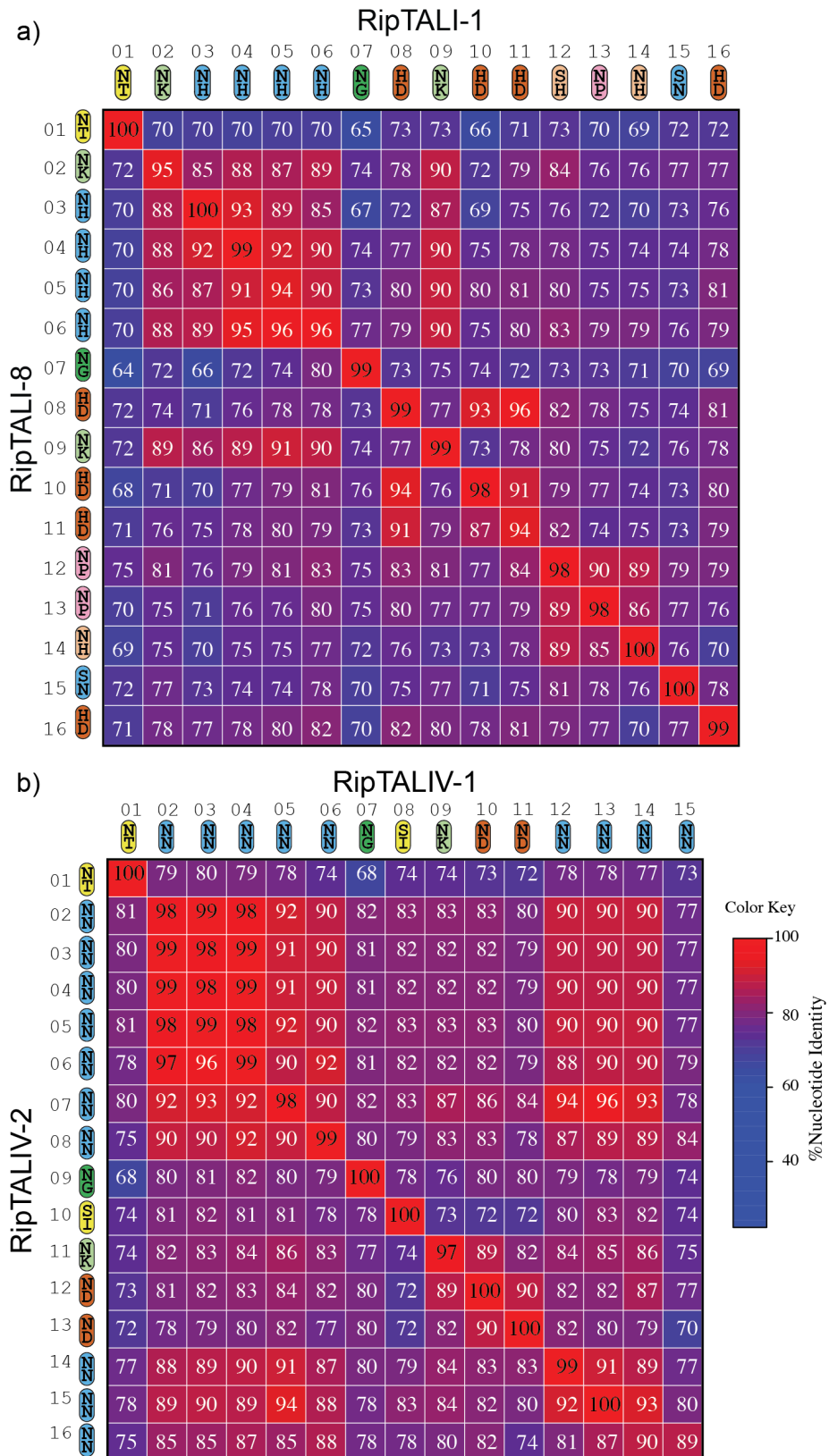


Figure 17. Per-repeat comparison of a) *RipTALI-1* (columns) and *RipTALI-8* (rows) and b) *RipTALIV-1* (columns) and *RipTALIV-2* (rows). Cells are colored by value according to the color code to the right. Values ≥ 97 are colored in black, all others in white. Repeats are numbered according to their position

in the *CRD*, and ovals are used to represent RipTAL repeat amino acid translations with the RVD of that repeat given in black text.

However, the observed pattern of position dependent *repeat* conservation in Figure 17 does not hold when comparing repeats stemming from distantly related Rssc strains. For example, phylotype III and phylotype II are phylogenetically distant (Wicker et al. 2012), and a comparison of the RipTAL *CRDs* found in these phylotypes is accordance with the strain phylogeny. When comparing RipTALII-1 to RipTALIII-1, the range of repeat identities drops to 63-87% (Figure 18, compared to 64% to 97% in Figure 17). While these identities are higher than the ones observed for NTR and CTR (59% and 66%, respectively, Figure 6), the position specific conservation observed for repeats from closely related RipTALs (Figure 17) diminishes.

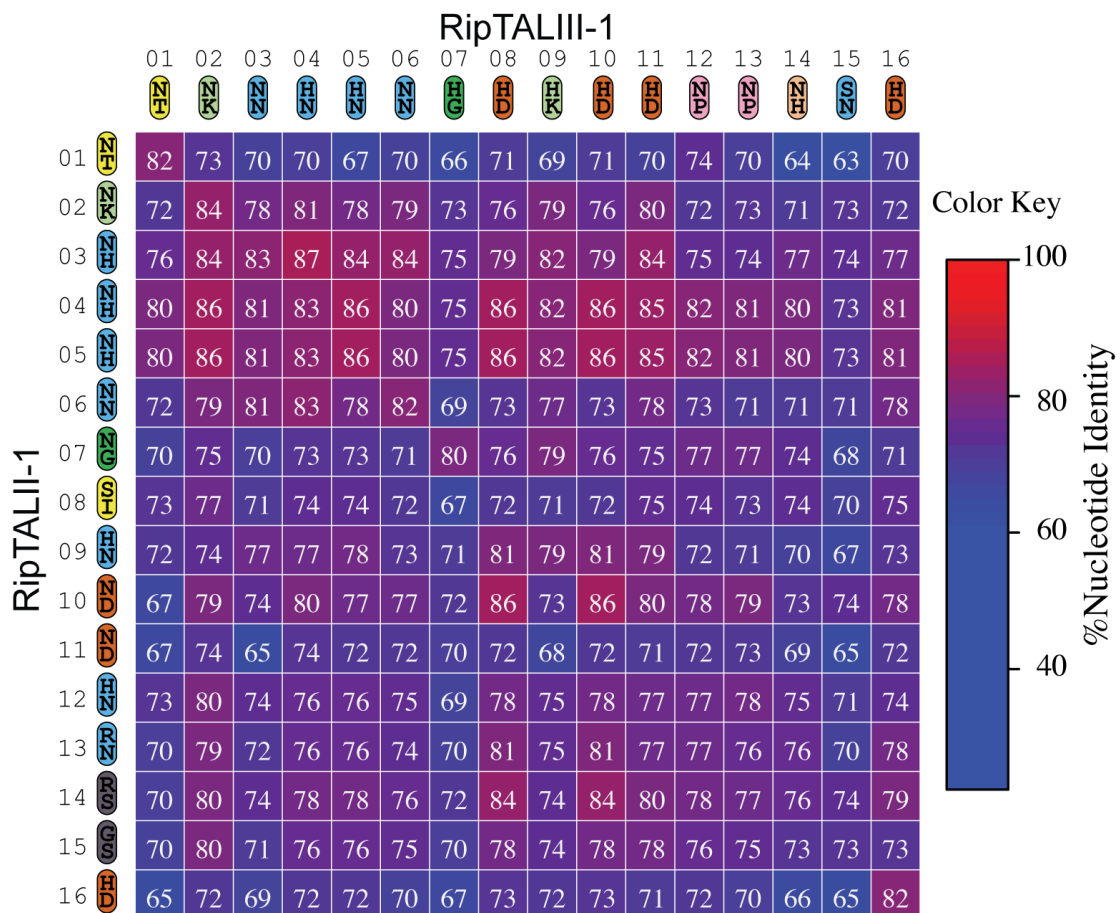


Figure 18. Per-repeat comparison of *RipTALIII-1* (columns) and *RipTALII-1* (rows). Cells are colored by value according to the color code to the right. *Repeats* are numbered according to their position in the *CRD*, and ovals are used to represent RipTAL repeat amino acid translations with the RVD of that repeat given in black text.

Therefore, the most meaningful insights on the *CRD* evolution on the *repeat* level can be made based on the comparison of closely related RipTAL sequences.

2.1.6.2 Mechanistic principles of RipTAL CRD evolution

Close inspection of the *repeat* identities found for *repeats* from closely related *CRDs* could provide a way to understand how *CRDs* evolve.

Two closely related *CRDs*, from *ripTALI-1* and *ripTALI-7*, show drastic differences in the number of repeat units. RipTALI-1 contains 16 repeats, but RipTALI-7 contains one repeat only. However, the alignment of the single *repeat* from *ripTALI-7* to the *CRD* of *ripTALI-1* suggests that the single *ripTALI-7 repeat* is a genetic fusion of the *repeats* 1 and 16 from *ripTALI-1*. This is evident from the alignment shown in Figure 19, where all polymorphic bases between *ripTALI-1 repeats* 1 (pink) and 16 (blue) are compared to the single *repeat* of *ripTALI-7*.

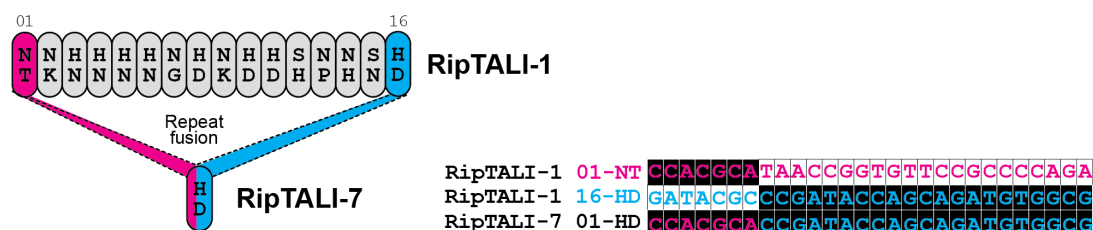


Figure 19. The single *ripTALI-7 repeat* is a fusion of *repeats* 1 and 16 of *ripTALI-1*. To the left a cartoon of the repeat fusion event is shown. To the right all polymorphic bases found in an alignment of the given *repeats* is shown. Pink text highlights bases as found in *repeat* 1 of *ripTALI-1*, blue text highlights bases found *repeat* 16 of *ripTALI-1*, and black background highlights the bases found in the single *repeat* of *ripTALI-7*.

The event depicted in Figure 19 is most parsimoniously explained by a recombination event, which leads to a loss of *repeats* 2-15 from the *CRD*. Notably, many sequenced phylotype I strains isolated from ginger plants carry *RipTALI-7*, which may indicate purifying selection during host specialization on ginger. However, as shown in this work (Figure 7), *RipTALI-7* can also be found in strains belonging to sequevar 15 of phylotype I, isolated from solanaceous plants (Table 2).

From a close inspection of sequence similarities shown in Figure 17, between *ripTALI-1* and *ripTALI-8* it is evident that their *repeats* 12 are 98% identical. The only differences across the 105 bases making up one *repeat* are to two SNPs in the two RVD codons. After translation into amino acids, repeats 12 from RipTALI-1 and RipTALI-8 exhibit RVDs SH and NP, respectively (Figure 7). Analysis of the *repeat* sequences revealed that the two SNPs found are limited to both RVD positions; both RVD codons differ by a non-synonymous exchange at triplet position 2 (Figure 20). Strikingly, this gives rise to identical predicted EBEs of RipTALIII-1 and RipTALI-8 (Figure 10b).

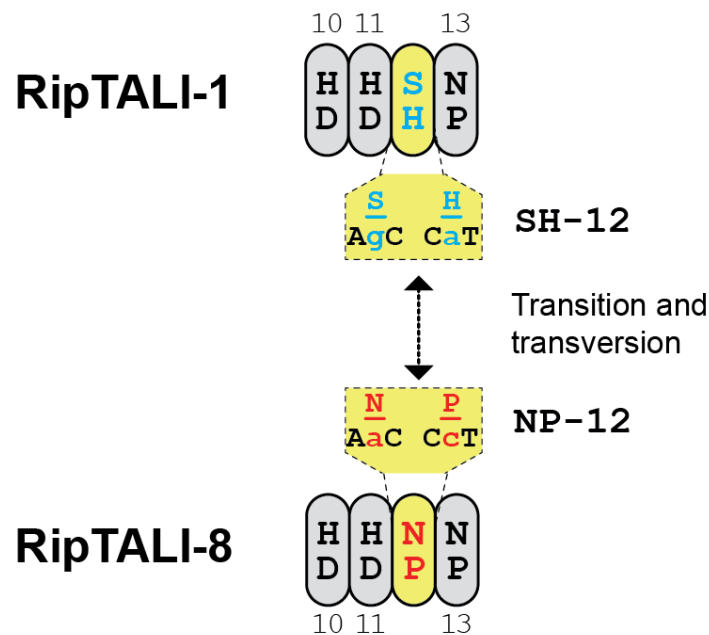


Figure 20. SNPs affecting the RVD codons and thereby the bound EBE diversify RipTAL CRDs. Repeats are depicted as ovals, and all nucleotide polymorphisms between *repeats* 12 are shown in yellow boxes, adjacent to the respective repeat.

As noted earlier, *repeats* 8, 10 and 11 of *RipTALI-1* are highly similar (Figure 14), with *repeats* 8 and 11 being more similar to each other, than to *repeat* 10. From Figure 18 it can be seen that *repeats* 8 and 10 of *RipTALIII-1* are identical in their sequence. This is evident from columns 8 and 10 in Figure 18, which are identical. *Repeats* at positions 8, 10 and 11 in *RipTALI-1* and *RipTALIII-1* have amino acids H and D at the RVD positions. However, the *repeat* similarities of *repeats* 8, 10 and 11 are not the same between those *repeat* arrays. In *RipTALI-1* *repeats* 8 and 11 are more similar to each other than either is to *repeat* 10, whereas in *RipTALIII-1* *repeats* 8 and 10 are more

similar to each other than either is to *repeat* 11. In Figure 21 all polymorphic bases of *repeats* 8, 10 and 11 of *RipTALI-1* and *RipTALIII-1* are displayed.

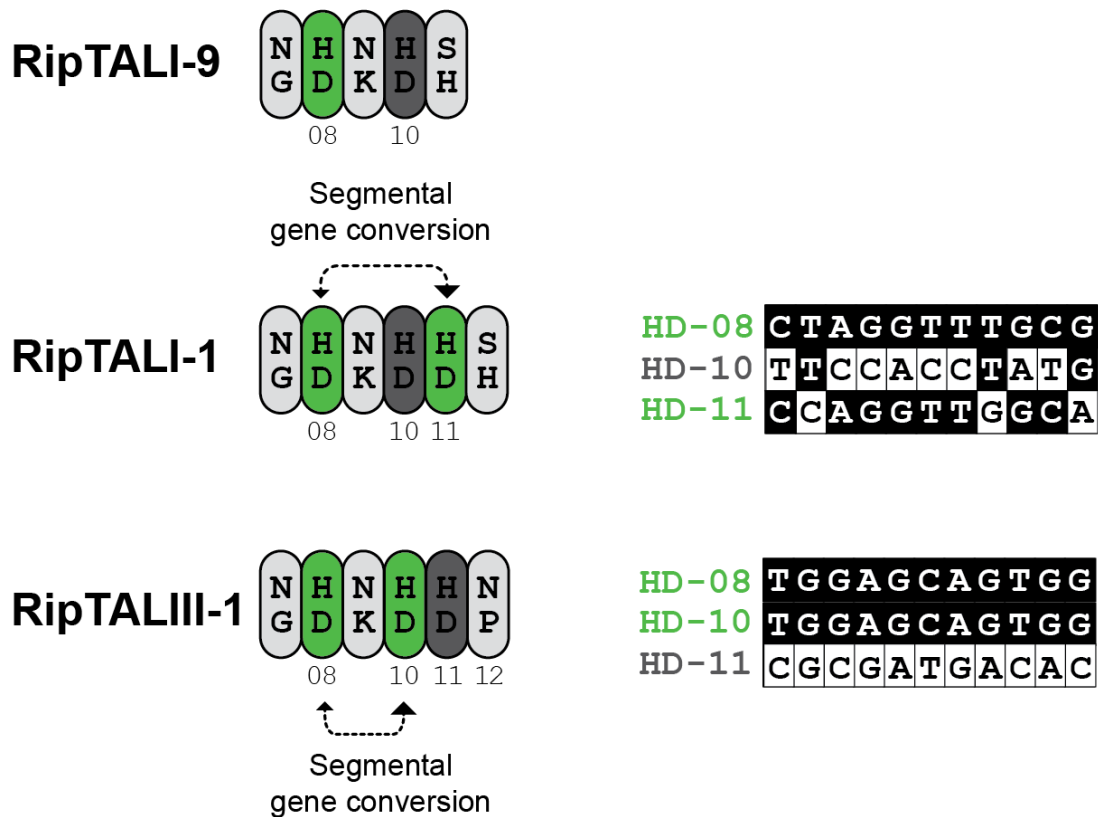


Figure 21. Segmental gene conversion drives *RipTAL* CRD evolution. Comparison between HD *repeats* 8, 10 and 11 within *RipTALI-1* and *RipTALIII-1*. RipTALI-9 is shown as a reference. Repeats are displayed as ovals and green color indicates similar *repeats* within an a CRD. Proposed segmental gene conversion events are shown with dashed arrows. To the right *all* polymorphic bases from *repeats* 8, 10 and 11 of the respective *RipTAL* are aligned, with a color code identical to the one to the left.

Based on these similarities it appears that *repeats* 8 and 11 in *RipTALI-1* and *repeats* 8 and 10 in *RipTALIII-1* are the result of duplication events. Judging by a comparison to *RipTALI-9*, which lacks HD repeat 11, it appears likely that both *repeat* 11 of *RipTALI-1* and *repeat* 10 in *RipTALIII-1* are the result of a duplication of *repeat* 8 from the same array (Figure 21). Mechanistically, it appears most likely that these events were facilitated by segmental gene conversion of *repeat* 8 (Figure 21).

Besides the duplication events described above, direct, adjacent *repeat* duplication events can be traced in RipTAL CRDs. From the comparison of *RipTALII-1 repeats* against all other *RipTALII-1 repeats* (Figure 15) and from that of *RipTALIV-2 repeats* against themselves (Figure 15) it can be seen that

some *repeats*, which are next to each other are perfectly identical. For example, *repeats* 4 and 5 of *RipTALII-1* are completely identical (Figure 15). Additionally, *repeats* 3 and 4, as well as *repeats* 2 and 5 of *RipTALIV-2* exhibit 100% identity (Figure 15). The direct *repeat* duplication is probably the result of slipped strand mis-pairing during genome replication (Ferreira et al. 2015). As shown in Figure 22 for *RipTALII-1*, slipping of the synthesized DNA strand during replication of tandem-repeated sequence stretches can lead to a looping out of the synthesized strand, which will cause a duplication of the looped out repeat unit after replication.

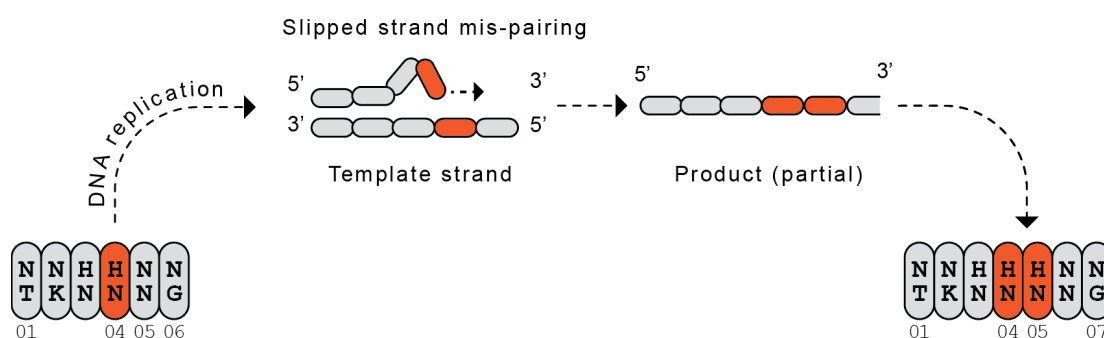


Figure 22. Slipped strand mis-pairing event during DNA replication. To the left the ancestral *repeat* array is shown, and the mutation leading to a new *repeat* array containing an additional *repeat* (right) is shown in the middle section.

It appears very likely that the pattern of *repeat* identities observed for *repeats* 3 and 4 as well as 2 and 5 of *RipTALIV-2*, also trace back to multiple slipped strand mis-pairing events. For example, one possible route to such a pattern could be an initial *repeat* duplication, leading to two identical, adjacent *repeats* (pattern AA). Another slipped strand mis-pairing event could give rise to a third identical *repeat* (pattern AAA). The central identical *repeat* may acquire a polymorphism leading to a slightly polymorphic *repeat*, surrounded by two *repeats* which are identical to each other (pattern ABA). A third slipped strand mis-pairing event leading to duplication of the central of the three related *repeats* would then lead to the pattern of repeat identities observed for *repeats* 2-5 of *RipTALIV-2* (ABBA) (Figure 15, Figure 17b).

In summary, analysis of *ripTAL* CRD compositions suggests four distinct mechanisms driving *ripTAL* CRD diversity. Namely these are recombination, SNP accumulation in RVD positions, segmental gene conversion and slipped strand mis-pairing.

2.2 RipTALs in disease

2.2.1 Natural recognition in *A. thaliana*

To gain insights into the biological role of RipTALs in a plant-microbe interaction, *Arabidopsis thaliana* plants were assessed for a differential reaction to treatment with RipTALI-1. The plant lines analyzed were the core collection of the 1001 Genomes project, encompassing 80 Ecotypes, which cover much of the diversity found within *A. thaliana* (Cao et al. 2011). The goal of this project was to uncover any RipTAL responsive plant accessions in that plant collection, using a heterologous delivery systems and validating the initial results with Rssc strains GMI1000 (phylotype I, (Salanoubat et al. 2002)) and the corresponding *RipTALI-1* mutant, GRS216 (Macho et al. 2010).

2.2.1.1 *P. fluorescens* as a heterologous delivery system for RipTALs

An initial screening of all 80 *A. thaliana* accessions in the core collection, using a non-pathogenic *Pseudomonas fluorescens* strains was performed. A particular strain of *P. fluorescens* was engineered to express a type III secretion system, and named Effector-to-Host-Analyzer (EtHAn) (Thomas et al. 2009). *RipTALI-1*_{GMI1000} (predicted molecular weight = 131 kDa) was cloned into a modified pENTR, with a 3xFLAG epitope tag (see 4.1.3.2), and from there into the broad host range vector *pDSK602*, sequence verified and transformed into *P. fluorescens* EtHAn. Expression was confirmed by western Blotting on two separate clones (11 and 16, Figure 23).

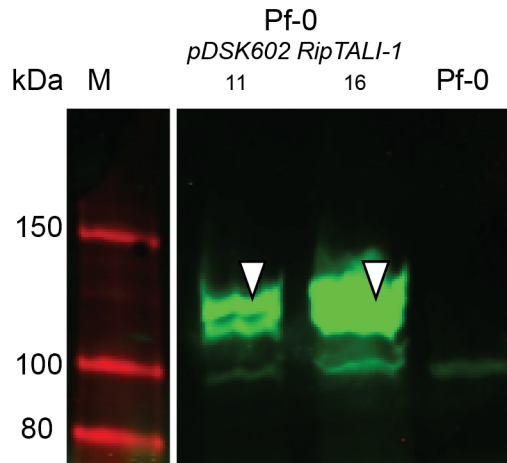


Figure 23. Confirmation of RipTALI-1 expression in *P. fluorescens* by Western blot. Two clones of *P. fluorescens* transformed with plasmid pDSK602 RipTALI-1 were tested for RipTAL expression using a commercial anti-FLAG antibody (mouse), and detected using an anti-mouse antibody (goat) coupled to IRDye600 in an Odyssey scanner. White arrows indicate expected molecular weight. The blot was spliced to remove lanes not of interest.

Subsequently, clone 16 (Figure 23) and an untransformed *P. fluorescens* EtHAn clone were used to leaf-infiltrate 3-4 week old *A. thaliana* plants (5 per ecotype and experiment, experiments were repeated once). Leaves were scored visually for phenotypic changes such as color changes or tissue aberrations seven days after infection. These data are given in Table 3.

Ecotype	Leaf phenotype after infiltration with	
	Pf-0-EtHAn	EtHAn-RipTALI-1
Agu-1	normal green	shriveled up green tissue
Aitba-2	normal green	normal green
Altenb-2	dead, dry tissue	dead, dry tissue
Angel-1	translucent patches	normal green
Angit-1	normal green	normal green
Apost-1	normal green	dead, dry tissue
Bak-2	normal green	normal green
Bak-7	normal green	normal green
Bolin-1	normal green	yellowing patches
Borsk-2	yellowing patches	yellowing patches
Bozen-1.1 (Ice169)	normal green	normal green
Bozen-1.2 (Ice173)	normal green	normal green
Capac-1	normal green	normal green
Castelfed 4	normal green	normal green
Cdm-0	normal green	normal green

Ciste-1	normal green	normal green
Ciste-2	normal green	normal green
Dobra-3	normal green	normal green
Dog-4	normal green	normal green
Don-0	normal green	normal green
Ey1.5-2	normal green	normal green
Fei-0	yellowing patches	normal green
Galdo-1	normal green	normal green
HKT2-4	yellowing patches	normal green
Jablo-1	normal green	normal green
Kastel-1	normal green	normal green
Kidr-1	normal green	dead, dry tissue
Kly-1	dead, dry tissue	normal green
Kly-4	dead, dry tissue	normal green
Koch-1	normal green	normal green
Koz2	dead, dry tissue	normal green
Krazo-2	some yellowing patches	normal green
Lag2-1	normal green	normal green
Lago-1	normal green	dead, dry tissue
Lecho-1	normal green	normal green
Leo-1	normal green	slight yellowing
Lerikl-3	normal green	normal green
Mammo-1	normal green	normal green
Mammo-2	normal green	normal green
Mer-6	normal green	normal green
Mittenberg-1	dead, dry tissue	dead, dry tissue
Monte-1	normal green	normal green
Moran-1	normal green	normal green
Niel-2	dead, dry tissue	dead, dry tissue
Ped-0	normal green	normal green
Petro-1	normal green	normal green
Pra-6	normal green	slight yellowing
Qui-0	normal green	normal green
Rovero-1	normal green	normal green
Sha	normal green	normal green
Shigu-2	normal green	yellowing patches
Sij-1	normal green	normal green
Sij-2	yellow and grey patches	normal green
Sij-4	normal green	normal green
Slavi-1	normal green	normal green
Star8	normal green	dead, dry tissue
stepn-1	dead, dry tissue	dead, dry tissue
Stepn-2	normal green	dead, dry tissue
Timpo-1	normal green	normal green
Toufl-1	some dead, dry patches	normal green

Tu-Sha-9	normal green	dead, dry tissue
TU-V-13	normal green	yellow tissue
Tu-Wal-2	normal green	normal green
Valsi-1	normal green	normal green
Vash-1	yellow tissue	yellow tissue
Vezzano-1	normal green	normal green
Vezzano-2	yellow tissue	normal green
Vie-0	normal green	dead, dry tissue
Voeran-1	normal green	normal green
WalHas B-4	dead, dry tissue	dead, dry tissue
Ws-0	normal green	normal green
Xan-1	dead, dry tissue	dead, dry tissue

Table 3. Leave phenotypes of different Ecotypes 7 days after infiltration with *P. fluorescens* strains. Dd-10, Istisu-1, Leb-3, Nemrut-1, Ru3.1-31, Shiju-1, Tu-SB30-3 and Yeg-1 are missing as these plants were lost after harvesting material for trypan blue staining at 3 days after infection.

3 days after infection leaves were detached and stained with trypan blue and de-stained. Trypan blue staining data were recorded and are given in Table 4.

Ecotype	<i>P. fluorescens</i> EtHAN	
	WT	RipTALI-1
Agu-1	+/-	+
Aitba-2	+/-	+
Altenb-2	-	-/+
Angel-1	+/-	+/-
Angit-1	+/?	-
Apost-1	-/?	+
Bak-2	-	-
Bak-7	+	+
Bolin-1	+/-	+/-
Borsk-2	+	+
Bozen-1.1 (N76357/lce169)	+/-	-
Bozen-1.2 (N76358/lce173)	+	+/-
Capac-1	-	-
Castelfed 4 (N76355)	+/?	+
Cdm-0	+/-	+
Ciste-1	-	-
Ciste-2	+/-	+/-
Dd-10	+/?	?
Dobra-3	+	+/-
Dog-4	+	+
Don-0	-	-
Ey1.5-2	-	-

Fei-0	+	+/?
Galdo-1	+	?
HKT2-4	+/-	+/-
Istisu-1	-	+/-
Jablo-1	?	?
Kastel-1	-	-
Kidr-1	+	-/?
Kly-1	+	+
Kly-4	+	+/?
Koch-1	-	+/-
Koz2	+	+/-
Krazo-2	+	+
Lag2-1	+/?	+
Lago-1	+/-	-
Leb-3	+	+/-
Lecho-1	+/-	+/-
Leo-1	+	-
Lerikl-3	+/?	+/?
Mammo-1	?	?
Mammo-2	+/?	-
Mer-6	-/?	+/?
Mittenberg-1	+/?	+/-
Monte-1	-	-/?
Moran-1	+	-
Nemrut-1	+	+
Niel-2	+	+
Ped-0	+/-	+
Petro-1	+/?	+/?
Pra-6	+/-	+/-
Qui-0	+/?	+/-
Rovero-1	+/-	+/-
Ru3.1-31	+/-	+/-
Sha	+/-	+
Shigu-2	+	+
Shiju-1	+/-	+
Sij-1	+	+/-
Sij-2	+	+/-
Sij-4	+	+
Slavi-1	+/?	-
Star8	+/?	+
Stepn-1	+	+/?
Stepn-2	+	+/?
Timpo-1	-	?
Toufl-1	+/-	+/-
Tu-SB30-3	+/-	+

Tu-Sha-9	+/-	+/-
TU-V-13	-	-/?
Tu-Wal-2	+/?	?
Valsi-1	+/?	+/-
Vash-1	+/?	?
Vezzano-1	+/-	+/-
Vezzano-2	+/-	-/?
Vie-0	+	+/?
Voeran-1	?	+/?
WalHas B-4	+/-	+
Ws-0	+	+/-
Xan-1	+	+/-
Yeg-1	-/?	+/?

Table 4. Summary of the results of the analysis of 80 *A. thaliana* ecotypes after treatment with *P. fluorescens* strains as given. Three Leaves were stained with trypan blue staining and destained. "+" indicates cell death (dark blue staining), "-" indicates no dark blue staining and "?" indicates inconclusive results after destaining.

Trypan blue staining revealed instances of cell death not visible from unstained leaves, but sometimes a whole leaf was blue even after destaining (see Figure 24, Apost-1 *P. fluorescens* EtHAn), possibly due to a mistake during handling or staining.

However, some interesting candidate accessions, which reacted differently to treatment with Pf-0 and Pf-RipTALI-1, were found and these results are shown in detail in Figure 24.

The ecotypes shown in Figure 24 were tested in collaboration with the group of Stephane Genin (INRA/CNRS) using *R. solanacearum* strains. Col-0 was used as a control and the tested accessions were, with the rationale according to Figure 24 given in brackets:

Mammo-2 (suppression of cell death with *P. fluorescens* delivering RipTALI-1)

Moran-1 (suppression of cell death with *P. fluorescens* delivering RipTALI-1)

Koz-2 (suppression of cell death with *P. fluorescens* delivering RipTALI-1)

Ciste-1 (no differential reaction)

Kidr-1 (Cell death with *P. fluorescens* delivering RipTALI-1)

Sha (Cell death with *P. fluorescens* delivering RipTALI-1)

Apost-1 (Cell death with *P. fluorescens* delivering RipTALI-1)

Istisu-1 (Cell death with *P. fluorescens* delivering RipTALI-1)

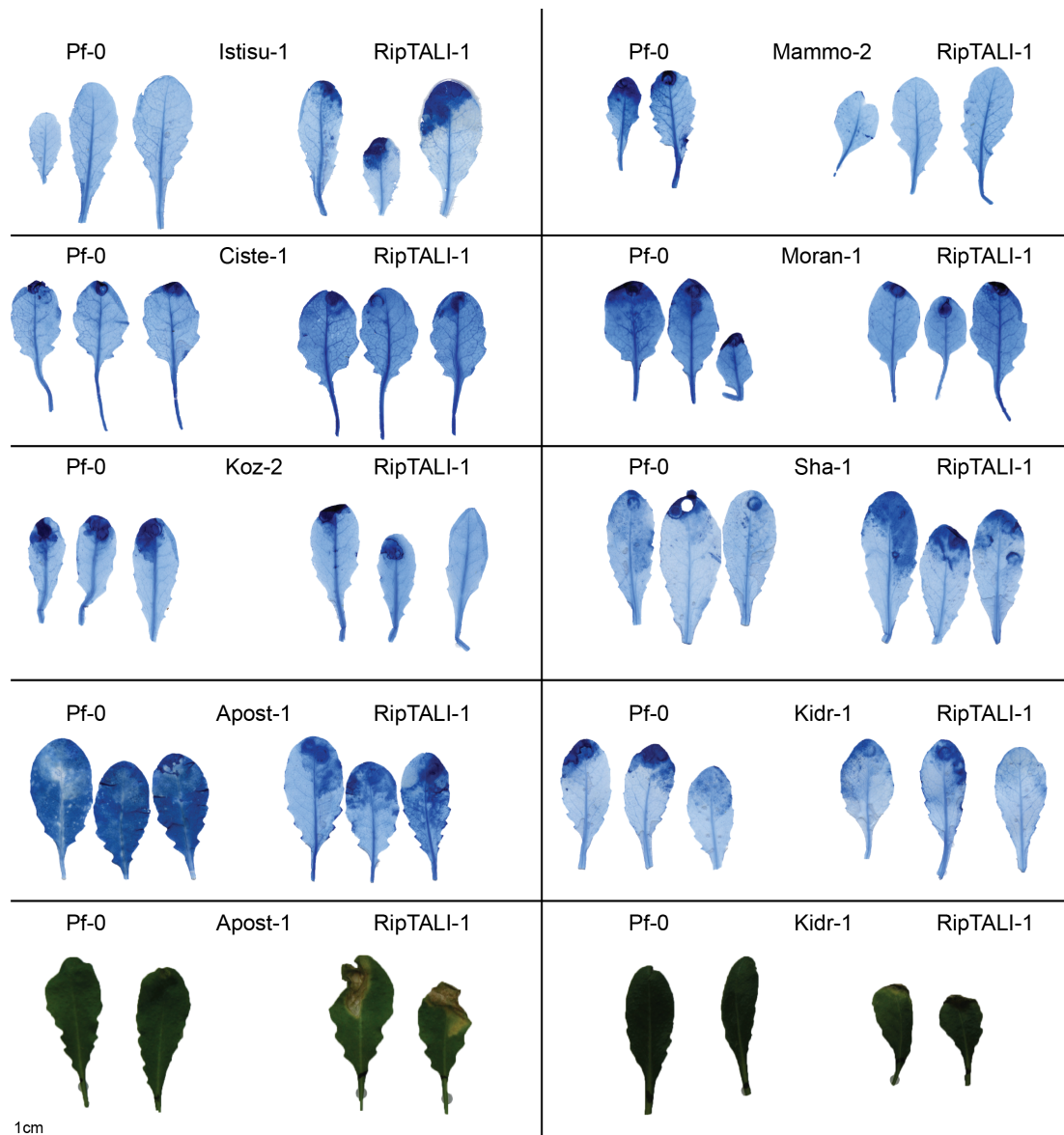


Figure 24. Phenotyping of *A. thaliana* ecotypes regarding differential reactions upon RipTALI-1 delivery, compared to non-delivering *P. fluorescens* EtHAn control strain (Pf-0). Rows one to four display the results of trypan blue staining performed on leaves three days after infection with either Pf-0 or RipTALI-1 expressing Pf-0 for different Ecotypes, as depicted. Row five shows the result of phenotyping unstained leaves seven days after infection for ecotypes Apost-1 and Kidr-1 as depicted. Scalebar is given at the bottom left.

2.2.1.2 Analysis of candidate accessions using Rssc strains

Testing of all *A. thaliana* candidate accessions was performed in the laboratory of S. Genin near Toulouse using *R. solanacearum* strains GMI1000 (wildtype) and GRS216 (RipTALI-1 K/O). In total 5 batches of experiments were performed and data was recorded according to the instructions given by the local supervisors. Disease was scored daily, based on wilting of the plant. In this disease scoring, wilted leaves are counted and put in relation to the

total number of leaves. This is then turned into a 5 level scoring (disease index), where no wilting is coded as 0, 25% wilting corresponds to 1, until a maximum score of 4, which relates to 100% wilted leaves. Due to the variability of the root inoculation assay of *A. thaliana* plants, statistical validation of all results is mandatory. Since the disease scoring is a rather crude approach to monitor disease, statistical analysis of these data is challenging, due to high variance and difficult interpretation of the actual score. Therefore, statistical tools based on survival analysis have been suggested to be useful to differentiate disease outcomes between plant lines and treatments (Lonjon et al. 2015).

However, a convenient analysis tool for these kinds of assays was not available. A script to analyze differential disease progression was therefore developed on the basis of survival analysis using R (R Core Team 2014) on a Macintosh computer. To use this script on a different operating system (e.g. Microsoft® Windows™), the functions used for saving plot outputs to a file need to be changed accordingly.

2.2.1.3 A R based statistical analysis tool for Rssc infections

The raw data generated and used to develop the following script can be found in Table S3 and this data is also used as an example dataset in this section. This tool reads the data from a comma separated value (.csv) file with a header as in Table 5

2.2.1.3.1 Input data formatting

StrainPlant	X0	X1	...	Xn	Batch
-------------	----	----	-----	----	-------

Table 5. Input table header required for the R based survival analysis

Where X0 to Xn in the cells between StrainPlant and Batch needs to be replaced with the day after inoculation (in arabic numerals) the disease was scored. Batch is used to discriminate between experiments done at separate times. Below the header each row is used to track one plant over time. An exemplary header and first row is given in Table 6

StrainPlant	3	4	5	6	7	8	Batch
GMI1000 / Sha-1	0	0	0.5	1	2	2,5	10

Table 6. Exemplary header and first row of the input table.

Replicates of the same experiment need to have completely identical names, but have to be in separate rows and the StrainPlant fields need to be filled with “Strainname / Plantname” (see Table 6). After the disease has been scored and recorded in such a table, the table needs to be exported from Excel into a .csv file and the script can be run.

2.2.1.3.2 Loading of require packages

The R script begins with:

```
#####Libraries#####
library(survival)
library(coin)
library(party)
```

Which loads the required libraries. After the libraries were loaded, the working directory needs to be specified. The working directory is where the input .csv file is located, and will contain the script output. The working directory needs to contain subdirectories named “fits” and “cumhazards”. Both of these folders need to contain the folder “stratified”.

2.2.1.3.3 Data import

```
#####Set working directory#####
wd <- c("~/Example/Path") ###replace Example/Path with true path
setwd(wd)
```

After the working directory has been specified, the name of the table has to be saved in the variable table and subsequently the table is imported.

```
#####Read table#####
table <- c("Table Name.csv") ###Name of the file to be read
```

```
ralsto <- as.data.frame( read.table( table, header = T, sep = "," ),
  stringsAsFactors = F) ###reads table
```

2.2.1.3.4 Converting disease indeces to survival data

After the table has been read into the data frame called ralsto, this table is converted into survival data. This script considers every plant that has a disease score equal to, or greater than 2 dead. The reason is that bacterial wilt is a non-reversible disease, and plants, which reach 50% wilt, will die.

```
### Create Survival table from input table
ralstoSurv <- data.frame()
### convert scored data to survival data, everything above or equal
2 is dead
for (ralrow in 1:nrow(ralsto)) {
  for (ralcol in 2:(ncol(ralsto) - 1)) {
    #
    if (is.na(ralsto[ralrow, ralcol]) == F) {
      if (ralsto[ralrow, ralcol] >= 2) {
        ralstoSurv[ralrow, 1] <- ralsto[ralrow, 1] #name
        ralstoSurv[ralrow, 2] <- 0 #start
        ralstoSurv[ralrow, 3] <- unlist(strsplit(colnames(ralsto[ralcol]),
          "X"))[[2]] #day of event (colname), string splitting is necessary because after csv import an X is added before the numbers
        ralstoSurv[ralrow, 4] <- 1 # status (1=dead)
        ralrow <- ralrow + 1 #next row
        ralcol <- 2 ###start from column 2 (first event)
      } else {
        if (((ralcol == ncol(ralsto) - 1) && (ralsto[ralrow, ralcol] < 2)) || ((sum(is.na(ralsto[ralrow, (ralcol + 1):(ncol(ralsto) - 1)])) == (((ncol(ralsto) - 1) - (ralcol)))) && (ralsto[ralrow, ralcol] < 2))) {
          ## if threshold is not passed until the end of all
```



```
#### Name Columns ####
colnames(ralstoSurv) <- c("StrainPlant", "Start", "End", "Death", "Batch", "Strain", "Plant")
ralstoSurv[,3] <- as.numeric(ralstoSurv[,3])
ralstoSurv[,6] <- as.factor(ralstoSurv[,6])
ralstoSurv[,7] <- as.factor(ralstoSurv[,7])
```

With this, the survival table has been fully generated, and can be used for analysis. The table should be inspected. The survival table should look similar to the one shown in Table 7.

StrainPlant	Start	End	Death	Batch	Strain	Plant
GMI1000 / Sha-1	0	8	1	10	GMI1000	Sha-1
GMI1000 / Sha-1	0	8	1	10	GMI1000	Sha-1

Table 7. Exemplary header and first two rows of the survival table generated.

2.2.1.3.5 *Plotting Kaplan-Meier survival curves and statistical analysis of plant lines treated with a single strain*

Depending on the data that has been generated, different analysis can be performed. In the case were only one bacterial strain has been used, the following plots the Kaplan-Meier survival curves (Bland and Altman 1998) for the individual plant lines, treated with strain GMI1000 (Figure 25).

```
plot(survfit(Surv(as.numeric(End[Strain=="GMI1000"]), Death[Strain=="GMI1000"]) ~Plant[Strain=="GMI1000"] , data=ralstoSurv), col=c("red", "blue", "green", "black", "orange", "yellow", "pink", "purple", "lightblue"))
legend("topleft", legend=levels(ralstoSurv$Plant), fill=c("red", "blue", "green", "black", "orange", "yellow", "pink", "purple", "lightblue"))
```

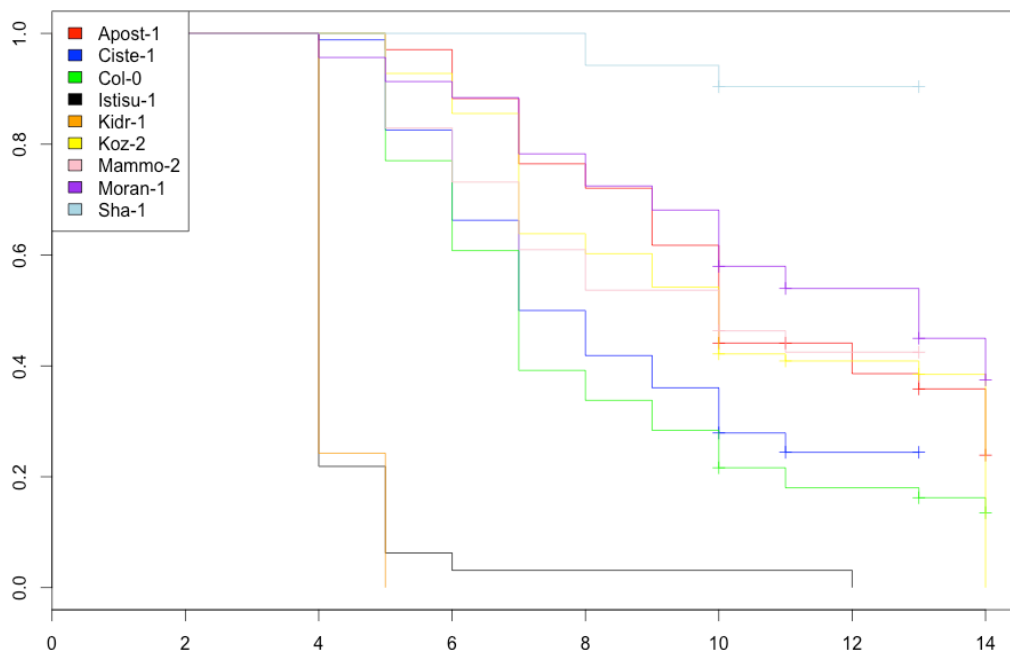


Figure 25. Kaplan-Meier survival curves of different plant lines treated with Rssc strain GMI1000

To generate statistics for these data, the following will return a logrank test of all plants in the dataset, and the p-value returned indicates if any of the plants is different from others.

```
survdiff(Surv(as.numeric(End[Strain=="GMI1000"]), Death[Strain=="GMI1000"]) ~Plant[Strain=="GMI1000"] , data=ralstoSurv, rho=1)
```

Call:

```
## survdiff(formula = Surv(as.numeric(End[Strain == "GMI1000"]),
##   Death[Strain == "GMI1000"]) ~ Plant[Strain == "GMI1000"],
##   data = ralstoSurv, rho = 1)
```

##

```
##           N Observed Expected (O-E)^2/
E
```

## Plant[Strain == "GMI1000"]=Apost-1	68	24.70	37.37	4.29
## Plant[Strain == "GMI1000"]=Ciste-1	86	45.17	38.78	1.05
## Plant[Strain == "GMI1000"]=Col-0	74	44.20	31.98	4.67
## Plant[Strain == "GMI1000"]=Istisu-1	32	30.65	4.53	150.81
## Plant[Strain == "GMI1000"]=Kidr-1	33	32.20	4.23	184.66
## Plant[Strain == "GMI1000"]=Koz-2	83	33.29	43.56	2.42

```
## Plant[Strain == "GMI1000"]=Mammo-2 41 16.49 20.23 0.68
## Plant[Strain == "GMI1000"]=Moran-1 69 21.61 38.32 7.28
## Plant[Strain == "GMI1000"]=Sha-1 52 2.68 32.01 26.86
##
## (O-E)^2/V
## Plant[Strain == "GMI1000"]=Apost-1 7.58
## Plant[Strain == "GMI1000"]=Ciste-1 1.80
## Plant[Strain == "GMI1000"]=Col-0 7.71
## Plant[Strain == "GMI1000"]=Istisu-1 188.01
## Plant[Strain == "GMI1000"]=Kidr-1 222.46
## Plant[Strain == "GMI1000"]=Koz-2 4.36
## Plant[Strain == "GMI1000"]=Mammo-2 1.11
## Plant[Strain == "GMI1000"]=Moran-1 13.11
## Plant[Strain == "GMI1000"]=Sha-1 47.72
##
## Chisq= 493 on 8 degrees of freedom, p= 0
```

2.2.1.3.6 Visual assessment of predictors in the dataset

However, depending on the number of replicates and the actual data used this test may not be sufficient. Data should always be visually assessed and a visualization of the behavior of different plants can be performed using the command, which uses the plant field as the sole predictor:

```
plot(ctree(Surv(End, Death) ~Plant, data=ralstoSurv),main="Batch cTree")
```

Which will generate a conditional inference tree, grouping plant lines based on their survival curves as shown in Figure 26.

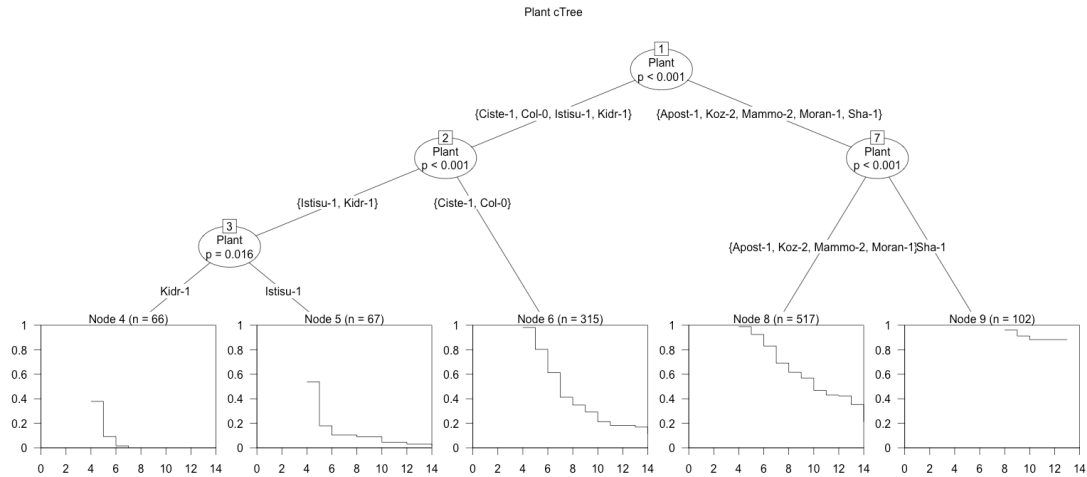


Figure 26. Conditional inference tree, conditioned only by plant.

However, depending on the conducted experiment, more than one bacterial strain may have been used on a multiple plant lines. In that case a conditional inference treeing considering Plant and Strain fields as predictors (Figure 27) should be plotted, using the following command:

```
plot(ctree(Surv(End, Death) ~Plant+Strain, data=ralstoSurv), main="Plant & Strain cTree")
```

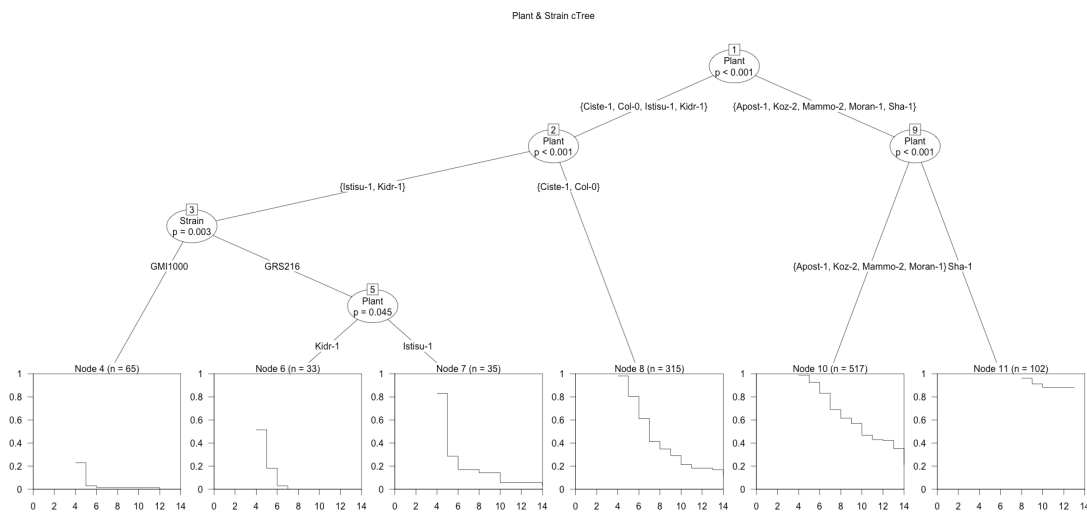


Figure 27. Conditional inference tree, conditioned by plant and strain.

In the case of multiple batches of experiments available, it is advisable to also check for batch effects in the data. A conditional inference tree considering plant, strain and batch as predictors (Figure 28) can be plotted using:

```
plot(ctree(Surv(End, Death) ~Plant+Strain+Batch, data=ralstoSurv), m
ain="Plant, Strain & Batch cTree")
```

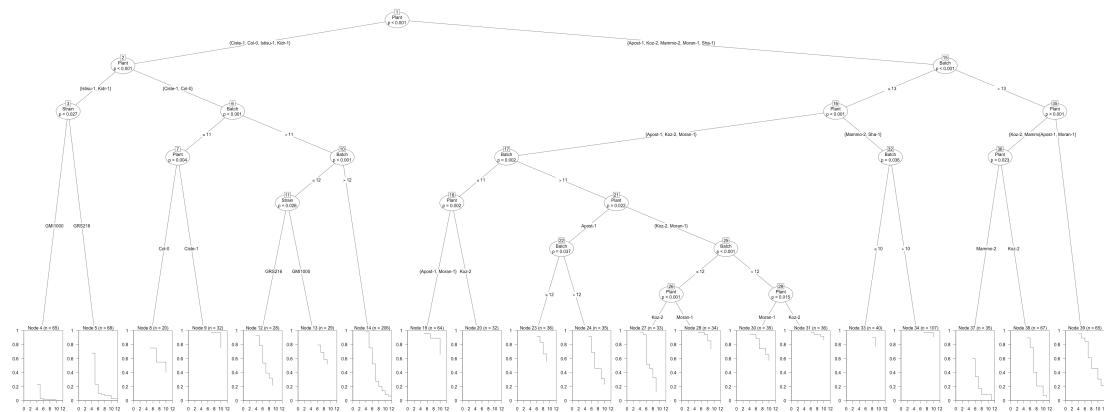


Figure 28. Conditional inference tree, conditioned by plant, strain and batch.

2.2.1.3.7 Excluding batches from subsequent analysis

Should one of the batches in the dataset be excluded from subsequent analysis this can be done with the next code chunk. This will overwrite the current survival table with one that only contains the specified batches. Since rebuilding the original survival table may take some time, the original table is copied to `ralstoSurv.backup` before subsetting.

```
ralstoSurv.backup <- ralstoSurv

batches.to.check <- c() ##define batches to be used here

ralstoSurv <- subset(ralstoSurv, ralstoSurv$Batch %in% batches.to.ch
eck)

droplevels(ralstoSurv)
```

2.2.1.3.7.1. Statistical analysis of differential survival using variants of the log-rank test

Since the conditional inference tree on a large dataset containing many plants and batches can turn out to be very complex (Figure 28), subsequent testing of the individual plants by strain is recommended. This requires an array containing all used plants in the dataset. This array is created by extracting all available plant identifiers from the dataset.


```
plants.array <- array(levels(as.factor(ralstoSurv$Plant)))
names(plants.array) <- levels(as.factor(ralstoSurv$Plant))
```

Subsequently, the plants will be tested for differential response to the strains used. This test is stratified by replicates (batches), to make the analysis more robust to batch effects.

```
plants.by.strain <- sapply( plants.array,
  function(x) {
    survdiff(Surv(as.numeric(End[Plant==x]), Death[Plant==x]) ~Strain[Plant==x] + strata(Batch[Plant==x]), data=ralstoSurv, rho=1)
  },simplify=F)
```

Depending on the value entered for rho, the test used changes. If rho is set to 1, the test weights earlier deaths differently from later deaths, if this is not desired, rho can be set to 0 (resulting in the use of the log-rank test (Bland and Altman 2004)).

```
plants.by.strain.logrank <- sapply( plants.array,
  function(x) {
    survdiff(Surv(as.numeric(End[Plant==x]), Death[Plant==x]) ~Strain[Plant==x] + strata(Batch[Plant==x]), data=ralstoSurv, rho=0)
  },simplify=F)
```

The contents of either variable can be inspected by calling the variable:

```
plants.by.strain.logrank
```

Calling either of the above objects will return the test statistic for each plant in the dataset. As an example, below is the log-rank test output for plant line Apost-1.

```
## $`Apost-1`
## Call:
## survdiff(formula = Surv(as.numeric(End[Plant == x]), Death[Plant ==
##      x]) ~ Strain[Plant == x] + strata(Batch[Plant == x]), data =
##      ralstoSurv,
##      rho = 0)
```

```
##
##
##              N Observed Expected (O-E)^2/E (O-E)^2
/V
## Strain[Plant == x]=GMI1000 68          42      46.8      0.497      1.
49
## Strain[Plant == x]=GRS216  67          44      39.2      0.594      1.
49
##
## Chisq= 1.5  on 1 degrees of freedom, p= 0.222
```

Next, one can fit the data to a Kaplan-Meier survival regression curve

```
fits <- sapply( plants.array,
  function(x) {
    survfit(Surv( as.numeric(End[Plant==x]), Death[Plant==x]) ~Strain[Plant==x] +strata(Batch[Plant==x]), data=ralstoSurv)
  },simplify=F)
```

Depending on the number of different strains used in the analysis, differential colouring helps understanding the output. In this version nine colors, to discriminate a maximum of 9 strain unambiguously, are defined

```
StrainColors <- c("red", "blue", "green", "black", "orange", "yellow", "pink", "purple", "lightblue")
```

Subsequently, the individual fits for each plant, stratified by batch are plotted and saved to /fits/stratified.

```
setwd(paste(wd, "/fits/stratified", sep=""))
for (x in plants.array) {
  plotcolors <- unlist(lapply( 1:nlevels (ralstoSurv$Strain) ,
    function(k) {
      rep(StrainColors[k], nlevels (as.factor (ralstoSurv$Batch[ ralstoSurv$Plant==x & ralstoSurv$Strain==levels(ralstoSurv$Strain)[[k]] ])) ) )
    })))
  plot(fits[[paste(x)]], main=paste(c(names(fits[x])), "Survival Plot"),
  ),
  col = plotcolors,
```

```

lty = c(cbind (rep( c(1:nlevels(as.factor(ralstoSurv$Batch[ralstoSurv$Plant==x]))), nlevels(ralstoSurv$Strain))))
)
legend("bottomleft", levels(ralstoSurv$Strain), fill=StrainColors)
text(3,0.2,labels=paste("Logrank pvalue=",round(pchisq(plants.by.strain.logrank[[x]]$chisq, df=1, lower=F),digits=5)) )
quartz.save(paste(x,"survival plot stratified.pdf",sep=" "),type="pdf")
dev.off()
}
setwd(wd)

```

This will generate Kaplan-Meier survival plots for each plant, paste the corresponding logrank p-value into the plot and save the plot as a .pdf file. The survival plot for the ecotype Col-0 is shown in Figure 29.

Col-0 Survival Plot

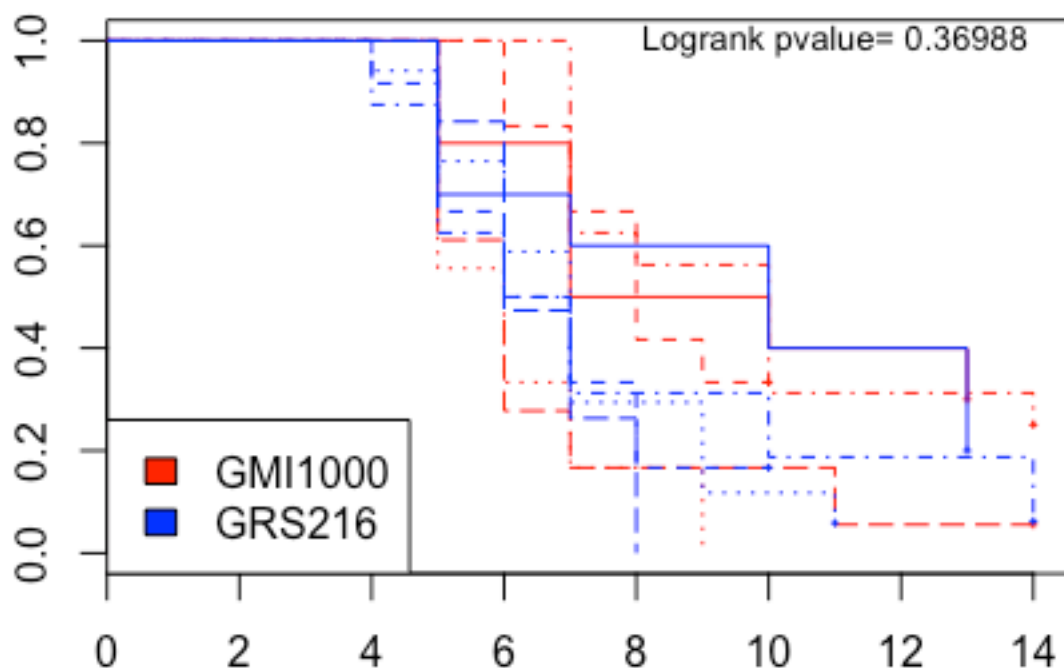


Figure 29. Kaplan-Meier Survival regressions of Col-0, different replicates are plotted with different line types, and strain treatment is color coded as shown in the legend. The p-value of the log-rank test is given in the top-right corner of the plot.

These plots show the survival of the plants used and provide the logrank test p-value for a difference between the groups analyzed. However, the logrank

test has some down-sides, such as poor performance on survival curves which cross over time (as seen in Figure 29) Sometimes it may be more intuitive to investigate the cumulative hazard the population is exposed to. The cumulative hazard will increase over time, as it is the sum of the probabilities of dying for each time interval recorded. The cumulative hazards for all plants in the data set can be plotted and saved into “/cumhazards/stratified” using

```
setwd(paste(wd, "/cumhazards/stratified", sep = ""))
for (x in plants.array) {
  plotcolors <- unlist(lapply(1:nlevels(ralstoSurv$Strain), function(k) {
    rep(StrainColors[k], nlevels(as.factor(ralstoSurv$Batch[ralstoSurv$Plant ==
      x])))
  })))
  plot(fits[[paste(x)]], main = paste(c(names(fits[x])), "Cumulative Hazards"),
    col = plotcolors, lty = c(cbind(rep(c(1:nlevels(as.factor(ralstoSurv$Batch[ralstoSurv$Plant ==
      x]))), nlevels(ralstoSurv$Strain))))), fun = "cumhaz")
  legend("topleft", levels(ralstoSurv$Strain), fill = StrainColors)
)

quartz.save(paste(x, "cumulative hazards stratified.pdf", sep =
" "), type = "pdf")
dev.off()
}
setwd(wd)
```

In Figure 30 the cumulative hazard fits for ecotype Col-0 are plotted.

Col-0 Cumulative Hazards

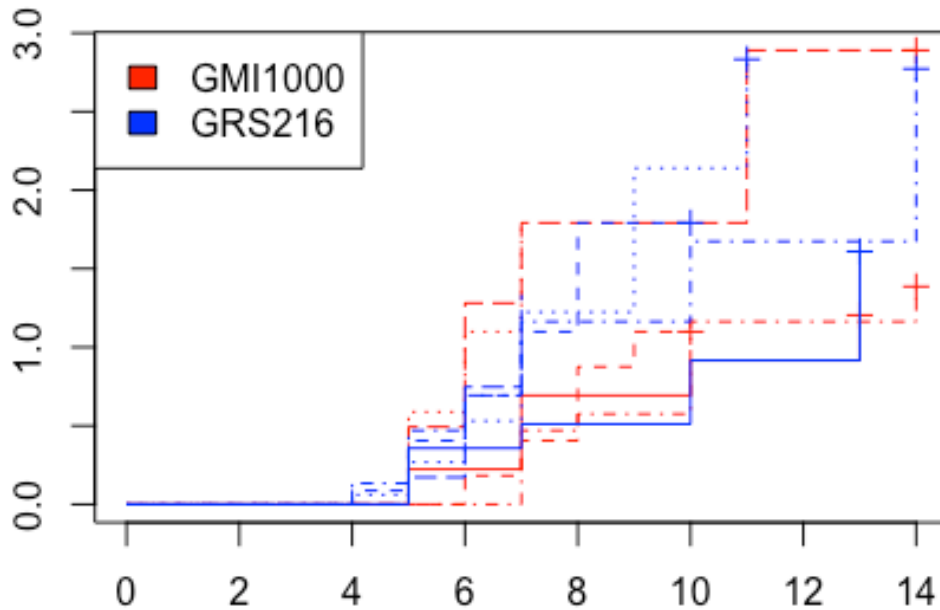


Figure 30. Cumulative hazards of ecotype Col-0. Different experiments are plotted with different line types, and strain treatment is color coded as shown in the legend

2.2.1.3.8 Statistical analysis of differential survival based on Cox-proportional hazards

Sub-optimal testing can result in misinterpretation of the data, and one important characteristic of survival curves is whether they exhibit a proportional behavior, which makes them applicable for the use of proportional hazard models. Proportional hazard models generally assume that the hazard is continuous over time and between groups, i.e. does not increase or decrease over time. Cox-proportional hazards can be generated for all plants using

```
plant.cox <- sapply(plants.array, function(x) {  
  coxph(Surv(as.numeric(End[Plant == x])), Death[Plant == x]) ~ Strain[Plant ==  
    x] + strata(Batch[Plant == x]), data = ralstoSurv)  
}, simplify = F)
```

These models can then be tested regarding the assumption of proportional hazards.

```
testCox <- rbind(sapply(plants.array, function(x) {
  print(cox.zph(plant.cox[[x]]))
}))
rownames(testCox) <- c("rho", "chisq", "p")
```

This test can subsequently filtered for p-values below 0.05.

```
which(testCox[3,]<0.05)
```

In the dataset used here, one plant line significantly violates the assumption of proportional hazards:

```
## Istisu-1
```

2.2.1.3.9 *Statistical analysis assuming non-proportional hazards*

To circumvent these problems, one can perform statistical analysis assuming non-proportional hazards. Currently, four separate distributions are used to generate four separate non-proportional hazard regressions. The distributions used are weibull, gaussian, logistic and lognormal distributions. The regressions are computed with the following code:

```
plant.NPH.wei <- sapply(plants.array,
  function(x) {
    survreg(Surv( as.numeric(End[Plant==x]), Death
[Plant==x]) ~Strain[Plant==x] + strata(Batch[Plant==x]), data=ralsto
Surv, dist="weibull")
  },simplify=F)
```

```
plant.NPH.gau <- sapply(plants.array,
  function(x) {
    survreg(Surv( as.numeric(End[Plant==x]), D
eath[Plant==x]) ~Strain[Plant==x] + strata(Batch[Plant==x]), data=ra
lstoSurv, dist="gaussian")
  },simplify=F)
```

```

plant.NPH.logist <- sapply(plants.array,
                          function(x) {
                            survreg(Surv( as.numeric(End[Plant==x]
), Death[Plant==x]) ~Strain[Plant==x] + strata(Batch[Plant==x]), dat
a=ralstoSurv, dist="logistic")
                            },simplify=F)

plant.NPH.lognorm <- sapply(plants.array,
                            function(x) {
                              survreg(Surv( as.numeric(End[Plant==x]), D
eath[Plant==x]) ~Strain[Plant==x] + strata(Batch[Plant==x]), data=ra
lstoSurv, dist="lognormal")
                              },simplify=F)

```

To then test which of these distributions is the best fit for the data, the Akaike Information Criterion (AIC) can be used. These AIC scores and degrees of freedom are extracted and collected into `aic.scores`:

```

aic.scores <- rbind(
  sapply(plants.array , function(x) {
    extractAIC(plant.NPH.wei[[x]])
  }),
  sapply(plants.array , function(x) {
    extractAIC(plant.NPH.gau[[x]])
  }),
  sapply(plants.array , function(x) {
    extractAIC(plant.NPH.logist[[x]])
  }),
  sapply(plants.array , function(x) {
    extractAIC(plant.NPH.lognorm[[x]])
  }))
rownames(aic.scores) <- c("WEI-df", "WEI-AIC", "GAU-df", "GAU-AIC", "log
ist-df", "logist-AIC", "lognorm-df", "lognorm-AIC")

```

Finally, one has to evaluate the resulting scores by calling the `aic.scores` object with

```

aic.scores

```

The model with the lowest overall AIC scores should be the one best fitting to the data at hand. For the data used here, this is the log-normal model, which can be called using

```
plant.NPH.lognorm
```

Which returns the p-values for this particular hazard model, for example for Apost-1 in the dataset used here this returns:

```
## `$`Apost-1`  
## Call:  
## survreg(formula = Surv(as.numeric(End[Plant == x]), Death[Plant == x]) ~ Strain[Plant == x] + strata(Batch[Plant == x]), data = ralst  
oSurv, dist = "lognormal")  
##  
## Coefficients:  
##           (Intercept) Strain[Plant == x]GRS216  
##           2.2970767           -0.1252916  
##  
## Scale:  
## Batch[Plant == x]=11 Batch[Plant == x]=12 Batch[Plant == x]=13  
##           0.8631574           0.2636134           0.3943303  
## Batch[Plant == x]=14  
##           0.2513453  
##  
## Loglik(model)= -249.5   Loglik(intercept only)= -251.5  
## Chisq= 3.98 on 1 degrees of freedom, p= 0.046  
## n= 135
```

However, a better overview of the results generated can be obtained using

```
for (i in 1:length(plants.array)) {  
  print(summary(plant.NPH.lognorm[[i]]))  
}
```

For Apost-1, the summary of the non-proportional hazard model is as follows:

```
##  
## Call:
```



```

## survreg(formula = Surv(as.numeric(End[Plant == x]), Death[Plant =
= x]) ~ Strain[Plant == x] + strata(Batch[Plant == x]), data = ralst
oSurv,
##      dist = "lognormal")
##
##              Value Std. Error      z      p
## (Intercept)      2.297      0.0458  50.154 0.00e+00
## Strain[Plant == x]GRS216 -0.125      0.0616  -2.033 4.21e-02
## Batch[Plant == x]=11     -0.147      0.2867  -0.513 6.08e-01
## Batch[Plant == x]=12     -1.333      0.1745  -7.641 2.15e-14
## Batch[Plant == x]=13     -0.931      0.1476  -6.304 2.90e-10
## Batch[Plant == x]=14     -1.381      0.1369 -10.086 6.36e-24
##
## Scale:
## Batch[Plant == x]=11 Batch[Plant == x]=12 Batch[Plant == x]=13
##              0.863              0.264              0.394
## Batch[Plant == x]=14
##              0.251
##
## Log Normal distribution
## Loglik(model)= -249.5   Loglik(intercept only)= -251.5
## Chisq= 3.98 on 1 degrees of freedom, p= 0.046
## Number of Newton-Raphson Iterations: 4
## n= 135

```

2.2.1.4 Validation of the initial Pf-0 phenotypes with *R. solanacearum*

From the original 9 plant lines identified using *P. fluorescens* to react differentially to delivery of RipTALI-1, four phenotypes could be confirmed in the *R. solanacearum* assays. Based on the p-values for the non-proportional hazard model best fitting to the data (log normal), the following plant lines reacted differentially in a stratified test, with a p-value cutoff of 0.05:

Apost-1 (p=0.046), Istisu-1 (p=4.3*10⁻⁸), Kidr-1 (p=0.0049), Sha-1 (p=0.00024).

All *A. thaliana* ecotype seeds (Table 4), seeds of the lines given in Table 8, bacterial strains (GMI1000, GRS216) and data, as well as analysis tools were handed over to Dousheng Wu for follow-up experiments.

Plant background	Details	Number of lines
Col-0, Dex::AvrPto	pGWB3* Bs3p-EBE Brg11	2
Col-0, Dex::AvrPto	pGWB3* Bs3p-EBE RipTALI-14 (this RipTAL was renamed to RipTALI-4)	7
Col-0, Dex::AvrPto	pGWB5 pNarrow	None. Plants were lost during the move from Munich.
Sha (male) x Don-0 (female)	Crossing; performed by S. Urbanus	Seeds
Sha (male) x Ciste-1 (female)	Crossing; performed by S. Urbanus	Seeds
Sha (male) x Altenb.-2 (female)	Crossing; performed by S. Urbanus	Seeds
medium flowering Istisu- 1 (Female) x DEX AvrPto (male)	Crossing; performed by S. Urbanus	Seeds

Sha (female) x medium flowering Istisu-1 (male)	Crossing performed by S. Urbanus	Seeds
Altenb.-2 (female) x medium flowering Istisu-1 (male)	Crossing performed by S. Urbanus	Seeds

Table 8. Additional seeds lines generated. Col-0 Dex::AvrPto was described in (Tsuda et al. 2012).

2.3 Engineering resistance based on synthetic RipTAL receptors

2.3.1 Project definition

This approach aims to control bacterial wilt disease of dicotyledonous plants, in the model plant *A. thaliana* as well as the crop model *Solanum lycopersicum* by generating a synthetic plant *R* gene. Conceptually the envisaged approach adapts available knowledge on the native mechanisms of TALE-activated resistance, outlined in the introduction of this work and the insights gained from the analysis of RipTALs.

Generally this project should be understood as a translational biological engineering project, rather than one aimed at answering basic biological research questions. The goal of this project is creating a plant, which shows elevated resistance to RipTAL carrying Rssc strains (Figure 31).

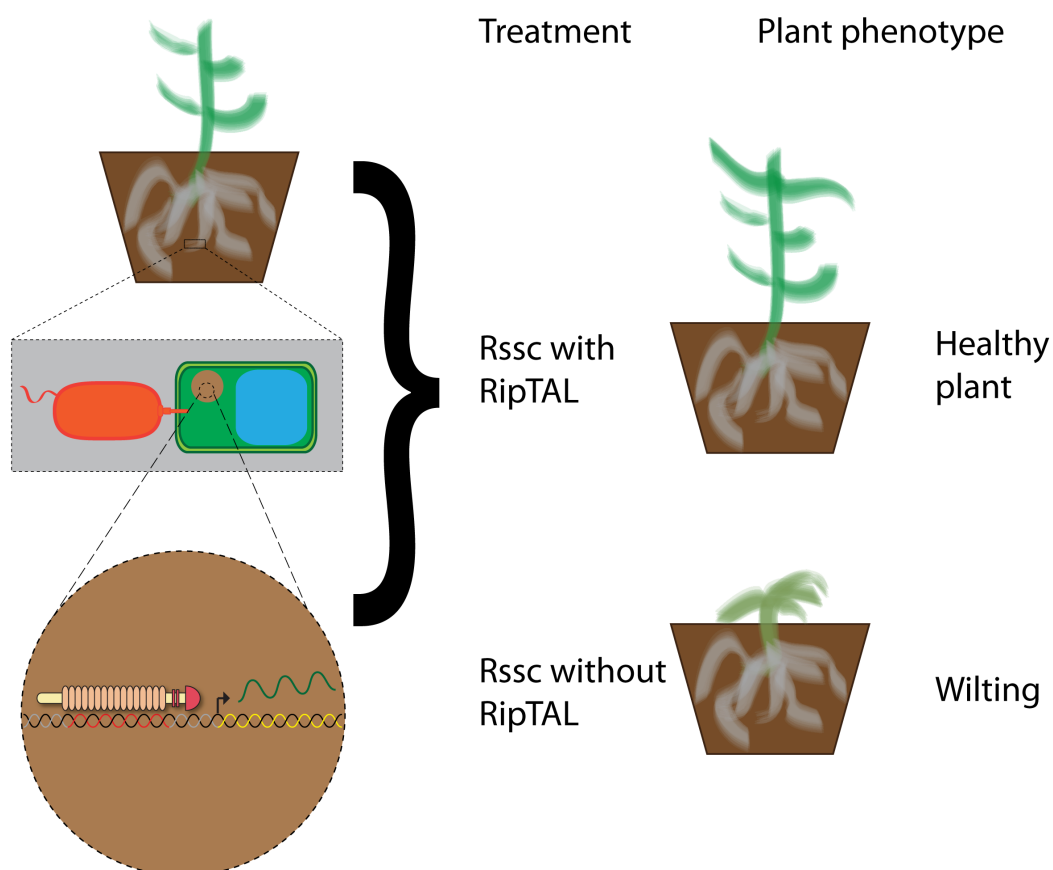


Figure 31. Overview of the engineered resistance concept. To the left, a schematic plant is shown (top), a zoom on the cellular level of infection is shown (middle, grey box), and the binding of a RipTAL to its EBE (red double helix) downstream of a coding sequence (yellow double helix) with the resulting mRNA

in green is shown (bottom, brown circle). To the right the expected plant phenotypes, of plants containing the generated construct, are shown.

2.3.2 Strategy

Research on the promoters activated by certain TALEs from certain *Xanthomonas* strains, has shown that promoters can be expanded to recognize additional TALEs, by the addition of new EBEs to the promoter, increasing spectrum of strains recognized by this *R* promoter (Römer et al. 2009; Hummel et al. 2012). Executor *R* genes are transcriptionally activated by TALEs, and the encoded *R* proteins often elicit a hypersensitive response in the infected tissue (Zhang et al. 2015).

As all known TALE regulated *R* proteins are only known to confer resistance to *Xanthomonas*, their ability to control *Rsc* infection is not predictable. To maximize chances of creating a functional synthetic *R* gene, a combination of different executor CDSs was used. In total four different executor protein CDSs are expressed under the control of a single synthetic promoter. Each of the executor proteins has a unique peptide tag, detectable by commercial antibodies and suitable for expression analysis, e.g. by immuno-blots. Additionally promoter activity can be monitored by expression of superfolder (sf) GFP reporter (Pédrelacq et al. 2006) which is located at the 3' end of the transcript. All CDSs are separated by 2A peptide sequences, which do not successfully form amino bonds during translation by the eukaryotic ribosome, resulting in separate peptide chains in equimolar ratios (Figure 32) (Burén et al. 2012; Sun et al. 2012; Szymczak-Workman et al. 2012).

2.3.3 Composition of the synthetic RipTAL-activated *R* gene.

2.3.3.1 Promoter

The promoter driving the expression of the CDS constitutes the sensor (input) part of the synthetic *R* gene described here. The promoter is based on the well-characterized *Bs3* promoter, found in pepper accession ECW-30R (Römer et al. 2007). This promoter responds to TALE AvrBs3 and is transcriptionally silent in the absence of AvrBs3 (Römer et al. 2007). The *Bs3*

promoter has further been experimentally shown to be transcriptionally silent in a variety of assays and contexts, such as random T-DNA insertion. Two *Bs3* promoter derivatives were designed to recognize RipTALs. Due to high diversity of the *Rssc*, one promoter was designed to recognize strains of *Rssc* phylotypes I & III (corresponds to the species *R. pseudosolanacearum* (Safni et al. 2014)). This promoter is referred to as “p-Narrow”. Additionally, a second promoter derivative was created to recognize RipTALs from across the species complex (“p-Broad”). As nothing was known on biological targets of RipTALs, and therefore no information was available on the natural distance between native *EBEs* it was anticipated that the distance between the RipTAL binding site and the transcriptional start site was similar as for TALEs (Grau et al. 2013). Accordingly, predicted RipTAL *EBEs* were inserted across all 300 bp of the *Bs3*-promoter (Figure 32).

2.3.3.2 Coding sequence

The executor *R* proteins employed span all groups defined by Zhang et al (Zhang et al. 2015), and namely include *Bs3*, *Bs4C*, *Xa10* as well as *Xa27*. Each executor is C-terminally fused to a unique, well-described peptide tag: *Bs3* is 3xFLAG tagged, *Bs4c* was fused to 3xMYC tag, a 3xHA tag decorates *Xa10*, and finally *Xa27* was tagged with 3xV5. All executor CDS are the native ones, with the exception of that of *Xa27*, which was synthesized with an improved dicotyledonous plant codon usage and free of *Typells* restriction sites. Commercial antibodies are available for all of the employed epitopes. All executor *R* protein-tag fusions, are separated by 2A peptides. Each *executor-tag-2A* fusion is considered one *building block* of the coding sequence, resulting in the *building blocks*: *Bs3-3xFLAG-F2A*, *Bs4C-3xMyc-E2A*, *Xa10-3xHA-P2A* and *Xa27-3xV5-T2A* (Table 9).

Building block	Other name used	Combined name (executors only)
pNarrow	PromoterA	-
pBroad	PromoterB	-
<i>Bs3-3xFLAG-F2A</i>	<i>Bs3</i>	All
<i>Bs4C-3xMyc-E2A</i>	<i>Bs4C</i>	
<i>Xa10-3xHA-P2A</i>	<i>Xa10</i>	

<i>Xa27-3xV5-T2A</i>	<i>Xa27</i>	
----------------------	-------------	--

Table 9. Overview of the cloning elements used, and designation of alternative terms used to refer to these.

Downstream of *Xa27-3xV5-T2A* is the sequence of *sfGFP*, with the intron of pepper bs3 (Figure 35, Figure 32). The intron was inserted 120bp after the ATG codon of *sfGFP*. The addition of an intron to the *sfGFP* sequence allows for efficient analysis of mature transcripts, as it will be spliced during mRNA maturation.

In summary, the CDS designed for this synthetic *R* gene allows for control of expression at the transcript and protein level. Analysis of transcripts are facilitated by the use of an intron, allowing for an easy distinction between nucleic acid sequences stemming from the genomic versus processed mRNA sequence. Analysis of protein levels can be conducted using GFP fluorescence for a binary (on/off) expression scoring *in vivo*, and analysis of expression of the individual executor proteins can be performed using the appropriate peptide tags in *in vitro* assays. The concept, divided into Input and both levels of output is shown in Figure 32

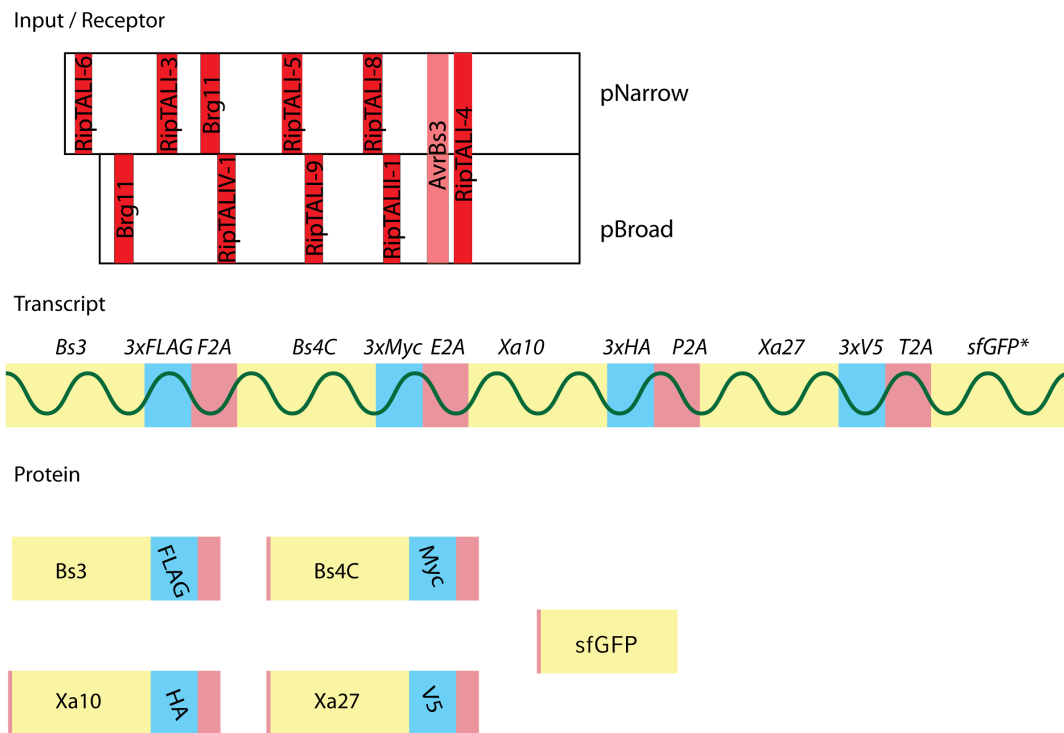


Figure 32. Schematics of input and output components of the synthetic RipTAL immune-receptor. Both promoter variants are shown, with inserted RipTAL EBEs highlighted in red, and the AvrBs3 EBE in light red (top). The transcriptional output, as one single mRNA is shown in the middle, * indicates spliced product. At the bottom, the peptide chains translated from the mRNA are shown. Color code for middle and bottom graphics is yellow: executor *R* protein; blue: peptide tag, light red: 2A peptide.

2.3.3.3 Selection markers, terminator sequences and cloning of the construct

The final part of the RipTAL responsive construct is the *ocs* terminator, to efficiently terminate transcription after transcription of *sfGFP*.

Additionally the DNA sequence flanked by LB and RB (T-DNA sequence) contains the herbicide resistance gene *bar*. *bar* expression confers resistance against the natural herbicide bialaphos and synthetic bialaphos derivatives such as Glufosinate (Basta®), when expressed in plants (Thompson et al. 1987). This gene is constitutively expressed, driven by the NOS promoter and the NOS terminator terminates transcription Figure 33.

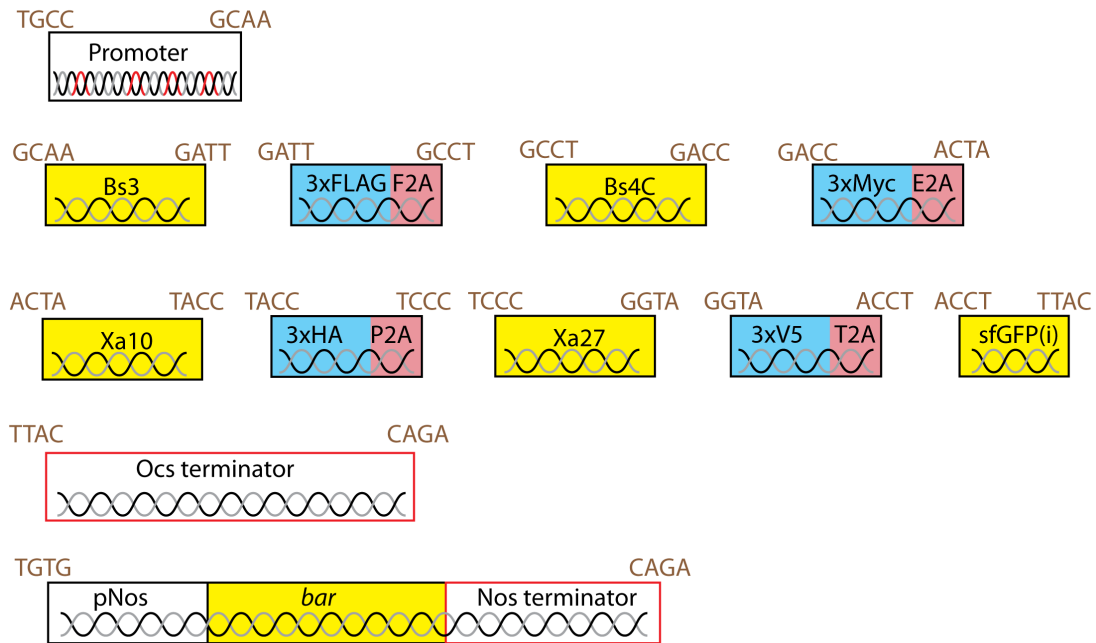


Figure 33. Schematic drawings of level 0 fragments. Yellow background indicates protein coding sequences, (i) indicates intron in the CDS, blue background indicates encoded peptide tags, and pink background indicates 2A peptide encoding sequences. Promoter blocks are framed in black, with no fill, and terminator sequences are framed in red with no fill. Brown text in capital letters shows overlaps generated upon Bsal digestion.

Cloning of this construct was performed using the Golden Gate modular cloning toolkit described by Weber et al. 2011. Xa27 was synthesized by Genscript, free of Bsal and Bpil restriction sites in the protein coding sequence, but flanked by Bsal sites with overlaps generated as depicted in Figure 33. All executors (level 0) were cloned into pUC vectors and internal Bsal or Bpil recognition sites were removed by site directed mutagenesis, if necessary and flanking sites were added by PCR. Subsequently modified cut-ligations were performed into level 1 Icon vectors. These modified cut-ligations were carried out as described (Weber et al. 2011); except that the level 1 Icon vector was digested with Bpil and dephosphorylated prior to Bsal based cut-ligation. All level 1 fragments were sequence verified. The level 1 fragments are shown in Figure 34

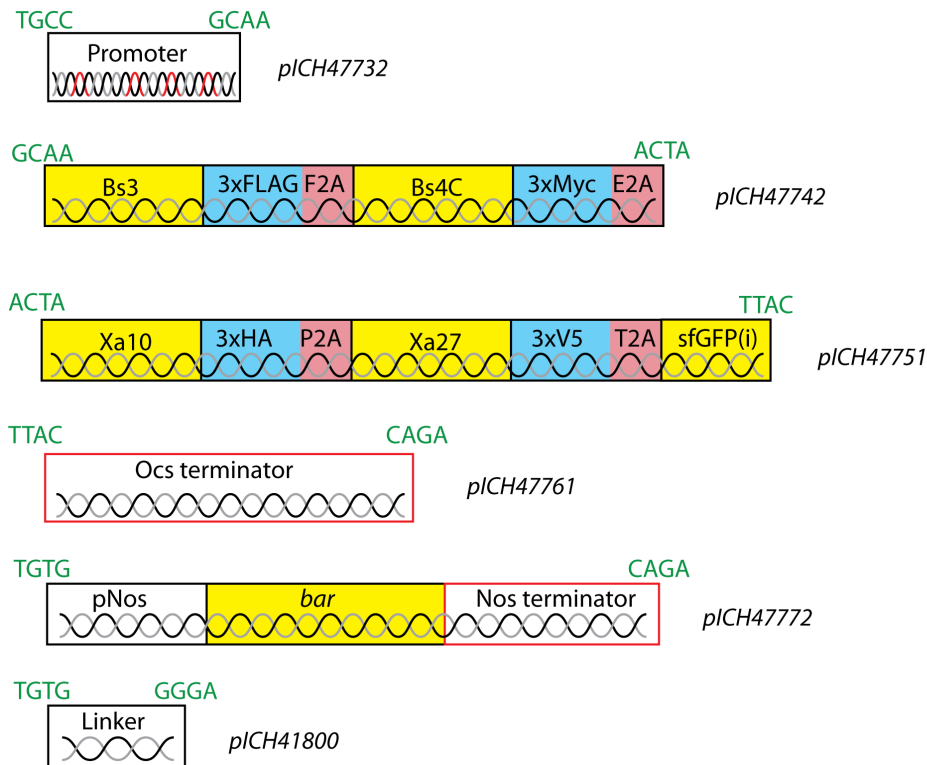


Figure 34. Schematic drawings of level 1 fragments assembled via cut-ligation of level 0 building blocks. Green capital letters indicate overlaps generated upon Bpil digestion, black italicized text gives the level 1 vector the fragments were assembled in. Yellow background indicates protein coding sequences, (i) indicates intron, blue background indicates encoded peptide tags, and pink background indicates 2A peptide encoding sequences. Promoter blocks are framed in black, with no fill, and terminator sequences are framed in red, with no fill. The linker sequence in pICH41800 is identical to the one described in (Weber et al. 2011)

Next, all fragments were cloned into pICH50505 (Weber et al. 2011) by Bpil cut-ligation, and the resulting vector is shown in Figure 35. The herbicide resistance conferring ORF is in inverse orientation in relation to the RipTAL responsive part of the construct, to minimize transcription of the *R* protein *building blocks* from any constitutive promoter in the construct. As a secondary precautionary measure, the constitutively expressed part was inserted in such a way that the RipTAL-inducible promoter and the constitutive promoter are as far physically separated as possible, and insulated by two inversely oriented transcription terminator sequences (Figure 35).

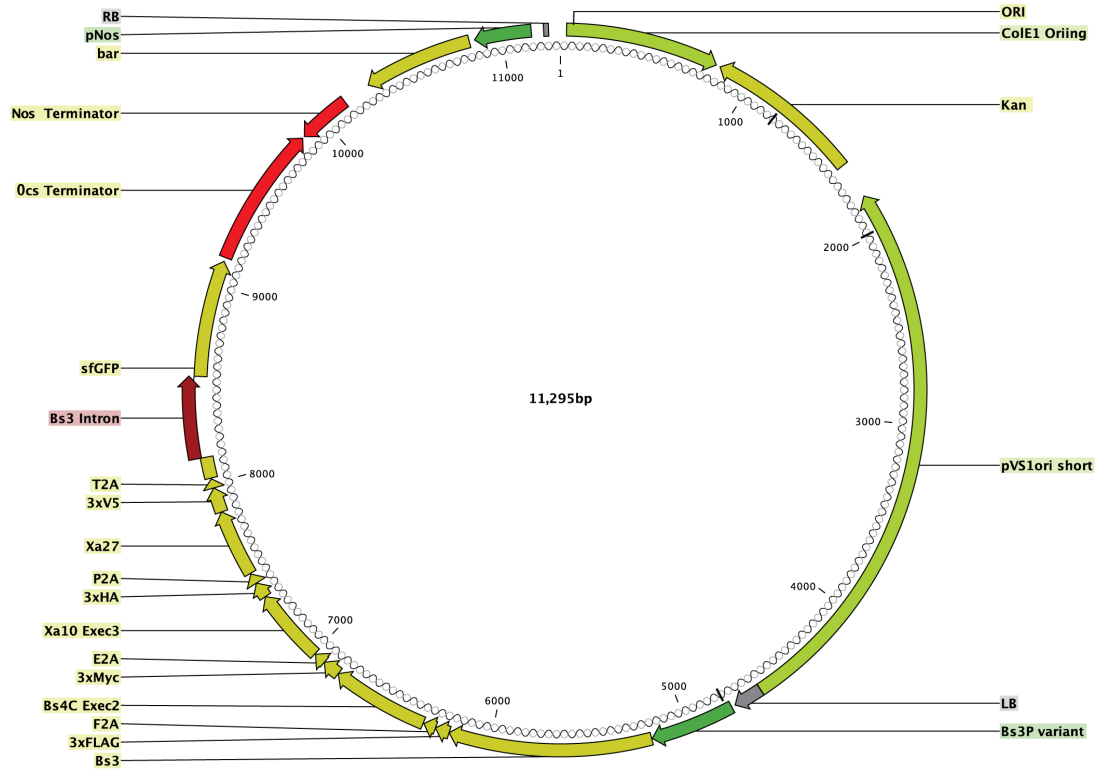


Figure 35. Vector map of the final RipTAL receptor construct assembled into vector pICH50505. Translated sequences are shown in yellow, introns in dark red, terminator sequences is bright red, promoters are annotated in dark green, bacterial origin of replications are depicted in light green and tDNA border sequences are annotated with RB and LB in grey.

To allow for further downstream investigation of the contribution of each executor R protein to RipTAL mediated resistance against Rssc strains, constructs were generated which only contain one *building block*, and therefore only one (executor) R gene. The constructs encoding for only one individual executor are otherwise identical to the construct described above (Figure 35).

Individual executor constructs, containing only one of the four *building blocks*, were derived from the construct containing all four building blocks by inFusion cloning (ClonTech), as depicted in Figure 36. All other parts of the construct are retained as in given in Figure 35.

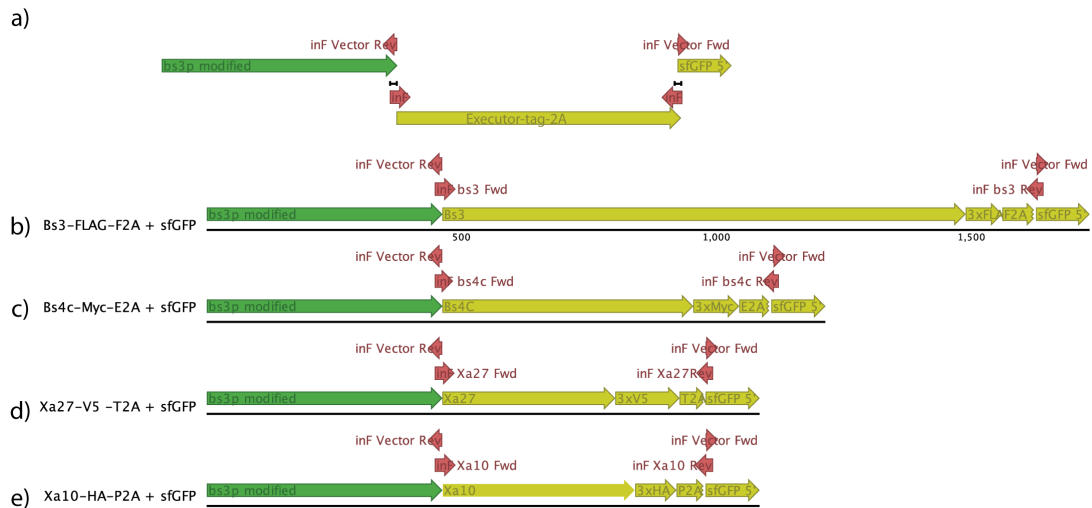


Figure 36. Cloning of individual executor variants from the full construct. a) Overview of the inFusion based cloning strategy. The vector backbone, including the promoter (green) and sGFP (sequence 5' of the intron is shown, yellow), is amplified with inF Vector primers (red), and the *building block* is amplified with inF primers as shown in b-e. Black bars indicate 15basepair overlaps between the two DNA fragments, required for inFusion cloning. b) cloning strategy for *Bs3-3xFLAG-F2A*. c) Cloning of *Bs4C-3xMyc-E2A*. d) Cloning of *Xa27-3xV5-T2A*. e) Cloning strategy for *Xa10-3xHA-P2A*. Number of bases is indicated in b, c-e are scaled identical to b.

2.3.4 Functional validation of hypersensitive response elicitation

To functionally validate the induction of the synthetic receptors described in the previous sections, all generated receptor constructs were analyzed in transient transformation assays in *N. benthamiana* leaves. *A. tumefaciens* strains transformed with a receptor construct were co-infiltrated with strains transformed with t-DNA vectors containing a TALE or RipTAL CDS downstream of a 35S promoter.

Promoter	Executor	TAL-like
A (pNarrow)	All	AvrBs3
A (pNarrow)	All	RipTALIV-1
A (pNarrow)	All	RipTALI-8
B (pBroad)	All	AvrBs3
B (pBroad)	All	RipTALIV-1
B (pBroad)	All	RipTALI-8
A (pNarrow)	Bs3	AvrBs3

A (pNarrow)	Bs3	RipTALIV-1
A (pNarrow)	Bs3	RipTALI-8
B (pBroad)	Bs3	AvrBs3
B (pBroad)	Bs3	RipTALIV-1
B (pBroad)	Bs3	RipTALI-8
A (pNarrow)	Bs4C	AvrBs3
A (pNarrow)	Bs4C	RipTALIV-1
A (pNarrow)	Bs4C	RipTALI-8
B (pBroad)	Bs4C	AvrBs3
B (pBroad)	Bs4C	RipTALIV-1
B (pBroad)	Bs4c	RipTALI-8
A (pNarrow)	Xa10	AvrBs3
A (pNarrow)	Xa10	RipTALIV-1
A (pNarrow)	Xa10	RipTALI-8
B (pBroad)	Xa10	AvrBs3
B (pBroad)	Xa10	RipTALIV-1
B (pBroad)	Xa10	RipTALI-8
A (pNarrow)	Xa27	AvrBs3
A (pNarrow)	Xa27	RipTALIV-1
A (pNarrow)	Xa27	RipTALI-8
B (pBroad)	Xa27	AvrBs3
B (pBroad)	Xa27	RipTALIV-1
B (pBroad)	Xa27	RipTALI-8

Table 10. Promoter-Executor and TAL-like elicitor combinations infiltrated into *N. benthamiana* leaves for conductivity measurements.

All combinations shown in Table 10 were infiltrated in one older and one younger leaf. 48 hours after infiltration, leave discs were harvested using a cork borer and ion leakage was monitored using a CM100-2 multiple cell conductivity meter (Reid & Associates, Glenwood South Africa) over 72hours with hourly conductivity measurements.

Data were retrieved from the machine and plotted over time (Figure 37, Tables S4.1-S4.3).

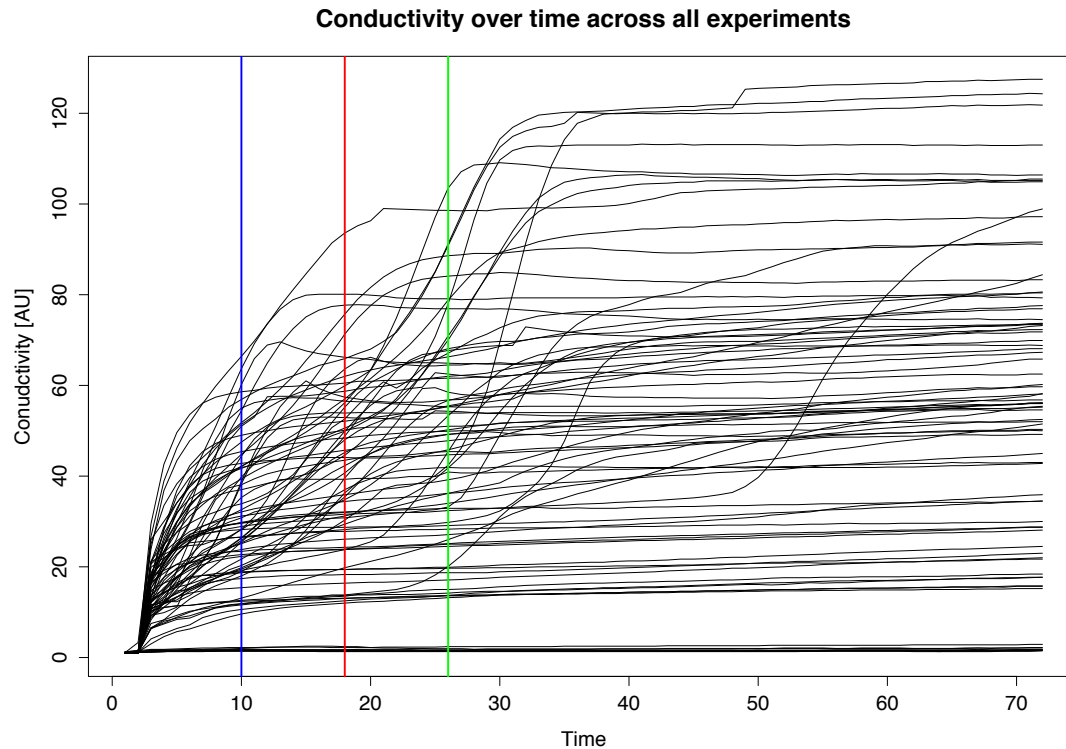


Figure 37. Conductivity plot of all leaf discs over 72 hours. Blue vertical line marks 10h time-point, red vertical line marks 18h time-point and green vertical line marks 26h time-point used in subsequent analysis.

For subsequent statistical evaluation, the 10h, 18h and 26h measurements were fitted to a generalized linear regression model, and analyzed using ANOVA regarding influence of Promoter, Executor, TAL-like effector used as an elicitor and leaf age on the observed conductivity, with the results shown below.

Output of ANOVA analysis for the 10 hour time-point:

```
anova(glm(Conduc[1:60,10]~Executor+Effector+Promoter+Age, data=Conduc[1:60,]),test="F")

## Analysis of Deviance Table
##
## Model: gaussian, link: identity
##
## Response: Conduc[1:60, 10]
##
## Terms added sequentially (first to last)
##
```

```
##
##           Df Deviance Resid. Df Resid. Dev      F    Pr(>F)
## NULL                    59      10639.0
## Executor  4   2838.48      55       7800.6  5.6107  0.0008043 ***
## Effector  2   1233.55      53       6567.0  4.8766  0.0115351 *
## Promoter  1     1.09      52       6565.9  0.0086  0.9262811
## Age       1    115.65      51       6450.3  0.9144  0.3434640
## ---
## Signif. codes:  0 '***' 0.001 '**' 0.01 '*' 0.05 '.' 0.1 ' ' 1
```

Output of ANOVA analysis for the 18 hour time-point:

```
anova(glm(Conduc[1:60,18]~Executor+Effector+Promoter+Age, data=Conduc[1:60,]),test="F")
```

```
## Analysis of Deviance Table
##
## Model: gaussian, link: identity
##
## Response: Conduc[1:60, 18]
##
## Terms added sequentially (first to last)
##
##
##           Df Deviance Resid. Df Resid. Dev      F    Pr(>F)
## NULL                    59      18919
## Executor  4   3772.5      55      15147  3.6166  0.01139 *
## Effector  2   1625.4      53      13521  3.1165  0.05285 .
## Promoter  1     62.4      52      13459  0.2394  0.62675
## Age       1    159.4      51      13300  0.6113  0.43791
## ---
## Signif. codes:  0 '***' 0.001 '**' 0.01 '*' 0.05 '.' 0.1 ' ' 1
```

Output of ANOVA analysis for the 26 hour time-point:

```
anova(glm(Conduc[1:60,26]~Executor+Effector+Promoter+Age, data=Conduc[1:60,]),test="F")

## Analysis of Deviance Table
##
## Model: gaussian, link: identity
##
## Response: Conduc[1:60, 26]
##
## Terms added sequentially (first to last)
##
##
##           Df Deviance Resid. Df Resid. Dev      F Pr(>F)
## NULL                    59      29260
## Executor  4    7160.8      55    22099 4.2928 0.004537 **
## Effector  2     707.6      53    21392 0.8483 0.434080
## Promoter  1     111.0      52    21281 0.2661 0.608180
## Age       1      12.3      51    21268 0.0296 0.864154
## ---
## Signif. codes:  0 '***' 0.001 '**' 0.01 '*' 0.05 '.' 0.1 ' ' 1
```

These statistical analyses reveal that the significance of certain predictors defined for these analysis changes dependent on the time-point chosen for analysis. It could be observed that, independent of time-point, the choice of Executor(s) appears to be the most significant predictor on the measured conductivity. As it is known that different executors are likely to use different cellular pathways to elicit HR (Zhang et al. 2015), this may be an indication that these differences can be measured through conductivity, which relates to ion release from the leaf disc used in the measurement. In particular, it is known that Xa27 does not elicit HR like the other executors employed do, but instead confers resistance to bacteria through other, unknown, means (Wu et al. 2008). From the summary statistics of the generalized linear model at any time-point it becomes evident that within the executors used, Xa27 appears to be responsible for most of the variance observed within the measurements

performed. This can be seen in the summary statistics shown below, for the 18 hour time-point:

```
summary(glm(Conduc[1:60,18]~Executor+Effector+Promoter+Age, data=Conduc[1:60,]))

##
## Call:
## glm(formula = Conduc[1:60, 18] ~ Executor + Effector + Promoter +
##      Age, data = Conduc[1:60, ])
##
## Deviance Residuals:
##      Min        1Q    Median        3Q        Max
## -43.410  -10.311   -0.822   11.804   38.520
##
## Coefficients:
##              Estimate Std. Error t value Pr(>|t|)
## (Intercept)      44.492      6.254   7.114 3.6e-09 ***
## Executor Bs3      -7.125      6.593  -1.081  0.2849
## Executor Bs4C     -3.058      6.593  -0.464  0.6447
## Executor Xa10      9.817      6.593   1.489  0.1426
## Executor Xa27     13.958      6.593   2.117  0.0391 *
## Effector RipTALI-8 -12.430      5.107  -2.434  0.0185 *
## Effector RipTALIV-1 -8.670      5.107  -1.698  0.0956 .
## Promoter B         2.040      4.170   0.489  0.6268
## AgeYoung           3.260      4.170   0.782  0.4379
## ---
## Signif. codes:  0 '***' 0.001 '**' 0.01 '*' 0.05 '.' 0.1 ' ' 1
##
## (Dispersion parameter for gaussian family taken to be 260.7737)
##
##      Null deviance: 18919  on 59  degrees of freedom
## Residual deviance: 13299  on 51  degrees of freedom
## AIC: 514.34
##
## Number of Fisher Scoring iterations: 2
```

Besides the significant influence of the expressed executor on all samples, for the earlier time-points (10h, 18h) the choice of effector used for transcriptional activation seems to account for some of the observed variance, with a decrease in significance over time and it appears that the use of RipTALI-8 accounts for some additional variance. However, it is important to note here that the analysis presented here was performed across both promoters, which are likely to respond differentially to the different RipTALs employed. Promoter A is not expected to respond to RipTALIV-1, but only to RipTALI-8, while for promoter B the opposite behavior is expected. However, both promoters should be responsive to AvrBs3 (Figure 32).

Yet, the choice of promoter, or leaf age, does not appear to significantly influence the measured conductivity across the full dataset.

To understand, how the choice of effector may affect the measured conductivity, the dataset was split by promoter (A (pNarrow) or B (pBroad)) and subsequently both datasets were inspected using ANOVA on a generalized linear model, as previously. ANOVA for both promoters for time-points 10 and 18hrs confirmed significant influence of effectors across all measurements. Leaf age appeared to significantly account for some variance at 18hrs with promoter B.

Inspection of the summary statistics of all generalized linear models generated for the promoter variants indicated that RipTALI-8 significantly influences the conductivity measurements at the 10 hour time-point of constructs containing promoter A (pNarrow). These summary statistics are shown below.

```
summary(glm(Conduc.pA[,10]~Executor+Effector+Age, data=Conduc.pA))  
  
##  
## Call:  
## glm(formula = Conduc.pA[, 10] ~ Executor + Effector + Age, data =  
##   Conduc.pA)  
##  
## Deviance Residuals:  
##      Min       1Q   Median       3Q      Max   
## -25.113   -5.392    1.210    4.622   21.253
```

```

##
## Coefficients:
##              Estimate Std. Error t value Pr(>|t|)
## (Intercept)      47.747      6.163   7.747  1e-07 ***
## Executor Bs3     -11.300      6.891  -1.640  0.1153
## Executor Bs4C    -10.467      6.891  -1.519  0.1430
## Executor Xa10      1.967      6.891   0.285  0.7780
## Executor Xa27      3.567      6.891   0.518  0.6099
## Effector RipTALI-8 -12.860      5.338  -2.409  0.0248 *
## Effector RipTALIV-1 -9.880      5.338  -1.851  0.0776 .
## AgeYoung         -8.800      4.358  -2.019  0.0558 .
## ---
## Signif. codes:  0 '***' 0.001 '**' 0.01 '*' 0.05 '.' 0.1 ' ' 1
##
## (Dispersion parameter for gaussian family taken to be 142.4575)
##
##      Null deviance: 5827.9  on 29  degrees of freedom
## Residual deviance: 3134.1  on 22  degrees of freedom
## AIC: 242.6
##
## Number of Fisher Scoring iterations: 2

```

However, the statistical analysis on the sub-setted dataset may not be very powerful, as the number of samples is halved, and therefore these interpretations should be taken with caution.

Besides performing conductivity measurements on leaf discs of leaves infiltrated as given in Table 10, HR was assessed visually on a different set of infiltrated leaves. The results from the visual assessment of HR are given in Table 11

Construct	TALE(-like)	HR
A:All	AvrBs3	++
A:All	Brg11	+-
B:All	AvrBs3	++
B:All	Brg11	+-
A:Bs3	AvrBs3	+
A:Bs3	Brg11	+

B:Bs3	AvrBs3	++
B:Bs3	Brg11	+
pBs4c:Bs4C	AvrBs4	+
A:Bs4C	AvrBs3	++
A:Bs4C	Brg11	+
B:Bs4C	AvrBs3	++
B:Bs4C	Brg11	-
A:Xa10	AvrBs3	+
A:Xa10	Brg11	+ -
B:Xa10	AvrBs3	++
B:Xa10	Brg11	+ -
A:Xa27	AvrBs3	-
A:Xa27	Brg11	-
B:Xa27	AvrBs3	-
B:Xa27	Brg11	+ -
-	AvrBs3	-
A:All	AvrBs4	-
B:All	AvrBs4	-
-	Brg11	-
-	AvrBs4	-

Table 11. Visual HR assessment on *N. benthamiana* leaves as shown. HR was scored on a scale from - (no) to ++(very strong). +- indicates cell death reaction, which could not be clearly identified as HR. pBs4c:Bs4C was described in (Strauss et al. 2012).

Generally, it appears that conductivity measurements can be used to approximate HR, and further it appears that all synthetic receptor constructs are able to elicit HR, with the exception of the construct containing *Xa27* only.

2.3.5 Plant lines generated and project continuation

All constructs in *pICH50505* were transformed into *A. tumefaciens* strain GV3101 and transgenic plant lines were generated. Both promoter variants of the construct containing all *building blocks* were transformed into *S. lycopersicum* cv. *Heinz* by cotyledon transformation in collaboration with the ZMBP transformation facility. All ten generated constructs (containing all *building blocks*, individual *building block* constructs, with both promoters) were transformed into *A. thaliana* Col-0 plants by floral dipping. Transgenic offspring were selected using Basta®. Lines were propagated to the stage given in Table 12. All constructs, bacterial strains, plant lines and seeds generated in this project as well as the analysis tools described in 2.2.1.3 were handed over to Patrizia Ricca in April 2015 for subsequent studies.

Plant background transformed	Construct used	Line designation	Comment
<i>S. lycopersicum</i> cv. Heinz	pICH50505 pNarrow All executors	200 #11.5	Seeds from transformed plants
		200 #11.5	Seeds from transformed plants
		200 #15.2	Seeds from transformed plants
		200 #15.2	Seeds from transformed plants
		200 #15.2	Seeds from transformed plants
		200 #15.2f	Seeds from transformed plants
		200 #15.2m	Seeds from transformed plants
		200 #22.1	Seeds from transformed plants
		200 #22.3	Seeds from transformed plants
		200 #22.4	Seeds from transformed plants
		200 #29	Seeds from transformed plants
		200 #36	Seeds from transformed plants
		200 #39.5	Seeds from transformed plants
		200 #41	Seeds from transformed plants
		200 #41	Seeds from transformed plants
		200 #60.3	Seeds from transformed plants
		200 #60.4	Seeds from transformed plants
200 #61	Seeds from transformed plants		
<i>S. lycopersicum</i> cv. Heinz	pICH50505 pBroad All executors	201 #1.3	Seeds from transformed plants
		201 #1.3	Seeds from transformed plants
		201 #1.4	Seeds from transformed plants
		201 #1.4	Seeds from transformed plants

		201 #1.4	Seeds from transformed plants
		201 #10	Seeds from transformed plants
		201 #10	Seeds from transformed plants
		201 #10	Seeds from transformed plants
		201 #11.1	Seeds from transformed plants
		201 #13.1	Seeds from transformed plants
		201 #14	Seeds from transformed plants
		201 #15.3	Seeds from transformed plants
		201 #19	Seeds from transformed plants
		201 #20.1	Seeds from transformed plants
		201 #20.1	Seeds from transformed plants
		201 #24	Seeds from transformed plants
		201 #24.1	Seeds from transformed plants
		201 #26.1	Seeds from transformed plants
		201 #4.4	Seeds from transformed plants
		201 #4.4	Seeds from transformed plants
		201 #5.2	Seeds from transformed plants
		201 #6	Seeds from transformed plants
		201 #6	Seeds from transformed plants
		201 #6.1	Seeds from transformed plants
		201 #8.2	Seeds from transformed plants
		201 #8.2	Seeds from transformed plants
		201 #11.4	Seeds from transformed plants

		200 #39.3	Seeds from transformed plants
<i>A. thaliana</i> Col-0	pICH50505 pNarrow All executors	A 1-1	T2 seeds Offspring of line A1 (T1)
		A 1-2	
		A 1-3	
		A 1-4	
		A 1-5	
		A 1-6	
		A 1-7	
		A 1-8	
		A 1-9	
		A 1-10	
<i>A. thaliana</i> Col-0	pICH50505 pNarrow All executors	A 2-1	T2 seeds Offspring of line A2 (T1)
		A 2-2	
		A 2-3	
		A 2-4	
		A 2-5	
		A 2-6	
		A 2-7	
		A 2-8	
		A 2-9	
		A 2-10	
<i>A. thaliana</i> Col-0	pICH50505 pBroad All executors	B 2-1	T2 seeds Offspring of line B2 (T1)
		B 2-2	
		B 2-3	
		B 2-4	
		B 2-5	
		B 2-6	
		B 2-7	
		B 2-8	
		B 2-9	
		B 2-10	
<i>A. thaliana</i> Col-0	pICH50505 pBroad All executors	B 3-1	T2 seeds Offspring of line B3 (T1)
		B 3-2	
		B 3-3	
		B 3-4	
		B 3-5	
		B 3-6	
		B 3-7	
		B 3-8	
		B 3-9	
		B 3-10	
<i>A. thaliana</i> Col-0	pICH50505 pBroad	B 4-1	T2 seeds Offspring of line B4 (T1)
		B 4-2	

	All executors	B 4-3	
		B 4-4	
		B 4-5	
		B 4-6	
		B 4-7	
		B 4-8	
		B 4-9	
		B 4-10	
<i>A. thaliana</i> Col-0	pICH50505 pBroad All executors	B 5-1	T2 seeds Offspring of line B5 (T1)
		B 5-2	
		B 5-3	
		B 5-4	
		B 5-5	
		B 5-6	
		B 5-7	
		B 5-8	
		B 5-9	
		B 5-10	
<i>A. thaliana</i> Col-0	pICH50505 pNarrow Bs3	A-Bs3 1	Basta resistant offspring of dipped plants, handed over before seed harvesting
<i>A. thaliana</i> Col-0	pICH50505 pNarrow Bs4C	A-Bs4C 1	Basta resistant offspring of dipped plants, handed over before seed harvesting
		A-Bs4C 2	
		A-Bs4C 3	
<i>A. thaliana</i> Col-0	pICH50505 pNarrow Xa10	A-Xa10 1	Basta resistant offspring of dipped plants, handed over before seed harvesting
		A-Xa10 2	
<i>A. thaliana</i> Col-0	pICH50505 pNarrow Xa27	A-Xa27 1	Basta resistant offspring of dipped plants, handed over before seed harvesting
		A-Xa27 2	
		A-Xa27 3	
		A-Xa27 4	
		A-Xa27 5	
		A-Xa27 6	
		A-Xa27 7	
<i>A. thaliana</i> Col-0	pICH50505 pBroad Bs3	B-Bs3 1	Basta resistant offspring of dipped plants, handed over before seed harvesting
<i>A. thaliana</i> Col-0	pICH50505 pBroad Bs4C	none	No Basta resistant offspring obtained from dipped plants.
<i>A. thaliana</i> Col-0	pICH50505 pBroad Xa10	B-Xa10 1	Basta resistant offspring of dipped plants, handed over before seed harvesting
		B-Xa10 2	
		B-Xa10 3	
		B-Xa10 4	
		B-Xa10 5	

		B-Xa10 6	
<i>A. thaliana</i> Col-0	pICH50505 pBroad Xa27	B-Xa27 1	Basta resistant offspring of dipped plants, handed over before seed harvesting
		B-Xa27 2	

Table 12. Transgenic plant lines generated as part of this project

3 Discussion

3.1 RipTALs are part of the accessory effectome in Rssc

3.1.1 Abundance, distribution and phylogeny of RipTALs in the Rssc indicates monophyletic origin

ripTAL abundance between phlotypes differs (Figure 5), with *ripTALs* being prevalent in phlotypes I and IV, and less frequent in phlotypes II and III. Generally, the absence from several strains indicates that *ripTALs* are not part of the core Rssc effectome, but instead are part of the accessory effectome of the species complex (Peeters, Carrère, et al. 2013).

Others have previously suggested that *ripTALs* in the Rssc are the result of horizontal gene transfer of *TALEs* from *Xanthomonas* strains (Salanoubat et al. 2002; Heuer et al. 2007; Peeters, Carrère, et al. 2013). These suggestions were based on evidence such as an alternative codon usage region (ACUR) partially overlapping with the GMI1000 *rsc1815* (*ripTALI-1_{GMI1000}*) locus (Salanoubat et al. 2002; Heuer et al. 2007). Additionally it has been noted that *ripTALI-1_{GMI1000}* contains three putative Crossover hotspot instigator (CHI) sites and has been shown to exhibit an increased recombinatorial rate (Fall et al. 2007). However, the ACUR partially overlapping with *rsc1815* is in an inverse orientation to the *rsc1815* ORF, and only overlaps in the first 500 bases of the *rsc1815* sequence (Salanoubat et al. 2002). Further, *ripTALs* can be found across all Rssc phlotypes (Figure 5), and the sequence similarities of NTRs and CTRs within and between classes (Figure 6) fit to the general genome identities found for Rssc strains from different phlotypes. For example, RipTAL classes I and III are most similar, as are phlotypes I and III within the Rssc (Wicker et al. 2012). Further, a close correlation between RipTAL RVD composition and strain sequevar can be observed (Figure 7), indicating that these effectors co-evolve with the genome they are located in, and generally abide to strain phylogeny. These observations are consistent with a *ripTAL* ancestor in the last common ancestor of the Rssc, which probably predates the fragmentation of

Gondwana into modern continents (Wicker et al. 2012), and subsequent *ripTAL* diversification in the geographically separated phylotypes. This is further supported by the GC content of *ripTALs*, which matches well to the overall GC content of Rssc genomes (around 66%, Remenant et al. 2010).

3.1.2 RipTALs in comparison to other Rips

Generally, the picture observed for the abundance of *ripTALs* within and between phylotypes fits to the general picture reported for Rips (Peeters, Carrère, et al. 2013). About half to two thirds of Rips are conserved between strains found in the species complex, when compared across phylotypes. This number can drastically change depending on the distance between the analyzed strains (Peeters, Carrère, et al. 2013). For example, between Phylotype I, II and IV strains, 46 out of 71-72 Rips found per strain are conserved across all strains (Peeters, Carrère, et al. 2013). As one would expect, between closely related strains, more Rips are conserved. Strains Psi07 and BDBR229, both belong to phylotype IV, have markedly different host preferences but are near identical on the genome level (Remenant et al. 2011). Yet, out of the 56 BDB R229 effectors annotated, 52 are also found in Psi07 (Peeters, Carrère, et al. 2013). However, any attempts to link *rip* repertoire directly to strain host range have failed to provide any meaningful insights (Peeters, Carrère, et al. 2013). It thus may well be that subtle differences in *Rip* sequence influence their action in host cells.

3.1.3 Functional overlap between RipTALs indicates role in host adaptation

As discussed above, so far no clear-cut correlations between *rips* and strain host range have been established. Superficially, the same picture emerges for *RipTAL* bearing strains. Strains containing a *ripTAL* can be found across all phylotypes (Figure 5), and the host ranges of the strains containing *ripTALs* range from broad host range strains able to infect many solanaceous hosts (phylotypes I and III, and IV-10) to strains able to infect both, tomato and banana (Moko disease causing phylotype II strain Molk2), to those exhibiting

a remarkable degree of host specialization (Blood disease bacterium strains, phylotype IV-10-BDB) (Figure 7) (Remenant et al. 2010; Genin and Denny 2012; Ailloud et al. 2015).

However, the detailed molecular characterization of overlaps in *in planta* reporter activation (Figure 12), has unveiled significant overlap in EBE activation by certain RipTALs. RipTALs from broad host range strains belonging to phylotype I and III, largely overlap in their activated sequences, possibly indicating a shared host target gene (Figure 12). As these RipTALs generally have similar CRDs, this is result is in-line with expectations. But, RipTALII-1 and RipTALIV-2, both from banana infecting strains, are able to activate the predicted EBE of RipTALIV-2, which based on a comparison of the CRDs (Figure 7) and aligned EBEs (Figure 10b) was not anticipated. This observed overlap can be explained by a close inspection of the CRDs, and predicted EBEs. As shown in Figure 38, RipTALII-1 may be able bind to EBE_RipTALIV-1 with an offset of +2, relative to RipTALIV-2 and thereby activate the reporter. Reciprocal activation of EBE_RipTAL-II-1 by RipTALIV-2 with an offset of -2 was not observed. This may be explained by the NTR mediated requirement of a Guanosine base at position 0, which is not fulfilled (Figure 10, Figure 38) (de Lange et al. 2013).

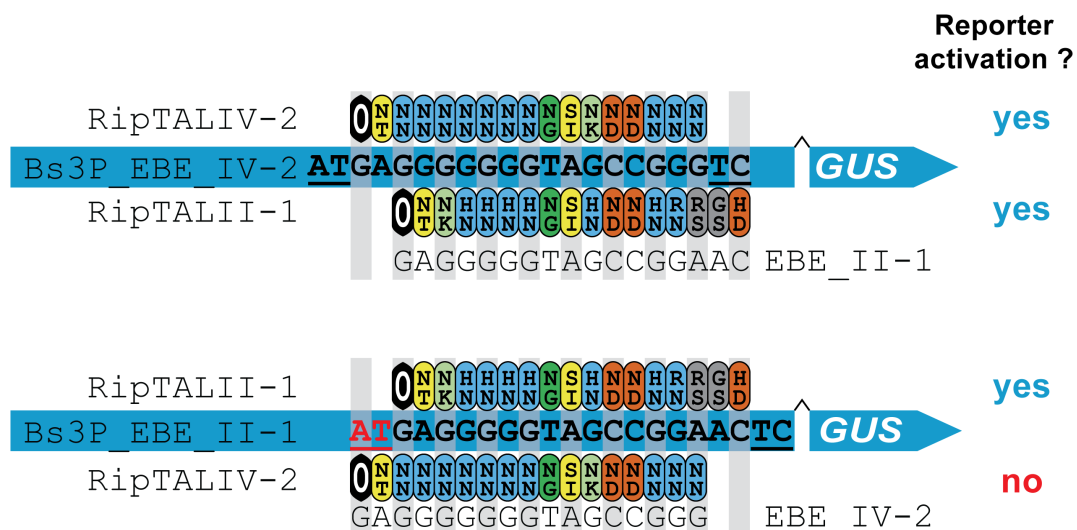


Figure 38. Reciprocal reporter activation by RipTALII-1 and RipTALIV-2. Each EBE is shown in the context of the reporter construct used (blue background, underlined bases are part of the bs3 promoter), with the best possible matching of each RipTAL shown. Successful binding leads to reporter activation. Bases discriminated against by the lower RipTAL are highlighted in red.

This unexpected overlap in sequence activation by RipTALs found in distantly related, geographically separated strains independently evolved to non-solanaceous hosts of the *Musa* family, indicates functional convergence of these effectors on a common host target, despite divergence in their CDSs.

Taken together, the results summarized in Figure 12 lend credence to the previously formulated hypothesis that RipTALs are involved in host adaptation, in a CRD dependent manner (Heuer et al. 2007), which was based solely on the observed number of RipTAL repeats and strain host range, but did not consider factors such as RVD composition. The role of RipTALs in host adaptation, and the characterization of evolutionary mechanisms driving RipTAL diversity (Figure 19, Figure 20, Figure 21, Figure 22) warrant a discussion of the evolutionary and adaptive characteristics of TALE-like effectors.

3.2 Evolutionary constraints of TALE-like effectors

3.2.1 Analysis of repetitive sequences in an evolutionary context

RipTALs and TALEs, are directly injected into the host cell. This facilitates molecular co-evolution of these effectors and host genes, such as host *R* genes. TALE-likes are inherently modular proteins, conceptually divided into NTR, CRD and CTR. The CRD itself is made up of modular repeat units, which can be shuffled and mutated to create new DNA targeting preferences. The high sequence similarities, in particular of TALEs, makes *a posteriori* definitions of natural breakpoints for recombinatorial processes within *repeat* arrays near impossible, as virtually all residues are conserved across *repeats* (Figure 14, Figure 16). Therefore, most recombinatorial events would lead to seamless integration, irrespective of position, with the exception of the RVD. However, as long as the resulting RVD is within the expectations of the observer, even recombinatorial events leading to RVD changes cannot be unambiguously distinguished from any other recombination event.

In practical terms, any breakpoint defined as the *repeat* boundary is equally arbitrary and while informed choices of functional units can be made on the

protein level based on structural information, this knowledge is unlikely to be available to the mechanisms driving the diversification of TALE-like *repeat* arrays on the nucleotide level. Therefore, shifting of the start of a *repeat* unit along the repeated sequence, should not strongly influence the outcome of any sequence based analysis performed on *repeat* arrays, as the total number of informative residues contained in the window defined by the *repeat* length does not change when the window is shifted along the repetitive stretch, with the exception of border effects at the end of the repetitive sequence stretch. However, in TALE-likes the CRD is flanked by non-canonical repeats (Mak et al. 2013), which slightly reduces the influence of border effects on the sequence similarities obtained. Therefore any analysis performed based on sequence similarities of *repeat* units should produce similar results regardless of the offset of the window used to define the start and end of *repeats*, justifying the use of the *ripTAL repeat* sequences annotated on the basis of *TALE repeats* throughout this work. As shown in Figure 19, Figure 20, Figure 21 and Figure 22 the comparatively high number of *repeat* specific polymorphisms found in *ripTALs*, allows for the formulation of specific mechanisms driving *ripTAL* diversity.

3.2.2 RipTALs provide an angle to trace evolutionary mechanisms acting on TALEs

In total four different traces of (functionally) diversifying mechanisms could be deduced from a comparison of RipTAL *repeats*. Namely, these are SNP accumulation in *RVD codons* (Figure 20), recombinatorial events encompassing multiple *repeats* (Figure 19), segmental gene conversion of individual *repeats* (Figure 21), and *repeat* duplication (or loss) by slipped strand mis-pairing (Figure 22). These mechanisms will be discussed in detail in the context of TALEs, the only other class of TALE-likes known to be directly involved as effectors in host-pathogen interactions.

SNP occurrence in *RVD* residues can lead to a complete switch in target specificity. Exchange of RVDs, in particular the second RVD residue (position 13), can change the base recognized by the repeat affected by that mutation (de Lange, Binder, et al. 2014). Often, exchange of a single nucleotide can switch the specificity of a repeat, for example, amino acid aspartic acid (D) at

position 13 confers a strong Cytosine base for that repeat, while amino acid asparagine (N) at the same position confers a strong Guanosine preference (Miller et al. 2015). Yet, assuming that aspartic acid is encoded by a GAT codon, only a single mutation at codon position one, could give rise to an AAT codon, encoding asparagine, and lead to a specificity switch of the protein. It appears reasonable that many of the residues of the structural helical scaffold of an repeat are under stabilizing selection, as interactions between helices of TALE repeats are not limited to one repeat, but these interactions structurally stabilize the whole repeat array (Bochtler 2012). While, as long as transcriptional activation of the bound sequence entails a fitness benefit, the RVD should also be under stabilizing selection, mutations in a TALE, which lead to new beneficial targeting, should be under directional selection. It is important to note here that *TALEs* are often multi-copy in *Xanthomonas* (Booher et al. 2015; Pérez-Quintero et al. 2015; Wilkins et al. 2015), thereby enabling neo-functionalization of redundant *TALEs* without affecting fitness benefits of other *TALEs*. In summary, the occurrence of SNPs, especially at *RVD* positions is likely to contribute to *TALE* diversification.

Figure 19 shows how a recombination event, encompassing multiple *repeats*, leads to the loss of *repeats* from a *CRD*. Mechanistically, this may be the result of a large slipped strand mis-pairing event encompassing multiple repeats, or it might be facilitated by other cellular components such as *recA* (Bzymek and Lovett 2001). Strikingly, this event is in-frame, resulting in a full RipTAL that is functionally deprecated, as it is unable to bind DNA (de Lange et al. 2013). Interestingly, similar *CRDs* containing only few *repeats* have been reported for *TALEs* (Booher et al. 2015; Pérez-Quintero et al. 2015), and comparative analysis have shown that these short *CRD* variants were generated from longer repeat arrays (Booher et al. 2015). As *TALE repeat* arrays have been shown to be prone to recombination in various cellular systems (Holkers et al. 2013; Lau et al. 2014), such recombination events, leading to partial loss of the *CRD*, probably occur rather frequently in a bacterial population. Ecologically, *CRD* loss can be an adaptive advantage, if the given *TALE* is deleterious to the pathogen due to, for example, activation of an executor *R* gene.

Slipped strand mis-pairing has probably lead to the adjacent *repeat* duplications observed in *ripTALII-1* and *ripTALIV-2* (Figure 15, Figure 22).

Slipped strand mis-pairing has also been implicated to affect *TALE CRDs* during replication and possibly transposition (Ferreira et al. 2015). Mechanistically, a higher per-*repeat* sequence identity should positively correlate with the probability of slipped strand mis-pairing events, as more identical *repeats* should be able to pair more perfectly during mis-pairing. Thereby, compared to RipTAL *CRDs*, slipped strand mis-pairing should occur more frequently in TALE *CRDs*.

Finally, segmental gene conversion is likely to influence the diversity of RipTAL *CRDs* (Figure 21). So far, gene conversion has not been implicated to drive TALE *CRD* evolution. However, it is know that gene conversion is biased towards GC rich sequences over GC poor sequences (Lassalle et al. 2015), termed GC biased gene conversion (GCBGC). Both, *ripTALs* and *TALEs* exhibit GC contents of about 66% across their coding sequence (Figure 39).

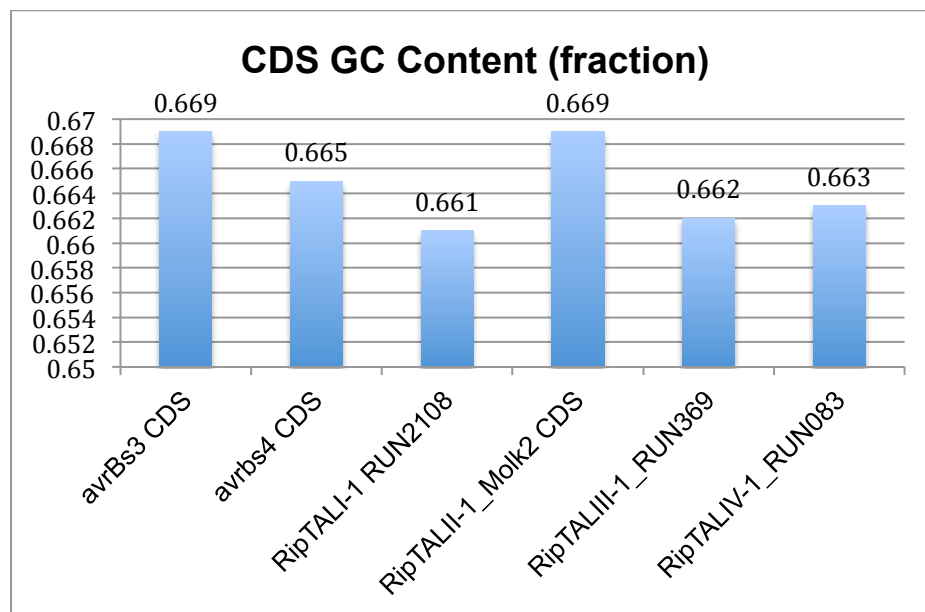


Figure 39. GC contents of RipTAL and TALE coding sequences.

However, while the GC content of RipTALs is rather equally distributed across the 3 modules (*NTR* (5'), *CRD* and *CTR* (3')), Figure 40), this is not the case for TALEs. Instead the TALE *NTR* and *CTR* are relatively GC poor, while the *CRD* is GC rich, with GC contents of 70% and 69% for TALEs *avrBs3* and *avrBs4*, respectively (Figure 40).

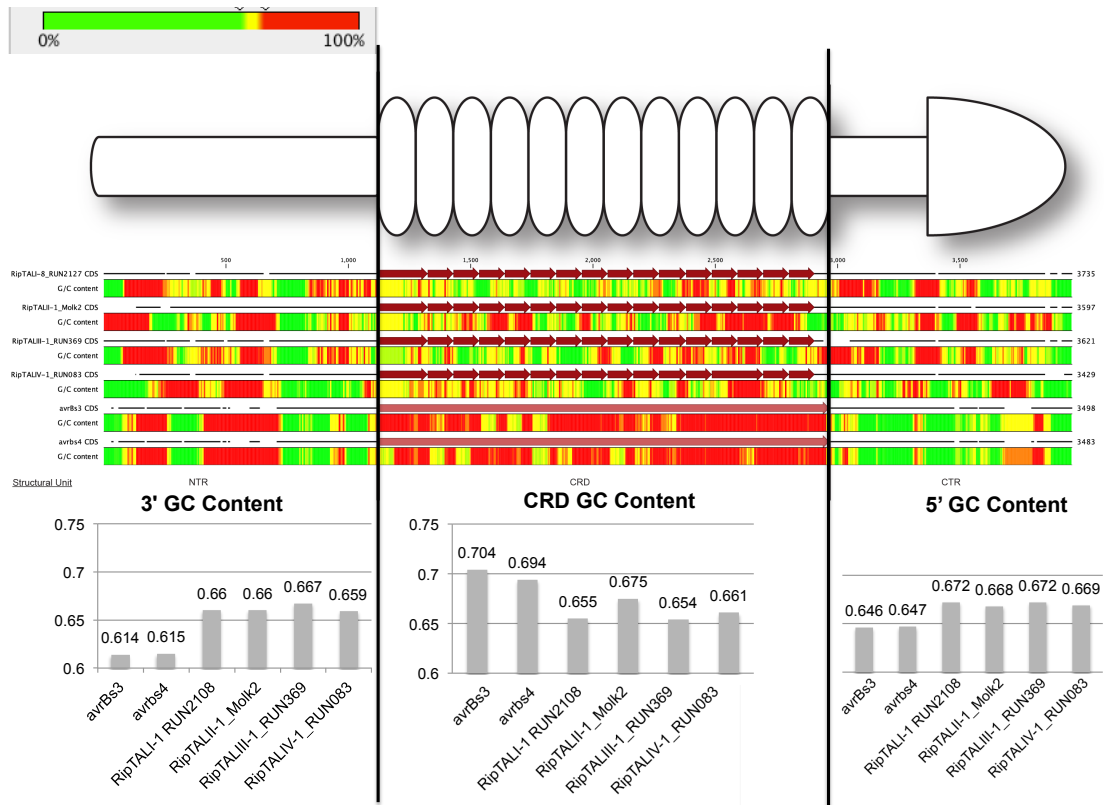


Figure 40. GC contents of the subdivided, aligned CDSs of *ripTAL*s and *TALE*s. On the top the color code is given. Below the color code a schematic representation of a TALE-like is shown with black vertical lines dividing *NTR*, *CRD* and *CTR*. GC contents for *ripTAL*s and *TALE*s across the CDS were calculated with a 61bp sliding window and are shown in the order of RipTALI-8, RipTALII-1, RipTALIII-1, RipTALIV-1, avrBs3, avrBs4 (top to bottom). Below, the average GC contents of 3' (corresponds to the *NTR*), *CRD*, and 5' (corresponds to the *CTR*) are plotted, with identically scaled axis.

The elevated GC content found for the TALE *CRD* may indicate that gene conversion acts frequently on the *CRD*, but not *NTR* and *CTR* of *TALE*s. Frequent occurrence of gene conversion acting on the *CRD* of *TALE*s would not only increase the GC content of the *CRD*, but would also account for the proliferation of near-identical *repeats* in this region and between different TALE copies found in one genome. As shown in Figure 14 and Figure 16 TALE *repeats* found within the same array are near-identical, supporting the hypothesis that gene conversion acts on TALE *CRDs*.

Taken together, it appears that all diversifying mechanisms identified for *RipTAL* *CRDs* are also likely to act on TALE *CRDs* and some, such as slipped strand mis-pairing and (segmental) gene conversion, are likely to act more

frequently on *TALE CRDs* due to the more pronounced repetitive character of the *TALE CRD*.

3.2.3 Evolvability of host-exposed pathogen proteins

The high potential for various diversifying molecular mechanisms of the *TALE CRD* leads to a higher rate of evolution of *TALEs* compared to the overall genome. This trait is commonly referred to as evolvability (Kirschner and Gerhart 1998). Conceptually it is logical that any biological feature has to be evolvable to some extent, as this is the basic requirement for evolution to happen. Further, generally one would expect heightened evolvability in features that are directly exposed to other evolving organisms, than for example for features involved in basic metabolism. However, the evolvability of *TALE-likes* is remarkably high, as outlined in the previous section. The evolvability of *TALEs* in particular is further heightened in contrast to *RipTALs*, due to the fact that *TALEs* are often multi-copy genes in *Xanthomonas*, and often *TALEs* are found in clusters in the genome (Booher et al. 2015). Multiple copies of a gene found in close physical proximity enables additional diversifying mechanisms, such as large recombination events encompassing multiple *TALEs*, which can easily give rise to altered DNA binding domains, possibly resulting in the deletion of one, or multiple, intervening *TALEs* during recombination (Booher et al. 2015). Such mechanisms could facilitate rapid evasion of host recognition, by recombinatorial loss of a *TALE* located between two other *TALEs*, recombining into a novel *TALE*. Further, gene conversion events, which do not act on the same gene, but lead to conversion of *repeat(s)* between one *TALE* locus and another, may also increase the overall evolvability of *TALE* genes located in one genome.

Functionally, any mutation affecting the RVDs found in the *TALE CRD* can lead to a complete change of the sequence bound and activated by that *TALE*. Thereby, a constantly evolving *TALE* repertoire with changing host target sequences can be understood as a long-term fitness benefit, as this mechanism undermines natural selection for disease resistant plants. For example, should a plant acquire mutations, which for example abolish *TALE* binding to a host susceptibility gene, this constitutes a fitness benefit for that host genotype in the context of a bacterial infection by a *TALE* carrying strain.

However, it is unlikely that natural bacterial populations are fully clonal. It has been shown that within house-keeping genes, natural bacterial populations exhibit various variants, likely the result of recombinatorial mechanisms (Feil et al. 2001). One would expect this to be more pronounced for highly evolvable genes like TALEs, resulting in a high diversity in TALE genes in a given natural bacterial population. Conceptually, the observations detailed above bear a remarkable resemblance to the antigenic variation systems of pathogens of vertebrate animals, which are also selected for increased evolvability and diversity in host-exposed residues (Graves et al. 2013).

3.2.4 Mechanistic, structural and ecological comparison of antigenic variation and *Xanthomonas* TALEs

Antigenic variation systems, found in bacterial and protistic pathogens of vertebrates, constantly alter host-exposed surface antigens (Morrison et al. 2014; Norris 2015). This enables a pathogen population to continuously evade recognition by the adaptive host antibody complement. As the host immune system is constantly trained to recognize the pathogen based on its exposed peptides, antigenic variation systems often entail tight expression control of the antigens, and often a single variant is predominantly expressed within a pathogen population at a given time point (Vink et al. 2012). Yet, a basic prerequisite for antigenic variation systems to be useful, is the evasion of host recognition. Therefore, at least one individual in the pathogenic population has to express a surface antigen different from the one expressed by the majority and recognized by host antibodies. This is known as “switching”, meaning that a subset of the pathogen population switches to the expression of a different antigen allele. Depending on the pathogen different ways evolved to tightly regulate the expression of a single epitope in the majority of a population.

Genetic diversity of antigenic variants is maintained by a number of evolutionary mechanisms, such as gene conversion, which maintain and create diversity between alleles (Norris 2015). The mechanisms identified in this work as drivers of RipTAL and TALE diversity, are largely the same as the ones maintaining antigen diversity in respective pathogens (Vink et al. 2012; Morrison et al. 2014; Norris 2015).

One structural feature of *Borrelia* antigenic variation systems, is a mixture of high sequence conservation and high diversity within the repetitive *visE* locus (Graves et al. 2013). Protein residues, which form a structural scaffold to properly expose a short peptide to the host, are kept constant, with little diversity. However, the exposed peptide stretch is highly variable between allelic variants found. Thereby, the exposed peptide, which is the molecular interface between host and pathogen, is varied with minimal impact on the residues responsible for its proper exposition (Figure 41a) (Graves et al. 2013).

Strikingly, hypervariable residues embedded in a fixed scaffold is what one finds in the TALE CRD. The RVDs are embedded in a fixed scaffold, defined by the remaining 32 amino acids forming a TALE repeat (Bochtler 2012; Mak et al. 2012). These non-RVD residues are largely conserved in sequence and highly conserved in structure and mediate the proper exposition of the RVDs inside the host nucleus towards the DNA bases (Figure 41b).

Despite overall different structural shapes between VisE proteins and TALEs, certain shared features can be identified. For one, high structural conservation of a helical scaffold, responsible for the proper exposition of variable host-interacting residues, can be observed in both (Figure 41a, b). Secondly, diversity is found in residues, or structures, which are exposed to and interact with the host (Figure 41a, b).

However, in TALEs, the individual repeats form an array, which interacts with multiple, sequential host features (DNA bases) (Figure 41c). This functional property is not shared between the two systems, as antigens only interact with a single host feature (an antibody).

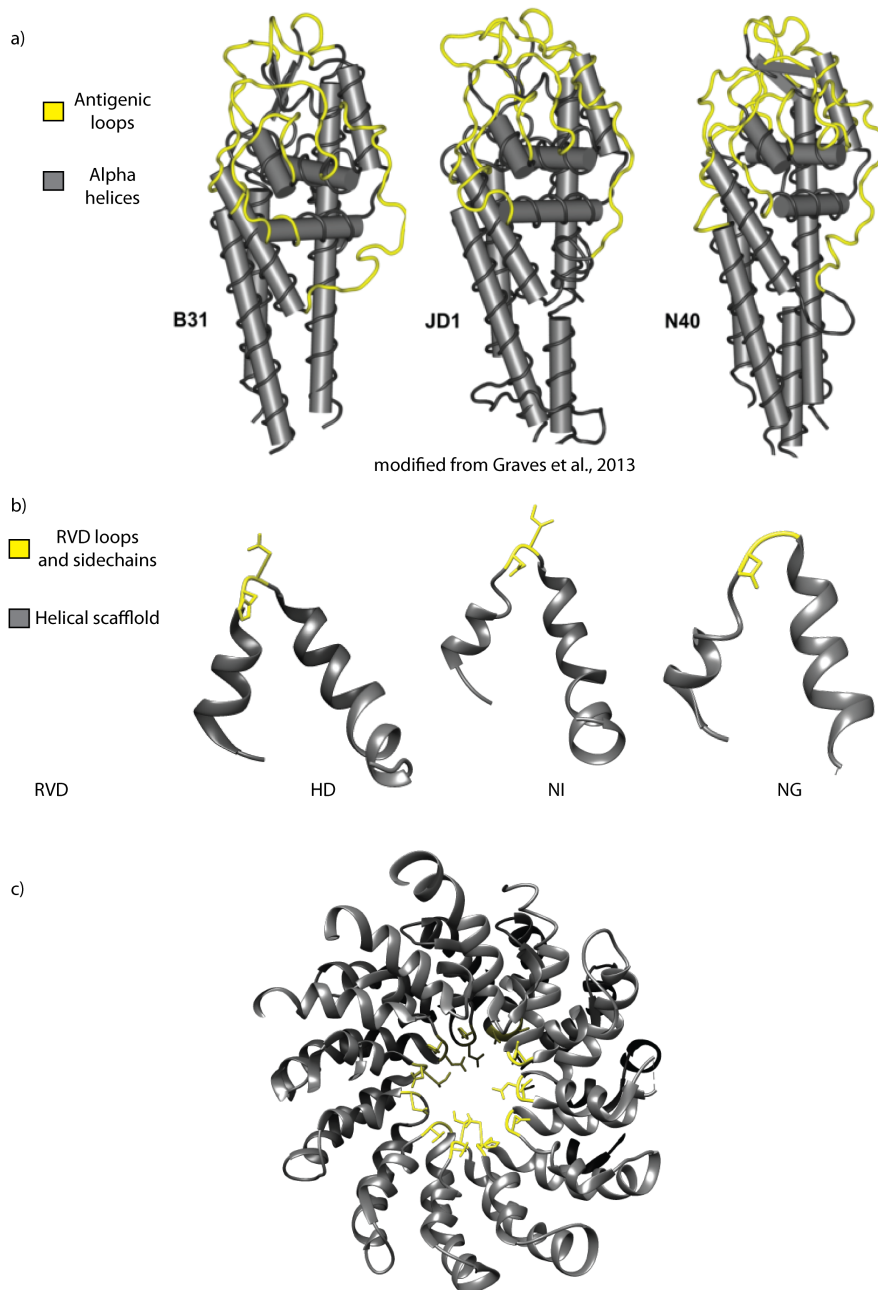


Figure 41. Structural comparison of the *Borrelia* VisE proteins and a *Xanthomonas* TALE. a) Figure modified from Graves et al, 2013. Structures of VisE proteins from different *Borrelia* strains. Conserved helical regions are colored in grey, and hypervariable antigenic loops in yellow. b) Three individual repeats from PthXo1, exhibiting a conserved helical scaffold (grey) and exhibiting diverse residues towards the host (RVDs, yellow). c) Partial structure of the CRD of a TALE. Conserved regions between individual repeats are colored in grey, and hypervariable RVD residues and side-chains and colored yellow. Structures in b) and c) were rendered using UCSF Chimera (Pettersen et al. 2004) based on the PthXo1 structure (Mak et al., 2012, pdb: 3UGM).

Ecologically, high diversity in RVD compositions across TALEs found in a single individual, and diversity between individuals making up a population,

gives rise to an increased number of molecular pathogen-host interfaces during initial infection. Unlike antigens, TALEs do not interface with an adaptive immune system, but directly with the host genome, which may contain some variation in natural populations, but is largely static in an agricultural setting relying on monoculture of cultivated crops. During the initial infection step, the *Xanthomonas* population is under strong selection, as any subset of the population, which does not carry a TALE repertoire adapted to the host genome, will be selected against. If any subset of the *Xanthomonas* population is able to successfully infect the host, this population will grow and may initially be clonal with regards to its TALE repertoire. In contrast to antigenic variation systems, which are selected for evolvability by the adaptive host immune system, TALEs are probably selected for evolvability by the standing variation found in the genomes of natural plant populations over generations. In agricultural settings, these evolvable systems allow these pathogens to rapidly adapt to new genotypes deployed in fields.

3.2.5 Relationship between evolvability of pathogen features and host range

The benefits of the high evolvability of *TALEs* to *Xanthomonas* populations are evident. However, *ripTALs* are less evolvable than *TALEs*, but still members of the Rssc are highly successful pathogens, causing drastic damages across more than 200 host plants. Unlike *Xanthomonas* strains, many of the *ripTAL* bearing Rssc strains exhibit a broad host range (Table 2, Figure 12). The reason for decreased evolvability of *ripTALs* in contrast to *TALEs* is that high evolvability is not necessarily advantageous to broad host range pathogens. For example if a certain RipTAL is recognized in a specific host plant genotype, but advantageous in multiple other hosts, the population wide fitness benefit of colonizing an alternative plant and retaining the *ripTAL* may be greater than that of losing that *ripTAL* to gain the ability to infect the RipTAL recognizing genotype. This ecological model implies that host specialization and evolvability of certain features should correlate. Thereby pathogens, which show a higher degree of host specialization, should also exhibit increased evolvability of pathogenicity determinants. Examples of host-specialized strains can be found within the Rssc. Two evolutionary lineages of

the Rssc, within phylotypes II and IV, have independently undergone host specialization on members of the Musa family, causing Moko and Blood disease respectively. Musa plants, such as banana and plantain, constitute important crops in tropical regions and blood and Moko diseases can have drastic impacts on yields. Moko causing strain MolK2 carries *RipTALII-1*, and all analyzed blood disease bacterium strains carry *RipTALIV-2* (Figure 7). Evidence for increased evolvability compared to other *RipTALs* can be identified for both *RipTALII-1* and *RipTALIV-2*. *RipTALII-1* is the only *RipTAL* that exhibits a higher GC content in the *CRD* than in the *NTR* or *CTR* (Figure 40). As stated above, elevated GC content may imply higher rates of gene conversion (Lassalle et al. 2015). *RipTALIV-2* exhibits traces of multiple slipped strand mis-pairing (Figure 15), and overall median per repeat identities of *RipTALIV-2* (82%) are higher than those of other *RipTALs*, e.g. *RipTALI-1* shows median per repeat identities of 77%. These observations indicate an increase of *ripTAL* evolvability in strains that underwent host-specialization compared to *ripTALs* from broad host range strains. In summary, it appears that increased evolvability of *TALE-like* effectors in pathogens positively correlates with increased host specialization (Figure 42).

Relationship between TALE-like effector evolvability and host range

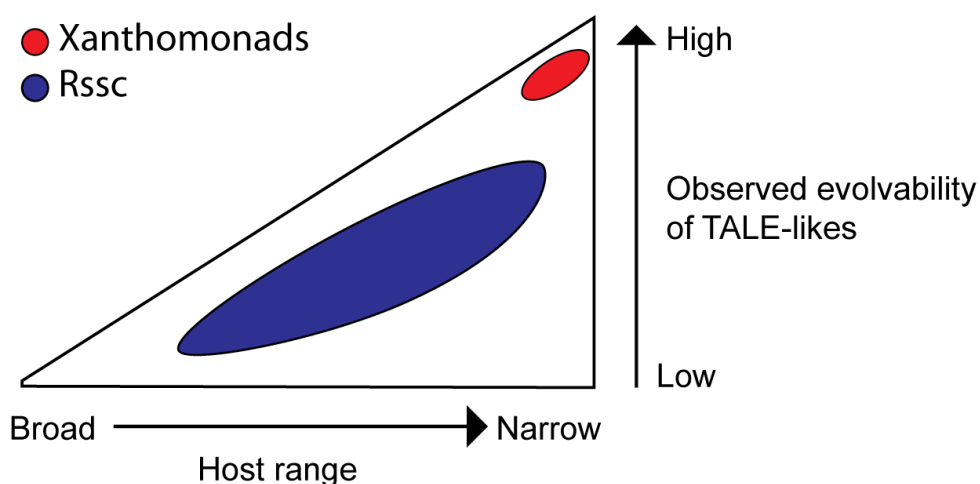


Figure 42. Proposed model of the relationship between strain host range and the assumed evolvability of *TALE-like* effectors in Xanthomonads and Rssc.

3.3 RipTAL recognition in plants

3.3.1 Natural recognition in *A. thaliana*

Despite the advances presented in this work, from the general characterization and classification of RipTALs (Figure 5, Figure 6, Figure 7) to the implication of these effectors in disease as highlighted by their convergent target preferences dependent on host range (Figure 12), no direct RipTAL target gene has been experimentally validated. It appears likely that a putative RipTAL susceptibility promoter and gene is conserved among multiple solanaceous plant species, due to the convergent DNA targeting specificities of RipTALs from strains isolated from different solanaceous host plants (Figure 12, Table 2).

The foundations for the future characterization of RipTAL responsive *A. thaliana* genes have been established in this work. Initially by using heterologous delivery to screen for differential responses to RipTAL delivery in a number of ecotypes, and followed up by a second, biologically distinct assay using Rssc strains.

The initial use of a heterologous delivery system in an engineered non-pathogenic *P. fluorescens* strain has uncovered a total of 7 ecotypes, which were subsequently analyzed further using GMI1000 and the corresponding *ripTALI-1* knockout strain. While the use of heterologous delivery using biosafety level (BSL) 1 organisms, such as *P. fluorescens*, was necessary due to the lack of BSL 2 facilities, required for handling Rssc strains, with the current availability of BSL2 facilities such a delivery system may be obsolete. One major drawback of using *P. fluorescens* EtHAn is the uncertainty of successful type III delivery of Rssc effectors by the type III secretion system recombineered into that strain, as it stems from *P. syringae* (Thomas et al. 2009). While *Ralstonia* and *Pseudomonas* are closely related and were previously classified as the same species (Hayward 1991; Safni et al. 2014), successful delivery of Rssc effectors using that secretion system has not been shown. However, as some of the accessions identified by the *P. fluorescens* mediated delivery could be confirmed using Rssc strains it appears likely that RipTALs were type III secreted successfully (Table 3, Table 4, Figure 24, page 76). The overall experimental procedure used to uncover differential

recognition is time consuming, and involves the use of expensive and toxic reagents (e.g. phenol, chloral hydrate). Compared to a screen involving Rssc strains, which involves growing plants, infecting these plants with wild-type and knockout strains, and a subsequent non-invasive disease scoring for about 10 days, the use of *P. fluorescens* EtHAN involved growing plants, infection of individual leaves by syringe infiltration, harvesting of leaf material, staining of leaf material and subsequent de-staining for about one week followed by detailed visual inspection of all samples. In summary, the use of *P. fluorescens* as heterologous delivery system for RipTALs entails the use of more expensive and toxic chemicals more direct handling of plants, likely to increase experimental variance and, due to the long time required for de-staining, time consuming. Further, the results obtained using *P. fluroescens* EtHAN, were sometimes inconclusive for certain ecotypes (Figure 24, Table 3, Table 4). The reasons for this are unclear, but it is likely that for some leaves the trypan blue staining procedure did not work properly.

However, the use of Rssc strains to assess a number of plant ecotypes regarding their survival in a strain-dependent manner may be more reliable, especially in combination with the statistical analysis script developed in this work, which was tailored towards the analysis of Rssc infections.

3.3.2 Considerations on the survival analysis of Rssc infected plants

One of the most defining features of Rssc infection in the context of plant diseases is the fact that successful infection entails death of the host. This is different from strictly biotrophic pathogens such as *Xanthomonas*, which primarily cause disease without killing their host. However, survival analysis could theoretically be applied to analyze kind of host-pathogen interaction that can be conceptualized into a “time-to-event” experiment (Altman and Bland 1998). The event analyzed does not necessarily have to be death of the host, it could also be understood as a certain severity of symptoms. As long as the event can be defined based on certain features, the experiment is suitable for survival analysis. Theoretically, it is possible to stop observing an individual for unrelated reasons, termed censoring in the context of survival analysis (Altman and Bland 1998). While this may be relevant in clinical settings where

multiple, unrelated factors can influence the event, this is considered unlikely to occur and be relevant in the case of Rssc infections, with the exception of survivors at the end of observation. In these experiments, the event recorded is actually not death, but the disease severity as approximated by the percentage of wilted leaves per plant. If more than 50% of the plant leaves are wilted (corresponds to a disease index of 2), the plant is considered as dead on that day. Reality is of course different, as the plant is not truly dead at that point. However, infections by Rssc members are generally not reversible, and any therefore plant that exhibits 50% wilting is committed to dying. In experimental setups, 50% of wilted leaves can be scored much easier and more precisely than time of death. Further, disease progression within one experimental set, done in parallel, should be comparable; therefore an arbitrary, but consistent definition of the event analyzed (death) does not change the relative times to event between the groups analyzed.

While the precise method used to obtain the time of death does not strongly influence the statistical analysis of the survival times, differences in the underlying statistical model used will and different approaches are therefore discussed below.

One of the basic tools in survival analysis is comparing the differences in fitted survival curves between two groups using the logrank test (Bland and Altman 2004) (Figure 29). Briefly, this test ranks the probabilities of the event in each group over time, based on the observations across both groups. The outcomes of both groups are then individually tested against the null hypothesis (no difference) using the X^2 test (Bland and Altman 2004). Generally, the logrank test has limited power when survival curves cross (Bland and Altman 2004; Sedgwick 2013). However, crossing of the survival curves has been observed in Rssc infection assays (compare Figure 29, continuous lines) and therefore testing with the logrank test may lead to misleading test statistics.

More complex statistical approaches, relying on the comparison of hazard ratios exist, such as Cox-proportional hazard regression (Sedgwick 2013). Generally hazard regression analysis builds on the transformation of survival curves into hazards, which represent the probability of death at any given time point. Hazards are calculated by dividing the cumulative hazard of dying at a

certain time point by the time passed from the beginning of observation to that point. As implied by the name, Cox-proportional hazard regression models assume proportional hazards over time, meaning that the rates of death are not changing between the groups compared during the time of observation (Sedgwick 2013). Proportional hazards result in the formulation of hazard ratio describing the relation between the treatments. E.g. hazard ratio of 2 for one group (A) compared to another group (B), implies that at any time an individual belonging to group A has twice the risk of dying than an individual that is part of group B (Sedgwick 2013). As shown (page 72), this assumption does not necessarily hold for Rssc infections comparing different strains. This is likely rooted in the disease progression of Rssc infection and the experimental setup used. In the assay used, plants are all infected at the same time. Theoretically, as disease is lethal, infection success determines the fate of any plant analyzed. However, the hazard experienced by any individual is not constant over time. Disease progression usually takes place in certain phases. Initially, no symptoms are visible on the aerial parts of a plant, while the infection is established in the root and xylem vessels. Then, disease progresses at a certain rate. This rate should primarily depend on the plant (or bacterial strain) genotype used, and abiotic factors, which should be controlled, or at least similar for all plants analyzed in a set. Further, the relative risk of dying for each individual is most likely not constant over time. An individual, which does not show any disease symptoms by the time all of its peers have developed disease, is unlikely to die at any point from Rssc infection, as it was probably not infected. For all other infected individuals, there is a certain window where they will reach disease incidence that will be scored as an event (Figure 43), giving rise to a bell shaped curve when plotting discrete hazards of an ideal experiment over time (Figure 44).

Day of death across all plant lines from all experiments

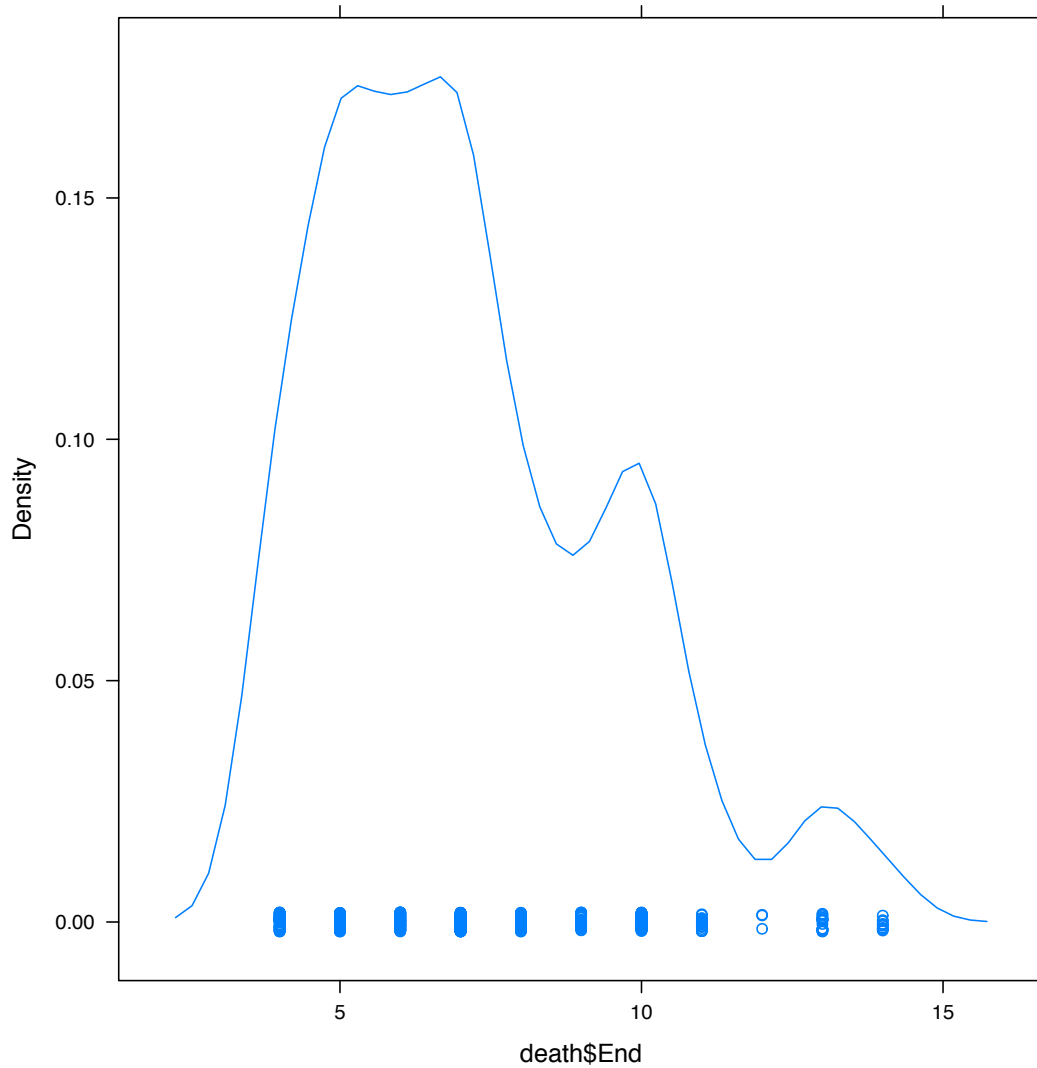


Figure 43. Density distribution of the observed times to event (death\$End) across all Rssc infection experiments analyzed.

Therefore, the cumulative hazard (each hazard added to the previous one) function of plants infected with Rssc is not a linear line, but resembles a sigmoid curve (Figure 44). Such regressions can be calculated using the non-proportional hazard regression models implemented in the R survival package. As the precise shape of the underlying hazard curve is difficult to predict, four different regression analyses are performed, tested for the quality of the fit using the Akaike information criterion (AIC) and the one with the lowest AIC is subsequently inspected. In the dataset used in this work, the best matching regression curve was a log-normal regression curve.

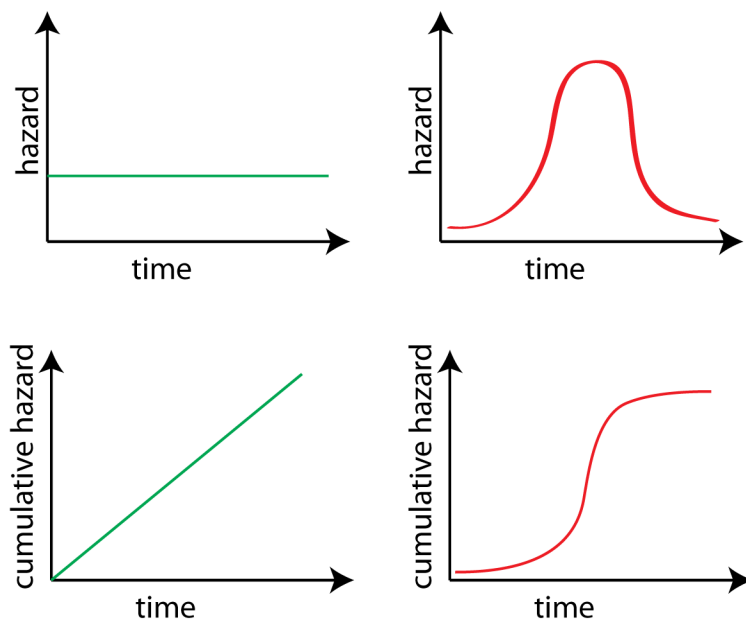


Figure 44. Schematics illustrating hazards (top) and cumulative hazards (bottom) for proportional (left, green) and non-proportional hazards (right, red).

In conclusion, based on the biology of bacterial wilt disease, the assumptions entailed in a non-proportional hazard model should fit best to the data obtained from such infection experiments. The analysis tool developed as part of this work (see 2.2.1.3) can be used to analyze the infection of any plant species, and allows for a flexible statistical analysis of the obtained data depending on experimental assumptions.

3.3.3 Engineered RipTAL recognition

The synthetic resistance construct created as part of this work has the potential to control bacterial wilt disease in crop plants in a RipTAL dependent manner. The construct drives the expression of 4 executor *R* proteins from a single mRNA. However, the effect of any of these executors on Rssc infected tissues is not characterized. Phenotypically three of the four executor *R* proteins (Bs3, Bs4C, Xa10) elicit a hypersensitive response in plant cells (Römer et al. 2007; Strauss et al. 2012; Tian et al. 2014). The fourth (Xa27) does not trigger an HR, but appears to be secreted into the apoplastic space, where it presumably interferes with bacterial growth (Wu et al. 2008; Hummel et al. 2012). However, the precise modes of action are unknown for all of these *R* proteins (Zhang et al. 2015), and therefore how the expression of these proteins affects the development of bacterial wilt is unpredictable. It has

been shown that elicitation of hypersensitive response in Rssc infected plants may constitute a mechanism conferring resistance in certain pepper lines (Rahman et al. 1999) and *A. thaliana* (Ho and Yang 1999).

Preliminary results indicate that the constructs developed here can elicit HR in transiently transformed *N. benthamiana* leaves, if a TALE-like matching to the promoter used is co-delivered. Whether there is a synergistic effect by the simultaneous expression of multiple executor R proteins on resistance remains to be elucidated, although the results shown in section 2.3.4 indicate that the “all” executor construct behaves differentially from the individual executor constructs. The individual *building block* constructs developed here (Figure 36) may provide a valuable tool in dissecting the contribution of each individual R protein to HR elicitation or Rssc resistance.

3.3.4 Broad range synthetic resistance

In the design of the synthetic, RipTAL receptive promoters, EBE_AvrBs3 was retained in the Bs3 promoter derivatives used (Figure 32). The retention of this EBE in the promoter may expand the spectrum of resistance conferred in the transgenic tomatoes to *Xanthomonas* strains secreting a TALE matching to that EBE, in particular against *X. gardneri* strains secreting AvrHaH1, which is able to transcriptionally activate promoters containing EBE_AvrBs3 (Schornack et al. 2008). Thereby, this construct may constitute a first step in the development of synthetic, TALE-like dependent, broad-spectrum bacterial resistance, which can be expanded in a strain specific manner by the addition of new EBEs to the promoter (Hummel et al. 2012). Even if the resistance conferred by such a construct may eventually be overcome, it could present an advance towards desperately needed resistance against bacterial wilt in solanaceous plants, in particular tomato, for agricultural use (Jyothi and Santhosha 2012; Huet 2014).

4 Material and Methods

All chemicals, technical equipment and consumables, such as plastic- and glassware, enzymes, primers, PCR buffers, kits or chemical compounds and solutions were bought from one of the following companies / suppliers:

Amersham Biosciences Europe GmbH (Freiburg), Applichem GmbH (Darmstadt), Applied Biosystems (Weiterstadt), BD Becton Dickinson GmbH (Heidelberg), BioRad Laboratories GmbH (München), Biozym Scientific GmbH (Hess. Oldendorf), BRAND GmbH (Wertheim), Carl Roth GmbH (Karlsruhe), Takara Bio Europe/Clontech, DIAGONAL GmbH & Co.KG (Münster), Difco (Augsburg), Eppendorf Vertrieb Deutschland GmbH (Wesseling-Berzdorf), Eurofins Genomics GmbH (Ebersberg), Merck KGaA (Darmstadt), Merck Biosciences GmbH (Bad Soden), metabion GmbH (Martinsried), New England Biolabs GmbH (Frankfurt), peqlab Biotechnologie GmbH (Erlangen), Qiagen GmbH (Hilden), Roche Diagnostics GmbH (Mannheim), Schleicher und Schüll Biosciences GmbH/Whatman (Dassel), SCHOTT DURAN (Mainz), Schütt Labortechnik GmbH (Göttingen), Sigma-Aldrich Chemie GmbH (Steinheim), Thermo Fisher Scientific Biosciences GmbH (St. Leon-Rot), VWR International GmbH (Darmstadt).

4.1 Methods for the isolation and modification of Deoxyribonucleic acids (DNA)

4.1.1 Transformation of bacteria

Chemically competent *E. coli* strains were transformed with a maximum of 10% (v/v) plasmid solution using heat-shock transformation and selected using appropriate antibiotics. *A. tumefaciens* and *P. fluorescens* were transformed using electroporation (BioRad), and selected using appropriate antibiotics. Competent cells were generated using standard protocols.

4.1.2 DNA Isolation

DNA isolations were performed using appropriate laboratory kits according to manufacturers instructions. Plasmid DNA was isolated using GeneJet Plasmid

MiniPrep kits (Thermo Scientific) or Machery & Nagel MidiPrep kits, depending on the required amount and concentration of plasmid.

Ralstonia solanacearum genomic DNA was isolated using the Wizards Genomic DNA extraction kit (Promega) according to instructions, with an initial wash step with a 0.5M NaCl solution, to remove extracellular sugars from the bacterial suspension.

4.1.3 Polymerase chain reaction and related methods

4.1.3.1 General Procedure

Polymerase chain reactions were performed in thermal cyclers (Analytic Jena, Sensoquest) using standard protocols. PCRs were routinely performed in GC Phusion Buffer (ThermoFischer) supplemented with 1x or 2x preCESI (Ralsler et al. 2006) with Phusion polymerase. Primer annealing temperatures (T_m) were routinely calculated using the following formula:

$$T_m = 64.9 + \frac{41 * (yG + zC - 16.4)}{wA + xT + yG + zC}$$

Where yG is the number of G nucleotides, zC is the number of C nucleotides, wA is the number of A nucleotides and xT is the number of T nucleotides found in the primer. Generally, primers were designed to have GC contents in the range of 40-80%, with a length between 18 and 42 nucleotides, and a T_m between 50°C and 70°C, and primers which were used as pairs were designed to have a similar calculated T_m . PCR cycling was performed for 25-35 cycles, depending on required product yield. All non-standard primers necessary to repeat experimental procedures described in this work are listed in Table 13

#	Name	Sequence	Application	Len	%GC	Tm
18	pENTR-EcoRI-MUT R	P- TTCAAGGGGGCGGCCGCG GAGCC	Introduction of EcoRI Site before TATG for transfer into pDSK	23	78,3	67,8
19	pENTR-TATG F-L-GFP11 Sall-Ascl F	gtcgaccGGTCTCAggtGACT ACAAGGACGACGATG	Cloning of FLAG-Linker-GFP11 Fragment into pENTR 3' Bsal Site. Contains HindIII for transfer into pDSK. Cloning into pENTR via	36	58,3	70,1

20	pENTR F-L-GFP11 Sall-Ascl R	GGCGCGCCAAGCTTTATGT GATTCC	Cloning of FLAG-Linker-GFP11 Fragment into pENTR 3' Bsal Site. Contains HindIII for transfer into pDSK. Cloning into pENTR via Sall, Ascl	25	56,0	61,0
21	pENTR-CACC F-L-GFP11 Sall-Ascl F	gtcgaccGGTCTCAaagGACT ACAAGGACGACGATG	Cloning of FLAG-Linker-GFP11 Fragment into pENTR 3' Bsal Site. Contains HindIII for transfer into pDSK. Cloning into pENTR via Sall, Ascl	36	55,6	69,0
22	pENTR-CACC-EcoRI-MUT F	TTCcaccTGAGACCgcgcccc t	Introduction of EcoRI Site before CACC for transfer into pDSK	23	69,6	64,2
29	pENTR Mut ECO REV NEU	P- GGGGCGGCCGCGGAGCCT G	Introduction of EcoRI Site for transfer into pDSK	19	89,5	66,2
30	pENTR Mut ECO FWD NEU TATG	CTTGAATTCTATGTGAGACC gcgccccctc	Introduction of EcoRI Site before TATG for transfer into pDSK	30	56,7	65,7
31	pENTR Mut ECO FWD NEU CACC	CTT GAA TTC CAC CTG AGA CCG CGG CCC	Introduction of EcoRI Site before CACC for transfer into pDSK	27	63,0	65,8
48	RipTAL allPhT F	CTCGGCTATTCCCGTGAGC AG	Amplification of RipTAL CRDs from any Phylotype from gDNA	21	61,9	58,3
49	RipTAL allPhT R	TTTGCCGGCACGCTTGCCG		19	68,4	57,6
50	RipTAL allPT REP F	TCGTGGACATCGCTCGGCA G	Sequencing of repeat region of RipTALs from any Phylotype	20	65,0	57,9
51	RipTAL allPT REP R	ACCCGCTCGGGACTCAGG		18	72,2	57,2
82	Bs3Ex1 Fwd	ATGGTCTCAGCAATGATGA ATCAGAATTGCTTTAATTC	Amplification of Bs3 CDS for Complex Resistance (Exec #1)	38	34,2	61,2
83	Bs3Ex1 Rev	TAGGTCTCGAGTCCATTTGT TCTTTCAAATTTTGG	Amplification of Bs3 CDS for Complex Resistance (Exec #1)	36	38,9	62,2
84	Bs3 dBsal Fwd	GGGAGGATGGcCTCTATGC AGTTGG	Bs3 CDS Bsal Free	25	60,0	62,6
85	Bs3 dBsal Rev	CAACTGCATAGAGgCCATC CTC	Bs3 CDS Bsal Free	22	54,5	56,7
86	Bs4C Ex2 Fwd	CGGTCTCAGCCAATGGAGT TTGATCTCAGATACTTGA	Amplification of Bs4C CDS for Complex Resistance (Exec #2)	37	45,9	65,6

87	Bs4C Ex2 Rev	TAGGTCTCAGTTCGACGAG CAGGCGATTTGTTGAG	Amplification of Bs4C CDS for Complex Resistance (Exec #2)	36	50,0	66,7
88	Xa10 Ex3 Fwd	CGGTCTCAACTAATGCAAC TGATGCTGACGTTCTG	Amplification of Xa10 CDS for Complex Resistance (Exec #3)	35	48,6	65,6
89	Xa10 Ex3 Rev	TTGGTCTCTGGTACACCGG GCTGATTTCTTCGTC	Amplification of Xa10 CDS for Complex Resistance (Exec #3)	34	52,9	66,8
90	Xa27Ex4 Fwd	cCGGTCTCAccaatggcggatt gggcatg	Amplification of Xa27 CDS for Complex Resistance (Exec#4)	31	61,3	68,3
91	Xa27 Ex4 Rev	agaGGTCTCATTCCgagtgacc agaaaccaccaagc	Amplification of Xa27 CDS for Complex Resistance (Exec#4)	36	52,8	67,9
92	Xa27 dBpil Fwd	ccggccgcgtgttcctgctcctc	Xa27 CDS Bpil Free	23	69,6	64,2
93	Xa27 dBpil Rev	gaggagcatgaacacggccgg	Xa27 CDS Bpil Free	23	69,6	64,2
94	sfGFP Repo5 Fwd	GAGGGTCTCGACCGATGGT GTCTAAGGGCGAA	superfolder GFP as Reporter, Peptide Chain 5	32	59,4	68,2
95	sfGFP Repo5 Stopp Rev	CggtctcGGTAATTATGTGAT TCCGGCGGCGTTG	superfolder GFP as Reporter, Peptide Chain 5, with Stop	34	55,9	68,0
96	Oct Term GGAG Fwd	TGTGGTCTCAGGAGGTCTCT GCTTTAATGAG	Moving Oct Term into 1 F-4	30	50,0	63,0
97	Oct Term CGCT Rev	GTGGTCTCAAGCGTCTCTG CTGAGCC	Moving Oct Term into 1 F-4	26	65,4	65,8
98	Bs3F2A-sfGFP fwd	TGGCCCTGGATTAGATTCC ACATC	Fusion of Bs3 to sfGFP (control)	24	50,0	57,4
99	Bs3F2A-sfGFP rev	ATGGTGTCTAAGGGCGAAG AACTC	Fusion of Bs3 to sfGFP (control)	24	50,0	57,4
112	Xa27 nested F	aagtgaccatagagagcatcaga gc	Xa27 amplification from gDNA (nested)	26	50,0	59,5
113	Xa27 nested R	gtttcgaaagcataacgtgtagggc ac		27	48,1	59,7
114	Bs3P-360PTI- CACC	GGTCTCCACCTCATAGAG GGGT	Amplification of pNarrow with Bsal	23	60,9	60,6
115	Bs3P-360PTI- AAGG	GGTCTCCCTTCAAATATAT GTGCAACTAG	CACC-AAGG	30	43,3	60,3
116	inF-Bs3I-sGFP-F	GGGGAGAGGGAGAAGGTA AGGAAATACACAAGTTTTA TTT		40	40,0	64,5
117	inF-Bs3I-sGFP-R	CGATGGTAGCGTCGCCTGT ATCAGTAAAATTCTCATTAG A	Primers to inFusion clone Bs3 Intron into sfGFP	40	42,5	65,5
118	inF-sfGFP-Bs3I-F	CTTCTCCCTCTCCCCTGACG GAGAAC		26	61,5	64,3
119	inF-sfGFP-Bs3I-R	GCGACGCTACCATCGGAAA GCTCACAC		27	59,3	64,3
120	inF-Xa27-sfGFP- R	GCCCTTAGACACCATCGGT CCAGGGTTCTCTTC	InFusion fusion of Xa27 to Bs3p from all exec construct	33	57,6	68,1
121	inF-Bs3P-Xa27-F	CACATATATTTGCAATGGC TGATTGGGCTATGCACCAC		39	46,2	66,6
122	Bs4C dBpi R	ACGATGAAACTGGGATGGT C	Removal of Bpil sites from Bs4C cds	20	50,0	51,8

123	Bs4C dBpi F	GTTTCATCAATAAGCTCTTCT TTCTTTTC		28	32,1	54,1
124	inF vector Rev	TGCGAAATATATGTGCAAC TAGGACTAC	Backbone primers inFusion	28	39,3	57,0
125	inF vector Fwd	ATGGTGTCTAAGGGCGAAG AACTC		24	50,0	57,4
126	inF Bs3 Rev	GCCCTTAGACACCATTGGC CCTGGATTAGATT	Generation of Bs3 single executor	32	50,0	64,4
127	inF Bs3 Fwd	CACATATATTTTCGCAATGAT GAATCAGAATTGCTTTAATT C		41	29,3	60,5
128	inF Bs4C Fwd	CACATATATTTTCGCAATGG AGTTTGATCTCAGATACTTG ATC	Generation of Bs4C single executor	42	35,7	63,5
129	inF Bs4C Rev	GCCCTTAGACACCATTAGT GGGCCAGGGTTGG		32	59,4	68,2
130	inF Xa10 Fwd	CACATATATTTTCGCAATGCA ACTGATGCTGACGTTCTGT AC	Generation of Xa10 single executor	41	41,5	65,5
131	inF Xa10 Rev	GCCCTTAGACACCATTGGA CCAGGATTCTCTTCAAC		36	50,0	66,7
132	inF Xa27 Rev	GCCCTTAGACACCATTGGA CCAGGTTCTCTTC	Generation of Xa27 single executor	33	57,6	68,1
133	inF Xa27 Fwd	CACATATATTTTCGCAATGGC TGATTGGGCTATGCACCAC		39	46,2	66,6
140	RipTAL_N_out R	CTGCTCACGGGAATAGCCG AG	Sequencing of RipTAL N-terminal from +680 in Brg11	21	61,9	58,3
141	RipTAL_C_out F	CGGCAAGCGTGCCGGCAA A	Sequencing of RipTAL C-terminal from -250 in Brg11	19	68,4	57,6
142	PTI_FL_FWD	ATGAGAATAGGCAAATCAA GCGGTTGG	Amplification of FullLength PTI RipTALs	27	44,4	58,2
143	PTI_FL_NOSTOP _R	CGTTTCCAATATTTGCAGAA GCCAGTC	Amplification of FullLength PTI RipTALs	27	44,4	58,2
144	PTII_FL_FWD	ATGCGTCGCCGGACCGCC	Amplification of FullLength PTII RipTALs	18	77,8	59,4
145	PTII_FL_NOSTO P_R	CACATCCAACATTTGCAGG AACGAGTC	Amplification of FullLength PTII RipTALs	27	48,1	59,7
146	PTIV_FL_FWD	ATGAGAGTAGGCAAAGCAC GAGAGC	Amplification of FullLength PTIV RipTALs	25	52,0	59,3
147	PTIV_FL_NOSTO P_R	CAGGTCCAGTAGCTGCAGG AGC	Amplification of FullLength PTIV RipTALs	22	63,6	60,4
148	PTI_FL_CACC_F WD	AGGTCTCACACCATGAGAA TAGGCAAATCAAGCGGTTG G	Amplification of FullLength PTI RipTALs for pENTR CACC-AAGG	39	48,7	67,6
149	PTI_FL_AAGG_N OSTOP_R	TCAGGTCTCTCTTCGTTTC CAATATTTGCAGAAGCCAG TC		41	46,3	67,5
150	PTII_FL_CACC_F WD	AGGTCTCACACCATGCGTC GCCGACCGCC	Amplification of FullLength PTII RipTALs	30	70,0	71,2

151	PTII_FL_AAGG_NOSTOP_R	TCAGGTCTCTCCTTCACATC CAACATTTGCAGGAACGAG TC	for pENTR CACC-AAGG	41	48,8	68,5
152	PTIV_FL_CACC_FWD	AGGTCTCACACCATGAGAG TAGGCAAAGCACGAGAGC	Amplification of FullLength PTIV	37	54,1	68,9
153	PTIV_FL_AAGG_NOSTOP_R	TCAGGTCTCTCCTTCAGGTC CAGTAGCTGCAGGAGC	RipTALs for pENTR CACC-AAGG	36	58,3	70,1
156	GWalk_Adap_Long	GTAATACGACTCACTATAG GGCACGCGTGGTCGACGG CCCGGGCTGGT	Genome Walking Adaptor. Ordered @ 50mM	48	62,5	76,5
157	GWalk_Adap_Short	P-ACCAGCCC-H2N	Genome Walking Adaptor. Ordered @ 50mM	8	75,0	11,6
158	GWalk_AP1	GTAATACGACTCACTATAG GGC	Genome Walking Primer, outer	22	45,5	53,0
159	GWalk_AP2	ACTATAGGGCACGCGTGGT	Genome Walking Primer, inner	19	57,9	53,2
160	RUN369 COUT 1	TGGCTCCACCGCAGGAAAC GTACCGCT	Genome walking, GSP outer, RUN369 Cterminus	27	63,0	65,8
161	RUN369 COUT 2	CCGCTCGTTCGCACATACG GGCCGATT	Genome walking, GSP inner, RUN369 Cterminus	27	63,0	65,8
162	RipTAL Reps out N	CTGCTCACGGGAATAGCCG AG	Reverse complement of 48,49	21	61,9	58,3
163	RipTAL Reps out C	CCTGAGTCCCGAGCGGGT		18	72,2	57,2
164	RUN369 NOUT1	CTTCGCAATTTGCTCAGGC TCTCCTG	Genome walking, GSP outer, RUN369 Nterminus	27	55,6	62,8
165	RUN369 NOUT2	AGTTTCCGGATCTGCTCAC GGGAATAG	Genome walking, GSP inner, RUN369 Nterminus	27	51,9	61,3
166	RUN369 NOUT1.1	CCTTGTCTGTCAAGGTGG CGTGATACTTCGC	See 164, 165	32	56,3	67,0
167	RUN369 NOUT2.1	CGCTCAGGCTCTCCTGTTT AGTTTCCGGATC		32	56,3	67,0
168	RUN369 COUT1.1	GGCCTGATCAACTGGCATG GCTCCACCGC	See 160, 161	29	65,5	68,6
169	RUN369 COUT2.1	CGTACCGCTCGTTTCGCACAT ACGGGCCGA		29	65,5	68,6
170	RUN369 NOUT3.1	ACACGTCACGGCCGATGCG GGATGACGAG	See 164, 165	29	65,5	68,6
171	RUN369 NOUT3.2	GCCAAGAACAGTCGGGGC CGGCCAAGCAT		29	65,5	68,6
172	RUN369 NOUT150.1	CAGATCGGGGAGCGCCGC AGCCAACTCC	New Set 150 bp down of allPTN, attempt to make the genome walking work better by priming further away	28	71,4	70,2
173	RUN369 NOUT150.2	TGGCGACCACCCGGAGCGA CTGCCGTC		27	74,1	70,4
174	RUN369 NOUT250.1	GCTCGCCGCACTGCGCAAC GGTCGCAA	.2 is 250 down of allPTN	27	70,4	68,8
175	RUN369 NOUT250.2	GGGTAGCAGCGCTTGACAGC GCCAAGTCG		28	67,9	68,7

176	RUN369 NOUT500.1	CGGTGCTCAGTTCATAGGG GGCCGCGC	.1 is 500 bp down of allPTN	27	70,4	68,8
177	RUN369 NOUT500.2	CAACGCCCGCTTGCCGCCA GTGTTGCTG		28	67,9	68,7
178	PTIII_FL_NOSTO P_R	TGCATCCAATATTTGCAGG AGCCAGTC	Primers to amplify fulllength ripTAL from class III	27	48,1	59,7
179	PTIII_FL_AAGG_ NOSTOP_R	TCAGGTCTCTCCTTTGCATC CAATATTTGCAGGAGCCAG TC		41	48,8	68,5
180	PTI_200_BsaI_F	TCGGTCTCCGGCGCCGCGC CGCTC	Set of Primers to subclone individual RipTAL Pieces from PTI based on natural BsaI Sites to be used with primers 148 and 149 in this table	24	83,3	71,1
181	PTI_200_BsaI_R	CTGGTCTCACGCCGGTGAC CGAGCCCCG		28	75,0	71,6
182	PTI_3300_BsaI_ F	CGGGTCTCCGGTATGGCA GGGCAATCGGC		30	70,0	71,2
183	PTI_3300_BsaI_ R	TTGGTCTCAACCGGGAGAG CCGAGCGTGCGCTC		33	66,7	71,9
184	PTIII_3300_BsaI_ _F	CAGGTCTCCAGCGTAGCT GGGCAATCGGC	Cterminal set for Subcloning and subsequent CL of PTIII, no primers for Nterm, PTI fwd works.	30	66,7	69,8
185	PTIII_3300_BsaI_ _R	TTGGTCTCAGCTGGGTGAC CTGAGCGTGCGCTC		33	63,6	70,6
186	PTIII/I_3300_Bs al_F	CAGGTCTCCGGTGTAGCT GGGCAATCGGC	Set of Primers to generate Chimeras of PTI/III, based on PTI Overlap (not done)	30	66,7	69,8
187	PTIII/I_3300_Bs al_R	TTGGTCTCAACCGGTGAC CTGAGCGTGCGCTC		33	63,6	70,6
188	PTIV/I_3300_Bs al_F	AAGGTCTCACGGTACGACC GAGCAATCGGCGTCCC	Set of Primers to generate C terminal chimeras based on PTI overlap (not done)	35	62,9	71,5
189	PTIV/I_3300_Bs al_R	TTGGTCTCAACCGGAGGAC ATGAGCGAGCGTTCCAGCG		38	60,5	72,0
190	PTII/I_3300_Bsa I_F	AAGGTCTCACGGTATCGCC GAGCAATCGGCATCTCCAC C	Set of Primers to generate C terminal chimeras based on PTI Overlap (not done)	39	59,0	71,8
191	PTII/I_3300_Bsa I_R	CTGGTCTCAACCGGGCGAC AGCATCGAACGCTCAAGTG		38	60,5	72,0
192	PTIII_200_BsaI_ F	GGTCTCCGGCGCCGCGCCG CCC	See 180,181 same approach for phylotype III (dont want to change aa therefore need new primers, there is a polymorphism in the priming region	22	90,9	71,6
193	PTIII_200_BsaI_ R	GGTCTCACGCCGGTGACCG AGCCCCGGTTC		30	73,3	72,6
194	EBEs-A0- RipTALs-Bs3P-	P- acccccttATAAAATTGGTCA	These Primers also work for: RipTALII-1,	28	42,9	58,5

	Rev	GGCAAAC	Brg11(new), RUN64, IV-1/1327, RUN63			
195	EBEs-T0- RipTALs-Bs3P- Rev	accccctaATAAAATTGGTCA GGCAAAC		28	42,9	58,5
196	EBEs-G0- RipTALs-Bs3P- Rev	accccctcATAAAATTGGTCA GGCAAAC		28	46,4	59,9
197	EBEs-C0- RipTALs-Bs3P- Rev	accccctgATAAAATTGGTCA GGCAAAC		28	46,4	59,9
198	Bs3P-RUN2127- 369-FWD	cgcccttgTCACAACCTCAAGT TATC		26	46,2	58,0
199	Bs3P-RipTALII-1- FWD	agccggaacTCACAACCTCAA GTTATC		27	44,4	58,2
200	Bs3P-Brg11- new-FWD	cgccgtggcTCACAACCTCAA GTTATC	Specific primers to be used with 194-197	27	51,9	61,3
201	Bs3P-RUN064- FWD	cgcgtggcTCACAACCTCAAG TTATC		26	50,0	59,5
202	Bs3P-RipTALIV- 1-1327-FWD	agccggggTCACAACCTCAAG TTATC		26	50,0	59,5
203	Bs3p-RUN063- FWD	agccggggTCACAACCTCAA GTTATC		27	51,9	61,3
204	EBE-A0-BDB- Bs3P-Rev	cccccccttATAAAATTGGTCA GGCAAAC		29	48,3	61,5
205	EBE-T0-BDB- Bs3P-Rev	ccccccctaATAAAATTGGTCA GGCAAAC		29	51,7	62,9
206	EBE-G0-BDB- Bs3P-Rev	ccccccctcATAAAATTGGTCA GGCAAAC	Generation of BDB (RipTALIV-2) EBEs	29	51,7	62,9
207	EBE-C0-BDB- Bs3P-Rev	ccccccctgATAAAATTGGTCA GGCAAAC		29	51,7	62,9
208	EBE-BDBs-Bs3P- Fwd	tagccgggTCACAACCTCAAG TTATC		26	46,2	58,0
228	Bs3P-Brg11-8A- FWD	agccgtggcTCACAACCTCAA GTTATC	Testing HD specificity in Brg11 / RipTALI-1	27	48,1	59,7

Table 13. Oligonucleotide primers used in this work

4.1.3.2 PCR amplification and cloning of *ripTALs*

PCRs to screen for *ripTALs* were performed with primers allPT-F and allPT-R, using Phusion polymerase (NEB) in GC buffer (NEB), supplemented with 20% preCESI (Ralser et al. 2006) and PCR clean up (Fermentas) was performed if a fragment >1.5kb was visible on a Agarose Gel. PCR products were sequenced using primers allPTRepF and R and repeats were annotated to identify the RVD composition. *ripTAL* genes with RVD compositions not previously described, were amplified from genomic DNA with class specific primers, generating Bsal flanked fragments while removing internal Bsal recognition sites after cutligation into pENTR-CACC-GW-AAGG (de Lange, Wolf, et al. 2014). Cloned RipTALs were validated by sanger sequencing and

transferred into pGWB641 (Nakamura et al. 2010) via an LR Gateway cloning reaction (Life Technologies). Genome walking on genomic DNA from strain RUN369, to elucidate sequences of the *NTR* and *CTR*, was performed according to the instructions in the genome walking kit (Clontech).

ripTAL sequences have been deposited at ENA and are accessible with accessions LN874044-63.

For the heterologous delivery using *P. fluorescens*, RipTALs were cloned into a modified variant of pENTR-CACC-GW-AAGG, where an *EcoRI* restriction site was inserted upstream of the *BsaI* site flanking the *ccdB/camR* fragment on the 5' via site directed mutagenesis. Downstream of the 3' flanking *BsaI* site a FLAG tag, followed by a Serine/Glycine linker, and β -sheet 11 of sfGFP, followed by a *UAA stop-codon* and a *HindIII* restriction site. The FLAG-Linker-sfGFP11-Stop-*HindIII* fragment was cloned via *Sall* and *Ascl*. pENTR-*EcoRI*-CACC-GW-AAGG-FLAG-L-GFP11-*HindIII* was generated by Max Fürst as part of lab-rotation (Figure 45).

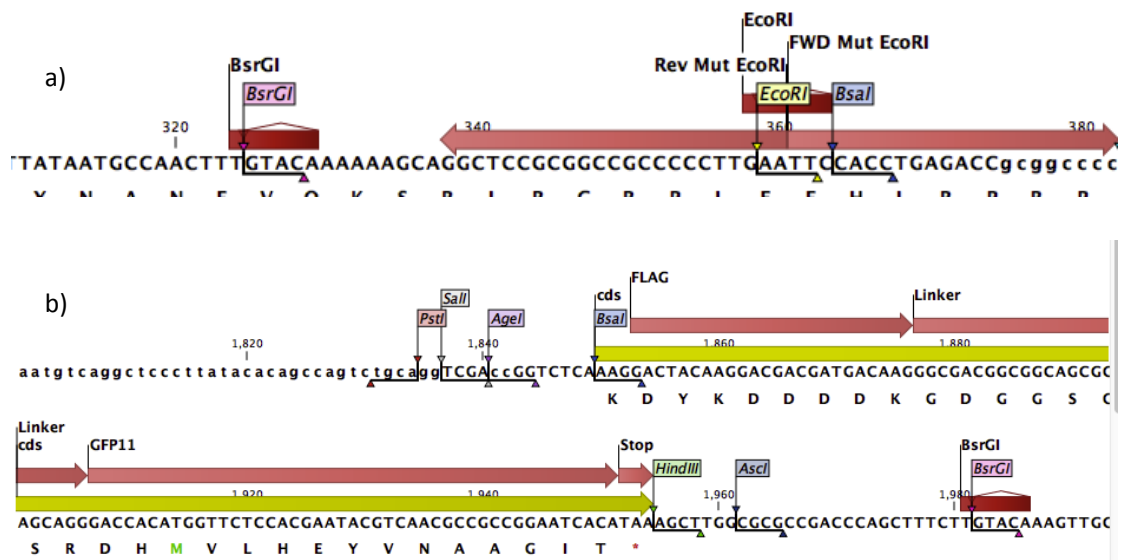


Figure 45. Generation of pENTR-*EcoRI*-CACC-GW-AAGG-FLAG-L-GFP11-*HindIII*. a) Modifications on the 5' end of the *ccdB* cassette. b) modifications on the 3' end of the *ccdB* cassette.

Subsequently, *ripTALs* were cloned into pENTR-*EcoRI*-CACC-GW-AAGG-FLAG-L-GFP11, sequence validated, and transferred into broad host range vector pDSK602 via *EcoRI* and *HindIII* (Murillo et al. 1994). To avoid co-transformation of (undigested) pENTR and pDSK602 (due to compatible origins of replications), the ligation product was digested with *BsrGI*, for which

no recognition site exists in pDSK602, prior to transformation into *E. coli* Top10 cells.

4.1.3.3 Cloning of GUS reporter constructs

EBEs were cloned as described previously (de Lange et al. 2013) and subsequently transferred into pENTR-ccdB-uidA, for protoplast assays, or pGWB vectors, for plant transformation, via cutligation.

4.1.3.4 Gel electrophoresis of DNA

DNA was routinely visually assessed regarding size and approximate concentration using Agarose Gel electrophoresis with an Agarose concentration of 1% to 2% in TAE (40 mM Tris, 40 mM Acetic acid, 1 mM EDTA, pH 8,0), depending on expected DNA fragment size. TAE was used as running buffer and electrophoresis was performed at voltages ranging from 80V to 120V. DNA was visualized using Ethidium Bromide (EtBr, 3ul of a 10mg/ml stock per 100ml of liquid gel) excited with UV light in a gel imaging system. 100bp or 1kb DNA size-markers (ThermoFischer) were used as size references.

4.2 Protein methods

4.2.1 Protein extraction, PAGE, and Western blot on *P. fluorescens*

To confirm the expression of RipTALI-1 in *P. fluorescens*, clones were grown overnight and adjusted to an OD600 of 1.0. 1ml was pelleted and resuspended in 200µl of 1xLämmli sample buffer (2x stock: 200mM Tris-HCl (pH 6,8), 10% β- Mercaptoethanol, 10% SDS, 10% Glycerin, 0,012% Bromophenol blue in ddH2O) , boiled at 95°C for 10 minutes, spun down at 8000g for 1 minute, and stored on ice, for immediate use, or at -20°C for longer term storage. 20µl of crude extract were loaded on an polyacrylamide (PA) gel electrophoresis (GE) system and gel electrophoresis was performed in 1x running buffer (diluted from 10x stock: 25 mM Tris-Base (pH 8,8), 1% SDS, 1,92M Glycine, in ddH2O) at 120V until the required degree of separation was reached in. Subsequently, the gel was sandwiched as shown in Figure 46 between pre-soaked “Whatman” papers (Anode buffer: 300mM

Tris-HCl (pH 10,4), 20% Ethanol, in ddH₂O; Cathode buffer: 25mM Tris-HCl (pH 7,6) 40mM ϵ -Aminocaproic acid, 20% Ethanol, in ddH₂O) and a PVDF membrane (Milipore) and semi-dry blotting was performed at $0.8 \frac{mA}{cm^2}$ of gel (about 40-50mA for one gel) for 1 hour.

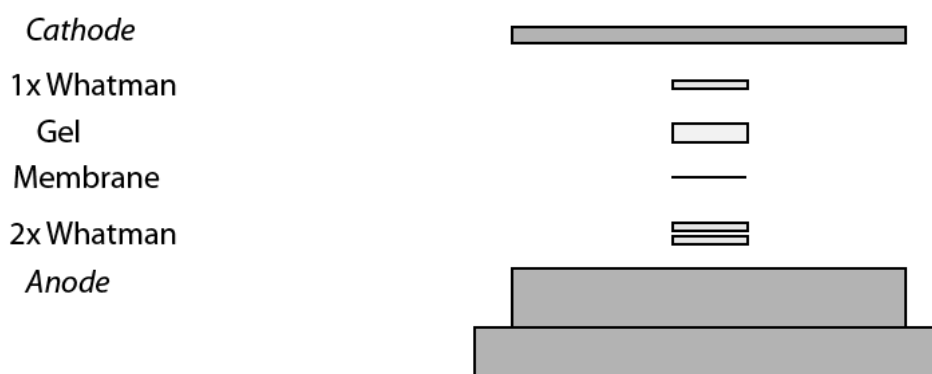


Figure 46. Assmbeily of the gel sandwhich for semi-dry western blotting.

After blotting, the membrane was blocked using 3% milk in TBS for one hour, incubated with the primary antibody solution according to manufacturers instructions, washed 4x 5 minutes with TBS/0.2%Tween-20, incubated with the secondary antibody (fluorophore coupled) according to manufacturers instructions, washed 4x 5 minutes with TBS/0.2%Tween-20 and rinsed with water. The membrane was then dried between two filter papers, and subsequently imaged using either an Odyssey or Typhoon laser scanning system according to antibody and machine specific instructions.

4.2.2 GUS-Assays using *A. thaliana* protoplasts

Arabidopsis thaliana root cell culture was maintained as described (Li et al. 2010). Protoplasts were pelleted by centrifugation at 50 x g for 5 minutes and resuspended in MM (0,4 M Mannitol, 5 mM MES, pH 6) at a cell density of 10^7 cells per ml. 30 μ l of protoplasts were transferred into wells of a 2 ml deep well plate together with 3 μ g of RipTAL expression plasmid, 3 μ g of GUS-reporter plasmid and 1 μ g of luciferase expression plasmid. 30 μ l of PEG1500 were added to each well and mixed gently. After incubation for 5 minutes 30 μ l of MM were to each well added to stop the transformation. Then 300 μ l of

K3 (Schütze et al. 2009) were added to each well and the plate was sealed with parafilm and stored at 21°C in the dark.

20 hours after transfection 1.7 ml of MMg (MM with 15 mM MgCl₂) were added to each well and cells were pelleted at 400 x g for 10 minutes at room temperature. Supernatant was removed to leave 70 µl volume. Protoplasts were lysed in 70µl of 2x Cell culture lysis reagent (promega, plus 1 Roche EDTA-free protease inhibitor tablet per 20ml) on ice by pipetting up and down 10 times per well, whilst avoiding the introduction of air bubbles. 100µl of lysed protoplasts were transferred into a PCR plate and stored on ice for 30 minutes. After centrifugation at 4000 x g for 30 minutes at 4°C the supernatant was transferred into a new plate and used to determine Luciferase and GUS activity in a plate reader (Berthold). GUS enzyme activity was measured as 4-MU fluorescence (excitation at 355nm, emission at 460nm) at 37°C over 80 minutes for 10µl of protoplast supernatant in 90 µl GUS buffer (100mM Tris-HCl, 2mM MgCl₂, 4mM 4MUG at pH 8.2). A single reading of Luciferase activity was carried out with 50 µl of reconstituted Promega luciferase assay reagent injected into 10 µl of protoplast supernatant.

4.2.3 Confocal laser scanning microscopy of *ripTAL* expressing protoplasts

Microscopy of *A. thaliana* root-cell culture protoplasts was carried out 24 to 36 hours after transfection with pGWB641 *ripTAL* constructs, which results in expression of C-terminal YFP fusion proteins. To mark out nuclei within the cell, a plasmid bearing a 35-S driven mCherry-NLS construct was co-transfected together with each *ripTAL* expression plasmid. A Leica DMI6000B-CS SP8 confocal laser-scanning microscope with an HC PL APO CS2 40x/1.10 water objective was used for imaging. Excitation was performed at 513 and 594 nm using Argon and HeNe Lasers for YFP and mCherry, respectively. Emission spectra were 522 - 556 nm for YFP and 604 - 627 nm for mCherry. A single focal plane is shown in Figure 8. Image analysis and processing of imaging stacks was performed using Fiji (Schindelin et al. 2012).

4.2.4 Analysis of RipTAL-YFP fusion protein levels in protoplasts by flow cytometry

A MoFlo XDP Cell Sorter (Beckman Coulter) was used outfitted with an Argon 488 nm 50 mW laser and solid state 532 nm 50 mW laser. Flow parameters were: trigger FCS 0.1% threshold, FL1-LH(YFP) = 513/17 (to avoid 532 scatter), FL8-LH(mCherryNLS) = 670/30 (to reduce YFP spillover). Cells were gated from debris using FSC-LA vs. SSC-LA and mCherryNLS positive cells were identified by comparison with a mock transfection control. The ratio of YFP/mCherryNLS fluorescence intensities was calculated from mCherryNLS positive cells directly in Summit 5.2 (Beckman Coulter) in a separate database.

4.3 Plant and microbe Methods

4.3.1 Leaf infiltration of *A. thaliana* plants and cell death assays

P. fluorescens strains were grown overnight in liquid medium with appropriate antibiotics, pelleted at 12000g for 5 minutes, resuspended in 10mM MgCl₂, adjusted to an OD600 of 0.4 and infiltrated into leaves of five 5-7 week old *A. thaliana* plants using a needle-less syringe. 3 days after inoculation leaves were harvested from three of the infiltrated plants, and stained for cell death using trypan blue, and subsequently de-stained, as previously described (Koch and Slusarenko 1990) with the exception that the de-staining procedure was performed for at least 2 days to minimize background. The remaining 2 plants per infiltration and ecotype were monitored for up to 7 days regarding phenotypic tissue aberrations visible to the naked eye.

4.3.2 Transient transformation of leaf cells via *A. tumefaciens* infiltration of *N. benthamiana*

A. tumefaciens strains were re-suspended in water to an OD600 of 0.4 per strain and subsequently infiltrated into leaves using a needle-less syringe. In cases where two strains were co-infiltrated, the OD600 per strain was set to 0.8 and the two strains were mixed before infiltration.

4.3.3 Transformation of *A. thaliana* by floral dip

A. thaliana plants were transformed by floral dip as described by (Clough and Bent 1998).

4.3.4 Cotyledon transformation of *S. lycopersicum*

S. lycopersicum cv. *Heinz* transformations were performed as described in (Wittmann et al. 2015) with support from C. Brancato of the ZMBP transformation facility.

4.3.5 Infection of *A. thaliana* with Rssc strains by soil soaking

R. solanacearum strains GMI1000 (wt) and GRS216 (RipTALI-1 K/O) were kindly provided by the group of Stephane Genin. Bacteria were grown in Phi medium (Bactopeptone: 10 g/L, Casaminoacids 1 g/L, Yeast extract 1 g /L), supplemented with: Agar Agar 15 g/L, 25ml/L glucose (20%) and 5 ml/L TTC (1%) for plates. Bacterial strains were grown at 28°C.

A. thaliana plants were grown for four weeks in Gifi pots in a short day growth chamber. On the day of infection, a bacterial over-night culture was adjusted to an OD600 of 0.01. The lower 3rd of each gifi pot was cut off using scissors, and the plants were placed into the bacterial suspension for 15-20 minutes, and then transferred onto soil and kept in a long day growth chamber (27°C/26°C, HR75%, 12h Day /12h Night). Disease was scored from the third day after infection using the disease index (see section 2.2.1.2).

4.4 Computational methods and additional R scripts

4.4.1 Alignments and calculations of alignment sequence identities or similarities

Alignments were performed using the CLC Main Workbench (Quiagen) implementation of ClustalW in the additional alignments plugin. Pairwise sequence identities and pairwise sequence similarities were calculated from ClustalW alignments using the “Create Pairwise Comparison” tool in CLC Main Workbench (found in the “Alignments & Trees” toolbox).

All R scripts presented in this work, including the ones in the results section, were conceived and written by me and have been deposited on the group internal server MN01131 (ZMBP, Tübingen).

4.4.2 Extraction of individual *repeat* sequences from *repeat* arrays (*CRD* sequences)

Repeat arrays were initially extracted from the full CDS, with the starting point defined as the first Leucine codon of the first canonical *repeat*, using CLC Main workbench. All repeat arrays of interest were exported as a multi-fasta file, and subsequently individual repeats were extracted, numbered and collected into a new multi-fasta file using the following R script (RepeatSplitter.R).

```
require("Biostrings")
require("seqinr")

filename <- c("Arrays.fa") #define file name here (input)
outputname <- c("Repeats.fa") #define file name here (output)

RepeatSeqs <- readDNASTringSet(paste("/path/where/files/are", filename,
sep=""), format="fasta", nrec=-1L, skip=0L, use.names=T)

RepeatType <- "" ## Options are TAL or RipTAL

#OFFSET FOR shifted Repeat starts.
offset <- 0
#Section to set repeat length (nucleotides) based on RepeatType
if (RepeatType == "RipTAL") {
  RepLength <- 105
}
if (RepeatType == "TAL") {
  RepLength <- 102
}
```

```
for (i in 1:20) {#number of Loops, defines the number of repeats extracted. With the current setting 20 repeats are extracted (RipTALs only have 17). If more repeats are defined here, these have to be added in the RepeatSeqs_IndReps container
```

```
  outputContainer <- paste("RepeatSeqs_Reps", i, sep = "") #name of Output containers, one per Repeat(Numbered)
  startBase <- (offset+(i*RepLength)-(RepLength-1)) #Defines starting point of the extracted sequence
  endBase <- offset+i*RepLength #end of extracted sequence
  assign(outputContainer, substring(RepeatSeqs, startBase, endBase)) #puts the extracted sequence into the corresponding output container, outputcontainer is a variable, defined in the first step of this Loop
}
```

```
RepeatSeqs_IndReps <- DNASTringSet(c(RepeatSeqs_Reps1,RepeatSeqs_Reps2,RepeatSeqs_Reps3,RepeatSeqs_Reps4,RepeatSeqs_Reps5,RepeatSeqs_Reps6,RepeatSeqs_Reps7,RepeatSeqs_Reps8,RepeatSeqs_Reps9,RepeatSeqs_Reps10,RepeatSeqs_Reps11,RepeatSeqs_Reps12,RepeatSeqs_Reps13,RepeatSeqs_Reps14,RepeatSeqs_Reps15,RepeatSeqs_Reps16,RepeatSeqs_Reps17,RepeatSeqs_Reps18,RepeatSeqs_Reps19,RepeatSeqs_Reps20))
```

```
seqnum <- length(RepeatSeqs) # number of Seqs in the StringSet (Number of Sequences the repeats were extracted from)
```

```
for (i in 1:20) {
  startSeq <- ((i*seqnum)-(seqnum-1))
  endSeq <- i*seqnum
  names(RepeatSeqs_IndReps)[startSeq:endSeq] <- paste(names(RepeatSeqs_IndReps[startSeq:endSeq]), "_Rep", i, sep="")
}
```

```
Ripreps <- RepeatSeqs_IndReps[which(width(RepeatSeqs_IndReps) != 0)] # Remove Sequences of length 0, collect all others in Ripreps
```

```
writeXStringSet(Ripreps, paste("/path/to/save/script/output/", output
```

```
tname ,sep=""), append=FALSE, format="fasta") #Write individual repeats
at fasta file to the directory given
```

4.4.3 Visualization of sequence similarities

Sequence similarities were calculated as described in 4.4.1, and the resulting table was exported, and subsequently imported into R and heatmaps were generated and saved using the following commands:

```
require(RColorBrewer)
require(gplots)
col_pwc <- colorRampPalette(c("blue", "red"))(n = 40) # define colors
s

col_breaks_pwc <- c(seq(0, 60, length=1),
                    seq(61,100,length=40))

# defines the values to be used for color breaks. The way this is here,
color block is used for values below 60, and the transitions happen
in steps of 1 from values of 61 to 100

table <- x #This is where the table or table subset that should be plotted
as a heatmap should be defined

heatmap.2(as.matrix(table),
          colsep = c(1:ncol(table)),
          rowsep = c(1:nrow(table)),
          sepcolor="black",
          sepwidth=c(0.05,0.05),
          cellnote =round(table) , # data set for cell labels
          main = "Repeat comparison\n A vs B", # heat map title
          notecol="black", # change font color of cell labels to
black
          density.info="none", # turns off density plot inside color
Legend
          trace="none", # turns off trace lines inside the heatmap
```

```
margins =c(12,12),      # widens margins around plot
col=col_pwc,           # use on color palette defined above
breaks=col_breaks_pwc, # enable color transition at spe
cified limits, defined above
dendrogram="none",    # control dendrogram
Colv = "NA",          # turn off column clustering
Rowv = "NA",          # turn off row clustering
cexCol=1.5
)
quartz.save("X.pdf",type="pdf")
dev.off()
```


References

- Abramovitch RB, Anderson JC, Martin GB. 2006. Bacterial elicitation and evasion of plant innate immunity. *Nat. Rev. Mol. Cell Biol.* 7:601–611.
- Van den Ackerveken G, Marois E, Bonas U. 1996. Recognition of the Bacterial Avirulence Protein AvrBs3 Occurs inside the Host Plant Cell. *Cell* 87:1307–1316.
- Ailloud F, Lowe T, Cellier G, Roche D, Allen C, Prior P. 2015. Comparative genomic analysis of *Ralstonia solanacearum* reveals candidate genes for host specificity. *BMC Genomics* 16:270.
- Albert I, Böhm H, Albert M, Feiler CE, Imkampe J, Wallmeroth N, Brancato C, Raaymakers TM, Oome S, Zhang H, et al. 2015. An RLP23–SOBIR1–BAK1 complex mediates NLP-triggered immunity. *Nat. Plants* 1:15140.
- Altman DG, Bland JM. 1998. Time to event (survival) data. *BMJ* 317:468–9.
- Angot A, Peeters N, Lechner E, Vailliau F, Baud C, Gentzbittel L, Sartorel E, Genschik P, Boucher C, Genin S. 2006. *Ralstonia solanacearum* requires F-box-like domain-containing type III effectors to promote disease on several host plants. *Proc. Natl. Acad. Sci. U. S. A.* 103:14620–5.
- Berendsen RL, Pieterse CMJ, Bakker PAHM. 2012. The rhizosphere microbiome and plant health. *Trends Plant Sci.* 17:478–486.
- Bland JM, Altman DG. 1998. Survival probabilities (the Kaplan-Meier method). *BMJ* 317:1572.
- Bland JM, Altman DG. 2004. The logrank test. *BMJ* 328:1073.
- Boch J, Bonas U. 2010. *Xanthomonas AvrBs3* family-type III effectors: discovery and function. *Annu. Rev. Phytopathol.* 48:419–36.
- Boch J, Scholze H, Schornack S, Landgraf A, Hahn S, Kay S, Lahaye T, Nickstadt A, Bonas U. 2009. Breaking the code of DNA binding specificity of TAL-type III effectors. *Science* 326:1509–12.
- Bochtler M. 2012. Structural basis of the TAL effector-DNA interaction. *Biol. Chem.* 393:1055–66.
- Bogdanove AJ, Schornack S, Lahaye T. 2010. TAL effectors: finding plant genes for disease and defense. *Curr. Opin. Plant Biol.* 13:394–401.
- Booher NJ, Carpenter SCD, Sebra RP, Wang L, Salzberg SL, Leach JE,

- Bogdanove AJ. 2015. Single molecule real-time sequencing of *Xanthomonas oryzae* genomes reveals a dynamic structure and complex TAL (transcription activator-like) effector gene relationships. *Microb. Genomics* 1.
- Burén S, Ortega-Villasante C, Otvös K, Samuelsson G, Bakó L, Villarejo A. 2012. Use of the foot-and-mouth disease virus 2A peptide co-expression system to study intracellular protein trafficking in Arabidopsis. *PLoS One* 7:e51973.
- Bzymek M, Lovett ST. 2001. Instability of repetitive DNA sequences: the role of replication in multiple mechanisms. *Proc. Natl. Acad. Sci. U. S. A.* 98:8319–25.
- Cao J, Schneeberger K, Ossowski S, Günther T, Bender S, Fitz J, Koenig D, Lanz C, Stegle O, Lippert C, et al. 2011. Whole-genome sequencing of multiple *Arabidopsis thaliana* populations. *Nat. Genet.* 43:956–963.
- Cao Y, Liang Y, Tanaka K, Nguyen CT, Jedrzejczak RP, Joachimiak A, Stacey G. 2014. The kinase LYK5 is a major chitin receptor in *Arabidopsis* and forms a chitin-induced complex with related kinase CERK1. *Elife* 3:e03766.
- Chen L. 2014. SWEET sugar transporters for phloem transport and pathogen nutrition. *New Phytol.* 201:1150–1155.
- Chisholm ST, Coaker G, Day B, Staskawicz BJ. 2006. Host-Microbe Interactions: Shaping the Evolution of the Plant Immune Response. *Cell* 124:803–814.
- Cho I, Blaser MJ. 2012. The human microbiome: at the interface of health and disease. *Nat. Rev. Genet.* 13:260–70.
- Clough SJ, Bent AF. 1998. Floral dip: A simplified method for *Agrobacterium*-mediated transformation of *Arabidopsis thaliana*. *Plant J.* 16:735–743.
- Cooper MD, Alder MN. 2006. The Evolution of Adaptive Immune Systems. *Cell* 124:815–822.
- D’Arcy. 2001. Illustrated Glossary of Plant Pathology. *Plant Heal. Instr.*
- Deng D, Yan C, Wu J, Pan X, Yan N. 2014. Revisiting the TALE repeat. *Protein Cell* 5:297–306.
- Deslandes L, Pileur F, Liaubet L. 1998. Genetic characterization of *RRS1*, a recessive locus in *Arabidopsis thaliana* that confers resistance to the bacterial soilborne pathogen *Ralstonia solanacearum*. *Mol. plant-* 11:659–67.

Doyle EL, Hummel AW, Demorest ZL, Starker CG, Voytas DF, Bradley P, Bogdanove AJ. 2013. TAL Effector Specificity for base 0 of the DNA Target Is Altered in a Complex, Effector- and Assay-Dependent Manner by Substitutions for the Tryptophan in Cryptic Repeat -1. PLoS One 8:e82120.

Fall S, Mercier A, Bertolla F, Calteau A, Gueguen L, Perrière G, Vogel TM, Simonet P. 2007. Horizontal gene transfer regulation in bacteria as a “spandrel” of DNA repair mechanisms. PLoS One 2:e1055.

Fegan M, Prior P. 2005. How complex is the “*Ralstonia solanacearum* species complex”?

Feil EJ, Holmes EC, Bessen DE, Chan MS, Day NP, Enright MC, Goldstein R, Hood DW, Kalia A, Moore CE, et al. 2001. Recombination within natural populations of pathogenic bacteria: short-term empirical estimates and long-term phylogenetic consequences. Proc. Natl. Acad. Sci. U. S. A. 98:182–7.

Ferreira RM, de Oliveira ACP, Moreira LM, Belasque J, Gourbeyre E, Siguier P, Ferro MIT, Ferro J a., Chandler M, Varani AM. 2015. A TALE of transposition: Tn3-like transposons play a major role in the spread of pathogenicity determinants of *Xanthomonas citri* and other xanthomonads. MBio 6:e02505–14.

Gao H, Wu X, Chai J, Han Z. 2012. Crystal structure of a TALE protein reveals an extended N-terminal DNA binding region. Cell Res. 22:1716–1720.

Genin S, Denny TP. 2012. Pathogenomics of the *Ralstonia solanacearum* species complex. Annu. Rev. Phytopathol. 50:67–89.

Gómez-Gómez L, Boller T. 2000. FLS2: an LRR receptor-like kinase involved in the perception of the bacterial elicitor flagellin in Arabidopsis. Mol. Cell 5:1003–1011.

Gómez-Gómez L, Boller T. 2002. Flagellin perception: A paradigm for innate immunity. Trends Plant Sci. 7:251–256.

Grant SR, Fisher EJ, Chang JH, Mole BM, Dangl JL. 2006. Subterfuge and Manipulation: Type III Effector Proteins of Phytopathogenic Bacteria. Annu. Rev. Microbiol. 60:425–449.

Grau J, Wolf A, Reschke M, Bonas U, Posch S, Boch J. 2013. Computational Predictions Provide Insights into the Biology of TAL Effector Target Sites. Tresch A, editor. PLoS Comput. Biol. 9:e1002962.

Graves CJ, Ros VID, Stevenson B, Sniegowski PD, Brisson D. 2013. Natural

selection promotes antigenic evolvability. Moxon R, editor. PLoS Pathog. 9:e1003766.

Gu K, Yang B, Tian D, Wu L, Wang D, Sreekala C, Yang F, Chu Z, Wang G-L, White FF, et al. 2005. R gene expression induced by a type-III effector triggers disease resistance in rice. Nature 435:1122–5.

Guidot A, Jiang W, Ferdy J-B, Thébaud C, Barberis P, Gouzy J, Genin S. 2014. Multihost Experimental Evolution of the Pathogen *Ralstonia solanacearum* Unveils Genes Involved in Adaptation to Plants. Mol. Biol. Evol. 31

Guidot A, Prior P, Schoenfeld J, Carrère S, Genin S, Boucher C. 2007. Genomic structure and phylogeny of the plant pathogen *Ralstonia solanacearum* inferred from gene distribution analysis. J. Bacteriol. 189:377–87.

Hacquard S, Garrido-Oter R, González A, Spaepen S, Ackermann G, Lebeis S, McHardy AC, Dangl JL, Knight R, Ley R, et al. 2015. Microbiota and Host Nutrition across Plant and Animal Kingdoms. Cell Host Microbe 17:603–616.

Hayward A. 1991. Biology and epidemiology of bacterial wilt caused by *Pseudomonas solanacearum*. Annu. Rev. Phytopathol. 29:65–87.

Heuer H, Yin Y-N, Xue Q-Y, Smalla K, Guo J-H. 2007. Repeat domain diversity of *avrBs3*-like genes in *Ralstonia solanacearum* strains and association with host preferences in the field. Appl. Environ. Microbiol. 73:4379–84.

Ho GD, Yang CH. 1999. A Single Locus Leads to Resistance of *Arabidopsis thaliana* to Bacterial Wilt Caused by *Ralstonia solanacearum* Through a Hypersensitive-like Response. Phytopathology 89:673–8.

Holkers M, Maggio I, Liu J, Janssen JM, Miselli F, Mussolino C, Recchia A, Cathomen T, Gonçalves M a F V. 2013. Differential integrity of TALE nuclease genes following adenoviral and lentiviral vector gene transfer into human cells. Nucleic Acids Res. 41:e63.

van der Hoorn RALL, Kamoun S. 2008. From Guard to Decoy: a new model for perception of plant pathogen effectors. Plant Cell 20:2009–17.

Huet G. 2014. Breeding for resistances to *Ralstonia solanacearum*. Front. Plant Sci.

Hummel AW, Doyle EL, Bogdanove AJ. 2012. Addition of transcription

activator-like effector binding sites to a pathogen strain-specific rice bacterial blight resistance gene makes it effective against additional strains and against bacterial leaf streak. *New Phytol.* 195:883–93.

Hutin M, Sabot F, Ghesquière A, Koebnik R, Szurek B. 2015. A knowledge-based molecular screen uncovers a broad spectrum *OsSWEET14* resistance allele to bacterial blight from wild rice. *Plant J.*:n/a–n/a.

Jones JDG, Dangl JL. 2006. The plant immune system. *Nature* 444:323–329.

Juillerat A, Bertonati C, Dubois G, Guyot V, Thomas S, Valton J, Beurdeley M, Silva GH, Daboussi F, Duchateau P. 2014. BurrH: a new modular DNA binding protein for genome engineering. *Sci. Rep.* 4:1–6.

Jyothi HK, Santhosha HM. 2012. Recent advances in breeding for bacterial wilt (*Ralstonia solanacearum*) resistance in Tomato -review. *Curr. Biot.* 6:370–398.

Kajava A V, Anisimova M, Peeters N. 2008. Origin and evolution of GALA-LRR, a new member of the CC-LRR subfamily: from plants to bacteria? *PLoS One* 3:e1694.

Kay S, Hahn S, Marois E, Hause G, Bonas U. 2007. A bacterial effector acts as a plant transcription factor and induces a cell size regulator. *Science* (80-.). 318:648–51.

Kim MG, da Cunha L, McFall AJ, Belkhadir Y, DebRoy S, Dangl JL, Mackey D. 2005. Two *Pseudomonas syringae* Type III Effectors Inhibit RIN4-Regulated Basal Defense in Arabidopsis. *Cell* 121:749–759.

Kirschner M, Gerhart J. 1998. Evolvability. *Proc. Natl. Acad. Sci. U. S. A.* 95:8420–7.

Kistner C, Parniske M. 2002. Evolution of signal transduction in intracellular symbiosis. *Trends Plant Sci.* 7:511–518.

Koch E, Slusarenko a. 1990. Arabidopsis is susceptible to infection by a downy mildew fungus. *Plant Cell* 2:437–45.

Lamb BM, Mercer a. C, Barbas CF. 2013. Directed evolution of the TALE N-terminal domain for recognition of all 5' bases. *Nucleic Acids Res.* 41:9779–9785.

de Lange O, Binder A, Lahaye T. 2014. From dead leaf, to new life: TAL effectors as tools for synthetic biology. *Plant J.* 78:753–71.

de Lange O, Schreiber T, Schandry N, Radeck J, Braun KH, Koszinowski J,

- Heuer H, Strauß A, Lahaye T. 2013. Breaking the DNA-binding code of *Ralstonia solanacearum* TAL effectors provides new possibilities to generate plant resistance genes against bacterial wilt disease. *New Phytol.* 199:773–86.
- de Lange O, Wolf C, Dietze J, Elsaesser J, Morbitzer R, Lahaye T. 2014. Programmable DNA-binding proteins from *Burkholderia* provide a fresh perspective on the TALE-like repeat domain. *Nucleic Acids Res.* 42:7436–49.
- de Lange O, Wolf C, Thiel P, Krüger J, Kleusch C, Kohlbacher O, Lahaye T. 2015. DNA-binding proteins from marine bacteria expand the known sequence diversity of TALE-like repeats. :1–16.
- Lassalle F, Périan S, Bataillon T, Nesme X, Duret L, Daubin V. 2015. GC-Content evolution in bacterial genomes: the biased gene conversion hypothesis expands. *PLoS Genet.* 11:e1004941.
- Lau C-H, Zhu H, Tay JC-K, Li Z, Tay FC, Chen C, Tan W-K, Du S, Sia V-K, Phang R-Z, et al. 2014. Genetic rearrangements of variable di-residue (RVD)-containing repeat arrays in a baculoviral TALEN system. *Mol. Ther. — Methods Clin. Dev.* 1:14050.
- Leoni C, Volpicella M, De Leo F, Gallerani R, Ceci LR. 2011. Genome walking in eukaryotes. *FEBS J.* 278:3953–77.
- Li L, Atef A, Piatek A, Ali Z, Piatek M, Aouida M, Sharakuu A, Mahjoub A, Wang G, Khan S, et al. 2013. Characterization and DNA-binding specificities of *Ralstonia* TAL-like effectors. *Mol. Plant* 6:1318–30.
- Li M, Doll J, Weckermann K, Oecking C, Berendzen KW, Schöffl F. 2010. Detection of in vivo interactions between *Arabidopsis* class A-HSFs, using a novel BiFC fragment, and identification of novel class B-HSF interacting proteins. *Eur. J. Cell Biol.* 89:126–132.
- Liebrand TWH, van den Burg H a., Joosten MH a J. 2014. Two for all: Receptor-associated kinases SOBIR1 and BAK1. *Trends Plant Sci.* 19:123–132.
- Van der Linden L, Bredenkamp J, Naidoo S, Fouché-Weich J, Denby KJ, Genin S, Marco Y, Berger DK. 2013. Gene-for-gene tolerance to bacterial wilt in *Arabidopsis*. *Mol. Plant. Microbe. Interact.* 26:398–406.
- Lonjon F, Turner M, Henry C, Rengel D, Lohou D, van de Kerkhove Q, Cazale A-C, Peeters N, Genin S, Vaillau F. 2015. Comparative Secretome Analysis

of *Ralstonia solanacearum* Type 3 Secretion-Associated Mutants Reveals a Fine Control of Effector Delivery, Essential for Bacterial Pathogenicity. *Mol. Cell. Proteomics*:mcp.M115.051078.

Macho AP, Guidot A, Barberis P, Beuzón CR, Genin S. 2010. A competitive index assay identifies several *Ralstonia solanacearum* type III effector mutant strains with reduced fitness in host plants. *Mol. Plant. Microbe. Interact.* 23:1197–205.

Mak AN-S, Bradley P, Bogdanove AJ, Stoddard BL. 2013. TAL effectors: function, structure, engineering and applications. *Curr. Opin. Struct. Biol.* 23:93–9.

Mak AN-S, Bradley P, Cernadas RA, Bogdanove AJ, Stoddard BL. 2012. The crystal structure of TAL effector PthXo1 bound to its DNA target. *Science* 335:716–9.

Miller JC, Zhang L, Xia DF, Campo JJ, Ankoudinova I V, Guschin DY, Babiarz JE, Meng X, Hinkley SJ, Lam SC, et al. 2015. Improved specificity of TALE-based genome editing using an expanded RVD repertoire. *Nat. Methods* 12.

Milling A, Meng F, Denny TP, Allen C. 2009. Interactions with hosts at cool temperatures, not cold tolerance, explain the unique epidemiology of *Ralstonia solanacearum* race 3 biovar 2. *Phytopathology* 99:1127–1134.

Miya A, Albert P, Shinya T, Desaki Y, Ichimura K, Shirasu K, Narusaka Y, Kawakami N, Kaku H, Shibuya N. 2007. CERK1, a LysM receptor kinase, is essential for chitin elicitor signaling in *Arabidopsis*. *Proc. Natl. Acad. Sci. U. S. A.* 104:19613–8.

Morbitzer R, Elsaesser J, Hausner J, Lahaye T. 2011. Assembly of custom TALE-type DNA binding domains by modular cloning. *Nucleic Acids Res.* 39:5790–9.

Morrison LJ, McCulloch R, Hall JPJ. 2014. DNA Recombination Strategies During Antigenic Variation in the African Trypanosome. In: *Mobile DNA III*. American Society of Microbiology. p. 409–435.

Moscou MJ, Bogdanove AJ. 2009. A simple cipher governs DNA recognition by TAL effectors. *Science* 326:1501.

Murillo J, Shen H, Gerhold D, Sharma A, Cooksey DA, Keen NT. 1994. Characterization of pPT23B, the Plasmid Involved in Syringolide Production by *Pseudomonas syringae* pv. *tomato* PT23. *Plasmid* 31:275–287.

- N'guessan C, Abo K, Fondio L. 2012. So Near and Yet so Far: The Specific Case of *Ralstonia solanacearum* Populations from Côte d'Ivoire in Africa. *Phytopathology*.
- Nakamura S, Mano S, Tanaka Y, Ohnishi M, Nakamori C, Araki M, Niwa T, Nishimura M, Kaminaka H, Nakagawa T, et al. 2010. Gateway binary vectors with the *bialaphos* resistance gene, *bar*, as a selection marker for plant transformation. *Biosci. Biotechnol. Biochem.* 74:1315–9.
- Norris SJ. 2015. The *vls* antigenic variation systems of Lyme disease *Borrelia*: eluding host Immunity through both random, segmental gene conversion and framework heterogeneity. In: *Mobile DNA III*. Vol. 2. American Society of Microbiology. p. 471–489.
- Nürnberg T, Brunner F, Kemmerling B, Piater L. 2004. Innate immunity in plants and animals: Striking similarities and obvious differences. *Immunol. Rev.* 198:249–266.
- Pédelacq J-D, Cabantous S, Tran T, Terwilliger TC, Waldo GS. 2006. Engineering and characterization of a superfolder green fluorescent protein. *Nat. Biotechnol.* 24:79–88.
- Peeters N, Carrère S, Anisimova M, Plener L, Cazalé A-C, Genin S. 2013. Répertoire, unified nomenclature and evolution of the Type III effector gene set in the *Ralstonia solanacearum* species complex. *BMC Genomics* 14:859.
- Peeters N, Guidot A, Vaillieu F, Valls M. 2013. *Ralstonia solanacearum*, a widespread bacterial plant pathogen in the post-genomic era. *Mol. Plant Pathol.* 14:651–62.
- Pereira A La, Carazzolle MF, Abe VY, de Oliveira ML, Domingues MN, Silva JC, Cernadas R a, Benedetti CE. 2014. Identification of putative TAL effector targets of the citrus canker pathogens shows functional convergence underlying disease development and defense response. *BMC Genomics* 15:157.
- Pérez-Quintero AL, Lamy L, Gordon JL, Escalon A, Cunnac S, Szurek B, Gagnevin L. 2015. QueTAL: a suite of tools to classify and compare TAL effectors functionally and phylogenetically. *Front. Plant Sci.* 6:545.
- Pettersen EF, Goddard TD, Huang CC, Couch GS, Greenblatt DM, Meng EC, Ferrin TE. 2004. UCSF Chimera - A visualization system for exploratory research and analysis. *J. Comput. Chem.* 25:1605–1612.

Prior P, Ailloud F, Dalsing BL, Remenant B, Sanchez B, Allen C. 2016. Genomic and proteomic evidence supporting the division of the plant pathogen *Ralstonia solanacearum* into three species. *BMC Genomics* 17:90.

R Core Team. 2014. R: A language and environment for statistical computing.

Rahman MA, Abdullah H, Vanhaecke M. 1999. Histopathology of susceptible and resistant *Capsicum annuum* cultivars infected with *Ralstonia solanacearum*. *J. Phytopathol.* 147:129–140.

Ralser M, Querfurth R, Warnatz H-J, Lehrach H, Yaspo M-L, Krobitsch S. 2006. An efficient and economic enhancer mix for PCR. *Biochem. Biophys. Res. Commun.* 347:747–51.

Remenant B, de Cambiaire J-C, Cellier G, Jacobs JM, Mangenot S, Barbe V, Lajus A, Vallenet D, Medigue C, Fegan M, et al. 2011. *Ralstonia syzygii*, the Blood Disease Bacterium and some Asian *R. solanacearum* strains form a single genomic species despite divergent lifestyles. Yang C-H, editor. *PLoS One* 6:e24356.

Remenant B, Coupat-Goutaland B, Guidot A, Cellier G, Wicker E, Allen C, Fegan M, Pruvost O, Elbaz M, Calteau A, et al. 2010. Genomes of three tomato pathogens within the *Ralstonia solanacearum* species complex reveal significant evolutionary divergence. *BMC Genomics* 11:379.

Remigi P, Anisimova M, Guidot A, Genin S, Peeters N. 2011. Functional diversification of the GALA type III effector family contributes to *Ralstonia solanacearum* adaptation on different plant hosts. *New Phytol.* 192:976–87.

Römer P, Hahn S, Jordan T, Strauss T, Bonas U, Lahaye T. 2007. Plant pathogen recognition mediated by promoter activation of the pepper Bs3 resistance gene. *Science* 318:645–8.

Römer P, Strauss T, Hahn S, Scholze H, Morbitzer R, Grau J, Bonas U, Lahaye T. 2009. Recognition of AvrBs3-like proteins is mediated by specific binding to promoters of matching pepper Bs3 alleles. *Plant Physiol.* 150:1697–1712.

Safni I, Cleenwerk I, De Vos P, Fegan M, Sly L, Kappler U. 2014. Polyphasic taxonomic revision of the *Ralstonia solanacearum* species complex: proposal to emend the descriptions of *R. solanacearum* and *R. syzygii* and reclassify current *R. syzygii* strains as *Ralstonia syzygii* subsp. *syzygii*, *R. solanacearum* phylotype IV. *Int. J. Syst. Evol. Microbiol.*

820940:ijs.0.066712-0-.

Salanoubat M, Genin S, Artiguenave F, Gouzy J, Mangenot S, Arlat M, Billault A, Brottier P, Camus JC, Cattolico L, et al. 2002. Genome sequence of the plant pathogen *Ralstonia solanacearum*. *Nature* 415:497–502.

Saucet SB, Ma Y, Sarris PF, Furzer OJ, Sohn KH, Jones JDG. 2015. Two linked pairs of Arabidopsis TNL resistance genes independently confer recognition of bacterial effector AvrRps4. *Nat. Commun.* 6:6338.

Schindelin J, Arganda-Carreras I, Frise E, Kaynig V, Longair M, Pietzsch T, Preibisch S, Rueden C, Saalfeld S, Schmid B, et al. 2012. Fiji: an open-source platform for biological-image analysis. *Nat. Methods* 9:676–82.

Schornack S, Ballvora A, Gürlebeck D, Peart J, Ganai M, Baker B, Bonas U, Lahaye T. 2004. The tomato resistance protein *Bs4* is a predicted non-nuclear TIR-NB-LRR protein that mediates defense responses to severely truncated derivatives of AvrBs4 and overexpressed AvrBs3. *Plant J.* 37:46–60.

Schornack S, Minsavage G V., Stall RE, Jones JB, Lahaye T. 2008. Characterization of AvrHah1, a novel AvrBs3-like effector from *Xanthomonas gardneri* with virulence and avirulence activity. *New Phytol.* 179:546–556.

Schütze K, Harter K, Chaban C. 2009. Bimolecular fluorescence complementation (BiFC) to study protein-protein interactions in living plant cells. *Methods Mol. Biol.* 479:189–202.

Sedgwick P. 2013. Cox proportional hazards regression. *BMJ* 347:f4919–f4919.

Strauss T, van Poecke RMP, Strauss A, Römer P, Minsavage G V, Singh S, Wolf C, Strauss A, Kim S, Lee H-A, et al. 2012. RNA-seq pinpoints a *Xanthomonas* TAL-effector activated resistance gene in a large-crop genome. *Proc. Natl. Acad. Sci. U. S. A.* 109:19480–5.

Streubel J, Blücher C, Landgraf A, Boch J. 2012. TAL effector RVD specificities and efficiencies. *Nat. Biotechnol.* 30:593–5.

Sun H, Lang Z, Zhu L, Huang D. 2012. Acquiring transgenic tobacco plants with insect resistance and glyphosate tolerance by fusion gene transformation. *Plant Cell Rep.* 31:1877–87.

Szymczak-Workman AL, Vignali KM, Vignali D a a. 2012. Design and construction of 2A peptide-linked multicistronic vectors. *Cold Spring Harb. Protoc.* 2012:199–204.

- Thomas WJ, Thireault C a, Kimbrel J a, Chang JH. 2009. Recombineering and stable integration of the *Pseudomonas syringae* pv. *syringae* 61 hrp/hrc cluster into the genome of the soil bacterium *Pseudomonas fluorescens* Pf0-1. *Plant J.* 60:919–28.
- Thompson CJ, Movva NR, Tizard R, Cramer R, Davies JE, Lauwereys M, Botterman J. 1987. Characterization of the herbicide-resistance gene *bar* from *Streptomyces hygroscopicus*. *EMBO J.* 6:2519–2523.
- Tian D, Wang J, Zeng X, Gu K, Qiu C, Yang X, Zhou Z, Goh M, Luo Y, Murata-Hori M, et al. 2014. The rice TAL effector-dependent resistance protein XA10 triggers cell death and calcium depletion in the endoplasmic reticulum. *Plant Cell* 26:497–515.
- Tsuda K, Qi Y, Nguyen L V, Bethke G, Tsuda Y, Glazebrook J, Katagiri F. 2012. An efficient *Agrobacterium*-mediated transient transformation of *Arabidopsis*. *Plant J.* 69:713–9.
- Turner TR, James EK, Poole PS. 2013. The Plant Microbiome. *Genome Biol.* 14:1–10.
- Verdier V, Triplett LR, Hummel AW, Corral R, Cernadas RA, Schmidt CL, Bogdanove AJ, Leach JE. 2012. Transcription activator-like (TAL) effectors targeting *OsSWEET* genes enhance virulence on diverse rice (*Oryza sativa*) varieties when expressed individually in a TAL effector-deficient strain of *Xanthomonas oryzae*. *New Phytol.* 196:1197–1207.
- Vink C, Rudenko G, Seifert HS. 2012. Microbial antigenic variation mediated by homologous DNA recombination. *FEMS Microbiol. Rev.* 36:917–948.
- Walter J, Ley R. 2011. The Human Gut Microbiome: Ecology and Recent Evolutionary Changes. *Annu. Rev. Microbiol.* 65:411–429.
- Weber E, Engler C, Gruetzner R, Werner S, Marillonnet S. 2011. A modular cloning system for standardized assembly of multigene constructs. *PLoS One* 6:e16765.
- Wicker E, Lefeuvre P, de Cambiaire J-C, Lemaire C, Poussier S, Prior P. 2012. Contrasting recombination patterns and demographic histories of the plant pathogen *Ralstonia solanacearum* inferred from MLSA. *ISME J.* 6:961–74.
- Wicky BIM, Stenta M, Dal Peraro M. 2013. TAL Effectors Specificity Stems from Negative Discrimination. Carloni P, editor. *PLoS One* 8:e80261.

- Wilkins KE, Booher NJ, Wang L, Bogdanove AJ. 2015. TAL effectors and activation of predicted host targets distinguish Asian from African strains of the rice pathogen *Xanthomonas oryzae* pv. *oryzicola* while strict conservation suggests universal importance of five TAL effectors. *Front. Plant Sci.* 6.
- Wittmann J, Brancato C, Berendzen KW, Dreiseikelmann B. 2015. Development of a tomato plant resistant to *Clavibacter michiganensis* using the endolysin gene of bacteriophage CMP1 as a transgene. *Plant Pathol.*
- Wu L, Goh ML, Sreekala C, Yin Z. 2008. XA27 depends on an amino-terminal signal-anchor-like sequence to localize to the apoplast for resistance to *Xanthomonas oryzae* pv *oryzae*. *Plant Physiol.* 148:1497–1509.
- Yang B, Sugio A, White FF. 2005. Avoidance of host recognition by alterations in the repetitive and C-terminal regions of AvrXa7, a type III effector of *Xanthomonas oryzae* pv. *oryzae*. *Mol. Plant. Microbe. Interact.* 18:142–9.
- Yang Y, Gabriel DW. 1995. Intragenic recombination of a single plant pathogen gene provides a mechanism for the evolution of new host specificities. *J. Bacteriol.* 177:4963–8.
- Zhang J, Yin Z, White F. 2015. TAL effectors and the executor R genes. *Front. Plant Sci.* 6:641.
- Zhu W. 1999. The C Terminus of AvrXa10 Can Be Replaced by the Transcriptional Activation Domain of VP16 from the Herpes Simplex Virus. *Plant Cell* 11:1665–1674.
- Zipfel C. 2008. Pattern-recognition receptors in plant innate immunity. *Curr. Opin. Immunol.* 20:10–16.
- Zipfel C, Kunze G, Chinchilla D, Caniard A, Jones JDG, Boller T, Felix G. 2006. Perception of the Bacterial PAMP EF-Tu by the Receptor EFR Restricts *Agrobacterium*-Mediated Transformation. *Cell* 125:749–760.

Acknowledgements

First and foremost I thank Prof. Dr. Thomas Lahaye for supervising me and giving me the opportunity to work on the projects presented in this work, and additional ones not presented here.

I am thankful for the nice working environment I experienced in his group, and in particular I would like to thank Orlando de Lange for his constant support and input. Annett Strauß, I thank you for inspiring the RipTAL diversity study. Dousheng Wu and Patrizia Ricca, I thank you for your interest and efforts in pursuing the *R. solanacearum* related projects.

I acknowledge the technical contributions by Karl-Heinz Braun, Markus Wunderlich and Angela Dressel and by HiWis and students: Max Fürst, Max Mattheuer, Stephanie Solle, Annette Zehrer, Jana Radeck and Isabel Blunck and those I forgot, who all contributed in some way to various parts of the work shown here. Out of the people who performed practical work. I would like to emphasize the contributions by Dr. Susan Urbanus, who was a great help in performing the *A. thaliana* screen.

Outside of the Lahaye Group I would like to thank Prof. Dr. Dirk Metzler (LMU) for taking the time to introduce me into the R scripting language.

I am thankful to Dr. Stéphane Genin, Dr. Nemo Peeters and Dr. Anne-Claire Cazalé-Noel at the LIPM near Toulouse for educating me on how to work with *R. solanacearum*.

Besides providing key materials, the patience, input and intellectual stimulation from Dr. Philippe Prior strongly influenced this work and I am grateful for this fruitful relationship.

Finally, I would like to thank my parents and Dr. U. Braun for their constant support throughout my life, studies and PhD.

Without the ongoing support from Steffi, through the ups and down of my Thesis, this work might not exist and words cannot express my gratitude.

Curriculum Vitae

Niklas Peter Schandry

Day of birth: 26.01.1987

Place of birth: Munich

2006: Abitur from the Erasmus-Grasser-Gymnasium, Munich

2006-2007: Civil service

2007-2012: Bachelor of Science (240ECTS), Ludwig-Maximilians-University Munich.

Bachelor Thesis: "Funktionelle Analyse des Brg11-Proteins aus *Ralstonia solanacearum*", supervised by Prof. Dr. Thomas Lahaye

Previous research experience: Lab rotations with Prof. Dr. C. Janzen (now University of Würzburg), partially published in Gassen A, Brechtefeld D, Schandry N, et al. 2012, Nucleic Acids Res. 40:10302–10311.

2012-2013: Doctoral studies at the LMU Munich

2013-2016: Doctoral studies at the University of Tübingen (cont.)

Diversity, evolution and function of *Ralstonia solanacearum* TALE-likes

Non-academic scientific work

2007-2012 KantarHealth (prev. TNS-Healthcare) Clinical Research

Conference Attendance

2013 SFB924, Plant Biology of the Next Generation; Freising; Poster presentation

2016 "Recontres Plantes-Bactéries 2016"; Aussois, France (unscheduled talk)

Data Supplement

Dissertation Niklas Schandry

This data supplement is primarily intended to copy and paste data from the electronic version into e.g. Excel.

TABLE S1 RAW GUS DATA, NORMALIZED TO LUCIFERASE	154
TABLE S2 BACKGROUND NORMALIZED GUS DATA	171
TABLE S3 DISEASE INDECES OF <i>R. SOLANACEARUM</i> INFECTED <i>A. THALIANA</i> PLANTS	183
TABLES S4.1-S4.3 CONDUCTIVITY MEASUREMENTS	207
Table S4.1 Conductivity measurements 0-24h	207
Table S4.2 Conductivity measurements 25-48h	213
Table S4.3 Conductivity measurements 49-72h	220

Table S1 Raw GUS data, normalized to luciferase

rep1	rep2	rep3	rep4	rep5	mean	sd	date	effector	expt	genotype	experiment
NA	0,0108 72263	0,0062 17804	0,0023 50751	0,0071 65692	0,0066 51628	0,0035 00656	Feb-12-15	I-1	I-9	G	n. d. Crossreactivity
0,0050 91775	0,0126 18842	0,0029 70024	0,0085 14247	0,0066 73668	0,0071 73711	0,0036 64082	Feb-12-15	I-8	I-9	G	n. d. Crossreactivity
0,0046 92254	0,0171 24468	0,0108 01454	0,0100 33972	0,0129 4709	0,0111 19848	0,0045 27382	Feb-12-15	III-1	I-9	G	n. d. Crossreactivity
0,0881 95991	0,0689 5393	0,2569 27281	0,2596 67118	0,1514 65488	0,1650 41962	0,0904 42476	Feb-12-15	I-9	I-9	G	n. d. Crossreactivity
0,0790 42342	0,0082 68204	NA	NA	NA	0,0436 55273	0,0500 44873	Feb-12-15	IV-1	I-9	G	n. d. Crossreactivity
0,0067 40157	0,0018 8885	0,0006 45748	0,0029 70868	0,0075 48293	0,0039 58783	0,0030 35516	Feb-12-15	BD B	I-9	G	n. d. Crossreactivity
0,0329 80218	0,0234 75858	0,0327 45285	0,0234 96077	0,0335 68122	0,0292 53112	0,0052 73187	Feb-12-15	II-1	I-9	G	n. d. Crossreactivity
0,0266 42042	0,0076 90018	0,0044 16234	0,0015 16698	0,0022 67174	0,0085 06433	0,0104 17309	Feb-12-15	Avr Bs3	I-9	G	n. d. Crossreactivity
0,0830 66009	0,0720 79985	0,0703 0579	0,0566 89421	0,0592 12297	0,0682 707	0,0106 50518	Feb-12-15	I-1	I-1	G	n. d. Crossreactivity
0,0217 86555	0,0279 59086	0,0783 18191	0,1225 23364	NA	0,0626 46799	0,0472 70824	Feb-12-15	I-8	I-1	G	n. d. Crossreactivity
0,0145 88025	0,0394 73314	0,1007 40359	0,0833 01208	0,0587 71738	0,0593 74929	0,0342 26709	Feb-12-15	III-1	I-1	G	n. d. Crossreactivity
0,0014 51832	0,0055 3716	0,0389 17222	0,0586 43097	0,0657 82389	0,0340 6634	0,0296 27167	Feb-12-15	I-9	I-1	G	n. d. Crossreactivity
0,0495 88985	0,0377 30147	0,0186 70587	0,0127 81991	0,0102 27185	0,0257 99779	0,0171 10332	Feb-12-15	IV-1	I-1	G	n. d. Crossreactivity
NA	0,0006 40463	0,0078 75272	0,0260 91365	0,0162 85849	0,0127 23237	0,0109 68063	Feb-12-15	IV- BD	I-1	G	n. d. Crossreactivity

07663	16662	76495	52731	63446	83399	7176	Feb-15		1		d.	ivity
0,0074		0,0089	0,0042	0,0062	0,0066	0,0020	Feb-15	Avr	IV-		n.	Crossreact
07456	NA	70235	05689	07092	97618	09891	19-15	Bs3	1	G	d.	ivity
NA	NA	NA	NA	NA	NA	NA	19-15	I-8	I-8	A	d.	ZeroB
NA	0,0024	0,0229	0,0136	0,0110	0,0125	0,0084	19-15				n.	ZeroB
	99287	36454	94503	62439	48171	1463	19-15	I-8	I-8	C	d.	ZeroB
0,1042	0,1281	0,0427	0,0340	0,0118	0,0641	0,0495	19-15	I-8	I-8	G	d.	ZeroB
08917	97343	05097	00208	52879	92889	24369	19-15				n.	ZeroB
0,0018	0,0013		0,0250	0,0056	0,0084	0,0111	19-15	I-8	I-8	T	d.	ZeroB
38919	56999	NA	09862	94568	75087	92795	19-15				n.	ZeroB
NA	NA	NA	0,0023	0,0042	0,0033	0,0013	19-15	III-1	I-8	A	d.	ZeroB
NA	NA	0,0005			0,0005		19-15	III-1	I-8	C	d.	ZeroB
		52614	NA	NA	52614	NA	19-15				n.	ZeroB
0,1245	0,0381	0,0284	0,0120	0,0170	0,0440	0,0461	19-15	III-1	I-8	G	d.	ZeroB
41301	22387	14826	88005	00665	33437	29381	19-15				n.	ZeroB
NA	1,21E-05	0,0074	0,0060	0,0044	0,0044	0,0032	19-15	III-1	I-8	T	d.	ZeroB
		65887	32939	04794	78931	29803	19-15				n.	ZeroB
0,0186	0,0148		0,0040	0,0115	0,0123	0,0061	19-15	Avr			n.	ZeroB
82018	77025	NA	99224	7577	08509	95379	19-15	Bs3	I-8	A	d.	ZeroB
0,0080	0,0008	0,0059	0,0405		0,0138	0,0180	19-15	Avr			n.	ZeroB
06314	51945	10783	32309	NA	25338	56139	19-15	Bs3	I-8	C	d.	ZeroB
0,0383	0,0123	0,0161	0,0079	0,0108	0,0171	0,0122	19-15	Avr			n.	ZeroB
35272	48494	74716	17083	22783	1967	28013	19-15	Bs3	I-8	G	d.	ZeroB
0,0055	0,0179	0,0199	0,0245	0,0017	0,0139	0,0097	19-15	Avr			n.	ZeroB
94094	42402	28405	0158	44727	42242	69928	19-15	Bs3	I-8	T	d.	ZeroB
0,0024	0,0026	0,0031		0,0135	0,0054	0,0053	19-15		IV-		n.	Crossreact
49264	73507	59446	NA	33225	53861	94393	19-15	I-1	B	G	d.	ivity
0,0117	0,0113	0,0109	0,0060	0,0061	0,0092	0,0029	19-15		IV-		n.	Crossreact
49668	98595	45189	3775	36005	53441	04906	19-15	I-8	B	G	d.	ivity
0,0089	0,0080	0,0112	0,0063	0,0108	0,0090	0,0020	19-15		IV-		n.	Crossreact
58519	37023	50652	18806	65562	86112	38782	19-15	III-1	B	G	d.	ivity

0,0117	0,0140	0,0134	0,0116	0,0079	0,0117	0,0023	19- Feb- 15	IV- BD I-9	n.	Crossreact ivity
7275	86072	26394	76323	78214	87951	7132		B G	d.	
0,0165	0,0242	0,0146	0,0174		0,0182	0,0041	19- Feb- 15	IV- BD 1	n.	Crossreact ivity
37921	36561	80182	17319	NA	17996	7145		B G	d.	
0,0620	0,0562	0,0443	0,0402		0,0507	0,0101	19- Feb- 15	IV- BD B	n.	Crossreact ivity
06949	27278	93044	54604	NA	20469	2061		B G	d.	
0,0211	0,0212	0,0230	0,0269	0,0307	0,0246	0,0041	19- Feb- 15	IV- BD II-1	n.	Crossreact ivity
57603	28628	99822	62576	83582	46442	61564		B G	d.	
0,0056	0,0107	0,0065	0,0065	0,0147	0,0088	0,0038	19- Feb- 15	IV- BD Avr Bs3	n.	Crossreact ivity
18043	39599	10222	27708	03266	19768	45123		B G	d.	
0,0453	0,0462	0,0656	0,0885	0,0525	0,0596	0,0180	19- Feb- 15	IV- BD I-1	n.	Crossreact ivity
9984	27418	21745	97693	3268	75875	79798		II-1 G	d.	
0,0960	0,0466	0,0707	0,1081	0,0651	0,0773	0,0246	19- Feb- 15	IV- BD I-8	n.	Crossreact ivity
66591	40625	11848	87417	77074	56711	80801		II-1 G	d.	
0,0086	0,0202	0,0154	0,0095	0,0164	0,0140	0,0048	19- Feb- 15	IV- BD III-1	n.	Crossreact ivity
27795	41318	85157	36507	59349	70025	98137		II-1 G	d.	
0,0293	0,0146	0,0213	0,0147	0,0213	0,0202	0,0060	19- Feb- 15	IV- BD I-9	n.	Crossreact ivity
39097	7095	01288	45605	51066	81601	48727		II-1 G	d.	
0,0632	0,0434	0,0371	0,0413	0,0578	0,0486	0,0112	19- Feb- 15	IV- BD 1	n.	Crossreact ivity
05988	93671	94603	91712	39721	25139	56346		II-1 G	d.	
0,0080	0,0066	0,0031			0,0059	0,0025	19- Feb- 15	IV- BD B	n.	Crossreact ivity
8951	14088	72375	NA	NA	58658	23241		II-1 G	d.	
0,0198	0,0136		0,0148	0,0088	0,0142	0,0044	19- Feb- 15	IV- BD II-1	n.	Crossreact ivity
21477	57708	NA	24121	7224	93887	95716		II-1 G	d.	
0,0033	0,0170	0,0185	0,0355	0,0216	0,0192	0,0115	19- Feb- 15	IV- BD Avr Bs3	n.	Crossreact ivity
36452	04428	85005	58671	88281	34567	1784		II-1 G	d.	
0,0094	0,0258	0,0225	0,0222	0,0090	0,0178	0,0079	26- Feb- 15	IV- BD I-1	n.	Crossreact ivity
49358	4252	64026	96402	05285	31518	79207		I-1 A	d.	ZeroB
0,0172	0,0196	0,0155	0,0040		0,0141	0,0068	26- Feb- 15	IV- BD I-1	n.	Crossreact ivity
05215	04371	7757	80336	NA	16873	92416		I-1 C	d.	ZeroB
0,0256	0,0839	0,0579	0,0854	0,0210	0,0548	0,0307	26- Feb- 15	IV- BD I-1	n.	Crossreact ivity
40731	01078	65788	8099	17945	01306	80303		I-1 G	d.	ZeroB
0,0099	0,0138	0,0121	0,0116	0,0057	0,0106	0,0030	26- Feb- 15	IV- BD I-1	n.	Crossreact ivity
62463	25283	82253	57878	20626	69701	90936		I-1 T	d.	ZeroB

							15							
							26-							
0,0082	0,0180	0,0139	0,0071	0,0040	0,0103	0,0056	Feb-	Avr				n.		
96197	53415	57105	57172	46882	02154	23253	15	Bs3	I-1	A	d.	ZeroB		
							26-							
0,0136	0,0175	0,0127	0,0128	0,0086	0,0130	0,0031	Feb-	Avr				n.		
84319	3292	80503	28549	69595	99177	54222	15	Bs3	I-1	C	d.	ZeroB		
							26-							
0,0061	0,0116	0,0078	0,0383	0,0120	0,0152	0,0131	Feb-	Avr				n.		
07242	76911	19129	66314	51403	042	92416	15	Bs3	I-1	G	d.	ZeroB		
							26-							
0,0118	0,0218	0,0152	0,0145	0,0115	0,0150	0,0041	Feb-	Avr				n.		
50736	62162	44613	33487	46744	07548	59606	15	Bs3	I-1	T	d.	ZeroB		
							26-							
NA	0,0398	0,0419	0,0478	0,0609	0,0476	0,0094	Feb-					n.		
	40501	93867	08026	61366	5094	90303	15	II-1	II-1	A	d.	ZeroB		
							26-							
0,0385	0,0088	0,0265	0,0372	0,0645	0,0351	0,0202	Feb-					n.		
76286	73117	04124	14545	52031	44021	83656	15	II-1	II-1	C	d.	ZeroB		
							26-							
0,0341	0,0550	0,0635	0,0528	0,0651	0,0541	0,0123	Feb-					n.		
18119	12252	29583	3422	99273	38689	87629	15	II-1	II-1	G	d.	ZeroB		
							26-							
0,0302	0,0198	0,0379	0,0215	0,0395	0,0298	0,0090	Feb-					n.		
85841	07221	83508	82274	96713	51111	90586	15	II-1	II-1	T	d.	ZeroB		
							26-							
0,0178	0,0116	0,0076	0,0223	0,0748	0,0268	0,0274	Feb-	Avr				n.		
32899	10438	27357	23371	99223	58658	42122	15	Bs3	II-1	A	d.	ZeroB		
							26-							
0,0202	0,0135	0,0094	0,0162	0,0317	0,0182	0,0085	Feb-	Avr				n.		
5659	49024	27701	29698	91789	5096	35517	15	Bs3	II-1	C	d.	ZeroB		
							26-							
0,0062	0,0202	0,0140	0,0269	0,0164	0,0167	0,0076	Feb-	Avr				n.		
81454	06826	13481	0214	36951	6817	18906	15	Bs3	II-1	G	d.	ZeroB		
							26-							
0,0156	0,0183	0,0105	0,0206	0,0193	0,0168	0,0040	Feb-	Avr				n.		
08131	2346	06216	17426	19411	74929	07658	15	Bs3	II-1	T	d.	ZeroB		
							26-							
0,0189	0,0216	0,0220	0,0116	0,0010	0,0150	0,0088	Feb-	IV-	IV-			n.		
92501	48933	05333	6189	823	78191	60557	15	1	1	A	d.	ZeroB		
							26-							
0,0080	0,0938	0,0172	0,0057	0,0032	0,0256	0,0384	Feb-	IV-	IV-			n.		
57247	6224	54902	74662	98503	49511	95165	15	1	1	C	d.	ZeroB		
							26-							
0,0286	0,1647	0,1022	0,0243	0,0210	0,0682	0,0636	Feb-	IV-	IV-			n.		
84834	78992	65095	32407	2665	17596	37783	15	1	1	G	d.	ZeroB		
							26-							
0,0019	0,0454	0,0184	0,0055	0,0014	0,0145	0,0185	Feb-	IV-	IV-			n.		
87394	21108	09523	17868	61449	59468	6495	15	1	1	T	d.	ZeroB		
0,0071	0,0469	0,0159	0,0017	0,0010	0,0145	0,0190	26-	Avr	IV-	A	n.	ZeroB		

04316	10338	08098	15731	0636	28969	48849	Mar-15					d.	
							23-						
NA	0,0063 13232	0,0230 46054	0,0176 59816	0,0282 45004	0,0188 16027	0,0093 8892	Mar-15	I-9	I-9	C		d.	ZeroB
							23-						
0,0636 03874	0,0987 39055	0,0557 21393	0,1185 43075	0,1391 01426	0,0951 41765	0,0355 02176	Mar-15	I-9	I-9	G		d.	ZeroB
							23-						
NA	0,0082 49466	0,0030 85417	0,0664 23772	0,0322 45639	0,0275 01074	0,0288 9196	Mar-15	I-9	I-9	T		d.	ZeroB
							23-						
0,0149 04762	0,0629 22002	0,0012 1876	NA	0,0038 41634	0,0207 2179	0,0287 51832	Mar-15	Avr Bs3	I-9	A		d.	ZeroB
							23-						
0,0083 89044	0,0376 48301	NA	0,0030 41271	NA	0,0163 59539	0,0186 29499	Mar-15	Avr Bs3	I-9	C		d.	ZeroB
							23-						
0,0131 04715	0,0893 16797	NA	0,0056 39255	NA	0,0360 20256	0,0463 06849	Mar-15	Avr Bs3	I-9	G		d.	ZeroB
							23-						
NA	0,0065 57713	0,0206 97145	0,0306 9808	0,0374 94341	0,0238 6182	0,0134 41569	Mar-15	Avr Bs3	I-9	T		d.	ZeroB
							23-						
NA	0,0021 32219	0,0201 52006	0,0288 27074	0,0310 52939	0,0205 4106	0,0131 42735	Mar-15	II-1	II-1	A		d.	ZeroB
							23-						
0,0024 34716	0,0044 1408	0,0156 50656	0,0169 61552	0,0152 83593	0,0109 48919	0,0069 32591	Mar-15	II-1	II-1	C		d.	ZeroB
							23-						
NA	NA	0,0241 1991	0,0225 7215	0,0174 75017	0,0213 89026	0,0034 7685	Mar-15	II-1	II-1	G		d.	ZeroB
							23-						
NA	0,0056 81369	0,0170 56694	0,0052 14695	0,0197 8787	0,0119 35157	0,0075 75613	Mar-15	II-1	II-1	T		d.	ZeroB
							23-						
NA	0,0049 30437	0,0101 66514	0,0142 94642	0,0195 14968	0,0122 2664	0,0061 88028	Mar-15	Avr Bs3	II-1	A		d.	ZeroB
							23-						
NA	0,0003 28908	0,0099 3117	NA	0,0069 71452	0,0057 43843	0,0049 17431	Mar-15	Avr Bs3	II-1	C		d.	ZeroB
							23-						
NA	0,0066 91682	0,0013 5933	NA	0,0031 01842	0,0037 17618	0,0027 18985	Mar-15	Avr Bs3	II-1	G		d.	ZeroB
							23-						
0,0022 92285	0,0052 16017	0,0093 19801	0,0142 64264	0,0428 94309	0,0147 97335	0,0163 39411	Mar-15	Avr Bs3	II-1	T		d.	ZeroB
							23-						
0,0290 67748	0,0252 82094	0,0253 13917	0,0061 73792	0,0072 54307	0,0186 18372	0,0109 82196	Mar-15	I-1	II-1	G		d.	Crossreact ivity

5349	41607	07623	7348	35351	2231	82136	Mar-15	Bs3	BD		d.		
							26-		B				
0,0167	0,0240	0,0160	0,0332	0,0272	0,0234	0,0072	Mar-15						TempCros
59279	93737	17803	13888	88184	74578	53962	26-	I-1	II-1	G	21		sreactivity
0,0177	0,0167	0,0179	0,0252	0,0027	0,0160	0,0081	Mar-15						TempCros
42754	01281	79566	52684	5728	86713	91335	26-	I-9	II-1	G	21		sreactivity
0,0212	0,0300	0,0315	0,0456	0,0390	0,0334	0,0092	Mar-15						TempCros
21024	98319	30308	02775	2568	95621	63296	26-	I-8	II-1	G	21		sreactivity
0,0086	0,0089	0,0110	0,0185	0,0173	0,0129	0,0047	Mar-15						TempCros
41707	27114	21368	97519	30113	03564	31112	26-	III-1	II-1	G	21		sreactivity
0,0218	0,0204	0,0290	0,0236	0,0274	0,0244	0,0036	Mar-15						TempCros
5867	16219	66375	65725	49449	91288	7085	26-	II-1	II-1	G	21		sreactivity
0,0171	0,0407	0,0419	0,0511	0,0514	0,0404	0,0139	Mar-15						TempCros
74285	21095	52684	51823	61171	92212	62955	26-	IV-1	II-1	G	21		sreactivity
0,0033	0,0127	0,0051	0,0055	0,0053	0,0064	0,0036	Mar-15						TempCros
72286	88782	48467	95863	9779	60638	4632	26-	BD	II-1	G	21		sreactivity
0,0038	0,0099	0,0040	0,0083	0,0089	0,0070	0,0028	Mar-15						TempCros
97256	31471	91378	87173	27887	47033	42119	26-	Avr	II-1	G	21		sreactivity
0,0370	0,0269	0,0354	0,0357	0,0417	0,0353	0,0053	Mar-15						TempCros
80225	75089	55054	3866	07589	91323	31634	26-	I-1	I-8	G	21		sreactivity
0,0180	0,0106			0,0190	0,0159	0,0045	Mar-15						TempCros
75972	83136	NA	NA	17285	25464	64321	26-	I-9	I-8	G	21		sreactivity
0,1087	0,0362	0,0631	0,0696	0,0981	0,0751	0,0288	Mar-15						TempCros
19651	85097	14416	47645	21346	77631	97285	26-	I-8	I-8	G	21		sreactivity
0,0350	0,0688	0,0696	0,0486	0,0497	0,0543	0,0147	Mar-15						TempCros
50703	80183	43401	69006	47717	98202	55679	26-	III-1	I-8	G	21		sreactivity
0,0248	0,0147	0,0237	0,0220	0,0385	0,0248	0,0086	Mar-15						TempCros
79074	46915	61489	54297	70077	0237	5019	26-	II-1	I-8	G	21		sreactivity
0,0115	0,0091	0,0176	0,0126	0,0130	0,0128	0,0030	Mar-15						TempCros
68774	27568	02345	52526	83747	06992	88981	26-	IV-1	I-8	G	21		sreactivity
0,0119	0,0089	0,0112	0,0069	0,0106	0,0099	0,0020	Mar-15						TempCros
87578	08177	2703	76306	1052	41922	0915	26-	BD	I-8	G	21		sreactivity
0,0211	0,0069	0,0163	0,0111	0,0109	0,0133	0,0055	Mar-15						TempCros
73518	56291	74869	1285	11812	05868	26677	26-	Avr	I-8	G	21		sreactivity

65088	41775	94413	34165	31247	93338	74012	Apr-15						sreactivity
							12-						
0,0155	0,0157	0,0039	0,0109		0,0115	0,0055	May-15					n.	
06073	63547	27967	22619	NA	30052	34495	15	I-9	I-9	A	d.	ZeroB	
							12-						
0,1436	0,0304	0,0177		0,0339	0,0564	0,0585	May-15	Avr				n.	
57984	69654	39047	NA	87069	63439	47221	15	Bs3	I-9	A	d.	ZeroB	
							12-						
0,0248	0,0205		0,0195	0,0060	0,0177	0,0081	May-15					n.	
27775	67211	NA	74894	52662	55636	27923	15	I-9	I-9	C	d.	ZeroB	
							12-						
0,0157	0,0181	0,0140	0,0167	0,0140	0,0157	0,0017	May-15	Avr				n.	
73133	80906	82257	68589	96513	8028	64806	15	Bs3	I-9	C	d.	ZeroB	
							12-						
0,0915	0,1107	0,0540	0,0991	0,1048	0,0920	0,0224	May-15					n.	
44153	68581	74074	43273	99683	85953	06665	15	I-9	I-9	G	d.	ZeroB	
							12-						
0,0499	0,0091	0,0212	0,0144	0,0029	0,0195	0,0182	May-15	Avr				n.	
6074	29512	04659	71068	17135	36623	93335	15	Bs3	I-9	G	d.	ZeroB	
							12-						
0,0239	0,0311		0,0121	0,0315	0,0246	0,0090	May-15					n.	
86424	25	NA	15892	47105	93605	74364	15	I-9	I-9	T	d.	ZeroB	
							12-						
0,0155	0,0114		0,0075	0,0097	0,0110	0,0033	May-15	Avr				n.	
06841	24279	NA	63912	69718	66188	56307	15	Bs3	I-9	T	d.	ZeroB	
							12-						
0,0307	0,0176	0,0161	0,0385	0,0221	0,0250	0,0094	May-15					n.	Crossreact
90268	91213	61273	93074	04818	68129	63076	15	I-1	I-9	G	d.	ivity	
							12-						
0,0499	0,0091	0,0212	0,0144	0,0029	0,0195	0,0182	May-15	Avr				n.	Crossreact
6074	29512	04659	71068	17135	36623	93335	15	Bs3	I-9	G	d.	ivity	
							12-		IV-				
0,0190	0,0293	0,0096	0,0255	0,0265	0,0220	0,0078	May-15		BD			n.	Crossreact
38885	08501	01463	98381	12456	11937	93288	15	I-1	B	G	d.	ivity	
							12-						
0,0404	0,0293	0,0385	0,0433	0,0365	0,0376	0,0052	May-15		IV-1			n.	Crossreact
62852	50456	90514	81247	91614	75337	8307	15	I-9	1	G	d.	ivity	
							12-		IV-				
0,0125	0,0100	0,0180	0,0085	0,0092	0,0116	0,0038	May-15		BD			n.	Crossreact
20361	92947	59683	82206	35669	98173	56641	15	III-1	B	G	d.	ivity	
							12-						
0,0801	0,0940	0,1027	0,0701		0,0867	0,0144	May-15					n.	
19681	4233	39844	22305	NA	5604	83259	15	I-1	I-1	G	d.	HD8	
							12-						
0,0434	0,0425	0,0456			0,0438	0,0016	May-15	Avr				n.	
19604	18072	88093	NA	NA	75256	33393	15	Bs3	I-1	G	d.	HD8	
							12-						
0,1459	0,4013	0,1195	0,1833		0,2125	0,1285	May-15					n.	
63699	39405	84349	02744	NA	47549	47253	15	I-8	I-1	G	d.	HD8	

Table S2 Background normalized GUS Data

rep1	rep2	rep3	rep4	rep5	mean	sd	date	effector	exposure	z	test	experiment
NA	1,2781 22422	0,7309 53133	0,2763 49787	0,8423 85032	0,7819 52593	0,4115 30364	Feb-12-15	I-1	I-9	G	n.	Crossreactivity
0,5985 7932	1,4834 46905	0,3491 50335	1,0009 18575	0,7845 43632	0,8433 27753	0,4307 42407	Feb-12-15	I-8	I-9	G	n.	Crossreactivity
0,5516 12396	2,0131 1967	1,2697 98251	1,1795 74537	1,5220 35111	1,3072 27993	0,5322 30326	Feb-12-15	III-1	I-9	G	n.	Crossreactivity
10,368 15184	8,1060 91987	30,203 87922	30,525 96922	17,805 99276	19,402 01701	10,632 2443	Feb-12-15	I-9	I-9	G	n.	Crossreactivity
9,2920 66386	0,9719 94231	NA	NA	NA	5,1320 30309	5,8831 7944	Feb-12-15	IV-1	I-9	G	n.	Crossreactivity
0,7923 59952	0,2220 49589	0,0759 12898	0,3492 49554	0,8873 62873	0,4653 86973	0,3568 49417	Feb-12-15	BD B	I-9	G	n.	Crossreactivity
3,8770 91282	2,7597 76918	3,8494 73008	2,7621 53825	3,9462 04151	3,4389 39837	0,6199 05806	Feb-12-15	II-1	I-9	G	n.	Crossreactivity
4,7240 86716	4,0992 95292	3,9983 942	3,2240 11168	3,3674 90855	3,8826 55646	0,6057 10679	Feb-12-15	I-1	I-1	G	n.	Crossreactivity
1,2390 33587	1,5900 74548	4,4540 71288	6,9680 84818	NA	3,5628 1606	2,6883 61661	Feb-12-15	I-8	I-1	G	n.	Crossreactivity
0,8296 42545	2,2449 05715	5,7292 53126	4,7374 62831	3,3424 35613	3,3767 39966	1,9465 23549	Feb-12-15	III-1	I-1	G	n.	Crossreactivity
0,0825 67832	0,3149 06474	2,2132 79941	3,3351 1961	3,7411 41699	1,9374 03111	1,6849 40769	Feb-12-15	I-9	I-1	G	n.	Crossreactivity
2,8201 98877	2,1457 69231	1,0618 23881	0,7269 30722	0,5816 35128	1,4672 71568	0,9730 89883	Feb-12-15	IV-1	I-1	G	n.	Crossreactivity
NA	0,0364 24078	0,4478 78359	1,4838 54494	0,9262 00306	0,7235 89309	0,6237 69977	Feb-12-15	BD B	I-1	G	n.	Crossreactivity
0,8916 44229	2,4949 85699	1,9788 36883	1,5814 31335	3,2330 52766	2,0359 90182	0,8892 48787	Feb-12-15	II-1	I-1	G	n.	Crossreactivity
1,6499	0,8810	1,5845	0,9076	1,5714	1,3189	0,3888	Feb-12-15	I-1	I-8	G	n.	Crossreactivity

36004	69938	51155	84129	85997	45444	27951	Feb-15							d.	ivity
5,3719	4,0914	3,6413	2,8608	3,0342	3,7999	1,0061	Feb-12-							n.	Crossreact
27856	28758	30413	10941	48904	49374	70308	Feb-15	I-8	I-8	G				d.	ivity
4,8403	2,1149	1,6640		1,5724	2,5479	1,5465	Feb-12-							n.	Crossreact
99853	03263	97845	NA	32325	58321	75267	Feb-15	III-1	I-8	G				d.	ivity
0,2018	0,4389	0,6469	0,2612	0,3620	0,3822	0,1738	Feb-12-							n.	Crossreact
08739	49314	79924	30968	54196	04628	60044	Feb-15	I-9	I-8	G				d.	ivity
1,3376	0,6114	0,5331	0,2841	0,1602	0,5853	0,4584	Feb-12-	IV-1						n.	Crossreact
6365	02926	79011	78509	93362	43492	63141	Feb-15	1	I-8	G				d.	ivity
0,3535	0,2738	0,2642	0,0937	0,2197	0,2410	0,0953	Feb-12-	BD						n.	Crossreact
26472	0754	68405	9886	32113	26678	94517	Feb-15	B	I-8	G				d.	ivity
0,6729	0,8396	0,6585	1,2194	0,7582	0,8297	0,2296	Feb-12-							n.	Crossreact
39542	42844	37326	27096	08825	51126	56018	Feb-15	II-1	I-8	G				d.	ivity
14,144	8,1427	4,3830	2,9046	3,0091	6,5168	4,7626	Feb-12-		IV-					n.	Crossreact
67472	34775	52004	13551	22945	39599	8586	Feb-15	I-1	1	G				d.	ivity
4,0346	3,8702	2,6479	4,5817	4,8930	4,0055	0,8634	Feb-12-		IV-					n.	Crossreact
10812	38046	14079	83106	29731	15155	22551	Feb-15	I-8	1	G				d.	ivity
2,0522	1,3643	1,3577		1,8147	1,6472	0,3444	Feb-12-		IV-					n.	Crossreact
58728	26093	82722	NA	13828	70343	38405	Feb-15	III-1	1	G				d.	ivity
1,8990	1,5708	1,7212		4,9817	2,5432	1,6311	Feb-12-		IV-					n.	Crossreact
94872	12489	87628	NA	41568	34139	99335	Feb-15	I-9	1	G				d.	ivity
18,320		12,575		7,8741	12,923	5,2320	Feb-12-	IV-	IV-					n.	Crossreact
74747	NA	10043	NA	34655	32752	05006	Feb-15	1	1	G				d.	ivity
0,7397	1,6148	1,6787	0,9831	1,3912	1,2815	0,4072	Feb-12-	BD	IV-					n.	Crossreact
527	35304	9461	91785	97324	74345	74104	Feb-15	B	1	G				d.	ivity
2,7633	3,4365	2,3555	2,2176	3,6973	2,8940	0,6527	Feb-19-		IV-					n.	Crossreact
20183	44455	38193	13934	51208	73595	33495	Feb-15	II-1	1	G				d.	ivity
NA	NA	NA	NA	NA	NA	NA	Feb-19-	I-8	I-8	A				d.	ZeroB
NA	0,1807	1,6590	0,9905	0,8001	0,9076	0,6086	Feb-19-							n.	
NA	75837	15817	36596	56871	2128	38261	Feb-15	I-8	I-8	C				d.	ZeroB
6,0870	7,4883	2,4945	1,9860	0,6923	3,7496	2,8928	Feb-19-							n.	
86926	07076	04742	31787	54425	56991	34387	Feb-15	I-8	I-8	G				d.	ZeroB

0,1318	0,0973		1,7938	0,4084	0,6078	0,8027	19- Feb-					n.	
95505	30045	NA	19295	39917	71191	97371	15	I-8	I-8	T	d.	ZeroB	
			0,1936	0,3492	0,2714	0,1099	19- Feb-					n.	
NA	NA	NA	73251	08414	40833	79969	15	III-1	I-8	A	d.	ZeroB	
		0,0399			0,0399		19- Feb-					n.	
NA	NA	71103	NA	NA	71103	NA	15	III-1	I-8	C	d.	ZeroB	
7,2747	2,2268	1,6597	0,7060	0,9930	2,5720	2,6945	19- Feb-					n.	
49099	17917	76541	88685	48663	96181	25177	15	III-1	I-8	G	d.	ZeroB	
	0,0008	0,5354	0,4327	0,3159	0,3212	0,2316	19- Feb-					n.	
NA	68175	86847	094	3155	48993	55941	15	III-1	I-8	T	d.	ZeroB	
0,2777	0,3031	0,3582		1,5344	0,6183	0,6116	19- Feb-		IV-			n.	Crossreact
01648	26695	23271	NA	19682	67824	25323	15	I-1	B	G	d.	ivity	
							19- Feb-		IV-			n.	Crossreact
1,3321	1,2923	1,2409	0,6845	0,6957	1,0491	0,3293	15	I-8	B	G	d.	ivity	
97007	91763	83833	70192	10508	70661	63132			IV-			n.	Crossreact
1,0157	0,9112	1,2756	0,7164	1,2319	1,0301	0,2311	19- Feb-		BD			n.	Crossreact
31866	51108	17738	36791	5559	98619	60497	15	III-1	B	G	d.	ivity	
							19- Feb-		IV-			n.	Crossreact
1,3348	1,5971	1,5223	1,3238	0,9045	1,3365	0,2688	15	I-9	B	G	d.	ivity	
14083	024	07005	81028	83245	37552	64283			IV-			n.	Crossreact
1,8750	2,7479	1,6644	1,9748		2,0655	0,4729	19- Feb-	IV-	BD			n.	Crossreact
9714	81818	63585	04756	NA	86825	6599	15	1	B	G	d.	ivity	
							19- Feb-	IV-	IV-			n.	Crossreact
7,0304	6,3751	5,0333	4,5641		5,7507	1,1474	15	BD	BD			n.	Crossreact
51573	4281	57568	3432	NA	71568	91637		B	B	G	d.	ivity	
							19- Feb-		IV-			n.	Crossreact
2,3988	2,4069	2,6190	3,0570	3,4902	2,7944	0,4718	15	II-1	B	G	d.	ivity	
84411	37344	96449	61957	94007	54833	45045						n.	Crossreact
2,3603	2,4033	3,4116	4,6061	2,7311	3,1025	0,9399	19- Feb-					n.	Crossreact
25504	51063	56921	70295	59943	32745	6383	15	I-1	II-1	G	d.	ivity	
							19- Feb-					n.	Crossreact
4,9944	2,4248	3,6762	5,6246	3,3885	4,0217	1,2831	15	I-8	II-1	G	d.	ivity	
76299	33584	90011	34792	38595	54656	48222						n.	Crossreact
0,4485	1,0523	0,8050	0,4958	0,8557	0,7314	0,2546	19- Feb-					n.	Crossreact
56748	40694	69159	00441	1714	96836	5282	15	III-1	II-1	G	d.	ivity	
							19- Feb-					n.	Crossreact
1,5253	0,7627	1,1074	0,7666	1,1100	1,0544	0,3144	15	I-9	II-1	G	d.	ivity	
31784	38755	4825	20049	36195	35006	71709						n.	Crossreact
3,2860	2,2612	1,9337	2,1519	3,0070	2,5280	0,5852	19- Feb-	IV-				n.	Crossreact
62363	24289	37434	44005	71581	07934	14387	1	II-1		G	d.	ivity	

								15						
								23-						
NA	13,161 31136	8,1458 38007	1,1641 59954	1,0666 07704	5,8844 79255	5,8753 53306	Mar- 15	IV- 1	II-1	G	d.	n.	Crossreact ivity	
								23-						
NA	NA	2,0250 40496	1,0969 22008	0,8065 12396	1,3094 91633	0,6364 68434	Mar- 15	BD B	II-1	G	d.	n.	Crossreact ivity	
								23-						
NA	1,5068 8075	1,7642 5523	3,5109 35766	4,7667 11104	2,8871 95712	1,5370 85389	Mar- 15	II-1	II-1	G	d.	n.	Crossreact ivity	
								23-						
0,5261 11108	2,0320 5618	0,9378 70373	0,5185 99132	1,1909 44271	1,0411 16213	0,6231 62203	Mar- 15	I-8	I-8	A	d.	n.	ZeroB	
								23-						
1,6489 7032	1,3429 49059	3,4452 66407	1,6051 68912	4,5266 43587	2,5137 99657	1,4021 05714	Mar- 15	I-8	I-8	C	d.	n.	ZeroB	
								23-						
21,347 75038	26,375 87047	16,085 32754	18,309 30755	22,076 94892	20,839 04097	3,9193 4385	Mar- 15	I-8	I-8	G	d.	n.	ZeroB	
								23-						
2,3773 63461	3,2542 84567	3,5582 65948	3,2015 43146	5,0430 28379	3,4868 971	0,9738 11896	Mar- 15	I-8	I-8	T	d.	n.	ZeroB	
								23-						
1,0507 53282	1,0920 80051	1,2285 304	1,7649 50203	2,2224 16117	1,4717 46011	0,5074 46859	Mar- 15	III-1	I-8	A	d.	n.	ZeroB	
								23-						
1,8818 22809	1,2837 07313	3,8737 62777	3,8953 32008	6,8632 05146	3,5595 66011	2,1863 12249	Mar- 15	III-1	I-8	C	d.	n.	ZeroB	
								23-						
19,664 35584	14,045 50571	8,5716 00678	5,0574 35759	11,438 024	11,755 3844	5,5429 27867	Mar- 15	III-1	I-8	G	d.	n.	ZeroB	
								23-						
0,1638 41375	1,0252 23671	4,8902 24877	11,260 2794	11,632 43836	5,7944 01538	5,4594 93922	Mar- 15	III-1	I-8	T	d.	n.	ZeroB	
								23-						
1,9461 8851	1,1888 22001	NA	1,8302 74663	0,8852 26792	1,4626 27991	0,5090 37234	Mar- 15	IV- 1	IV- 1	A	d.	n.	ZeroB	
								23-						
6,0539 07416	3,8452 67905	0,3409 37351	0,5137 80356	0,0467 25982	2,1601 23802	2,6686 88719	Mar- 15	IV- 1	IV- 1	C	d.	n.	ZeroB	
								23-						
3,2952 06346	10,069 11162	2,2317 95983	5,5447 45235	2,0234 18964	4,6328 55629	3,3446 96344	Mar- 15	IV- 1	IV- 1	G	d.	n.	ZeroB	
								23-						
2,5531 80177	5,2463 59301	1,7394 49019	1,2766 45352	NA	2,7039 08462	1,7752 0302	Mar- 15	IV- 1	IV- 1	T	d.	n.	ZeroB	
								23-						
2,2898 98315	1,5573 54769	0,6238 57837	0,7855 7582	NA	1,3141 71685	0,7674 90992	Mar- 15	BD B	BD B	A	d.	n.	ZeroB	
								23-						
1,6254	2,3360	1,8761	1,8740	NA	1,9279	0,2964	23-	IV- IV-	IV- IV-	C	n.		ZeroB	

								15											
								14-											
4,6583	3,8682	2,3631	2,3373			3,3067	1,1506	Apr-	IV-										TempCros
609	44102	34834	77863	NA		79425	83792	15	1	II-1	G	21							sreactivity
								14-											
0,5492	1,1557	0,6606	0,5360			0,7254	0,2922	Apr-	IV-										TempCros
81763	85651	20182	20613	NA		27052	9575	15	1	I-8	G	21							sreactivity
								14-											
1,6095	1,4636	3,8193	5,4159			3,0771	1,8954	Apr-	IV-	IV-									TempCros
51787	91561	28773	48945	NA		30266	24533	15	1	1	G	21							sreactivity
								14-											
1,8289	1,4511	0,9260	1,3560			1,3905	0,3709	Apr-	IV-										TempCros
12013	54097	00706	37811	NA		26157	58779	15	1	I-1	G	26							sreactivity
								14-											
2,2301	2,1781	1,9089	2,2904			2,1519	0,1683	Apr-	IV-										TempCros
41449	7167	03125	94082	NA		27581	92125	15	1	II-1	G	26							sreactivity
								14-											
0,9853	0,9468	0,5996	0,9996			0,8828	0,1901	Apr-	IV-										TempCros
65228	57602	67127	12881	NA		75709	16151	15	1	I-8	G	26							sreactivity
								14-											
19,586	12,618	1,8473	5,6026			9,9136	7,8427	Apr-	IV-	IV-									TempCros
4972	07325	55385	53729	NA		4489	81728	15	1	1	G	26							sreactivity
								14-											
3,4876	3,8117	3,7194	4,2962	5,2445		4,1119	0,6983	Apr-											TempCros
33101	45762	05003	76791	02503		12632	26085	15	III-1	I-8	G	21							sreactivity
								14-											
3,1486	3,2077	3,0794	1,9935	0,0056		2,2869	1,3701	Apr-											TempCros
30093	49236	10512	02252	32672		84953	16583	15	III-1	I-8	G	26							sreactivity
								12-											
0,2746	0,2791	0,0695	0,1934			0,2042	0,0980	May-										n.	
21479	81492	66557	4587	NA		0385	19087	15	I-9	I-9	A	d.							ZeroB
								12-											
1,5733	1,3033		1,2404	0,3835		1,1251	0,5150	May-										n.	
41894	4896	NA	656	58603		78764	68386	15	I-9	I-9	C	d.							ZeroB
								12-											
4,6857	5,6697	2,7678	5,0747	5,3693		4,7135	1,1469	May-										n.	
71637	91659	31193	39581	86719		04158	05742	15	I-9	I-9	G	d.							ZeroB
								12-											
2,1675	2,8126		1,0948	2,8507		2,2314	0,8200	May-										n.	
41802	21781	NA	56923	65451		4649	08201	15	I-9	I-9	T	d.							ZeroB
								12-											
1,5760	0,9055	0,8272	1,9754	1,1314		1,2831	0,4843	May-										n.	Crossreact
28176	41003	29617	21975	55433		35241	76224	15	I-1	I-9	G	d.							ivity
								12-		IV-									
0,8782	1,3520	0,4429	1,1808	1,2230		1,0154	0,3641	May-		BD								n.	Crossreact
91484	43821	29467	90584	58195		4271	28881	15	I-1	B	G	d.							ivity
								12-											
1,1900	0,8632	1,1349	1,2758	1,0761		1,1080	0,1553	May-		IV-								n.	Crossreact
4074	17412	73972	72775	84926		57965	78767	15	I-9	1	G	d.							ivity
								12-											
0,5775	0,4656	0,8331	0,3959	0,4260		0,5396	0,1779	12-	III-1	IV-	G	n.							Crossreact

82481	02339	1947	09658	54857	53761	12479	May-15		BD	d.	ivity
							12-		B		
1,8260	2,1434	2,3416	1,5982		1,9773	0,3301	May-15			n.	
78927	02406	35185	19836	NA	34089	00851	12-	I-1	I-1	G	d. HD8
3,3267	9,1472	2,7255	4,1778		4,8443	2,9298	May-15			n.	
88518	83424	53284	15911	NA	60284	34814	12-	I-8	I-1	G	d. HD8
6,7633	2,7720	2,2618	2,3456	6,1953	4,0676	2,2191	May-15			n.	
34891	78027	96187	14946	64465	57703	521	12-	III-1	I-1	G	d. HD8
8,1323	5,9895	3,2586	11,987	3,7914	6,6319	3,5635	May-15		I-1-	n.	
20839	75162	12995	73116	72203	42473	60951	12-	I-1	8A	G	d. HD8
6,5974	9,4927		10,329	6,0145	8,1086	2,1227	May-15		I-1-	n.	
11763	78638	NA	81297	55534	39726	69391	12-	I-8	8A	G	d. HD8
5,0566	2,5675	1,7777	3,7358	3,8807	3,4037	1,2661	May-15		I-1-	n.	
85392	91826	39188	39745	14966	14223	99652	12-	III-1	8A	G	d. HD8
1,5205	0,8795	0,9737	4,0975	1,3549	1,7652	1,3303	May-15		BD	n.	Crossreact
83342	17289	75386	64523	60114	80131	04955	12-	II-1	B	G	d. ivity
	0,7420	1,8624	4,0170		2,2071	1,6644	May-15		IV-1	n.	Crossreact
NA	49235	48611	09224	NA	69023	71344	12-	1	I-9	G	d. ivity
1,3402	2,2667	2,3091	0,1845		1,5252	0,9993	May-15		IV-1	n.	Crossreact
83852	85752	60078	92345	NA	05507	2739	19-	1	BD	G	d. ivity
17,564	4,8307	5,0484	4,5433	5,1809	7,4335	5,6683	May-15			n.	
28052	69506	16193	83885	68273	63676	81936	19-	I-1	I-1	G	d. HD8
9,1632	3,2036	4,3257	4,7234	6,1503	5,5132	2,2965	May-15			n.	
00134	97853	67558	63091	41467	9402	15324	19-	I-8	I-1	G	d. HD8
4,3404	3,8870	3,5816	2,7960	3,9649	3,7140	0,5799	May-15			n.	
61243	375	2508	49623	48515	24392	84231	19-	III-1	I-1	G	d. HD8
1,8890	1,8858	2,1494		3,2795	2,3009	0,6639	May-15		IV-1	n.	
78265	17101	93314	NA	69682	8959	80234	19-	1	I-1	G	d. HD8
4,1251	3,0780	4,3250	5,6406	6,3944	4,7126	1,3093	May-15		I-1-	n.	
97585	12418	89825	39959	8683	85324	01697	19-	I-1	8A	G	d. HD8
13,654	2,1607	6,8229	8,7082	12,339	8,7372	4,5845	May-15		I-1-	n.	
86586	86607	68459	74552	26571	32238	56878	19-	I-8	8A	G	d. HD8
6,2173	6,4660	4,7279	4,4956	8,6346	6,1083	1,6604	May-15		I-1-	n.	
7466	83913	86553	22122	71769	47803	55967	19-	III-1	8A	G	d. HD8

6,4086	6,5670	6,7782	6,1599	9,0481	6,9924	1,1711	19- May-	IV-	I-1-	n.	
91196	91507	86427	4525	78025	38481	80184	15	1	8A	G	d. HD8
10,227	7,4300		1,5851	1,0188	5,0653	4,4990	19- May-			n.	Crossreact
40514	00881	NA	79932	34074	55008	46637	15	II-1	I-9	G	d. ivity

Table S3 Disease Indexes of *R. solanacearum* infected *A. thaliana* plants

StrainPlant	3	4	5	6	7	8	9	10	11	12	13	14	Batch
GMI1000 / Sha-1	0	0		0,5	1	2	3	2,5					10
GMI1000 / Sha-1	0	0		0,5	1	3	4	4					10
GMI1000 / Sha-1	0	0		0,5	0,5	0,5	1	1					10
GMI1000 / Sha-1	0	0		0,5	1	1	1	1					10
GMI1000 / Sha-1	0	0		0,5	1	2	2	1,5					10
GMI1000 / Sha-1	0	0		0	0,5	1	1	1					10
GMI1000 / Sha-1	0	0		0	0,5	1	1,5	1,5					10
GMI1000 / Sha-1	0	0		0	0,5	0,5	1	1					10
GMI1000 / Sha-1	0	0		0,5	0,5	0,5	0,5	1					10
GMI1000 / Sha-1	0	0		0,5	0,5	1	1	1					10
GMI1000 / Sha-1	0	0		0	0	0,5	0,5	1					10
GMI1000 / Sha-1	0	0		0	0	0,5	0,5	1					10
GMI1000 / Sha-1	0	0		0	0	0	1	2					10
GMI1000 / Sha-1	0	0		0	0	0	0	0					10
GMI1000 / Sha-1	0	0,5		0,5	0,5	0,5	1	2					10
GMI1000 / Sha-1	0	0,5		0,5	0,5	1	1,5	1,5					10
GMI1000 / Sha-1	0	0		0	0	0,5	1	1,5					10
GMI1000 / Sha-1	0	0		0	0	0,5	1	1					10
GMI1000 / Sha-1	0	0		0	0,5	0,5	1,5	1,5					10
GMI1000 / Sha-1	0	0		0	0	0	0	0					10
GRS216 / Sha-1	0	0		0	0,5	0,5	2	3					10
GRS216 / Sha-1	0	0		0	0	0,5	2	3					10
GRS216 / Sha-1	0	0		0	0,5	0,5	1	2					10
GRS216 / Sha-1	0	0		0	0,5	1	3	3,5					10
GRS216 / Sha-1	0	0		0	0,5	1	2	2					10
GRS216 / Sha-1	0	0		0	0	0,5	0,5	1					10
GRS216 / Sha-1	0	0		0,5	1	1	2	2					10
GRS216 / Sha-1	0	0		0	0,5	1	1	1					10
GRS216 / Sha-1	0	0		0	0,5	0,5	1	1,5					10
GRS216 / Sha-1	0	0		0	0	0,5	1,5	1,5					10
GRS216 / Sha-1	0	0		0	0	1	1	1					10
GRS216 / Sha-1	0	0		0	0,5	1,5	1,5	1					10
GRS216 / Sha-1	0	0		1	1	2	2	2					10
GRS216 / Sha-1	0	0		0	0	1,5	1,5	1					10
GRS216 / Sha-1	0	0		0	0,5	1,5	1,5	1,5					10
GRS216 / Sha-1	0	0		0	0	1,5	1,5	1,5					10
GRS216 / Sha-1	0	0		0,5	0,5	1,5	1,5	1,5					10
GRS216 / Sha-1	0	1		0,5	1	1,5	1,5	1,5					10
GRS216 / Sha-1	0	0		0	0	1	1	1					10

GRS216 / Sha-1	0	0		0	0	1	1	1,5		10
GMI1000 / Col-0	0	0	0	0	3			4	4	11
GMI1000 / Col-0	0	0,5	0,5	0,5	0			0	2	11
GMI1000 / Col-0	0	0,5	0,5	0,5	0			4	4	11
GMI1000 / Col-0	0	0,5	2	4	4			4	4	11
GMI1000 / Col-0	0	0	0	1	0			0	0	11
GMI1000 / Col-0	0	0	0,5	0,5	0,5			0	0	11
GMI1000 / Col-0	0	0	1	1	2			4	4	11
GMI1000 / Col-0	0	0	2	2	2,5			4	4	11
GMI1000 / Col-0	0	0	0	0	0,5			0	0	11
GMI1000 / Col-0	0	0,5	0,5	0,5	2,5			4	4	11
GMI1000 / Apost-1	0	0	0	0	0			1	2	11
GMI1000 / Apost-1	0	0	0	0	0			3	4	11
GMI1000 / Apost-1	0	0	0,5	0,5	1,5			2	3	11
GMI1000 / Apost-1	0	0	0	0	0			0	0	11
GMI1000 / Apost-1	0	0	0	0	0			3	4	11
GMI1000 / Apost-1	0	0	0	0	0			0	0	11
GMI1000 / Apost-1	0	0	0	0	0			0	0	11
GMI1000 / Apost-1	0	0	0,5	0,5	1			4	4	11
GMI1000 / Apost-1	0	0	0	0	0			0	0	11
GMI1000 / Apost-1	0	0	0	0	0			0	0	11
GMI1000 / Apost-1	0	0	0	0	0			3	4	11
GMI1000 / Apost-1	0	0	0	0	0			0	0	11
GMI1000 / Apost-1	0	0	0	0	0			0	0	11
GMI1000 / Apost-1	0	0	0	0	0			0	0	11
GMI1000 / Apost-1	0	0	0	0	0			0	0	11
GMI1000 / Apost-1	0	0	0	0	0			0	0	11
GMI1000 / Ciste-1	0	0	0	0	0			0	0	11
GMI1000 / Ciste-1	0	0	0	0	0			2	4	11
GMI1000 / Ciste-1	0	0	0	0	0			0	0	11
GMI1000 / Ciste-1	0	0	0	0	0			0	0	11
GMI1000 / Ciste-1	0	0	0	0	0			0	1	11
GMI1000 / Ciste-1	0	0	0	0	0			0	0	11
GMI1000 / Ciste-1	0	0	0	0	0			0	0	11
GMI1000 / Ciste-1	0	0	0	0	0			4	4	11
GMI1000 / Ciste-1	0	0	0	0	2			4	4	11
GMI1000 / Ciste-1	0	0	0	0	0			0	1	11
GMI1000 / Ciste-1	0	0	0	0	0			0	0	11
GMI1000 / Ciste-1	0	0	0	0	0			0	0	11
GMI1000 / Ciste-1	0	0	0	0	0			0	0	11
GMI1000 / Ciste-1	0	0	0	0	0			0	0	11
GMI1000 / Ciste-1	0	0	0	0	0			0	0	11
GMI1000 / Kidr-1	0	3	4	4	4			4	4	11
GMI1000 / Kidr-1	0	2	2	4	4			4	4	11
GMI1000 / Kidr-1	0	2	3	4	4			4	4	11

GMI1000 / Kidr-1	0	2	3	4	4	4	4	11
GMI1000 / Kidr-1	0	0	3	4	4	4	4	11
GMI1000 / Kidr-1	0	2	3	4	4	4	4	11
GMI1000 / Kidr-1	0	2	2	4	4	4	4	11
GMI1000 / Kidr-1	0	0,5	2	4	4	4	4	11
GMI1000 / Kidr-1	0	2	3	4	4	4	4	11
GMI1000 / Kidr-1	0	2	3	4	4	4	4	11
GMI1000 / Kidr-1	0	3	3	4	4	4	4	11
GMI1000 / Kidr-1	0	3	3	4	4	4	4	11
GMI1000 / Kidr-1	0	3	3	4	4	4	4	11
GMI1000 / Kidr-1	0	2	3	4	4	4	4	11
GMI1000 / Kidr-1	0	3	4	4	4	4	4	11
GMI1000 / Koz-2	0	0	0	0	0	0	0	11
GMI1000 / Koz-2	0	0	0	0	0	0	0	11
GMI1000 / Koz-2	0	0	0	0	0	0	0	11
GMI1000 / Koz-2	0	0	0	0	0	0	0	11
GMI1000 / Koz-2	0	0	0	0	0	0	0	11
GMI1000 / Koz-2	0	0	0	0	0	0	0	11
GMI1000 / Koz-2	0	0	0	0	0	0	4	11
GMI1000 / Koz-2	0	0	0	0	0	0	0	11
GMI1000 / Koz-2	0	0	0	0	0	0	0	11
GMI1000 / Koz-2	0	0	0	0	0	3	4	11
GMI1000 / Koz-2	0	0	0	0	0	0	0	11
GMI1000 / Koz-2	0	0	0	0	0	0	0	11
GMI1000 / Koz-2	0	0	0	0	0	0	0	11
GMI1000 / Koz-2	0	0	0	0	0	0	0	11
GMI1000 / Koz-2	0	0	0	0	0	0	0	11
GMI1000 / Koz-2	0	0	0	0	0	0	0	11
GMI1000 / Koz-2	0	0	0	0	0	0	0	11
GMI1000 / Mammo-2	0	0	0	0	3	4	4	11
GMI1000 / Mammo-2	0	0	0	0	0	0	0	11
GMI1000 / Mammo-2	0	0	0	0	0	0	0	11
GMI1000 / Mammo-2	0	0	0	0	0	0	0	11
GMI1000 / Mammo-2	0	0	0	0	0	0	0	11
GMI1000 / Mammo-2	0	0	0	0	0,5	4	4	11
GMI1000 / Mammo-2	0	0	0	0	0,5	4	4	11
GMI1000 / Mammo-2	0	0	0	0	0	0	0	11
GMI1000 / Mammo-2	0	0	0	0	0	0	0	11
GMI1000 / Mammo-2	0	0	0	0	0	0	0	11
GMI1000 / Mammo-2	0	0	0	0	4	4	4	11
GMI1000 / Mammo-2	0	0	0	0	0	4	4	11
GMI1000 / Mammo-2	0	0	0	0	0	0	0	11
GMI1000 / Mammo-2	0	0	0	0	0	0	0	11
GMI1000 / Mammo-2	0	0	0	0	0	0	0	11
GMI1000 / Mammo-2	0	0	0	0	0	0	0	11
GMI1000 / Moran-1	0	0	0	0	0	0	2	11

GMI1000 / Moran-1	0	0	0	0	0	0	0	11
GMI1000 / Moran-1	0	0	0	0	0	2	4	11
GMI1000 / Moran-1	0	0	0	0	0	0	0	11
GMI1000 / Moran-1	0	0	0	0	0	4	4	11
GMI1000 / Moran-1	0	0	0	0	0	0	0	11
GMI1000 / Moran-1	0	0	0	0	0	3	4	11
GMI1000 / Moran-1	0	0	0	0	0	0	4	11
GMI1000 / Moran-1	0	0	0	0	0	0	0	11
GMI1000 / Moran-1	0	0	0	0	0	4	4	11
GMI1000 / Moran-1	0	0	0	0	0	0	2	11
GMI1000 / Moran-1	0	0	0	0	0	0	0	11
GMI1000 / Moran-1	0	0	0	0	0	0	0	11
GMI1000 / Moran-1	0	0	0	0	0	0	0	11
GMI1000 / Moran-1	0	0	0	0	0	0	0	11
GMI1000 / Sha-1	0	0	0	0,5	0,5	0,5	0,5	11
GMI1000 / Sha-1	0	0	0	0,5	1	1	1	11
GMI1000 / Sha-1	0	0	0	0	1	1	1	11
GMI1000 / Sha-1	0	0	0	0	0	0	0	11
GMI1000 / Sha-1	0	0	0	0	0	0	0	11
GMI1000 / Sha-1	0	0	0	0	0,5	0,5	0,5	11
GMI1000 / Sha-1	0	0	0	0	0	0	0,5	11
GMI1000 / Sha-1	0	0	0	0	0	0	0,5	11
GMI1000 / Sha-1	0	0	0	0	0	0	0,5	11
GMI1000 / Sha-1	0	0	0	0	0	0	1	11
GMI1000 / Sha-1	0	0	0	0	0	0	0,5	11
GMI1000 / Sha-1	0	0	0	0	0	0	0,5	11
GMI1000 / Sha-1	0	0	0	0	0,5	0,5	0,5	11
GMI1000 / Sha-1	0	0	0	0	0,5	0,5	0,5	11
GMI1000 / Sha-1	0	0	0	0	0,5	0,5	0,5	11
GMI1000 / Sha-1	0	0	0	0	0	0	0	11
GRS216 / Col-0	0	0	0	0	0	0	0	11
GRS216 / Col-0	0	0	0	0	2,5	4	4	11
GRS216 / Col-0	0	0	0	0,5	1	4	4	11
GRS216 / Col-0	0	1	3	4	4	4	4	11
GRS216 / Col-0	0	1	3	4	4	4	4	11
GRS216 / Col-0	0	1	3	4	4	4	4	11
GRS216 / Col-0	0	0	0	0	0	2	3	11
GRS216 / Col-0	0	0	0	0	0	0	2	11
GRS216 / Col-0	0	0	0	0	0	0	0	11
GRS216 / Col-0	0	0	0	0	0	0	3	11
GRS216 / Apost-1	0	0	0	0	0	0	0	11
GRS216 / Apost-1	0	0	0	0	0	0	0	11
GRS216 / Apost-1	0	0	0	0	0	0	0	11
GRS216 / Apost-1	0	0	0	0	0	3	4	11
GRS216 / Apost-1	0	0	0	0	0	0	0	11

GRS216 / Apost-1	0	0	0	0	0	0	0	11
GRS216 / Apost-1	0	0	0	0	0	0	0	11
GRS216 / Apost-1	0	1	2	2	4	4	4	11
GRS216 / Apost-1	0	0,5	0,5	1	1	0	0	11
GRS216 / Apost-1	0	0	0	0	4	4	4	11
GRS216 / Apost-1	0	0	0	0	0	1	3	11
GRS216 / Apost-1	0	0	0	0	0	0	0	11
GRS216 / Apost-1	0	0	0	0	0	0	0	11
GRS216 / Apost-1	0	0	0	0	0	0	0	11
GRS216 / Apost-1	0	0	0	0	0	0	0	11
GRS216 / Apost-1	0	0	0	0	0	0	0	11
GRS216 / Ciste-1	0	0	0	0	0	0	0	11
GRS216 / Ciste-1	0	0	0	0	0	0	0	11
GRS216 / Ciste-1	0	0	0	0	0	0	0	11
GRS216 / Ciste-1	0	0	0	0	0	3	4	11
GRS216 / Ciste-1	0	0	0	0	0	0	0	11
GRS216 / Ciste-1	0	0	0	0	0	0	0	11
GRS216 / Ciste-1	0	0	0	0	0	0	0	11
GRS216 / Ciste-1	0	0	0	0	0	2	2	11
GRS216 / Ciste-1	0	0	0	0	0	3	4	11
GRS216 / Ciste-1	0	0	0	0	0	0	0	11
GRS216 / Ciste-1	0	0	0	0	1	4	4	11
GRS216 / Ciste-1	0	1	1	1	1	0	0	11
GRS216 / Ciste-1	0	0	0	0	0	1	1	11
GRS216 / Ciste-1	0	0	0	0	0	2	4	11
GRS216 / Ciste-1	0	0	0	0	0	0	0	11
GRS216 / Ciste-1	0	0	0	0	0	0	0	11
GRS216 / Kidr-1	0	1	3	4	4	4	4	11
GRS216 / Kidr-1	0	0,5	3	4	4	4	4	11
GRS216 / Kidr-1	0	0	0	1	3	4	4	11
GRS216 / Kidr-1	0	2	3	4	4	4	4	11
GRS216 / Kidr-1	0	3	4	4	4	4	4	11
GRS216 / Kidr-1	0	3	4	4	4	4	4	11
GRS216 / Kidr-1	0	2	3	4	4	4	4	11
GRS216 / Kidr-1	0	2	3	4	4	4	4	11
GRS216 / Kidr-1	0	0	0	2	4	4	4	11
GRS216 / Kidr-1	0	0,5	2	3	4	4	4	11
GRS216 / Kidr-1	0	2	3	4	4	4	4	11
GRS216 / Kidr-1	0	1	2	4	4	4	4	11
GRS216 / Kidr-1	0	0	2	4	4	4	4	11
GRS216 / Kidr-1	0	0	0	2	4	4	4	11
GRS216 / Kidr-1	0	3	4	4	4	4	4	11
GRS216 / Kidr-1	0	0	3	4	4	4	4	11
GRS216 / Koz-2	0	0	0	0	0	0	4	11
GRS216 / Koz-2	0	0	0	0	0	0	4	11
GRS216 / Koz-2	0	0	0	0	0	0	0	11

GRS216 / Koz-2	0	0	0	0	0	0	0	11
GRS216 / Koz-2	0	0	0	0	0	0	4	11
GRS216 / Koz-2	0	0	0	0	0	0	0	11
GRS216 / Koz-2	0	0	0	0	0	0	0	11
GRS216 / Koz-2	0	0	0	0	0	0	0	11
GRS216 / Koz-2	0	0	0	0	0	0	0	11
GRS216 / Koz-2	0	0	0	0	0	0	4	11
GRS216 / Koz-2	0	0	0	0	0	0	0	11
GRS216 / Koz-2	0	0	0	0	0	0	4	11
GRS216 / Koz-2	0	0	0	0	0	0	4	11
GRS216 / Koz-2	0	0	0	0	0	0	4	11
GRS216 / Koz-2	0	0	0	0	0	0	0	11
GRS216 / Koz-2	0	0	0	0	0	0	0	11
GRS216 / Mammo-2	0	0	0	0	0	4	4	11
GRS216 / Mammo-2	0	0	0	0	0	0	0	11
GRS216 / Mammo-2	0	0	0	0	0	0	0	11
GRS216 / Mammo-2	0	0	0	0	0	0	0,5	11
GRS216 / Mammo-2	0	0	0	0	0	0	0	11
GRS216 / Mammo-2	0	0	0	0	0	0	1	11
GRS216 / Mammo-2	0	0	0	0	0	0	0	11
GRS216 / Mammo-2	0	0	0	0	0	0	4	11
GRS216 / Mammo-2	0	0	0	0	0	0	0	11
GRS216 / Mammo-2	0	0	0	0	0	0	2	11
GRS216 / Mammo-2	0	0	0	0	0	0	0,5	11
GRS216 / Mammo-2	0	0	0	0	0	0	3	11
GRS216 / Mammo-2	0	0	0	0	0	0	0,5	11
GRS216 / Mammo-2	0	0	0	0	0	0	0	11
GRS216 / Mammo-2	0	0	0	0	0	0	0	11
GRS216 / Mammo-2	0	0	0	0	0	0	0	11
GRS216 / Moran-1	0	0	0	0	0	4	4	11
GRS216 / Moran-1	0	0	0	0	0	0	2	11
GRS216 / Moran-1	0	0	0	0	4	4	4	11
GRS216 / Moran-1	0	0	0,5	0,5	0,5	0	2	11
GRS216 / Moran-1	0	0	0	0	0	4	4	11
GRS216 / Moran-1	0	0	0	0	0	4	4	11
GRS216 / Moran-1	0	0	0	0	0	3	4	11
GRS216 / Moran-1	0	0	0,5	0,5	0,5	1	1	11
GRS216 / Moran-1	0	0	0	0	0	0	0,5	11
GRS216 / Moran-1	0	0	0	0	0	0	2	11
GRS216 / Moran-1	0	1	4	4	4	4	4	11
GRS216 / Moran-1	0	0	0	0,5	3	4	4	11
GRS216 / Moran-1	0	0	0,5	1	2,5	4	4	11
GRS216 / Moran-1	0	0	0	0	0	0	0,5	11
GRS216 / Moran-1	0	0	0	0	0	4	4	11
GRS216 / Moran-1	0	0,5	4	4	4	4	4	11
GRS216 / Sha-1	0	0	0	0	0	0	1	11

GRS216 / Sha-1	0	0	0,5	0,5	0,5			0,5	0,5	11
GRS216 / Sha-1	0	0	0,5	0,5	0,5			0,5	1	11
GRS216 / Sha-1	0	0	0,5	0,5	0,5			0,5	1	11
GRS216 / Sha-1	0	0	0	1	1			1	1	11
GRS216 / Sha-1	0	0	0	0	0			0	0,5	11
GRS216 / Sha-1	0	0	0	0	0			0	0,5	11
GRS216 / Sha-1	0	0	0	0	0			0	0,5	11
GRS216 / Sha-1	0	0	0	0	0			0	0,5	11
GRS216 / Sha-1	0	0	0	0	0			0	0,5	11
GRS216 / Sha-1	0	0	0,5	0,5	0,5			0,5	0,5	11
GRS216 / Sha-1	0	0	0	0	0			0	0,5	11
GRS216 / Sha-1	0	0	0	0	0			0	0,5	11
GRS216 / Sha-1	0	0	0	0	0			0	1	11
GMI1000 / Col-0	0	0	0	0	0	0	0	0		12
GMI1000 / Col-0	0	0	0	0,5	1	3	4	4		12
GMI1000 / Col-0	0	0	0	0	0	2	4	4		12
GMI1000 / Col-0	0	0	0	0	0	0	0,5	1		12
GMI1000 / Col-0	0	0	0	0	0	0	0	0		12
GMI1000 / Col-0	0	0	0,5	3	4	4	4	4		12
GMI1000 / Col-0	0	0	0	0	0	0	0	0		12
GMI1000 / Col-0	0	0	0	0	0,5	3	4	4		12
GMI1000 / Col-0	0	0	0	0	0,5	1	4	4		12
GMI1000 / Col-0	0	0	0	0	2	3	4	4		12
GMI1000 / Col-0	0	0	0	2	2,5	4	4	4		12
GMI1000 / Col-0	0	0	0	0,5	2	3,5	4	4		12
GMI1000 / Apost-1	0	0	0	0	0	0,5	2	4		12
GMI1000 / Apost-1	0	0	0	1	2	3	4	4		12
GMI1000 / Apost-1	0	0	0	0	0	0	0	0		12
GMI1000 / Apost-1	0	0	0	0	0	0	0	0		12
GMI1000 / Apost-1	0	0	0	0	0	0	0	0		12
GMI1000 / Apost-1	0	0	0	2	2,5	4	4	4		12
GMI1000 / Apost-1	0	0	0	0	0	0	0	0		12
GMI1000 / Apost-1	0	0	0	0	0	0	2	2		12
GMI1000 / Apost-1	0	0	0	0	0	0	0	0		12
GMI1000 / Apost-1	0	0	0	0	0	0	0	0		12
GMI1000 / Apost-1	0	0	0	1	1	2	2	4		12
GMI1000 / Apost-1	0	0	0	0	0	0	0	0		12
GMI1000 / Apost-1	0	0	0	0	1	2	3	4		12
GMI1000 / Apost-1	0	0	0	0	0	0,5	2	3		12
GMI1000 / Apost-1	0	0	0	0	0	0	0	0,5		12
GMI1000 / Apost-1	0	0	0	0	0	0	0	0		12
GMI1000 / Apost-1	0	0	0	0	0	0	0	0		12
GMI1000 / Apost-1	0	0	0	0	0	0	0	0		12
GMI1000 / Ciste-1	0	0	0	0	0	0	0	0		12
GMI1000 / Ciste-1	0	0	0	0	0	0	1	2		12
GMI1000 / Ciste-1	0	0	0	4	4	4	4	4		12

GMI1000 / Ciste-1	0	0	0	0	0	0	0	0	12
GMI1000 / Ciste-1	0	0	0	0	0	0	0	2	12
GMI1000 / Ciste-1	0	0	0	4	4	4	4	4	12
GMI1000 / Ciste-1	0	0	0	0	0,5	0,5	1,5	2	12
GMI1000 / Ciste-1	0	0	0	0	0	0	2	3	12
GMI1000 / Ciste-1	0	0	0	0	0	0	0	0	12
GMI1000 / Ciste-1	0	0	0	4	4	4	4	4	12
GMI1000 / Ciste-1	0	0	0	0	0	0	0	0	12
GMI1000 / Ciste-1	0	0	0	0	0	0	0	0	12
GMI1000 / Ciste-1	0	0	0	0	0	0	0	0	12
GMI1000 / Ciste-1	0	0	0	0	0	0	0	0	12
GMI1000 / Ciste-1	0	0	0	2	4	4	4	4	12
GMI1000 / Ciste-1	0	0	0	0	0	0	0	0	12
GMI1000 / Ciste-1	0	0	0	1	2	4	4	4	12
GMI1000 / Kidr-1	0	2	3	4	4	4	4	4	12
GMI1000 / Kidr-1	0	3	3	4	4	4	4	4	12
GMI1000 / Kidr-1	0	3	3	4	4	4	4	4	12
GMI1000 / Kidr-1	0	3	3	4	4	4	4	4	12
GMI1000 / Kidr-1	0	0	3	4	4	4	4	4	12
GMI1000 / Kidr-1	0	2	3	4	4	4	4	4	12
GMI1000 / Kidr-1	0	3	3	4	4	4	4	4	12
GMI1000 / Kidr-1	0	1	3	4	4	4	4	4	12
GMI1000 / Kidr-1	0	1	3	4	4	4	4	4	12
GMI1000 / Kidr-1	0	0	3	4	4	4	4	4	12
GMI1000 / Kidr-1	0	3	4	4	4	4	4	4	12
GMI1000 / Kidr-1	0	3	3	4	4	4	4	4	12
GMI1000 / Kidr-1	0	0	3	4	4	4	4	4	12
GMI1000 / Kidr-1	0	2	0	4	4	4	4	4	12
GMI1000 / Kidr-1	0	2	3	4	4	4	4	4	12
GMI1000 / Kidr-1	0	1	3	4	4	4	4	4	12
GMI1000 / Kidr-1	0	3	3	4	4	4	4	4	12
GMI1000 / Koz-2	0	0	0	3	4	4	4	4	12
GMI1000 / Koz-2	0	0	0	0	3	3	4	4	12
GMI1000 / Koz-2	0	0	0	0	0	0	0	2	12
GMI1000 / Koz-2	0	0	0,5	3	4	4	4	4	12
GMI1000 / Koz-2	0	0	0	0	0	0	3	4	12
GMI1000 / Koz-2	0	0	0	2	4	4	4	4	12
GMI1000 / Koz-2	0	0	0	2	3	4	4	4	12
GMI1000 / Koz-2	0	0	0	0	0	0	2	4	12
GMI1000 / Koz-2	0	0	0	0	0	0	2	2	12
GMI1000 / Koz-2	0	0	0	2	4	4	4	4	12
GMI1000 / Koz-2	0	0	2	4	4	4	4	4	12
GMI1000 / Koz-2	0	0	0	0	0	0	0	0	12
GMI1000 / Koz-2	0	0	0	0	0	1	3	4	12
GMI1000 / Koz-2	0	0	0	0	0	0	0	1	12
GMI1000 / Koz-2	0	0	0	0	0	0	3	4	12

GRS216 / Col-0	0	0	2	3	4	4	4	4	12
GRS216 / Col-0	0	0,5	2,5	4	4	4	4	4	12
GRS216 / Col-0	0	0	0	0	1,5	2	4	4	12
GRS216 / Col-0	0	0,5	2,5	4	4	4	4	4	12
GRS216 / Col-0	0	0	1,5	4	4	4	4	4	12
GRS216 / Col-0	0	0	0	0	0,5	3	4	4	12
GRS216 / Col-0	0	0	0	0	0	0	0	0	12
GRS216 / Apost-1	0	0	0	0	0	0	0	1	12
GRS216 / Apost-1	0	0	0	0	0,5	1	2,5	3	12
GRS216 / Apost-1	0	0	0	0	0	0	0	0	12
GRS216 / Apost-1	0	0	0	0	0	0	0	0	12
GRS216 / Apost-1	0	0	0	0	0	0	0	0	12
GRS216 / Apost-1	0	0	0	0	0	0	0	4	12
GRS216 / Apost-1	0	0	0	0	3	4	4	4	12
GRS216 / Apost-1	0	0	0	0	1	2	4	4	12
GRS216 / Apost-1	0	0	0	0,5	2	4	4	4	12
GRS216 / Apost-1	0	0	0	0	1,5	4	4	4	12
GRS216 / Apost-1	0	0	0	0	0	0	0	1	12
GRS216 / Apost-1	0	0	0	0	0	3,5	4	4	12
GRS216 / Apost-1	0	0	0	0	1	3	4	4	12
GRS216 / Apost-1	0	0	0	0	0	0	0	0	12
GRS216 / Apost-1	0	0	0	0	0	0	0	2	12
GRS216 / Apost-1	0	0	0	0	0	0	0	0	12
GRS216 / Apost-1	0	0	0,5	4	4	4	4	4	12
GRS216 / Apost-1	0	0	0,5	4	4	4	4	4	12
GRS216 / Ciste-1	0	0	1	4	4	4	4	4	12
GRS216 / Ciste-1	0	0	0	0	0	1	2	2	12
GRS216 / Ciste-1	0	0	0	2	3	4	4	4	12
GRS216 / Ciste-1	0	0	0,5	2	3	4	4	4	12
GRS216 / Ciste-1	0	0	0	0	2	0	0	0	12
GRS216 / Ciste-1	0	0	0	2	3	3	4	4	12
GRS216 / Ciste-1	0	0	0	0	0	0	0	0	12
GRS216 / Ciste-1	0	0	0	0	0	0	0	0	12
GRS216 / Ciste-1	0	0	0	0	0	0	0	2	12
GRS216 / Ciste-1	0	0	0	2	3	3	4	4	12
GRS216 / Ciste-1	0	0	2	4	4	4	4	4	12
GRS216 / Ciste-1	0	0	0	0	1	1	2	3	12
GRS216 / Ciste-1	0	0	0	0	0	0	2	2	12
GRS216 / Ciste-1	0	0	0	0	0	0	0	0	12
GRS216 / Ciste-1	0	0	0	1	2	4	4	4	12
GRS216 / Ciste-1	0	2	2	4	4	4	4	4	12
GRS216 / Kidr-1	0	3	3	4	4	4	4	4	12
GRS216 / Kidr-1	0	3	2,5	4	4	4	4	4	12
GRS216 / Kidr-1	0	0	2	4	4	4	4	4	12
GRS216 / Kidr-1	0	3	3	4	4	4	4	4	12
GRS216 / Kidr-1	1	3	3	4	4	4	4	4	12

GRS216 / Kidr-1	0	0	0	4	4	4	4	4	12
GRS216 / Kidr-1	0	0	3	4	4	4	4	4	12
GRS216 / Kidr-1	0	0	1	4	4	4	4	4	12
GRS216 / Kidr-1	0	0	2,5	4	4	4	4	4	12
GRS216 / Kidr-1	0	3	3	4	4	4	4	4	12
GRS216 / Kidr-1	0	3	3	4	4	4	4	4	12
GRS216 / Kidr-1	0	3	3	4	4	4	4	4	12
GRS216 / Kidr-1	0	3	3	4	4	4	4	4	12
GRS216 / Kidr-1	0	0	0	4	4	4	4	4	12
GRS216 / Kidr-1	0	3	3,5	4	4	4	4	4	12
GRS216 / Kidr-1	0	1	3	4	4	4	4	4	12
GRS216 / Kidr-1	0	1	3	4	4	4	4	4	12
GRS216 / Koz-2	0	0	0	2	4	4	4	4	12
GRS216 / Koz-2	0	0	0	2	2	3	4	4	12
GRS216 / Koz-2	0	2	2,5	4	4	4	4	4	12
GRS216 / Koz-2	0	0	0	0,5	0	2	4	4	12
GRS216 / Koz-2	0	0	0	0,5	2	4	4	4	12
GRS216 / Koz-2	0	0	0	3	4	4	4	4	12
GRS216 / Koz-2	0	0	0	3	4	4	4	4	12
GRS216 / Koz-2	0	0	0	0	0	0	2	3	12
GRS216 / Koz-2	0	0	0	0	0	0	0	0	12
GRS216 / Koz-2	0	0	0	3	3	4	4	4	12
GRS216 / Koz-2	0	0	0	0	0	0	4	4	12
GRS216 / Koz-2	0	0	0	3	4	4	4	4	12
GRS216 / Koz-2	0	0	0	2	4	4	4	4	12
GRS216 / Koz-2	0	0	0	0	0	2	4	4	12
GRS216 / Koz-2	0	0	1,5	2	4	4	4	4	12
GRS216 / Koz-2	0	0	0,5	1	0	2	4	4	12
GRS216 / Koz-2	0	0	0	2	2	4	4	4	12
GRS216 / Mammo-2	0	0	0	0	4	4	4	4	12
GRS216 / Mammo-2	0	0	0	0	0	0	0	0	12
GRS216 / Mammo-2	0	0	0	0	0	0	0	0	12
GRS216 / Mammo-2	0	0	0	0	0	0	0	0	12
GRS216 / Mammo-2	0	0	0	0	0	0	0	0	12
GRS216 / Mammo-2	0	0	0	0	0	0	0	0	12
GRS216 / Moran-1	0	0	0	0	0	0	0	0	12
GRS216 / Moran-1	0	0	0	0	0	0	0	0	12
GRS216 / Moran-1	0	0	0	0	0	0	0	0	12
GRS216 / Moran-1	0	0	0	0	0	0	2	2	12
GRS216 / Moran-1	0	0	0	0	1	1	4	4	12
GRS216 / Moran-1	0	0	0	0	2	2	4	4	12
GRS216 / Moran-1	0	0	0	0	0	0	1	1	12
GRS216 / Moran-1	0	0	2	3,5	4	4	4	4	12
GRS216 / Moran-1	0	0	0	0	0	1	2,5	4	12
GRS216 / Moran-1	0	0	0	0	0	0	0	0	12
GRS216 / Moran-1	0	0	0	0	0	0	0	0	12

GRS216 / Moran-1	0	0	0	0	0	0	0	0	12	
GRS216 / Moran-1	0	0	0	0	0	0	0	0	12	
GRS216 / Moran-1	0	0	0	0	0	0	0	0	12	
GRS216 / Moran-1	0	0	0,5	0	0	0	0	0	12	
GRS216 / Moran-1	0	0	0	0	0	0	0	0	12	
GRS216 / Moran-1	0	0	0	0	0	0	0	0	12	
GRS216 / Sha-1	0	0	0	0	0	0	0	0	12	
GRS216 / Sha-1	0	0	0	0	0	0	0	0	12	
GRS216 / Sha-1	0	0	0	0	0	0	0	0	12	
GRS216 / Sha-1	0	0	0	0	0	0	0	0	12	
GRS216 / Sha-1	0	0	0	0	0	0	0	0	12	
GRS216 / Sha-1	0	0	0	0	0	0	0	0	12	
GRS216 / Sha-1	0	0	0	0	0	0	0	0	12	
GRS216 / Sha-1	0	0	0	0	0	0	0	0	12	
GRS216 / Sha-1	0	0	0	0	0	0	0	0	12	
GRS216 / Sha-1	0	0	0	0	0	0	0	0	12	
GRS216 / Sha-1	0	0	0	0	0	0	0	0	12	
GRS216 / Sha-1	0	0	0	0	0	0	0	0	12	
GRS216 / Sha-1	0	0	0	0	0	0	0	0	12	
GRS216 / Sha-1	0	0	0	0	0	0	0	0	12	
GRS216 / Sha-1	0	0	0	0	0	0	0	0	12	
GRS216 / Sha-1	0	0	0	0	0	0	0	0	12	
GRS216 / Sha-1	0	0	0	0	0	0	0	0	12	
GRS216 / Sha-1	0	0	0	0	0	0	0	0	12	
GRS216 / Sha-1	0	0	0	0	0	0	0	0	12	
GMI1000 / Col-0	0	0	0	0	3		4	4	4	13
GMI1000 / Col-0	0	0	3	3,5	4		4	4	4	13
GMI1000 / Col-0	0	0	3	4	4		4	4	4	13
GMI1000 / Col-0	0	0	2	3,5	4		4	4	4	13
GMI1000 / Col-0	0	0	1	0,5	0		3	4	4	13
GMI1000 / Col-0	0	0	0	1	3,5		4	4	4	13
GMI1000 / Col-0	0	0,5	1	3	4		4	4	4	13
GMI1000 / Col-0	0	1	2,5	3,5	4		4	4	4	13
GMI1000 / Col-0	0	1	3	3,5	4		4	4	4	13
GMI1000 / Col-0	0	0	3	3,5	4		4	4	4	13
GMI1000 / Col-0	0	0	0	0	0		2	3,5	4	13
GMI1000 / Col-0	0	1	3,5	3,5	4		4	4	4	13
GMI1000 / Col-0	0	0	0	2	3		4	4	4	13
GMI1000 / Col-0	0	1	3	4	4		4	4	4	13
GMI1000 / Col-0	0	0	0	0	1		4	4	4	13
GMI1000 / Col-0	0	0	1,5	3	4		4	4	4	13
GMI1000 / Col-0	0	0	0	1,5	3		4	4	4	13
GMI1000 / Col-0	0	0	0	2	3		4	4	4	13
GMI1000 / Apost-1	0	0,5	1	2	4		4	4	4	13
GMI1000 / Apost-1	0	0	0	2	3		4	4	4	13
GMI1000 / Apost-1	0	0,5	0,5	1	1		2	3	4	13
GMI1000 / Apost-1	0	0	0,5	1	1		2	2,5	3	13
GMI1000 / Apost-1	0	0	0,5	0	0		0	0	0	13
GMI1000 / Apost-1	0	0	0,5	2	4		4	4	4	13

GMI1000 / Apost-1	0	0,5	0	1	1	2	1	2	13
GMI1000 / Apost-1	0	0	0	0	0	0	0	0	13
GMI1000 / Apost-1	0	0,5	0,5	0,5	1	2	3	4	13
GMI1000 / Apost-1	0	0	1	2	4	4	4	4	13
GMI1000 / Apost-1	0	0	0,5	0,5	2	4	4	4	13
GMI1000 / Apost-1	0	0	1	2	4	4	4	4	13
GMI1000 / Apost-1	0	0	0	0,5	2	4	4	4	13
GMI1000 / Apost-1	0	0,5	0	1	2	3	3,5	3,5	13
GMI1000 / Apost-1	0	0	0	0,5	2	4	4	4	13
GMI1000 / Apost-1	0	0	0,5	0	0	0	1	1	13
GMI1000 / Apost-1	0	0	2	3	4	4	4	4	13
GMI1000 / Apost-1	0	0	2	3,5	4	4	4	4	13
GMI1000 / Koz-2	0	0	0	0	0	0	0	0	13
GMI1000 / Koz-2	0	0	0	0	0	0	0	0	13
GMI1000 / Koz-2	0	0	0	0	0	0	0	0	13
GMI1000 / Koz-2	0	0	0	0	0	0	0	0	13
GMI1000 / Koz-2	0	0	0	0,5	0	0	0	0	13
GMI1000 / Koz-2	0	0	0	0	0	0	2	4	13
GMI1000 / Koz-2	0	0	0	0	0	0	0	0	13
GMI1000 / Koz-2	0	0	0	0	0	0	0	0,5	13
GMI1000 / Koz-2	0	0	0	0	0	0	0	0	13
GMI1000 / Koz-2	0	0	0	0	0	0	3	4	13
GMI1000 / Koz-2	0	0	0	0	0	0	0	0	13
GMI1000 / Koz-2	0	0	0	0	0	0	0	1	13
GMI1000 / Koz-2	0	0	0	0	0	0	0	0	13
GMI1000 / Koz-2	0	0	0	0	0	0	0	0	13
GMI1000 / Koz-2	0	0	0	0	0	0	0	0	13
GMI1000 / Koz-2	0	0	0,5	0,5	3	4	4	4	13
GMI1000 / Koz-2	0	0	0	0	0	0	0	0	13
GMI1000 / Koz-2	0	0	0,5	0,5	0	0	0	0	13
GMI1000 / Moran-1	0	0	0,5	0,5	0	0	1	1,5	13
GMI1000 / Moran-1	0	0	0	0	0	0	0	0	13
GMI1000 / Moran-1	0	0	0	1	4	4	4	4	13
GMI1000 / Moran-1	0	0	0	0,5	4	4	4	4	13
GMI1000 / Moran-1	0	0	0	1	4	4	4	4	13
GMI1000 / Moran-1	0	0	0	0	0	0	0	0	13
GMI1000 / Moran-1	0	0	0	0	0	0	0	0	13
GMI1000 / Moran-1	0	0	0,5	0	0	0	0	2	13
GMI1000 / Moran-1	0	0	0	0	0	0	0	0	13
GMI1000 / Moran-1	0	0	0	0	0	0	3	4	13
GMI1000 / Moran-1	0	0	0	0	2	4	4	4	13
GMI1000 / Moran-1	0	0	0	0	0	0	0	0	13
GMI1000 / Moran-1	0	0,5	0,5	0	3	4	4	4	13
GMI1000 / Moran-1	0	0	0	0	0	0	0	0,5	13
GMI1000 / Moran-1	0	0	0	0	0	0	0	0	13
GMI1000 / Moran-1	0	0	0	0	0	2	3	4	13

GMI1000 / Moran-1	0	0	0	0	0	0	0	0	13
GMI1000 / Moran-1	0	0	0,5	0,5	1,5	3	3,5	4	13
GMI1000 / Ciste-1	0	0	0,5	0,5	0	4	4	4	13
GMI1000 / Ciste-1	0	4	4	4	4	4	4	4	13
GMI1000 / Ciste-1	0	0	1	0	2	4	4	4	13
GMI1000 / Ciste-1	0	0,5	1	3,5	4	4	4	4	13
GMI1000 / Ciste-1	0	0	0,5	0	1	3	4	4	13
GMI1000 / Ciste-1	0	0	0	0	0	0	0	1	13
GMI1000 / Ciste-1	0	0	1,5	1,5	2	4	4	4	13
GMI1000 / Ciste-1	0	0	0,5	0,5	2	4	4	4	13
GMI1000 / Ciste-1	0	0	1	0,5	0	0	1	3	13
GMI1000 / Ciste-1	0	0	2	3	4	4	4	4	13
GMI1000 / Ciste-1	0	1	2	3,5	4	4	4	4	13
GMI1000 / Ciste-1	0	0	2	2	4	4	4	4	13
GMI1000 / Ciste-1	0	0	1	0	0	0	0	2	13
GMI1000 / Ciste-1	0	0	0	0	0	3	4	4	13
GMI1000 / Ciste-1	0	0	3	3,5	4	4	4	4	13
GMI1000 / Ciste-1	0	0	2	1	0	3	4	4	13
GMI1000 / Ciste-1	0	0	2	0	0	3	4	4	13
GMI1000 / Ciste-1	0	0	1	1	0	3	4	4	13
GRS216 / Col-0	0	0	0	0	0	0	0,5	2	13
GRS216 / Col-0	0	0	0,5	2,5	4	4	4	4	13
GRS216 / Col-0	0	0	0	0	0	3	3	4	13
GRS216 / Col-0	0	0	0	0	0	0	0	0	13
GRS216 / Col-0	0	0	0,5	0	2	3	3,5	4	13
GRS216 / Col-0	0	0	0	0,5	0	2	3	4	13
GRS216 / Col-0	0	0	0	0,5	4	4	4	4	13
GRS216 / Col-0	0	1	3	3	4	4	4	4	13
GRS216 / Col-0	0	0	0	0,5	2	4	4	4	13
GRS216 / Col-0	0	0	0	0,5	1	2	3	4	13
GRS216 / Col-0	0	2	3	3,5	4	4	4	4	13
GRS216 / Col-0	0	0	0	3	4	4	4	4	13
GRS216 / Col-0	0	0	0	0,5	2	4	4	4	13
GRS216 / Col-0	0	0	0	1	3	4	4	4	13
GRS216 / Col-0	0	0,5	2	3	4	4	4	4	13
GRS216 / Col-0	0	0	3	3,5	4	4	4	4	13
GRS216 / Col-0	0	0	1	3	4	4	4	4	13
GRS216 / Apost-1	0	1	0,5	0,5	1	4	4	4	13
GRS216 / Apost-1	0	0,5	0,5	0	2	4	4	4	13
GRS216 / Apost-1	0	0	0	1	4	4	4	4	13
GRS216 / Apost-1	0	0	0,5	1	2	3	3	4	13
GRS216 / Apost-1	0	0	0	0	0	1	2	3	13
GRS216 / Apost-1	0	1	0,5	2	3	4	4	4	13
GRS216 / Apost-1	0	0,5	2	3	4	4	4	4	13
GRS216 / Apost-1	0	0,5	1	1	4	4	4	4	13
GRS216 / Apost-1	0	0,5	0	0	0	0,5	2	2	13

GRS216 / Apost-1	0	0	0	0	0	0	0	0	13
GRS216 / Apost-1	0	0,5	0	0	0	0	0	1	13
GRS216 / Apost-1	0	1	1	2	1	1	2	1	13
GRS216 / Apost-1	0	0	0,5	0,5	0	0	0	1	13
GRS216 / Apost-1	0	0	0	0,5	1	1	2	3	13
GRS216 / Apost-1	0	0,5	0,5	2,5	4	4	4	4	13
GRS216 / Apost-1	0	0	0	0	0	0	0	2	13
GRS216 / Apost-1	0	0	0	0,5	0	0	0	1	13
GRS216 / Koz-2	0	0	0	0	0	0	0	0	13
GRS216 / Koz-2	0	0	0	0	0	0	0	0	13
GRS216 / Koz-2	0	0	0	0	0	0	0	0	13
GRS216 / Koz-2	0	0	0	0	0	0	0	0	13
GRS216 / Koz-2	0	0	0	2,5	4	4	4	4	13
GRS216 / Koz-2	0	0	0	0	0	0	0	0	13
GRS216 / Koz-2	0	0	0	0	0	0	0	0	13
GRS216 / Koz-2	0	0	0	0	0	0	0	0	13
GRS216 / Koz-2	0	0	0	0	0	0	0	0	13
GRS216 / Koz-2	0	0	0	0	0	0	0	0	13
GRS216 / Koz-2	0	0	0	0	0	0	0	0	13
GRS216 / Koz-2	0	0	0	0	0	0	0	0	13
GRS216 / Koz-2	0	0	0	0	0	0	0	0	13
GRS216 / Koz-2	0	0	0	0	0	4	4	4	13
GRS216 / Koz-2	0	0	0	0	0	0	0	0	13
GRS216 / Koz-2	0	0	0	0	0	0	0	0	13
GRS216 / Koz-2	0	0	0	0	0	0	0	0	13
GRS216 / Koz-2	0	0	0	0	0	0	0	0	13
GRS216 / Koz-2	0	0	0	0	0	0	0	0	13
GRS216 / Koz-2	0	0	0	0	0	0	0	0	13
GRS216 / Koz-2	0	0	0	0	0	0	0	0	13
GRS216 / Moran-1	0	0	0,5	0,5	1	4	4	4	13
GRS216 / Moran-1	0	0	0	0	0	0	2	3	13
GRS216 / Moran-1	0	0	0	0	0	0	0	0	13
GRS216 / Moran-1	0	0	0	0	0	1	2	3	13
GRS216 / Moran-1	0	0	0	0	0	0	0	2	13
GRS216 / Moran-1	0	0	0	0	0	0	1	4	13
GRS216 / Moran-1	0	0	0	0	0	0	0	0	13
GRS216 / Moran-1	0	0	0	0	0	0	0	0	13
GRS216 / Moran-1	0	0	0,5	2,5	4	4	4	4	13
GRS216 / Moran-1	0	0	0	3,5	4	4	4	4	13
GRS216 / Moran-1	0	0	0	0	0	0	0	0	13
GRS216 / Moran-1	0	0	0	0	0	0	0	0	13
GRS216 / Moran-1	0	0	0	0	0	0	0	0	13
GRS216 / Moran-1	0	0	0	0	0	0	0	0	13
GRS216 / Moran-1	0	0	0	0	0	0	0	0	13
GRS216 / Moran-1	0	0	0	0	0	0	0	0	13
GRS216 / Moran-1	0	3	3,5	4	4	4	4	4	13
GRS216 / Moran-1	0	3	3	4	4	4	4	4	13
GRS216 / Moran-1	0	0	0	0	0	0	0	0	13
GRS216 / Ciste-1	0	0	0,5	0,5	3	4	4	4	13
GRS216 / Ciste-1	0	0	0	1	3	4	4	4	13
GRS216 / Ciste-1	0	0	0	0	0	0	0,5	2	13

GRS216 / Ciste-1	0	0,5	1	2	4	4	4	4	13	
GRS216 / Ciste-1	0	0	0	0	1	3	2	4	13	
GRS216 / Ciste-1	0	0	0,5	2	4	4	4	4	13	
GRS216 / Ciste-1	0	0,5	0,5	1	4	4	4	4	13	
GRS216 / Ciste-1	0	0	0,5	0,5	2	3	3,5	4	13	
GRS216 / Ciste-1	0	1	1	3	4	4	4	4	13	
GRS216 / Ciste-1	0	1	0,5	2	4	4	4	4	13	
GRS216 / Ciste-1	0	0	0,5	0	1	4	4	4	13	
GRS216 / Ciste-1	0	0,5	0	1	2	4	4	4	13	
GRS216 / Ciste-1	0	0	0	0,5	1	3	3,5	4	13	
GRS216 / Ciste-1	0	0	0,5	3	4	4	4	4	13	
GRS216 / Ciste-1	0	0,5	0,5	3	4	4	4	4	13	
GRS216 / Ciste-1	0	0,5	1	3,5	4	4	4	4	13	
GMI1000 / Col-0	0	0	0	0	1	2	4	4	4	14
GMI1000 / Col-0	0	0	0	0	0,5	1	4	4	4	14
GMI1000 / Col-0	0	0	0	0	0	0	0	0	0	14
GMI1000 / Col-0	0	0	0	0,5	2	3	4	4	4	14
GMI1000 / Col-0	0	0	0	0	0	0	0	0	0	14
GMI1000 / Col-0	0	0	0	1	4	4	4	4	4	14
GMI1000 / Col-0	0	0	0	0	3,5	4	4	4	4	14
GMI1000 / Col-0	0	0	1	1	4	4	4	4	4	14
GMI1000 / Col-0	0	0	0	0	3	3	4	4	4	14
GMI1000 / Col-0	0	0	0	0	0,5	1,5	4	4	4	14
GMI1000 / Col-0	0	0	0	0	0	0	3	4	4	14
GMI1000 / Col-0	0	0	0	0	2	2	4	4	4	14
GMI1000 / Col-0	0	0	0	0	0	0	0	1	3	14
GMI1000 / Col-0	0	0	0	0	0	0	4	4	4	14
GMI1000 / Col-0	0	0	0	0	0	0	0	0,5	0,5	14
GMI1000 / Col-0	0	0	0	0	0	0	0	0	0	14
GMI1000 / Apost-1	0	0	0	0	0,5	0,5	4	4	4	14
GMI1000 / Apost-1	0	0	0	0	0	0	1	2	3	14
GMI1000 / Apost-1	0	0	0	0	0	0	4	4	4	14
GMI1000 / Apost-1	0	0	0	0	0	0	1	2	3	14
GMI1000 / Apost-1	0	0	0,5	0,5	1	1,5	4	4	4	14
GMI1000 / Apost-1	0	0	0	0	0	0	4	4	4	14
GMI1000 / Apost-1	0	0	0	0	0	0,5	4	4	4	14
GMI1000 / Apost-1	0	0	0	0	0	0	0	0	0	14
GMI1000 / Apost-1	0	0	0,5	1	3	2	4	4	4	14
GMI1000 / Apost-1	0	0	0	0	0	0	3	4	4	14
GMI1000 / Apost-1	0	0	0	0	0	0	0	0,5	2	14
GMI1000 / Apost-1	0	0	0	0	2	2,5	4	4	4	14
GMI1000 / Apost-1	0	0	0	0	0	0	2	3	4	14
GMI1000 / Apost-1	0	0	0	0,5	1	3	4	4	4	14
GMI1000 / Apost-1	0	0	0	0	2	2	4	4	4	14
GMI1000 / Apost-1	0	0	0	0	0	0	0	0,5	1	14
GMI1000 / Koz-2	0	0	1	1	3	4	4	4	14	

GMI1000 / Koz-2	0	0	3	3	4	4	4	4	14	
GMI1000 / Koz-2	0	0	0	0	3	4	4	4	14	
GMI1000 / Koz-2	0	0	0,5	0,5	3	4	4	4	14	
GMI1000 / Koz-2	0	0	0	0	2	3	4	4	14	
GMI1000 / Koz-2	0	0	0	0	3	4	4	4	14	
GMI1000 / Koz-2	0	0	0	0	3	3	4	4	14	
GMI1000 / Koz-2	0	0	0	0	0,5	1	4	4	14	
GMI1000 / Koz-2	0	0	0	0	1	1	4	4	14	
GMI1000 / Koz-2	0	0	0	0	1	1	4	4	14	
GMI1000 / Koz-2	0	0	4	4	4	4	4	4	14	
GMI1000 / Koz-2	0	0	0	0	0,5	0	4	4	14	
GMI1000 / Koz-2	0	0	1,5	2	3	1,5	4	4	14	
GMI1000 / Koz-2	0	0	0	0	0,5	0	4	4	14	
GMI1000 / Koz-2	0	0	0	0	1	1	4	4	14	
GMI1000 / Koz-2	0	0	0,5	1	2	1,5	4	4	14	
GMI1000 / Istisu-1	0	4	4	4	4	4	4	4	14	
GMI1000 / Istisu-1	0	3,5	4	4	4	4	4	4	14	
GMI1000 / Istisu-1	0	3,5	4	4	4	4	4	4	14	
GMI1000 / Istisu-1	0	0	0	0	0	0	0	4	14	
GMI1000 / Istisu-1	0	3,5	4	4	4	4	4	4	14	
GMI1000 / Istisu-1	0	0	3,5	4	4	4	4	4	14	
GMI1000 / Istisu-1	0	4	4	4	4	4	4	4	14	
GMI1000 / Istisu-1	0	3	3	4	4	4	4	4	14	
GMI1000 / Istisu-1	0	4	4	4	4	4	4	4	14	
GMI1000 / Istisu-1	0	1	2	3,5	3,5	3,5	4	4	14	
GMI1000 / Istisu-1	0	4	4	4	4	4	4	4	14	
GMI1000 / Istisu-1	0	3,5	4	4	4	4	4	4	14	
GMI1000 / Istisu-1	0	3,5	4	4	4	4	4	4	14	
GMI1000 / Istisu-1	0	0,5	4	4	4	4	4	4	14	
GMI1000 / Istisu-1	0	3,5	4	4	4	4	4	4	14	
GMI1000 / Istisu-1	0	3,5	4	4	4	4	4	4	14	
GMI1000 / Ciste-1	0	0,5	0,5	0,5	3	2,5	4	4	4	14
GMI1000 / Ciste-1	0	0	0	0	0	0,5	4	4	4	14
GMI1000 / Ciste-1	0	0	0	0	0,5	2	4	4	4	14
GMI1000 / Ciste-1	0	0	0	0	0	3	4	4	4	14
GMI1000 / Ciste-1	0	0	0	0	0	1,5	2	3,5	4	14
GMI1000 / Ciste-1	0	0	0	0	0,5	3	3	4	4	14
GMI1000 / Ciste-1	0	0	1	2	4	3,5	4	4	4	14
GMI1000 / Ciste-1	0	0	0	0	2	3,5	4	4	4	14
GMI1000 / Ciste-1	0	1	2	2	4	3,5	4	4	4	14
GMI1000 / Ciste-1	0	0	0	0	1	2,5	4	4	4	14
GMI1000 / Ciste-1	0	0	0	0	2	3	4	4	4	14
GMI1000 / Ciste-1	0	0,5	1	1	3,5	3,5	4	4	4	14
GMI1000 / Ciste-1	0	0	0	0	3,5	4	4	4	4	14
GMI1000 / Ciste-1	0	0	0	0	0,5	2	4	4	4	14
GMI1000 / Ciste-1	0	0	0	0	1	3	4	4	4	14

GMI1000 / Ciste-1	0	0	0	0	2	3	4	4	4	14
GRS216 / Col-0	0	0	0	0	3	2	4	4	4	14
GRS216 / Col-0	0	0	3	4	4	4	4	4	4	14
GRS216 / Col-0	0	0	3	4	4	4	4	4	4	14
GRS216 / Col-0	0	0	0	0	0	0	0	1	3	14
GRS216 / Col-0	0	0	0	0	0	0	4	4	4	14
GRS216 / Col-0	0	0	4	4	4	4	4	4	4	14
GRS216 / Col-0	0	3,5	4	4	4	4	4	4	4	14
GRS216 / Col-0	0	0	1	3	4	4	4	4	4	14
GRS216 / Col-0	0	0	0	0	0	0	0	0	0	14
GRS216 / Col-0	0	0	0	0	2	3	4	4	4	14
GRS216 / Col-0	0	1	4	4	4	4	4	4	4	14
GRS216 / Col-0	0	2,5	4	4	4	4	4	4	4	14
GRS216 / Col-0	0	0	0	0	4	4	4	4	4	14
GRS216 / Col-0	0	0	1	2	4	4	4	4	4	14
GRS216 / Col-0	0	0	0	0	0	0	3,5	4	4	14
GRS216 / Col-0	0	0	0	0	0	0	0	0,5	3	14
GRS216 / Apost-1	0	0,5	1	1,5		4	4	4	4	14
GRS216 / Apost-1	0	0	1	0,5	1	4	4	4	4	14
GRS216 / Apost-1	0	0	0	0	4	3	4	4	4	14
GRS216 / Apost-1	0	0	0	0	4	0	2	4	4	14
GRS216 / Apost-1	0	0	0	0	3	0	1	2	4	14
GRS216 / Apost-1	0	0	0	0	0	0	3	4	4	14
GRS216 / Apost-1	0	0	0	1	0	3,5	4	4	4	14
GRS216 / Apost-1	0	1	3	3	0	4	4	4	4	14
GRS216 / Apost-1	0	0	0,5	0,5	4	3,5	4	4	4	14
GRS216 / Apost-1	0	0	0	0	4	0	0	0	0	14
GRS216 / Apost-1	0	0	0	0	2	0	3	4	4	14
GRS216 / Apost-1	0	0	0	0	0	0	0	0	3	14
GRS216 / Apost-1	0	0	1	1	0	2,5	4	4	4	14
GRS216 / Apost-1	0	0	0	0	0	1	4	4	4	14
GRS216 / Apost-1	0	0	0	0	2	3	4	4	4	14
GRS216 / Apost-1	0	0	0	0	0	1,5	3	4	4	14
GRS216 / Koz-2	0	0	0	0	0,5	3	4	4	4	14
GRS216 / Koz-2	0	0	0	0	0	0	4	4	4	14
GRS216 / Koz-2	0	0	0	0	0,5	2	4	4	4	14
GRS216 / Koz-2	0	0	0	0	1	3	4	4	4	14
GRS216 / Koz-2	0	0	0	0	0	0	3	4	4	14
GRS216 / Koz-2	0	0	0	0	3	4	4	4	4	14
GRS216 / Koz-2	0	0	0,5	1	2	3,5	4	4	4	14
GRS216 / Koz-2	0	0	0,5	0,5	3	4	4	4	4	14
GRS216 / Koz-2	0	0	1	1	4	4	4	4	4	14
GRS216 / Koz-2	0	0	0	0	1	3,5	4	4	4	14
GRS216 / Koz-2	0	0	4	4	4	4	4	4	4	14
GRS216 / Koz-2	0	0	1	1	4	4	4	4	4	14
GRS216 / Koz-2	0	0	0	0	0	2	4	4	4	14

GRS216 / Koz-2	0	0	1	3	3	4	4	4	4	14
GRS216 / Koz-2	0	0,5	4	4	4	4	4	4	4	14
GRS216 / Koz-2	0	0	0	0	0	0	4	4	4	14
GRS216 / Istisu-1	0	0	0	0	0	0	0	0	0	14
GRS216 / Istisu-1	0	0	0	0	0,5	3	4	4	4	14
GRS216 / Istisu-1	0	1,5	4	4	4	4	4	4	4	14
GRS216 / Istisu-1	0	0	0	0	0	0	4	4	4	14
GRS216 / Istisu-1	0	0	0	2	3	4	4	4	4	14
GRS216 / Istisu-1	0	2,5	4	4	4	4	4	4	4	14
GRS216 / Istisu-1	0	0	1	3	4	4	4	4	4	14
GRS216 / Istisu-1	0	0	0	0	0	1	4	4	4	14
GRS216 / Istisu-1	0	0	0	0	0	1	4	4	4	14
GRS216 / Istisu-1	0	3	4	4	4	4	4	4	4	14
GRS216 / Istisu-1	0	0	0	0	0	0	0	0	3	14
GRS216 / Istisu-1	0	0	0	3	4	4	4	4	4	14
GRS216 / Istisu-1	0	3,5	4	4	4	4	4	4	4	14
GRS216 / Istisu-1	0	3,5	4	4	4	4	4	4	4	14
GRS216 / Istisu-1	0	3,5	4	4	4	4	4	4	4	14
GRS216 / Istisu-1	0	4	4	4	4	4	4	4	4	14
GRS216 / Ciste-1	0	0	0,5	0,5	3	4	4	4	4	14
GRS216 / Ciste-1	0	0	0	0	0	0	2	4	4	14
GRS216 / Ciste-1	0	0	0	0	0	1,5	4	4	4	14
GRS216 / Ciste-1	0	0	0	0	2	3,5	4	4	4	14
GRS216 / Ciste-1	0	0	0	0	2	3	4	4	4	14
GRS216 / Ciste-1	0	0	2	1	4	4	4	4	4	14
GRS216 / Ciste-1	0	0	0	0	3	3,5	4	4	4	14
GRS216 / Ciste-1	0	0	0	0	1	3,5	4	4	4	14
GRS216 / Ciste-1	0	0,5	2	4	4	4	4	4	4	14
GRS216 / Ciste-1	0	1	3	4	4	4	4	4	4	14
GRS216 / Ciste-1	0	1	4	4	4	4	4	4	4	14
GRS216 / Ciste-1	0	0	0	0	0	1	4	4	4	14
GRS216 / Ciste-1	0	0	1	1	3,5	3,5	4	4	4	14
GRS216 / Ciste-1	0	0	0	4	4	4	4	4	4	14
GRS216 / Ciste-1	0	0	2	3	4	4	4	4	4	14
GRS216 / Ciste-1	0	0	0	0	0,5	2,5	4	4	4	14
GMI1000 / Col-0	0	0	0	0	0	0	3	4	15	
GMI1000 / Col-0	0	0	1,5	3	3	4	4	4	15	
GMI1000 / Col-0	0	0	3	4	4	4	4	4	15	
GMI1000 / Col-0	0	0	1	3	3	3	4	4	15	
GMI1000 / Col-0	0	0	0	0	0	0	0	0	15	
GMI1000 / Col-0	0	0	2	3	4	4	4	4	15	
GMI1000 / Col-0	0	0	0	2	4	4	4	4	15	
GMI1000 / Col-0	0	0	1	3	4	4	4	4	15	
GMI1000 / Col-0	0	0	2	3,5	4	4	4	4	15	
GMI1000 / Col-0	0	0	2	3,5	4	4	4	4	15	
GMI1000 / Col-0	0	0	1	2	2	3	4	4	15	

GMI1000 / Col-0	0	0	0	1	3	4	4	4	15
GMI1000 / Col-0	0	0	3,5	4	4	4	4	4	15
GMI1000 / Col-0	0	0	3	3,5	4	4	4	4	15
GMI1000 / Col-0	0	1	3,5	4	4	4	4	4	15
GMI1000 / Col-0	0	0	1	1	3	4	4	4	15
GMI1000 / Col-0	0	0	0	2	3	4	4	4	15
GMI1000 / Col-0	0	0	0	0	0	0	4	4	15
GMI1000 / Moran-1	0	0	3	3,5	4	4	4	4	15
GMI1000 / Moran-1	0	0,5	3,5	3,5	4	4	4	4	15
GMI1000 / Moran-1	0	0	3,5	4	4	4	4	4	15
GMI1000 / Moran-1	0	0	0	0	0	0	0	2	15
GMI1000 / Moran-1	0	0	0	0	0	0	0	0	15
GMI1000 / Moran-1	0	1	1	2	4	4	4	4	15
GMI1000 / Moran-1	0	0	0	0	0	1	3	4	15
GMI1000 / Moran-1	0	0	0	0	0	0	0	0	15
GMI1000 / Moran-1	0	0	0	0	0	0	0	0	15
GMI1000 / Moran-1	0	0	0	0	0	0	0	0	15
GMI1000 / Moran-1	0	0	1	1,5	3	4	4	4	15
GMI1000 / Moran-1	0	0	0	0	0	2	4	4	15
GMI1000 / Moran-1	0	0	0	0	0	0	0	1	15
GMI1000 / Moran-1	0	0	0,5	3,5	4	4	4	4	15
GMI1000 / Moran-1	0	0,5	0,5	1,5	3	4	4	4	15
GMI1000 / Moran-1	0	3,5	4	4	4	4	4	4	15
GMI1000 / Moran-1	0	2	4	4	4	4	4	4	15
GMI1000 / Moran-1	0	3	4	4	4	4	4	4	15
GMI1000 / Koz-2	0	0	0	0	2	4	4	4	15
GMI1000 / Koz-2	0	0	0	0	1	4	4	4	15
GMI1000 / Koz-2	0	0	0	1	3	4	4	4	15
GMI1000 / Koz-2	0	0	0,5	1,5	3	4	4	4	15
GMI1000 / Koz-2	0	0	0	0	0	0	0	4	15
GMI1000 / Koz-2	0	0	0,5	0,5	2	4	4	4	15
GMI1000 / Koz-2	0	0	0	0	2	4	4	4	15
GMI1000 / Koz-2	0	0	0	0	2	4	4	4	15
GMI1000 / Koz-2	0	0	0	1	4	4	4	4	15
GMI1000 / Koz-2	0	0	1	1	3	4	4	4	15
GMI1000 / Koz-2	0	0	0	0	1	2	4	4	15
GMI1000 / Koz-2	0	0	0	0,5	2	4	4	4	15
GMI1000 / Koz-2	0	0	0	0	0	0	4	4	15
GMI1000 / Koz-2	0	0	2	2	4	4	4	4	15
GMI1000 / Koz-2	0	0	2	3	4	4	4	4	15
GMI1000 / Koz-2	0	0	3	4	4	4	4	4	15
GMI1000 / Koz-2	0	0	0	0	0	0	0	4	15
GMI1000 / Istisu-1	0	3,5	3,5	4	4	4	4	4	15
GMI1000 / Istisu-1	0	2	3,5	4	4	4	4	4	15
GMI1000 / Istisu-1	0	3	4	4	4	4	4	4	15
GMI1000 / Istisu-1	0	2	3,5	4	4	4	4	4	15

GMI1000 / Istisu-1	0	3	4	4	4	4	4	4	15
GMI1000 / Istisu-1	0	2	4	4	4	4	4	4	15
GMI1000 / Istisu-1	0	2	4	4	4	4	4	4	15
GMI1000 / Istisu-1	0	2	3,5	4	4	4	4	4	15
GMI1000 / Istisu-1	0	2,5	3,5	4	4	4	4	4	15
GMI1000 / Istisu-1	0	3	4	4	4	4	4	4	15
GMI1000 / Istisu-1	0	0	3	3,5	4	4	4	4	15
GMI1000 / Istisu-1	0	2	3,5	4	4	4	4	4	15
GMI1000 / Istisu-1	0	0	1	3	4	4	4	4	15
GMI1000 / Istisu-1	0	2	4	4	4	4	4	4	15
GMI1000 / Istisu-1	0	3	4	4	4	4	4	4	15
GMI1000 / Istisu-1	0	1	4	4	4	4	4	4	15
GMI1000 / Mammo-2	0	0	0	0,5	4	4	4	4	15
GMI1000 / Mammo-2	0	0	0	0	0	3	4	4	15
GMI1000 / Mammo-2	0	0	0	2	4	4	4	4	15
GMI1000 / Mammo-2	0	0	1	4	4	4	4	4	15
GMI1000 / Mammo-2	0	0	0	0	0	1	3	4	15
GMI1000 / Mammo-2	0	0	0,5	3	4	4	4	4	15
GMI1000 / Mammo-2	0	0	0	0	3	3	4	4	15
GMI1000 / Mammo-2	0	0	2	3,5	4	4	4	4	15
GMI1000 / Mammo-2	0	0	2	3,5	4	4	4	4	15
GMI1000 / Mammo-2	0	0	2	3	3,5	3,5	4	4	15
GMI1000 / Mammo-2	0	0	3	3,5	4	4	4	4	15
GMI1000 / Mammo-2	0	0,5	3	3,5	4	4	4	4	15
GMI1000 / Mammo-2	0	1	1,5	3	4	4	4	4	15
GMI1000 / Mammo-2	0	0	2	3	4	4	4	4	15
GMI1000 / Mammo-2	0	0	2	3,5	4	4	4	4	15
GMI1000 / Mammo-2	0	0	0	1	3,5	4	4	4	15
GMI1000 / Mammo-2	0	0	0	0	0,5	2	3	4	15
GMI1000 / Mammo-2	0	0	0	0	1	2	3	4	15
GMI1000 / Ciste-1	0	0	2	3,5	4	4	4	4	15
GMI1000 / Ciste-1	0	1	3	3,5	4	4	4	4	15
GMI1000 / Ciste-1	0	1	3	3,5	4	4	4	4	15
GMI1000 / Ciste-1	0	1	2	3,5	4	4	4	4	15
GMI1000 / Ciste-1	0	0	1	2	3	3	4	4	15
GMI1000 / Ciste-1	0	1	0,5	3,5	4	4	4	4	15
GMI1000 / Ciste-1	0	1	4	4	4	4	4	4	15
GMI1000 / Ciste-1	0	0	0	2	3	4	4	4	15
GMI1000 / Ciste-1	0	0	0	1,5	4	4	4	4	15
GMI1000 / Ciste-1	0	0	1	1	4	4	4	4	15
GMI1000 / Ciste-1	0	0	1	2,5	4	4	4	4	15
GMI1000 / Ciste-1	0	0,5	1	3	4	4	4	4	15
GMI1000 / Ciste-1	0	0	0	3	4	4	4	4	15
GMI1000 / Ciste-1	0	0	0	0	0	2	4	4	15
GMI1000 / Ciste-1	0	0,5	1	3	4	4	4	4	15
GMI1000 / Ciste-1	0	1	0	0,5	3,5	4	4	4	15

GMI1000 / Ciste-1	0	1	2	4	4	4	4	4	15
GMI1000 / Ciste-1	0	0	0	2	3,5	4	4	4	15
GMI1000 / Ciste-1		0	3	3,5	4	4	4	4	15
GRS216 / Col-0	0	0	0	0	0,5	2	3	4	15
GRS216 / Col-0	0	0	0	1	1	2	4	4	15
GRS216 / Col-0	0	0,5	2	3	4	4	4	4	15
GRS216 / Col-0	0	0	0,5	3	4	4	4	4	15
GRS216 / Col-0	0	0	1,5	1,5	3	4	4	4	15
GRS216 / Col-0	0	0	2	4	4	4	4	4	15
GRS216 / Col-0	0	0	2	4	4	4	4	4	15
GRS216 / Col-0	0	0	0	1	3	4	4	4	15
GRS216 / Col-0	0	0	1	3,5	3,5	4	4	4	15
GRS216 / Col-0	0	0	0,5	3	3,5	4	4	4	15
GRS216 / Col-0	0	0	1	4	4	4	4	4	15
GRS216 / Col-0	0	0,5	0	0,5	1	4	4	4	15
GRS216 / Col-0	0	0	0	0	1	2	4	4	15
GRS216 / Col-0	0	0	0	0	1	3	4	4	15
GRS216 / Col-0	0	0	0	0	3,5	4	4	4	15
GRS216 / Col-0	0	0,5	0,5	3,5	4	4	4	4	15
GRS216 / Col-0	0	0	0	0,5	3	4	4	4	15
GRS216 / Col-0	0	0	0,5	2	3,5	4	4	4	15
GRS216 / Col-0	0	0	0	2	3,5	4	4	4	15
GRS216 / Moran-1	0	0	0	0	0,5	2	4	4	15
GRS216 / Moran-1	0	0	0	0	2	3	4	4	15
GRS216 / Moran-1	0	0	0	0	0	0	2	4	15
GRS216 / Moran-1	0	0	0	0	0,5	0,5	2	4	15
GRS216 / Moran-1	0	0	0	0	0	0	0	4	15
GRS216 / Moran-1	0	0	0	4	4	4	4	4	15
GRS216 / Moran-1	0	0	0,5	0,5	1,5	2	4	4	15
GRS216 / Moran-1	0	0	1	1,5	3	4	4	4	15
GRS216 / Moran-1	0	0	0	0	0	0	4	4	15
GRS216 / Moran-1	0	0	0	0	0	0	3	4	15
GRS216 / Moran-1	0	0	0	1	0	1	3	4	15
GRS216 / Moran-1	0	0	0	0	0	0	0	0	15
GRS216 / Moran-1	0	0	0	0,5	2	4	4	4	15
GRS216 / Moran-1	0	0	0	0	1,5	3	4	4	15
GRS216 / Moran-1	0	0	1	0,5	1	2	3,5	4	15
GRS216 / Koz-2	0	0	0	3,5	3,5	4	4	4	15
GRS216 / Koz-2	0	0	0	2	3,5	4	4	4	15
GRS216 / Koz-2	0	0	0	1	1	3	4	4	15
GRS216 / Koz-2	0	0	0	4	4	4	4	4	15
GRS216 / Koz-2	0	0	0	4	4	4	4	4	15
GRS216 / Koz-2	0	0	0	1	3,5	4	4	4	15
GRS216 / Koz-2	0	0	0	0	1	2	4	4	15
GRS216 / Koz-2	0	0	0,5	4	4	4	4	4	15
GRS216 / Koz-2	0	0	0	1	2	3	4	4	15

GRS216 / Koz-2	0	0	0	0	0,5	2	4	4	15
GRS216 / Koz-2	0	0	0	2	4	4	4	4	15
GRS216 / Koz-2	0	0	1	2	3,5	4	4	4	15
GRS216 / Koz-2	0	0	0	1,5	2	4	4	4	15
GRS216 / Koz-2	0	0	0	0	1	4	4	4	15
GRS216 / Koz-2	0	0	0,5	0,5	1	2	4	4	15
GRS216 / Koz-2	0	0	0	0	0	0	0	0	15
GRS216 / Koz-2	0	0	0	0	0	0	4	4	15
GRS216 / Koz-2	0	0	0	1	1	2	4	4	15
GRS216 / Istisu-1	0	0	4	4	4	4	4	4	15
GRS216 / Istisu-1	0	0	3	3	4	4	4	4	15
GRS216 / Istisu-1	0	0	4	4	4	4	4	4	15
GRS216 / Istisu-1	0	0	3	3	4	4	4	4	15
GRS216 / Istisu-1	0	0	2	3	4	4	4	4	15
GRS216 / Istisu-1	0	0,5	4	4	4	4	4	4	15
GRS216 / Istisu-1	0	0	3,5	4	4	4	4	4	15
GRS216 / Istisu-1	0	0	2	4	4	4	4	4	15
GRS216 / Istisu-1	0	1	3	4	4	4	4	4	15
GRS216 / Istisu-1	0	0,5	4	4	4	4	4	4	15
GRS216 / Istisu-1	0	0	2	3	4	4	4	4	15
GRS216 / Istisu-1	0	0	2	3	4	4	4	4	15
GRS216 / Istisu-1	0	0	0	3	3	4	4	4	15
GRS216 / Istisu-1	0	0	3	3,5	4	4	4	4	15
GRS216 / Istisu-1	0	1,5	4	4	4	4	4	4	15
GRS216 / Istisu-1	0	1	3,5	4	4	4	4	4	15
GRS216 / Istisu-1	0	0	2	3	4	4	4	4	15
GRS216 / Istisu-1	0	0	4	4	4	4	4	4	15
GRS216 / Istisu-1	0	1,5	4	4	4	4	4	4	15
GRS216 / Ciste-1	0	0	1	1	2	2	4	4	15
GRS216 / Ciste-1	0	0	0,5	2	3,5	4	4	4	15
GRS216 / Ciste-1	0	0	0,5	2	3,5	4	4	4	15
GRS216 / Ciste-1	0	0	0,5	3	4	4	4	4	15
GRS216 / Ciste-1	0	0	2	3	4	4	4	4	15
GRS216 / Ciste-1	0	0	0,5	1	3,5	3,5	4	4	15
GRS216 / Ciste-1	0	0	0	0	3	3	4	4	15
GRS216 / Ciste-1	0	0	1	2	4	4	4	4	15
GRS216 / Ciste-1	0	0	1	1,5	4	4	4	4	15
GRS216 / Ciste-1	0	0	4	4	4	4	4	4	15
GRS216 / Ciste-1	0	0	0,5	1	4	4	4	4	15
GRS216 / Ciste-1	0	0	3	4	4	4	4	4	15
GRS216 / Ciste-1	0	0	0	0,5	0	0	2	4	15
GRS216 / Ciste-1	0	0	0	1,5	4	4	4	4	15
GRS216 / Ciste-1	0	0	0,5	2	4	4	4	4	15
GRS216 / Ciste-1	0	0	0,5	3	4	4	4	4	15
GRS216 / Ciste-1	0	0	1	2	4	4	4	4	15
GRS216 / Mammo-2	0	0	0	0	0	0,5	3	4	15

GRS216 / Mammo-2	0	0	0	2	4	4	4	4	15
GRS216 / Mammo-2	0	0	0,5	2	3,5	4	4	4	15
GRS216 / Mammo-2	0	0	2	4	4	4	4	4	15
GRS216 / Mammo-2	0	0,5	3	4	4	4	4	4	15
GRS216 / Mammo-2	0	0	0,5	3	4	4	4	4	15
GRS216 / Mammo-2	0	0	0	1	3,5	4	4	4	15
GRS216 / Mammo-2	0	0	0,5	3	4	4	4	4	15
GRS216 / Mammo-2	0	0,5	0	0	3	4	4	4	15
GRS216 / Mammo-2	0	0,5	1,5	3	3,5	4	4	4	15
GRS216 / Mammo-2	0	0	3	4	4	4	4	4	15
GRS216 / Mammo-2	0	0,5	3	4	4	4	4	4	15
GRS216 / Mammo-2	0	0	0	0	0	0	4	4	15
GRS216 / Mammo-2	0	0	2	4	4	4	4	4	15
GRS216 / Mammo-2	0	0	0	1	3,5	4	4	4	15
GRS216 / Mammo-2	0	0	2	4	4	4	4	4	15
GRS216 / Mammo-2	0	0	2	4	4	4	4	4	15

Table S4.2 Conductivity measurements 25-48h

																				E	Pr	Eff		
																				x	o	ect		
																				e		or		
V	V	V	V	V	V	V	V	V	V	V	V	V	V	V	V	V	V	V	V	V	A	c	m	Eff
2	2	2	2	2	3	3	3	3	3	3	3	3	3	3	4	4	4	4	4	4	g	u	t	ect
5	6	7	8	9	0	1	2	3	4	5	6	7	8	9	0	1	2	3	4	5	e	o	r	or
6		6	6	6	6	6	6	6		6	6	6	6		6	6	6	6		6				
1		2	2	2	3	3	4	4		5	5	5	5		6	6	6	6		7	O			Av
,	6	,	,	,	,	,	,	,	6	,	,	,	,	6	,	,	,	,			I	Al		rB
7	2	2	4	7	3	8	3	7	5	3	6	7	8	6	2	5	6	8	7	1	d	I	A	s3
																				Y				
		6	6	6	6	6	6		6	6	6		6	6	6	6	6	6	6	6	o			
		4	4	4	4	4	4		5	5	5		6	6	6	7	7	7	7	8	u			Av
6	,	,	,	,	,	,	,	6	,	,	,	6	,	,	,	,	,	,	,	,	n	Al		rB
5	9	8	8	7	7	6	7	5	2	4	7	6	3	6	9	2	4	7	9	1	g	I	A	s3
6	6	6	7	7	7	7	7	7	7	7	7	7	7	7	7	7								Ri
5	7	8	0	1	2	3	4	5	5	5	6	6	6	6	6	6					O			pT
,	,	,	,	,	,	,	,	,	,	,	,	,	,	,	,	,					I	Al		AL
6	1	6	2	3	7	8	6	3	6	9	2	3	3	4	5	7	8	7	7	7	d	I	A	IV-1
																				Y				
3	3	3	4	4	4	4	4	4	4	4	4	4	4	4	4	5	5	5	5	5	o			Ri
8	9	9	0	1	2	3	3	4	5	6	7	7	8	9	9	0	0	1	1	1	u			pT
,	,	,	,	,	,	,	,	,	,	,	,	,	,	,	,	,	,	,	,	,	n	Al		AL
7	2	7	4	1	1	1	9	7	5	3	1	8	5	1	7	3	7	1	6	9	g	I	A	IV-1
1	1	1	1	1	1	1	1					2	2	2	2	2	2	2	2	2	O			Ri
9	9	9	9	9	9	9	9					0	0	0	0	0	0	0	0	0	I	Al		pT
,	,	,	,	,	,	,	2	2	2	,	,	,	,	,	,	,	,	,	,	,	d	I	A	AL
6	7	7	7	8	8	8	9	0	0	0	1	1	1	2	2	2	3	3	4	4	o			I-8
																				Y				
5	5		5	5		5	5	5	5	5	6	6		6	6	6	6	6	6	6	o			Ri
9	8		7	7		8	8	8	9	9	0	0		1	2	2	3	3	4	4	u			pT
,	,	5	,	,	5	,	,	,	,	,	,	,	6	,	,	,	,	,	,	,	n	Al		AL
5	5	8	8	6	8	2	4	8	2	6	1	6	1	5	1	7	1	6	1	4	g	I	A	I-8
5	5	5		5	5	5	5	5	5	5	5	5	5	5	5	5	5	5	5	5				
4	4	4		3	3	3	3	3	3	3	3	3	3	3	3	3	3	3	3	3	O			Av
,	,	,	5	,	,	,	,	,	,	,	,	,	,	,	,	,	,	,	,	,	I	Al		rB
4	3	2	4	8	8	6	5	4	3	3	3	3	3	3	4	4	5	5	5	6	d	I	B	s3
																				Y				
6	6	6	6	6		6	6	6	6	6	6	6	6	6		6	6		6	6	o			
4	4	4	4	4		4	4	5	5	5	6	6	7	7		8	8		9	9	u			Av
,	,	,	,	,	6	,	,	,	,	,	,	,	,	,	6	,	,	6	,	,	n	Al		rB
3	5	5	8	8	5	8	9	2	5	9	3	7	1	6	8	4	8	9	3	5	g	I	B	s3
2	2	3	3	3	3							3	3	4	4	5	6	6	6	6	O			Ri
9	9	0	0	1	2									6	8	2	7	4	0	4	I	Al		pT
,	,	,	,	,	,	3	,	,	,	,	,	,	,	,	,	,	,	,	,	,	d	I	B	AL
5	8	2	7	3	3	4	2	8	5	7	5	9	6	2	8	7	3	7	1	4	g	I	B	IV-1
																				Y				
1	1	1	1	1	1	1	1	1	1	1											o			Ri
4	4	4	4	4	4	4	4	4	4	4											u			pT
,	,	,	,	,	,	,	,	,	,	,	1	,	,	,	,	,	,	,	,	,	n	Al		AL
1	2	4	5	6	6	6	7	8	9	9	5	1	2	2	3	4	4	5	6	7	g	I	B	IV-1
		4	4	5	5		6	6	6	6	6	6	6	6	6	6	7	7	7	7	O			Ri
		5	9	3	6		1	2	3	4	5	6	7	8	8	9	9	0	0	0	I	Al		pT
4	,	,	,	,	5	,	,	,	,	,	,	,	,	,	,	,	,	,	,	,	d	I	B	AL
1	4	8	5	6	9	3	7	7	8	8	8	6	3	9	5	9	3	6	8	1	g	I	B	I-8
3	4	4	4	5	5	5	6	6	6	6	6	6	6	6	6	6	7	7	7	7	Y			B

9	1	4	7	0	4	7	0	2	4	6	7	8	8	9	9	9	0	0	0	0	0	0	1	o	Al	Ri		
,	,	,	,	,	,	,	,	,	,	,	,	,	,	,	,	,	,	,	,	,	,	,	,	u	l	pT		
4	8	4	5	7	2	4	2	6	6	3	6	4	9	3	5	8		3	4	6	8	9		n	AL			
																								g	I-8			
3		3	3	3	3	3	3	3	3	3	3	3	3	3	3		4	4	4	4	4	4	4			Ri		
3		4	4	5	5	6	6	6	7	7	8	8	8	9	9		0	0	1	1	1	2	2	O	B	Av		
,	3	,	,	,	,	,	,	,	,	,	,	,	,	,	,	4	,	,	,	,	,	,	,	l	s	rB		
6	4	4	8	2	7	2	6	9	3	7	1	4	8	2	6	0	4	7	2	5	9	3	6	d	3	A	s3	
																								Y				
				2	3	3	3	3	3	3	3	3	3	3	3		4	4	4	4	4	4	4	o				
				9	0	1	2	3	4	5	6	6	7	8	9		0	1	2	3	4	5	6	u	B	Av		
2	2	2	2	,	,	,	,	,	,	,	,	,	,	,	,	4	,	,	,	,	,	,	,	n	s	rB		
5	6	7	8	1	4	7	7	6	4	2	1	8	6	4	1	0	9	8	7	5	4	3	1	g	3	A	s3	
3	3	3	3	3		3	3	3	3	3	3	3	3	3	3	3	3	3	3	3	3	3		O	B	Ri		
2	2	2	2	2		3	3	3	3	3	3	3	3	3	3	3	3	3	3	3	3	3		5	5	5	6	AL
,	,	,	,	,	3	,	,	,	,	,	,	,	,	,	,	3	,	,	,	,	,	,	,	l	s	IV-		
2	4	5	7	8	3	1	3	4	5	6	8	9	4	2	3	5	6	8	5	2	5	9	4	d	3	A	1	
																								Y				
1	2	2	2	2		3	3		3	3	4	4	4	4	4		4	4	4	4	4	4	4	o		Ri		
8	0	2	5	7		3	5		8	9	1	2	3	4	4		5	5	6	7	7	7	7	u	B	pT		
,	,	,	,	,	3	,	,	3	,	,	,	,	,	,	,	4	,	,	,	,	,	,	,	n	s	IV-		
2	1	4	1	9	1	5	5	7	3	8	4	5	5	2	6	5	4	8	4	2	4	5	5	g	3	A	1	
									1	1	1	1	1	1	1	1	1	1	1	1	1	1	1					
6	7		7		8	9	9	9	9	0	0	0	0	0	0	0	0	0	0	0	0	0	0			Ri		
6	0		9		8	2	5	8	9	1	2	2	3	3	4	4	4	4	4	4	4	5	5	5	O	B	pT	
,	,	7	,	8	,	,	,	,	,	,	,	,	,	,	,	,	,	,	,	,	,	,	,	l	s	AL		
6	9	5	7	4	4	3	8	3	8	2	3	9	3	6	1	4	5	6	8	8	1	1	1	d	3	A	I-8	
																								Y				
4	5	5		5	5	5	5	5	5	5	5	5	5	5	5	5	5	5	5	5	5	5	o			Ri		
9	0	0		1	1	1	1	2	2	2	2	2	2	2	2	2	2	2	2	2	2	2	u	B	pT			
,	,	,	5	,	,	,	,	,	,	,	,	,	,	,	,	,	,	5	,	,	,	,	,	n	s	AL		
8	2	6	1	3	6	8	9	1	2	3	5	5	6	7	8	8	9	3	1	2	3	4	5	g	3	A	I-8	
3	3	3	3		5	5	6		7	7	7	7		7	7	7		8	8	8	8	8						
2	3	5	9		3	8	3		1	3	5	6		7	8	9		0	1	2	3	3	O	B	Av			
,	,	,	,	4	4	,	,	6	,	,	,	7	,	,	,	8	,	,	,	,	,	,	l	s	rB			
6	2	2	1	4	9	7	7	6	8	2	5	2	3	7	8	8	6	0	5	5	5	2	7	d	3	B	s3	
																							Y					
3	3	3	3	3	3	3	4	4		4	4		4	4	4	4		4	4	4	4	4	o			Ri		
5	6	6	7	7	8	9	1	2		3	4		5	5	6	6		7	7	8	8	8	u	B	Av			
,	,	,	,	,	,	,	,	4	,	,	4	,	,	,	,	4	,	,	,	,	,	4	n	s	rB			
5	2	8	4	9	5	9	1	1	3	8	5	5	5	9	2	6	7	4	8	1	5	7	9	g	3	B	s3	
2					2	2	2	2	2	2	2	2	2	2	2	2	2	2	2	2	2	2	2			Ri		
4					5	5	5	5	5	5	5	5	5	5	5	5	5	6	6	6	6	6	6	O	B	pT		
,	2	2	2	2	,	,	,	,	,	,	,	,	,	,	2	,	,	,	,	,	,	,	l	s	IV-			
8	5	5	5	5	2	3	4	5	5	6	7	8	9	9	6	1	2	3	4	4	6	6	7	d	3	B	1	
																							Y					
4	4	4	4	4	4	4	4	4	4					4	4	4	4		4	4	4	4	4	o		Ri		
8	9	9	9	9	9	9	9	9	8					9	9	9	9		8	8	8	8	8	u	B	pT		
,	,	,	,	,	,	,	,	,	4	4	4	,	,	,	,	4	,	,	,	,	,	,	n	s	IV-			
7	2	4	5	8	6	3	2	2	9	9	9	9	1	1	1	1	9	9	9	9	9	8	8	g	3	B	1	
3	3	3	3		3	3	3	3	3	3	3	3	3	3	3	3	3	4	4	4	4	4	4			Ri		
5	6	6	6		7	7	7	8	8	8	8	8	8	9	9	9	9	9	0	0	0	0	0	O	B	pT		
,	,	,	,	3	,	,	,	,	,	,	,	,	,	,	,	,	,	,	,	,	,	,	l	s	AL			
9	2	4	7	7	4	7	9	2	4	6	7	9	1	3	5	7	9	1	2	3	6	8	9	d	3	B	I-8	
																							Y					
5	5	5	5	5	5		5	5	5	5	5	5	5	5	5	5	5	5	5	5	5	5	o			Ri		
4	5	5	6	6	6		8	8	8	8	7	7	7	7	7	7	7	7	7	7	7	7	u	B	pT			
,	,	,	,	,	5	,	,	,	,	,	,	,	,	,	,	,	,	,	,	,	,	,	n	s	AL			
8	3	7	1	3	7	7	2	1	2	1	9	6	5	4	4	4	3	3	3	2	2	2	2	g	3	B	I-8	

5	6	5	4	6	6	7	7	7	8	8	8	8	8	9	9	8	7	8	4	5	4	4	3		1		s3	
																									0			
5	5	5	5	5	5	5	5	5	5		5	5	5	5	5	5	5	5	5	5	5	5						
4	4	4	4	4	4	4	4	4	4		5	5	5	5	5	5	5	5	5	5	5	5						
,	,	,	,	,	,	,	,	,	,	5	,	,	,	,	,	,	,	,	,	,	,	,	5	5				
3	4	4	5	5	7	8	9	9	9	5	1	2	3	3	5	6	6	7	8	7	8	8	6	6				
9	9	9	9	9	9	9	9	9	9	9	9	9	9	9	9	9	9		9	9	9	9	9					
5	5	5	5	5	6	6	6	6	6	6	6	6	6	6	6	6	6		6	6	7	7	7					
,	,	,	,	,	,	,	,	,	,	,	,	,	,	,	,	,	,	9	,	,	,	,	,					
4	6	7	9	9	1	2	4	3	4	5	6	5	6	7	7	8	8	7	9	9	1	2	2					
6	6	6	6	6	6	6	6	6	6	6	6	6	6	6	6	6	6	6	6	6	6	6	6	6	6	6	6	
2	2	2	2	2	2	2	2	2	2	2	3	3	3	3	3	3	4	4	4	4	4	5	5	5	5	5	5	
,	,	,	,	,	,	,	,	,	,	,	,	,	,	,	,	,	,	,	,	,	,	,	,	,	,	,	,	,
4	5	6	8	8	7	7	7	8	9	1	2	4	5	7	9	1	3	5	9	2	5	8	8					
2	2	2	2	2	2	2	2		2	2	2	2	2	2	2	2	2	2	2	2	2	2		2				
6	6	6	6	6	6	6	6		7	7	7	7	7	7	7	7	7	7	7	7	7	7		8				
,	,	,	,	,	,	,	,	2	,	,	,	,	,	,	,	,	,	,	,	,	,	,	2	,				
3	4	5	6	6	7	7	9	7	1	1	2	2	4	4	5	5	6	7	7	8	9	8	1					
6	6	6	6	6	6	6	6	6	6	6	6	6	6	6	6	6	6	6	6	6	6	6	6	6	6	6	6	
8	8	8	8	8	8	8	8	8	8	8	8	8	8	8	8	8	8	8	8	8	8	8	8	8	8	8	8	
,	,	,	,	,	,	,	,	,	,	,	,	,	,	,	,	,	,	,	,	,	,	,	,	,	,	,	,	,
7	7	7	6	7	7	7	7	7	7	7	7	7	8	8	9	9	9	9	8	8	8	8	8	8	8	8	8	
6	6	7	7	7	7		7	7	7	7	7	7	7	7	7	7	7	8	8	8	8	8	8					
8	9	0	0	1	2		3	4	4	5	6	6	7		8	9	9	0	1	1	2	3	4					
,	,	,	,	,	,	7	,	,	,	,	,	,	,	7	,	,	,	,	,	,	,	,	,					
8	5	1	7	5	3	3	6	3	9	5	2	8	4	8	6	3	9	6	2	8	5	5	4					
5	5	5	5	5	5	5	5	5	5	5	5	5	5	5	5	5	5	5	5	5	5	5	5	5	5	5	5	
5	5	5	5	5	6	6	6	6	6	6	6	6	6	6	6	6	6	6	6	6	6	6	6	6	6	6	6	
,	,	,	,	,	,	,	,	,	,	,	,	,	,	,	,	,	,	,	,	,	,	,	,	,	,	,	,	,
6	7	8	9	9	1	2	2	3	3	4	4	4	4	5	6	6	6	6	6	6	6	6	6	6	6	6	6	
1	1	1	1	1	1	1	1	1	1	1	1	1	1	1	1	1	1	1	1	1	1	1	1	1	1	1	1	
0	0	0	0	0	0	0	0	0	0	0	0	0	0	0	0	0	0	0	0	0	0	0	0	0	0	0	0	
6	6	6	6	6	6	6	6	6	6	6	6	6	6	6	6	6	6	6	6	6	6	6	6	6	6	6	6	
,	,	,	,	,	,	,	,	,	,	,	,	,	,	,	,	,	,	,	,	,	,	,	,	,	,	,	,	,
5	5	4	3	3	4	5	6	5	7	6	6	6	6	6	6	6	7	6	6	6	6	4	4	3	4	4	4	
6	6		6	6	6	6	6		6	6	6	6	6	6	6	6	6	6	6	6	6	6	6	6	6	6	6	
3	3		4	4	4	4	4		5	5	5	5	5	5	6	6	6	6	6	6	6	6	6	6	6	6	6	
,	,	6	,	,	,	,	,	6	,	,	,	,	,	,	,	,	,	,	,	,	,	,	,	6	,	,	,	,
8	9	4	2	4	6	8	9	5	2	4	7	7	9	1	2	4	5	7	7	8	7	2	3					
1	1	1	1	1	1	1	1	1	1	1	1	1	1	1	1	1	1	1	1	1	1	1	1	1	1	1	1	
0	0	0	0	0	0	0	0	0	0	0	0	0	0	0	0	0	0	0	0	0	0	0	0	0	0	0	0	
5	5	5	5	5	5	5	5	5	5	5	5	5	5	5	5	5	5	5	5	5	5	5	5	5	5	5	5	
,	,	,	,	,	,	,	,	,	,	,	,	,	,	,	,	,	,	,	,	,	,	,	,	,	,	,	,	,
6	6	4	3	2	2	3	4	4	3	4	4	3	3	4	4	4	3	4	2	2	2	2	2	2	2	2	2	
7	7		7	7	7	7	7	7		7	7	7	7	7	7	7	7	7	7	7	7	7	7	7	7	7	7	
0	0		1	1	1	1	1	1	1		2	2	2	2	2	2	2	2	2	2	2	2	2	2	2	2	2	
,	,	7	,	,	,	,	,	,	7	,	,	,	,	,	,	,	,	,	,	,	,	,	,	,	,	,	,	,
8	9	1	1	2	4	5	6	7	9	2	2	3	4	5	7	8	9	1	2	3	4	6	7					
1	1	0	0	0	0	0	0	0	0	1	1	1	1	1	1	1	1	1	1	1	1	1	1	1	1	1	1	
2	2	,	,	,	,	,	,	,	2	,	,	,	,	,	,	,	,	,	,	,	,	,	,	,	,	,	,	,
0	0	2	2	3	4	5	6	7	8	1	1	1	1	2	4	5	7	6	8	7	7	8	9	8				

